THÈSE

En vue de l'obtention du

DOCTORAT DE L'UNIVERSITÉ DE TOULOUSE

Délivré par l'Université Toulouse III Paul Sabatier (UT3 Paul Sabatier)

Présentée et soutenue le *15 Juin 2016* **par :**

Antony COSTES

Une Nouvelle Approche du Cyclisme : la Transition Assis-Danseuse comme Prétexte à l'Etude de l'Optimisation du Mouvement

---

JURY

Dr. BERTUCCI William	Université de Reims	Examinateur
Dr. BIDEAU Benoit	Université de Rennes	Rapporteur
Dr. GRAPPE Frédéric	Université de Besançon	Rapporteur
Pr. MORETTO Pierre	Université de Toulouse	Directeur de Thèse
Pr. PAILLARD Thierry	Université de Pau	Examinateur
Dr. SOUERES Philippe	LAAS-CNRS	Examinateur
Dr. WATIER Bruno	Université de Toulouse	Directeur de Thèse

École Doctorale et Spécialité :

CLESCO : Performance Motrice, Adaptation et Sports

Unité de Recherche :

Programme Interdisciplinaire de Recherche en Sciences du Sport et du Mouvement Humain (PRISSMH - EA 4561) - Equipe Laboratoire Adaptation Perceptivo-Motrice et Apprentissage (LAPMA)

COSTES Antony

Programme Interdisciplinaire de Recherche en Science du Sport et du Mouvement Humain (PRISSMH – EA 4561)

Laboratoire Adaptation Perceptivo-Motrice et Apprentissage (LAPMA)

Bureau 211

Université Toulouse III – Paul Sabatier

118 Route de Narbonne

31062 Toulouse Cedex 9

antony.costes@univ-tlse3.fr ou antony.costes@orange.fr

@AntonyCOSTES

Antony Costes

Résumé

L'objectif de ce travail a été d'approfondir la connaissance des choix spontanés effectués par les humains dans le but de réaliser des tâches locomotrices simples, avec un focus sur le mouvement de pédalage.

L'analyse de la transition spontanée de la position assise vers celle en danseuse en cyclisme a été le thème central de ces travaux. Peu étudiée en comparaison de la transition marche-course, cette transition est pourtant digne d'intérêt du fait des quelques possibilités de contraindre le mouvement de pédalage, et par sa nature abrupte facilitant ainsi la mise en valeur des critères optimisés lors du mouvement. Les analyses cinématiques, par électromyographie de surface, et par méthode de dynamique inverse du corps complet, ainsi que la mesure des efforts exercés en chacun des points d'appui du cycliste sur un ergocycle entièrement instrumenté ont permis l'analyse du pédalage sous un nouvel angle. La combinaison de ces procédés offre de nouvelles perspectives pour comprendre les choix spontanés effectués pour pédaler sous contrainte incrémentale de production de puissance.

Mots-clés : *biomécanique ; cyclisme ; optimisation.*

Abstract

The aim of this work has been to deepen the knowledge about the choices spontaneously made by humans in order to realize simple locomotor tasks, with a focus on the pedaling movement.

The analysis of the spontaneous transition from the seated to the standing position in cycling was the main topic of this thesis. Little studied in comparison to the walk-run transition, this transition is of interest given the possibilities to constrain the pedaling movement, and because of its abrupt nature making easier the identification of the criteria optimized in the movement. The combination of full-body kinematics, electromyography, inverse dynamics, and the measure of the efforts applied on each of the cyclist's supports on a fully instrumented cycling-ergometer offered a new perspective on the pedaling movement. These methods provide new leads to understand the spontaneous choices made in order to pedal under increasing power-output constraints.

Keywords: *biomechanics; cycling; optimization.*

Remerciements

En premier lieu, je tiens à remercier mes directeurs de thèse, Bruno Watier et Pierre Moretto. Grâce à vos soutiens, j'ai eu la chance d'être initié au domaine de la recherche scientifique et d'y découvrir une passion. Un immense merci à vous pour avoir été mes mentors pendant ces belles années.

Mes remerciements vont aussi à Nicolas Turpin et David Villeger, vous avez tous les deux été les collègues de travail dont tout doctorant peut rêver.

Je remercie tous les membres du laboratoire et en particulier Pier-Giorgio Zanone, Michelle Fourment et les anciens et actuels doctorants et ATER pour leur gentillesse et leur aide dans la réalisation de ces travaux de thèse. Mention spéciale à Arsène Thouzé pour les bons moments passés ensemble.

Je tiens aussi à remercier tous mes formateurs, du collège jusqu'à ce jour et en particulier Henri Broncan, Emmanuel Breuil, Bernard Thon, Pierre Luche, Julien Duclay, Didier Blanchi, Serge Vaucelle, Lionel Joubert, Jean-Paul Doutreloux, Gilles Pinna, Emmanuel Plisson, David Amarantini, et tous les autres, pour m'avoir tant apporté…

Merci à William Bertucci, Benoit Bideau, Frédéric Grappe, Thierry Paillard et Philippe Soueres pour avoir accepté d'expertiser ces travaux. Avoir vos noms sur cette thèse est un immense honneur pour moi.

Je ne peux oublier Benoit Renon et Jérémy Enjalby, qui ont eu une immense influence au commencement de ces travaux, et qui ont été des sujets « alpha » (beta ?) exemplaires. Cette thèse c'est un peu grâce à vous. J'en profite pour remercier tous les participants aux différentes expérimentations liées à cette thèse pour leur disponibilité.

A Georges Soto-Romero, pour les sushis et les nouveaux projets lancés.

A Nicolas Hemet, pour les années passées, et surtout celles à venir.

A Kévin Villeneuve et Simon Olivé, pour leur amitié éternelle.

A Jeanne B, Karin B, Robert W, Robert B et Mireille B, et mes beaux-parents, Marie et Patrick Dupouy, une famille en or.

Je ne remercierai jamais assez mes parents Gisèle et Didier, des parents formidables, pour tout.

A mon frère et mes sœurs, Joanna, Robin et Maïté, comme nous tous, vous avez encore beaucoup à apprendre, et vous êtes sur la bonne voie…

Enfin, Mathilde. Le grand hasard de la vie ne pouvait rien m'apporter de meilleur que toi.

"*If you can not measure it, you can not improve it.*" – Lord Kelvin

"*They did not know it was impossible, so they did it!"* – Mark Twain

"Ignoranti quem portum petat nullus suus uentus est." – Lucius Annaeus Seneca

Publications et communications

Communications Ecrites

COSTES, A., VILLEGER, D., MORETTO, P., WATIER, B. (2015) *Transferability Between Isolated Joint Torques And A Maximum Polyarticular Task: A Preliminary Study.* Journal of Human Kinetics, 50: 5-14. doi: 10.1515/hukin-2015-0136

COSTES, A., TURPIN, N.A., VILLEGER, D., MORETTO, P., WATIER, B. (2015) *Influence Of Position And Power Output On Upper Limb Kinetics In Cycling.* Journal of Applied Biomechanics, 32(2): 140-149. doi: 10.1123/jab.2014-0295

COSTES, A., TURPIN, N.A., VILLEGER, D., MORETTO, P., WATIER, B. (2015) *A Reduction Of The Saddle Vertical Force Triggers The Sit-Stand Transition In Cycling.* Journal of Biomechanics, 48(12): 2998-3003. doi: 10.1016/j.jbiomech.2015.07.035.

COSTES, A., TURPIN, N.A., VILLEGER, D., MORETTO, P., WATIER, B. (2016) *Minimization Of Cost Functions Is Associated With The Sit-Stand Transition In Cycling.* Submitted to *« Journal of Biomechanics ».*

MORETTO P., VILLEGER D., **COSTES A.**, WATIER B. (2016). *Elastic Energy in Locomotion: Simple vs. Complex Models.* Gait and Posture, 48: 183-188. doi: 10.1016/j.gaitpost.2016.05.015

TURPIN, N.A., **COSTES, A.**, VILLEGER, D., WATIER, B. (2014) *Selective Muscle Contraction During Plantarflexion Is Incompatible With Maximal Voluntary Torque Assessment.* European Journal of Applied Physiology.114(8):1667-77. doi: 10.1007/s00421-014-2900-3.

TURPIN, N.A., **COSTES, A.**, VILLEGER, D., MORETTO, P., WATIER, B. (2016) *Upper Limb And Trunk Muscles Activity Patterns During Seated And Standing Cycling.* Journal of Sports Science (In Press). doi : 10.1080/02640414.2016.1179777

TURPIN, N.A., **COSTES, A.**, VILLEGER, D., MORETTO, P., WATIER, B. (2016) *Muscles Activity Patterns Associated With The Seated And Standing Positions In Pedaling: Modularity And Evidences For An Optimal Transition.* Submitted to « *Journal of Science and Medicine in Sport ».*

VILLEGER D., **COSTES A.**, WATIER B., MORETTO P. (2015) *Froude and Strouhal Dimensionless Numbers to Ensure Dynamic Similarity in Human Walking*. Gait & Posture, 41(1):240-5. doi:10.1016/j.gaitpost.2014.10.016.

VILLEGER D., **COSTES A.**, WATIER B., MORETTO P. (2014). *Froude and Strouhal Dimensionless Numbers to Ensure Dynamic Similarity in Human Running.* Journal of Biomechanics, 47(16):3862-7. doi:10.1016/j.jbiomech.2014.10.012.

VILLEGER D., **COSTES A.**, WATIER B., MORETTO P. (2014). *An Algorithm to Decompose Ground Reaction Forces and Moments From a Single Force Platform in Walking Gait.* Medical Engineering & Physics, 36:1530-1535. doi: 10.1016/j.medengphy.2014.08.002

Communications Orales

COSTES, A., TURPIN, N.A., VILLEGER, D., MORETTO, P., WATIER, B. (2015) *Increasing Power Output And Movement Optimization In Cycling: Insights From A Fully Instrumented Ergometer.* International Society of Sports Biomechanics. Poitiers. France.

MANGIN, M., VALADE, A., **COSTES, A.**, BOUILLOD, A., SOTO-ROMERO, G. *An Instrumented Glove For Swimming Performance Monitoring.* 3rd International Congress on Sport Science Research and Technology Support. Lisbon. Portugal.

TURPIN, N.A., **COSTES, A.**, MORETTO, P., WATIER, B. (2014) *Variability in the Spatial Structure of Muscle Coordination in the Sit-To-Stand Transition in Pedaling.* 11th Motor Control Summer School. Bled. Slovenia.

VALADE, A., **COSTES, A.**, BOUILLOD, A., MANGIN, M., FOURNIOLS, J.Y., GRAPPE, F., SOTO-ROMERO, G. (2015) *Embedded Sensors System Applied To Wearable Motion Analysis In Sports.* Biomedical Circuits and Systems Conference. Atlanta. USA.

VILLEGER, D., **COSTES, A.,** WATIER, B., MORETTO, P. (2014). *Inter-Subject Variability in Running is Reduced with NMODELA-R Dimensionless Number - An Inverse Dynamic Study*.13th Symposium of 3DAHM, Lausanne, Swiss.

WATIER, B., **COSTES, A.**, MORETTO, P. (2013) *An Inverse Dynamic Study Suggests That Cyclists Marginally Use Hip Joint Torque At Maximal Power.* 24th Congress of the International Society of Biomechanics. Natal. Brazil.

WATIER, B., VILLEGER, D., **COSTES, A.**, MORETTO, P. (2015) *Similar Experimental Conditions Decrease Inter-Subject Variability Of Running Gait.* 21st Congress of the European Society of Biomechanics. Prague, Czech Republic.

WATIER, B., VILLEGER, D., **COSTES, A.**, MORETTO, P. (2015) *A Preliminary Study Suggests That Walk To Run Transition Is Consistent With Mechanical Optimization.* 40ème congrès de la Société de Biomécanique. Paris. France.

Table des matières

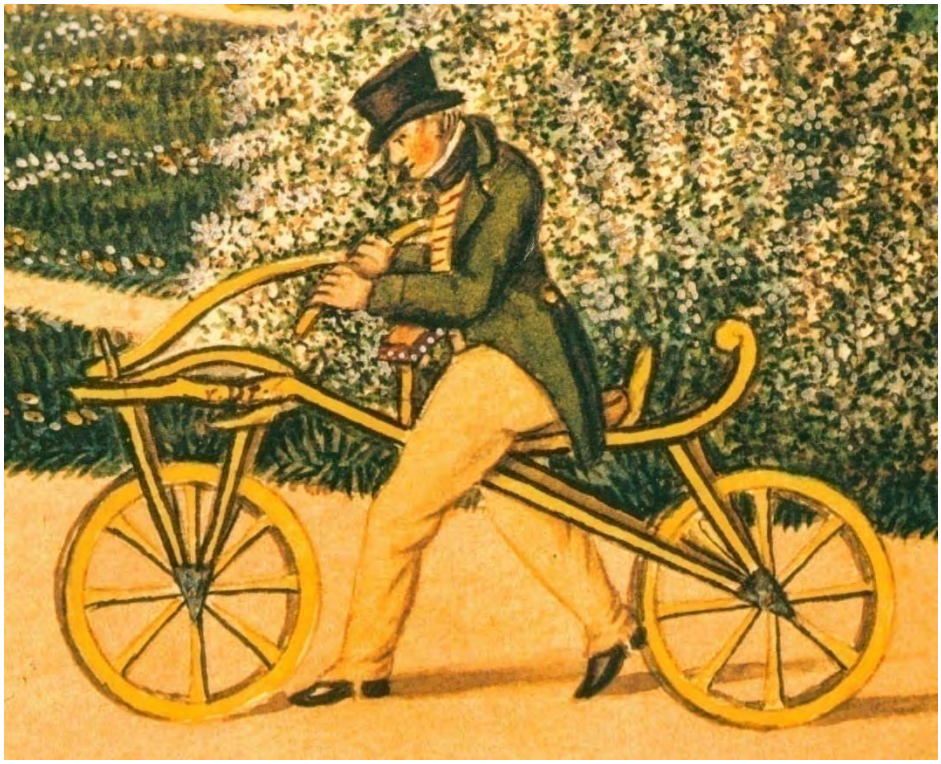

I) Introduction générale

Illustration : « Laufmaschine » ou « Draisienne », inventée en 1817 par le Baron Karl Von Drais pour se déplacer plus vite dans les jardins royaux de Paris. Considérée comme l'ancêtre de la bicyclette.

Depuis ses balbutiements avec la « Draisienne » du Baron Karl Von Drais, jusqu'aux bicyclettes modernes, le « vélo » est une invention qui a évolué pendant près de deux siècles. Au même titre que la marche ou la course, ce dernier est un moyen de déplacement utilisant l'énergie humaine, utile à environ 2 milliards de personnes dans le monde[1]. Le niveau de difficulté du déplacement à bicyclette paraît faible. Toutefois, le « problème de Bernstein » montre que le nombre de solutions possibles pour la réalisation de ce mouvement est la source d'une complexité computationnelle importante[2]. En effet, en raison de la redondance du système neuro-musculo-squelettique, un mouvement simple comme le pédalage peut être réalisé d'une infinité de manières par les différents muscles et articulations du corps humain. Cette complexité est d'autant plus importante lorsque des contraintes environnementales s'ajoutent. Se déplacer à une certaine vitesse en vélo, c'est principalement lutter contre des forces extérieures (traînée aérodynamique, poids, frottements…) en transférant les efforts musculaires d'un potentiel d'environ 790 muscles humains aux pédales. Selon ces contraintes, deux positions principales sur la bicyclette ont été observées : la position « assise », qui utilise les cinq possibilités d'appui proposées (selle, appuis manuels et pédales), et la position « danseuse », qui n'utilise que quatre appuis en supprimant celui sur la selle. Tout comme un bipède passe de la marche à la course, et inversement, selon sa vitesse de déplacement (Raynor et al. 2002), ou un quadrupède du pas au trot, puis au galop (Hoyt and Taylor 1981), il est couramment observé qu'un cycliste passe spontanément de la position « assise » à celle en « danseuse » en fonction de contraintes, à ce jour encore mal connues. Faisant suite aux travaux initiés par la thèse d'Eric Poirier (2009), ce manuscrit de thèse a pour objet principal l'approfondissement de la connaissance biomécanique de la transition assis-danseuse. L'intérêt de cette transition est sa nature abrupte, qui facilite l'étude des mécanismes impliqués lors de ce changement de stratégie choisie par l'humain (Alexander 1989). L'approche expérimentale utilisée se base sur une analyse biomécanique, en combinant les outils suivants : l'analyse cinématique du corps complet, l'analyse dynamique par la mesure des efforts appliqués sur les cinq appuis du cycliste sur sa bicyclette, l'approche dite par « dynamique inverse » sur le corps complet, ainsi que l'analyse électromyographique des principaux muscles impliqués dans le mouvement de pédalage.

[1] Source : Banque Mondiale.

[2] Nikolai Aleksandrovich Bernstein (1896-1966) est un physiologiste russe célèbre pour ses travaux sur le contrôle moteur.

Dans une première partie, l'état de l'Art recensera les méthodes ayant été utilisées pour l'analyse biomécanique du cyclisme, et conclura sur les principales études ayant comparé la position assise à celle en danseuse en cyclisme. Dans une seconde partie seront présentées nos contributions, concernant en premier lieu la mesure des efforts au membre supérieur lors du pédalage, la mesure des efforts appliqués par le cycliste sur ses différents appuis sous contraintes incrémentale de puissance mécanique à développer, les mesures par électromyographie, puis l'utilisation de fonctions de coût permettant d'expliquer la transition de la position assise vers celle en danseuse. Par la suite, une conclusion générale discutant les implications, limites et perspectives de ces travaux sera présentée. Enfin, en annexe seront reportés différents travaux réalisés parallèlement à cette thèse pour approfondir la connaissance du mouvement de pédalage selon différentes modalités.

II) Etat de l'Art

Illustration : Louison Bobet en « danseuse », en tête de son premier Tour de France victorieux (1953).

II.1. CONSIDERATIONS METHODOLOGIQUES

II.1.1. Analyse Cinématique et Anthropométrique

Dans le cadre de l'analyse cinématique du mouvement humain, les articulations et segments corporels peuvent être modélisés. Depuis les travaux de Muybridge (1883), Marey (1884) et Demeny (1904) utilisant la chronophotographie, les possibilités de mesure de la cinématique du corps humain ont évolué.

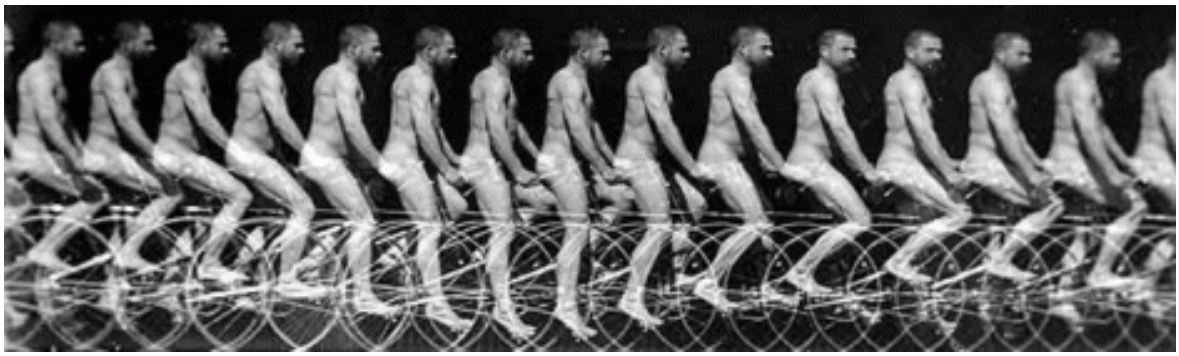

Figure 1 : décomposition image par image d'une scène de cyclisme, par Etienne Jules Marey.

D'un point de vue mécanique, le corps humain est généralement représenté comme un système composé de n segments S_i de centre de gravité G_i, de masse m_i et de rayon de giration r_i reliés par des articulations considérées « parfaites » (Hull and Jorge 1985, figure 2 pour illustration).

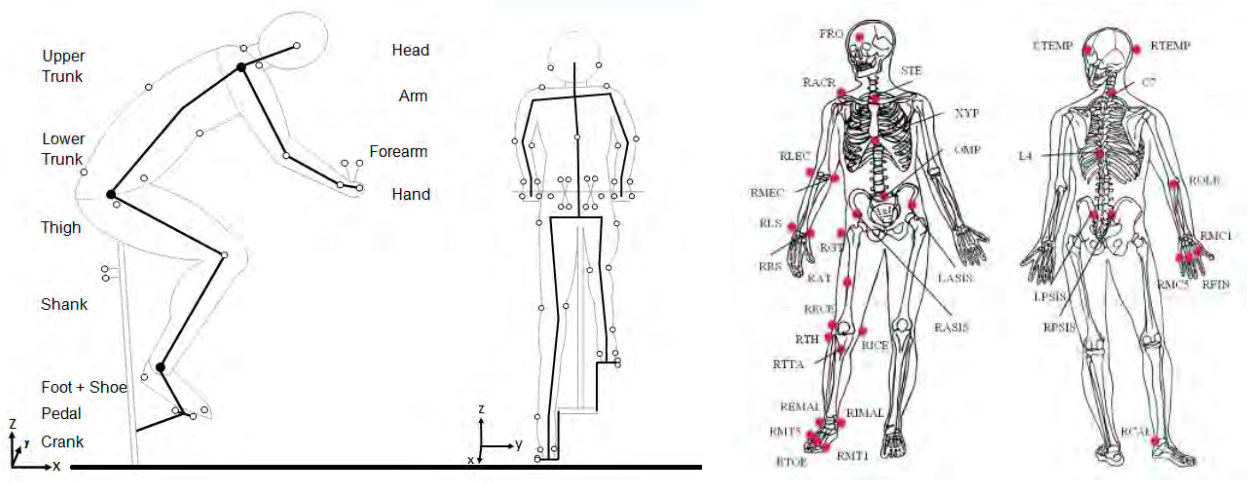

Figure 2 : modèle cinématique utilisé pour représenter un cycliste en 3 dimensions. (Gauche) : vue dans le plan saggital. (Centre) : vue dans le plan frontal. (Droite) positionnement de 54 marqueurs cutanés afin de décrire la cinématique du corps complet (adapté de Hayot, 2010).

Afin de capturer les positions de différents points d'intérêt du corps humain, puis d'en calculer par dérivation par rapport au temps les vitesses, accélérations, voire les jerks (variations d'accélération par rapport au temps), l'utilisation de système optoélectroniques s'est progressivement développée depuis les années 1970. Ces sytèmes permettent désormais l'enregistrement en temps réel des positions de plusieurs dizaines de marqueurs dans un espace en 3 dimensions, avec une précision de l'ordre du milimètre (Poirier 2009) et des fréquences d'acquisition dépassant 200 Hz. Classiquement, une articulation peut ainsi être repérée à partir de la position de deux marqueurs. Par exemple pour le coude, le centre de rotation est déterminé comme étant le milieu du segment reliant les marqueurs apposés sur l'épicondyle et l'épitrochlée (Figure 3).

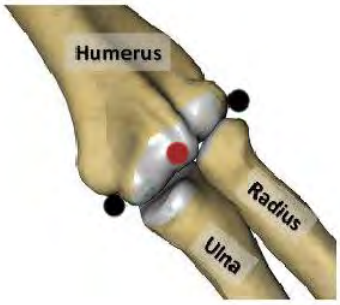

Figure 3 : localisation du centre articulaire du coude (point rouge) estimée à partir de marqueurs réfléchissants collés à la surface de la peau (points noirs).

Toutefois, quelques limitations existent à ces mesures. La première est la portée des caméras, qui restreint le champ d'analyse à quelques dizaines de mètres carrés, en fonction de la quantité de caméras utilisées. Pour y pallier dans le cas du cyclisme, trois principales méthodes expérimentales ont été utilisées : l'utilisation d'un ergocycle (Bini, Hume, and Kilding 2014; Martin and Brown 2009), celle d'un tapis roulant motorisé (Stone and Hull 1995; Duc et al. 2008), ou encore l'enregistrement en un point fixe sur un vélodrome (Bertucci, Taiar, and Grappe 2005), qui ne permet donc pas un enregistrement en continu. Une seconde limitation est que si la précision du repérage des marqueurs dans l'espace est devenue acceptable, le mouvement de ces derniers ne reproduit pas exactement celui des os du corps humain en raison d'artefacts liés aux mouvements des tissus mous (Thouzé et al. 2013; Dumas et al. 2014). En particulier dans le cas du cyclisme, la cinématique de la hanche a été décrite comme mesurée de façon imprécise par l'enregistrement du mouvement d'un marqueur collé à la surface de la peau au niveau de la tubérosité proximale du fémur (grand trochanter). Neptune et Hull (1995, 1997) ont étudié cette problématique et montré que l'erreur sur la position du centre articulaire de la hanche dans le plan saggital pouvait atteindre 4 cm (Figure 4).

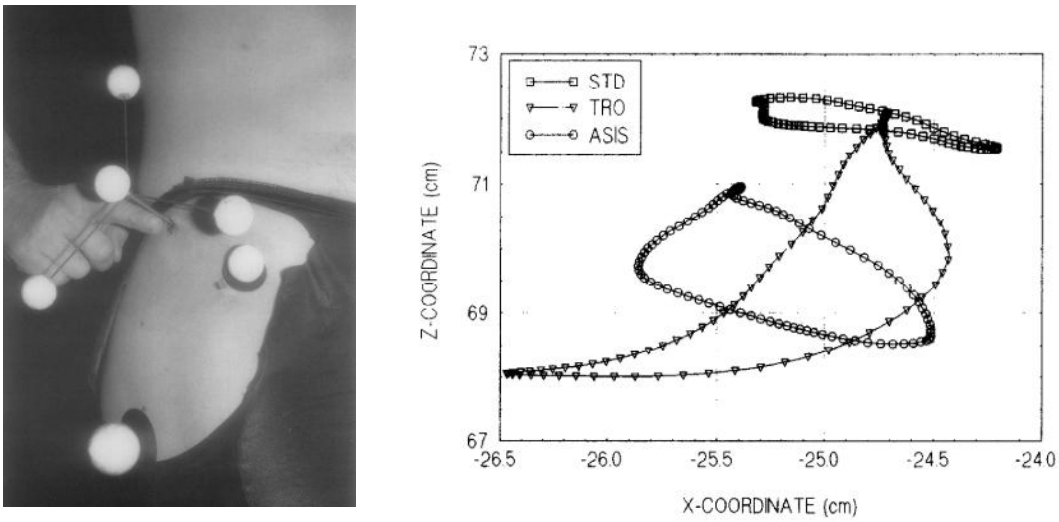

Figure 4 (Gauche): modèle expérimental utilisé par Neptune et Hull (1995). Noter la triade de marqueurs associée à un pin intracortical fixé à l'articulation de la hanche et utilisé comme standard afin de mesurer l'erreur cinématique entraînée par différentes configurations de marqueurs. (Droite) : Position du centre articulaire de la hanche au cours d'un cycle de pédalage à 225 W et 90 RPM. STD : référence basée sur le pin intracortical. TRO : marqueur cinématique placé sur le Grand Trochanter. ASIS : méthode basée sur l'utilisation d'un marqueur placé sur l'épine illiaque antéro-supérieure.

Pour diminuer cette erreur, ces auteurs proposent l'utilisation d'une méthode basée sur l'utilisation d'un marqueur placé sur l'épine illiaque antéro-supérieure. L'importance de la précision de la cinématique étant fondamentale lors de l'analyse biomécanique, et en particulier pour l'application de méthodes de dynamique inverse, d'autres méthodes ont été proposées. La méthode « SCoRE » (pour Symetrical Center of Rotation Estimation, voir Figure 5) est l'une d'entre elles et a notamment été utilisée dans les articles proposés dans le 3ème chapitre de cette thèse (Ehrig et al. 2006; Monnet et al. 2007). Son principe est d'estimer la position relative du centre articulaire en recherchant un point commun moyen appartenant à la fois au segment proximal et au segment distal, et implique donc de connaître la position et la matrice de rotation de ces deux segments et nécessitent la réalisation d'un enregistrement préalable sollicitant les mouvements de flexion-extension, abduction-adduction et de rotation interne et externe de l'articulation étudiée (Begon, Monnet, and Lacouture 2007). Cette méthode a été décrite en détail dans la littérature (Hayot 2010; Villeger 2014) et permet la localisation de l'articulation de la hanche avec une précision de 1,2 mm (Ehrig et al. 2006) et de 3 mm pour l'épaule (Monnet et al. 2007).

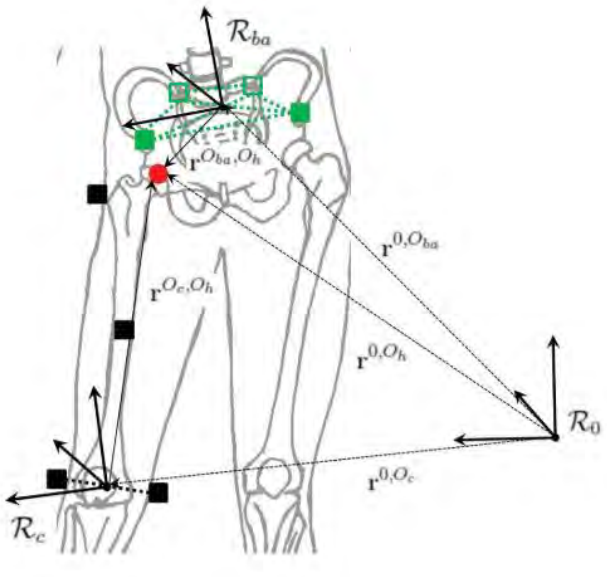

Figure 5 : localisation du centre articulaire de la hanche par la méthode SCoRE. R_0 désigne le référentiel global (du laboratoire), R_c le référentiel local associé à la cuisse, et R_{ba} le référentiel local associé au pelvis. Les points verts réprésentent les marqueurs passifs permettant la mesure de la cinématique du bassin, et les carrés noirs pour la cuisse. Le point rouge est le centre articulaire de la hanche dont la position est estimée à l'aide de la méthode SCoRE. (Adapté d'Hayot, 2010).

Malgré l'amélioration de la précision de la cinématique grâce à cette méthode, elle reste simplificatrice car décrivant le mouvement de centre de rotation moyen, alors que les articulations humaines possèdent des centres de rotation instantanés et donc mobiles du fait de la géométrie des surfaces de contact osseuses.

Enfin, une dernière source d'erreur en cinématique réside dans la propagation des erreurs dans la mesure des positions lors des opérations de dérivation. Pour y remédier, des méthodes d'optimisation du signal existent (Cahouët, Martin, et Amarantini (2002). L'approche la plus simple et la plus utilisée est de filtrer le signal à l'aide de filtres de type Butterworth, appliqués en aller-retour afin d'éliminer le déphasage temporel créé (Winter, 1990). Afin d'en déterminer de façon objective la fréquence de coupure passe-bas, une approche est de conserver un certain pourcentage de la puissance spectrale déterminée par transformée de Fourier (Amarantini 2003; Kamen and Gabriel 2010 / Figure 6).

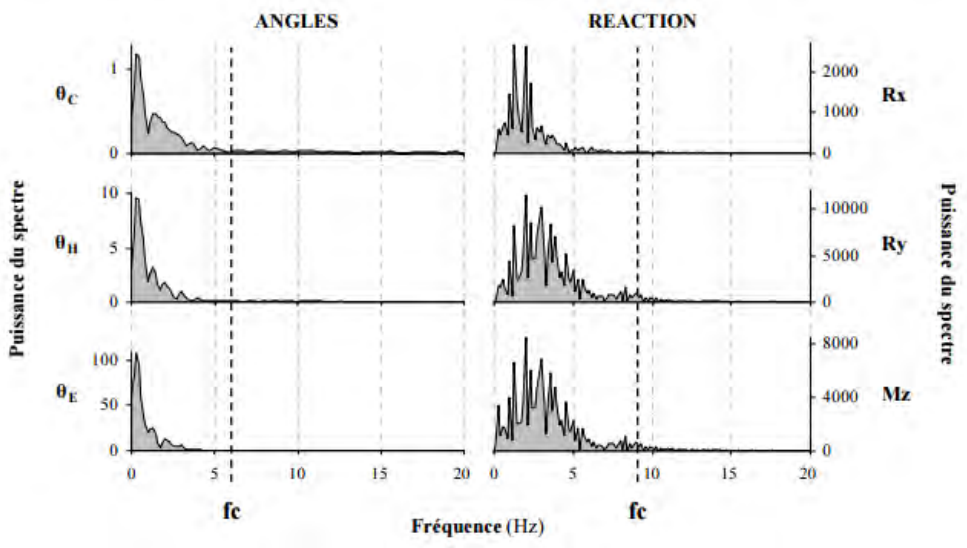

Figure 6 : exemple de représentation graphique de spectres de puissances de signaux cinématiques et analogiques déterminés par transformée de Fourier et permettant la définition objective d'une fréquence de coupure passe-bas permettant la conservation d'au moins 90% du signal (adapté d'Amarantini, 2003).

L'objectif des procédures de filtrage est d'éliminer une partie des sources de perturbation du signal non désirées liées notamment aux vibrations des marqueurs passifs, aux mouvements des câbles dans le cas de la mesure électromyographique, ou encore à l'imprécision instantanée inhérente à toute mesure physique.

Les données anthropométriques (masses et rayons de giration des différents segments corporels) ont aussi une importance cruciale dans l'analyse biomécanique. Ces dernières constituent une donnée d'entrée dans le calcul des moments dynamiques au niveau des articulations. Elles sont généralement issues de statistiques basées sur la taille et la masse de différentes populations, reportées dans des tables anthropométriques. Le choix de la table anthropométrique utilisée se doit donc être adapté à la population étudiée et peut constituer une source d'erreur (Rao et al. 2006).

Dans le cadre de ces travaux de thèse, la table anthropométrique proposée par de Leva (1996) a été utilisée au vu de la population de jeunes sportifs étudiée (Figure 7).

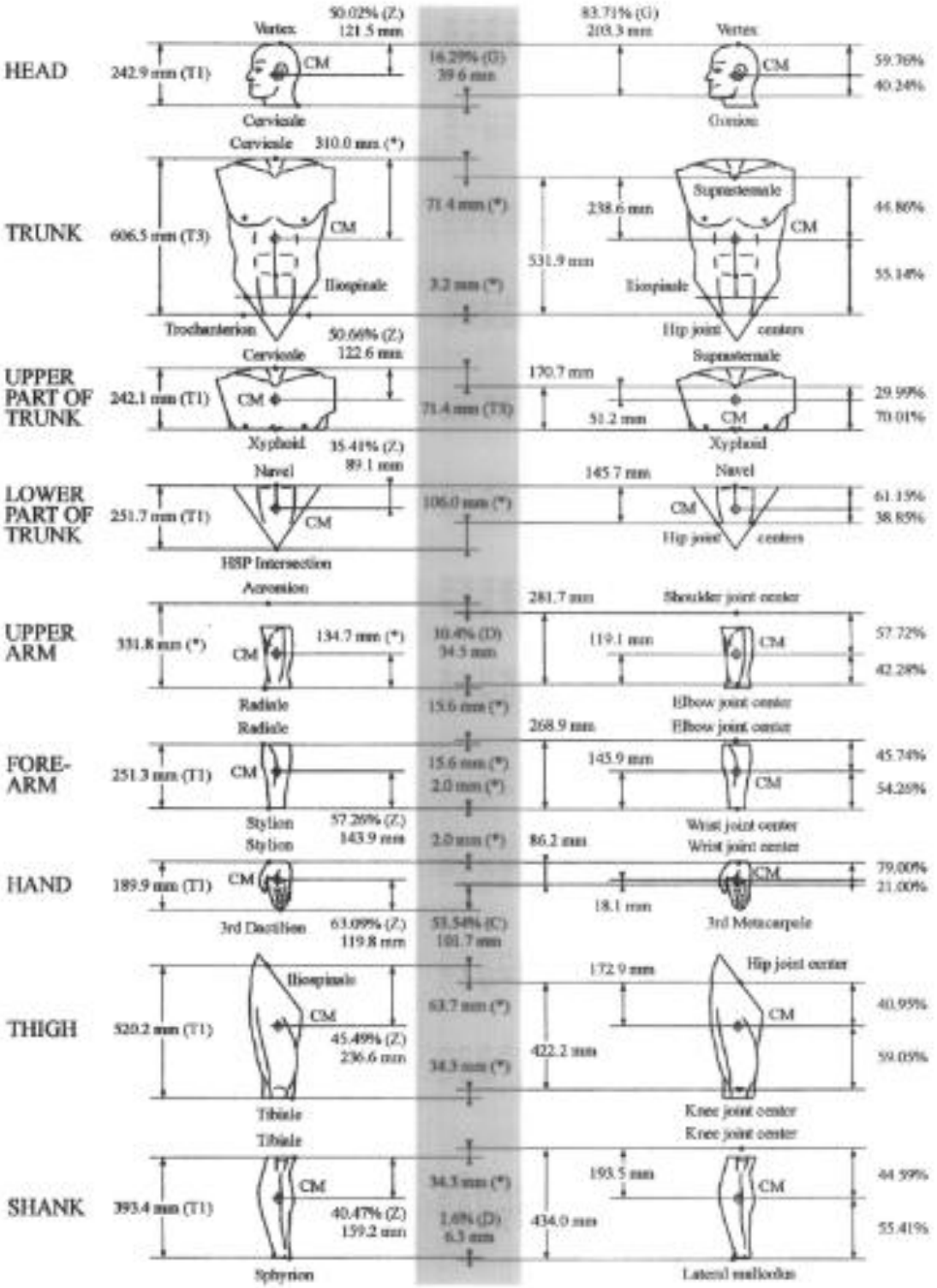

Figure 7 : représentation graphique de la position des centres de masse segmentaires selon la table anthopométrique de De Leva. (Adapté de De Leva, 1996).

II.1.2. Mesure des Efforts Externes

La mesure des efforts externes permet de caractériser l'intéraction entre le cycliste et sa bicyclette. Lors du pédalage en position assise, cinq appuis existent et sont répartis sur les pédales, le cintre et la selle. Dès ses débuts en l'an 1896, la littérature scientifique s'est focalisée sur la mesure des efforts appliqués sur les pédales (Figure 8). Ces premiers « cyclographes » avaient déjà permis de noter la présence de forces anti-propulsives lors du pédalage. Les méthodes se sont ensuite modernisées progressivement (Hoes et al. 1968; Sargeant and Davies 1977) pour permettre des mesures en 3 dimensions (Stone and Hull 1995; Gregersen and Hull 2003). En parallèle, en 1986, ont été développés les premiers capteurs SRM (Schoberer Rad Messtechnik, Jülich, Allemagne) permettant la mesure embarquée de la puissance mécanique développée au niveau de l'axe de pédalier.

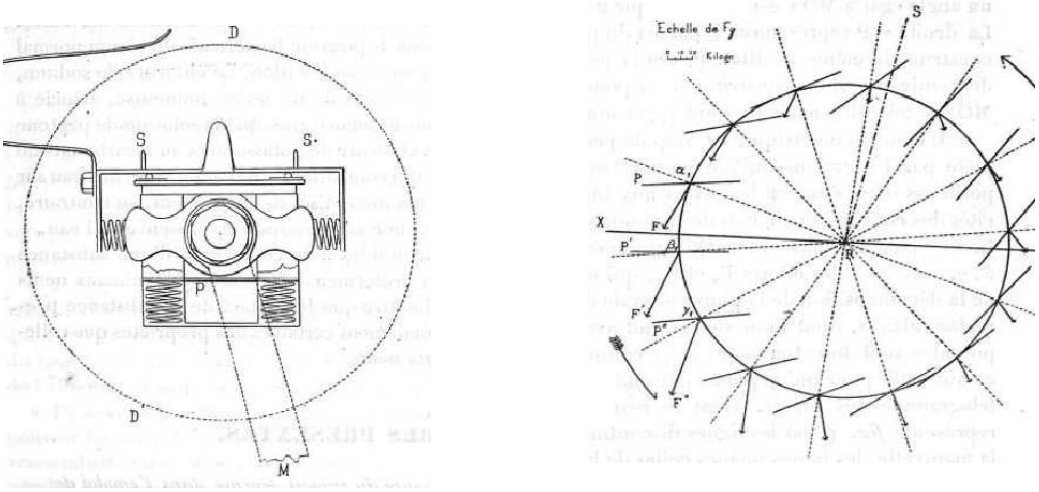

Figure 8 : (Gauche) « Cyclographe » premier outil permettant la mesure des forces appliquées sur la pédale en deux dimensions. (Droite) représentation du pattern de force appliquée sur la manivelle gauche (rotation dans le sens trigonométrique) grâce à une synchronisation avec des données issues de la chronophotographie. (Adapté de Marey, 1896).

La mesure de la puissance mécanique appliquée sur les pédales en cyclisme est fondamentale car c'est d'elle que dépend la vitesse de déplacement d'un cycliste en fonction des forces extérieures appliquées sur lui (traînée aérodynamique, poids et frottements des pneus et de la transmission, principalement). L'usage des capteurs de puissance se démocratise et l'offre se diversifie avec actuellement plus d'une dizaine de fabricants sur le marché. Mécaniquement, la puissance mécanique développée au niveau de l'axe du pédalier dépend de trois facteurs : la longueur de la manivelle, la valeur de la force appliquée sur la pédale perpendiculairement à la manivelle (le produit de ces deux premières variables représentant le couple mécanique), et la vitesse de rotation des manivelles. Il est à noter dans cette équation que seule la composante normale à la manivelle de la force appliquée sur la pédale créée un travail mécanique, la partie restante n'étant pas propulsive, mais pas non plus gratuite en terme d'effort musculaire ou de contrainte articulaire.

La puissance mécanique au pédalier n'étant pas suffisante pour quantifier l'effort global du système musculo-squelettique, il est nécessaire de quantifier les torseurs mécaniques à chaque contact entre le cycliste et sa bicyclette. Peu d'études ont été consacrées à la mesure des efforts appliqués sur le cintre et la selle. Les premiers dynamomètres permettant ce type de mesure datent de 1985 (Bolourchi et Hull, 1985 / Figure 9).

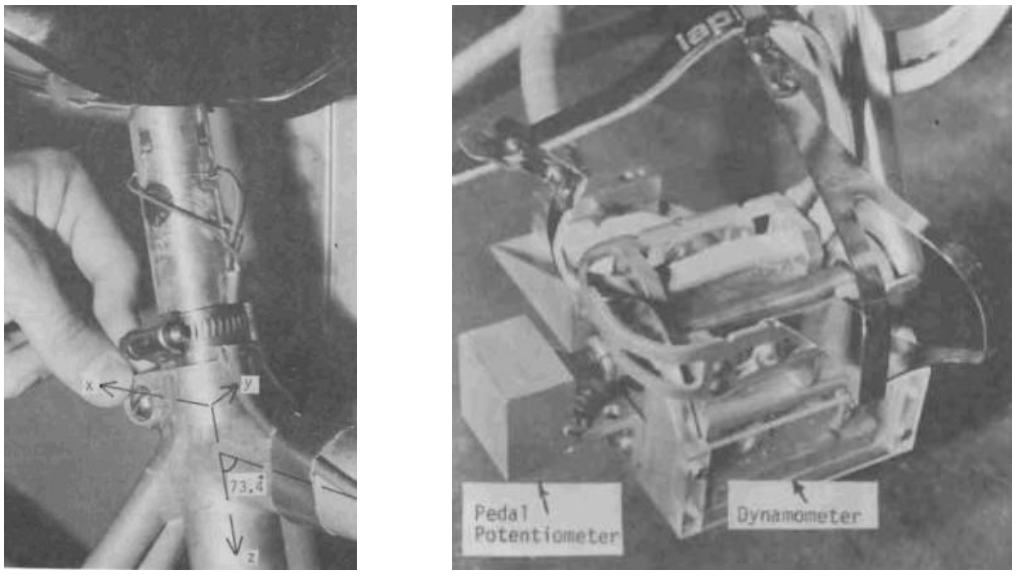

Figure 9 : dynamomètre pour la mesure des efforts appliqués sur la selle (Gauche), et sur la pédale (Droite). (Adapté de Boulourchi et Hull, 1985).

II.1.3. Détermination du Torseur des Actions Mécaniques par Dynamique Inverse

La combinaison des mesures de la cinématique, anthropométriques et des efforts externes exposés précédemment permet l'application de la « dynamique inverse en bottom-up ». Par l'application des lois fondamentales de Newton et d'Euler, ce procédé permet l'estimation du torseur des actions mécaniques aux articulations. A partir de ces torseurs, le travail, la puissance et l'énergie développés peuvent être calculés. Les forces résultantes au niveau des articulations sont associées aux forces de contact inter-articulaires, tandis que les couples développés sur ces mêmes articulations sont principalement associés à la création de force par les différents actionneurs du corps humain (muscles, tendons et ligaments) et à leurs caractéristiques visco-élastiques (Figure 10). Il est aussi à noter que la contraction d'un chef musculaire agoniste d'une articulation est systèmatiquement associée à une co-contraction plus ou moins importante des chefs antagonistes, qui créent donc un couple articulaire opposé à celui des agonistes. Les couples résultants sont donc associés aux couples créés simultanément par les agonistes et par les antagonistes (Amarantini and Martin 2004)

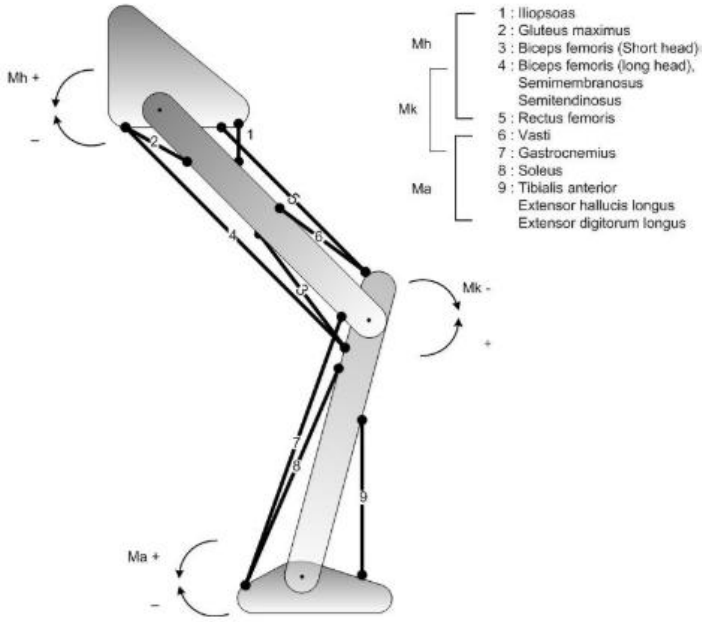

Figure 10 : représentation schématique des principaux muscles actionneurs du membre inférieur. Ma, Mk et Mh représentent les moments résultants au niveau de la cheville, du genou et de la hanche, respectivement. (Adapté de Poirier, 2009).

Cette technique qui permet de déterminer les actions mécaniques appliquées à un solide rigide est basée sur la deuxième loi de Newton (1687) :

$$\begin{Bmatrix} m_S.\vec{a}^{G}_{S/\Re_0} \\ \vec{\delta}^{A}_{S/\Re_0} \end{Bmatrix}_A = \begin{Bmatrix} \vec{F}_{\bar{s}\to S} \\ \vec{M}^{A}_{\bar{s}\to S} \end{Bmatrix}_A \qquad \text{(Equation 1)}$$

m_S représente la masse du solide S étudié, $\vec{a}^{G}_{S/R_0}$ l'accélération de son centre de gravité (G) par rapport à un référentiel galiléen$\Re_0$, $\vec{F}_{\bar{s}\to S}$ la somme des forces extérieures s'exerçant sur S, $\vec{\delta}^{A}_{S/R_0}$ le moment dynamique en un point A quelconque et $\vec{M}^{A}_{S/\Re_0}$ la somme des moments des forces. Avec $\vec{\delta}^{A}_{S/\Re_0} = \frac{d}{dt}\left(\bar{\bar{I}}^{A}.\vec{\Omega}_{S/\Re_0}\right) + m_s.\overrightarrow{AG} \wedge \vec{a}^{A}_{S/\Re_0}$ ou $\bar{\bar{I}}^{A}$ est le tenseur d'inertie en A du solide étudié et $\vec{\Omega}_{S/\Re_0}$ la vitesse de rotation du solide.

Afin de déterminer le torseur des actions mécaniques au niveau des articulations du corps humain, cette procédure implique l'utilisation d'un modèle faisant l'hypothèse que chaque segment humain est un solide indéformable (de masse constante et de centres de masse et d'inertie fixes par rapport au segment), et que ces derniers sont reliés par des articulations ne produisant pas de force de friction.

Pour exemple dans le cas du cyclisme, le moment articulaire résultant au niveau de la cheville (de la jambe sur le pied, noté $\vec{M}_{Cheville_{(j\to p)}}$ s'exprime de la façon suivante :

$$\vec{M}_{Cheville_{(j\to p)}} = \vec{M}_{Cheville_{(pesanteur\to pied)}} + \vec{M}_{Cheville_{(pédale\to pied)}} - \vec{\delta}_{Cheville_{(Pied/R_0)}} \qquad \text{(Equation 2)}$$

Où $\vec{M}_{Cheville_{(pesanteur\to pied)}}$ est le moment lié à l'action de la pesanteur sur le pied, $\vec{M}_{Cheville_{(pédale\to pied)}}$ est le moment des efforts de réaction mesurés par la pédale instrumentée, et $\vec{\delta}_{Cheville_{(Pied/R_0)}}$ est le moment dynamique du pied au niveau de la cheville dans le référentiel du laboratoire.

Le principe de la dynamique inverse « bottom-up » est d'itérer ces calculs au segment proximal suivant par déduction. Conséquemment, le moment articulaire résultant au niveau du genou $\vec{M}_{Genou_{(c\to j)}}$ peut être écrit :

$$\vec{M}_{Genou_{(c\to j)}} = \vec{M}_{Genou_{(pesanteur\to jambe)}} + \vec{M}_{Genou_{(Force\ p\to j)}} + \vec{M}_{Genou_{(p\to j)}} - \vec{\delta}_{Genou_{(Jambe/R_0)}} \qquad \text{(Equation 3)}$$

Où $\vec{M}_{Genou_{(pesanteur\to jambe)}}$ est le moment lié à l'action de la pesanteur sur la jambe, $\vec{M}_{Genou_{(Force\ p\to j)}}$ est le moment de la force de contact inter-osseuse du pied sur la jambe, $\vec{M}_{Genou_{(p\to j)}}$ est l'opposé du moment à la cheville calculé précédemment, et $\vec{\delta}_{Genou_{(Jambe/R_0)}}$ est le moment dynamique de la jambe au niveau du genou dans le référentiel du laboratoire. Il est à noter que la précision finale des données de sortie de la dynamique inverse est liée à celle des données d'entrée au niveau de la cinématique, de l'anthropométrie et de la mesure des efforts (Amarantini, 2003).

II.1.4. Calcul des Puissances aux Articulations

Dans le cadre de l'analyse biomécanique du cyclisme, les puissances développées au niveau des articulations ont aussi été source d'intérêt (G. Caldwell, van Emmerik, and Hamill 2000; Martin and Brown 2009; Elmer et al. 2011; McDaniel et al. 2014). Ces dernières peuvent être calculées sur la base du calcul des couples articulaires présentés lors des paragraphes précédents. Un des intérêts du calcul de ces puissances est sous-jacent à l'application du théorème de l'énergie mécanique pour les systèmes physiques conservatifs. Ce thèorème indique que la variation d'énergie mécanique d'un solide isolé dans un référentiel galiléen est égale à la somme des travaux des forces non conservatives internes et externes qui s'exercent sur le solide considéré.

Dans le cas du pédalage, il existe un système composé des deux jambes et des manivelles, qui peut être considéré comme isolé, proposant l'égalité suivante (Kautz, Hull, and Neptune 1994):

$$P_j = \frac{\mathrm{d}E_j}{\mathrm{d}t} = \sum_{j=1}^{3} P_j + \overrightarrow{F_p} \cdot \overrightarrow{V_p} + \overrightarrow{F_h} \cdot \overrightarrow{V_h} \qquad \text{(Equation 4)}$$

Où P_j est la puissance totale du système étudié, $\frac{\mathrm{d}E_j}{\mathrm{d}t}$ est la variation d'énergie mécanique de ce système, $\sum_{j=1}^{3} P_j$ est la somme des puissances articulaires résultantes au niveau de la cheville, du genou et de la hanche, $F_p \cdot V_p$ est le produit scalaire entre la force de réaction mesurée à la pédale et la vitesse de translation de la pédale (terme représentant la puissance mécanique appliquée sur les pédales), et $F_h \cdot V_h$ est le produit scalaire entre la force de réaction de la hanche et la vitesse de translation de la hanche. Cette égalité a été vérifiée expérimentalement à plusieurs reprises et permet une analyse approfondie des sources de productions de puissance dans le mouvement de pédalage en proposant une équivalence entre les puissances aux articulations et la puissance au pédalier (Martin and Brown 2009 / Figure 11).

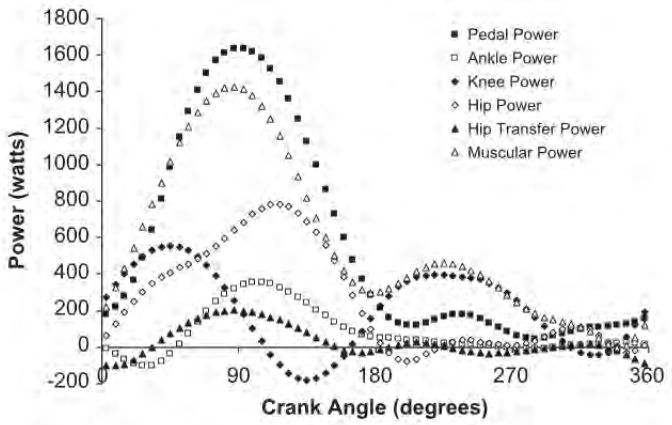

Figure 11 : puissance moyenne sur une pédale, par articulation, et pour la somme des articulations d'un membre inférieur au cours d'un cycle de pédalage lors de la 3ème seconde d'un test de Wingate (30 secondes à puissance maximale sur ergocycle). Il est à noter 1) que la variation d'énergie mécanique du système est nulle au cours d'un cycle et non représentée ici 2) que la puissance à la pédale est généralement supérieure à la somme des puissances articulaires durant la phase d'extension, et inférieure pendant la phase de flexion en raison de l'action du poids, qui agit toujours vers le bas et crée donc une puissance additionnelle pendant l'extension, mais coûte de la puissance pendant la phase de flexion. (Adapté de Martin et al, 2009).

Un des sujets d'intérêt de ces travaux de thèse est le test d'une hypothèse ancienne qui expliquerait la puissance liée à la force de réaction à la hanche par l'action mécanique des membres supérieurs (Kautz, Hull, and Neptune 1994). Cette question est discutée dans l'article 1 (section III.3) du chapitre « Contributions Personnelles » de cette thèse. Dans cet article, la participation en puissance du membre supérieur a été étudiée en position assise et danseuse à différents niveaux de puissance au pédalier. La puissance développée par le membre supérieur variant entre 1 et 2,5% de celle développée au pédalier, il semblerait que ces derniers ne soient que partiellement la cause de la puissance liée aux efforts de réaction à la hanche.

II.1.5. Analyse Electromyographique

L'électromyographie (souvent abrégée « EMG ») est définie comme « l'étude fonctionnelle du muscle à travers le recueil et l'analyse du signal électrique généré par les muscles en contraction » (De Luca 1997). D'un point de vue physiologique, ce signal électrique est le résultat de la stimulation de la cellule musculaire par les motoneurones *alpha* qui créent un potentiel d'action musculaire au niveau de la plaque motrice, qui en se propageant le long du sarcolemme provoque le déclenchement de la contraction. Cette activité électrique peut être mesurée de façon invasive à l'aide d'électrode-aiguilles placées en sous-cutané, ou de manière non invasive à l'aide d'électrodes collées à la surface de la peau, on parle alors « d'EMG de surface ». La méthode invasive étant difficilement applicable à l'analyse du mouvement, l'électromyographie de surface, pourtant moins précise, lui est majoritairement préférée. Dans le cadre de cette méthode, et après un traitement de la surface de la peau incluant rasage et nettoyage (www.seniam.org), le doublet d'électrodes enregistre la différence de potentiel entre deux points du muscle. La tension électrique mesurée représente la somme algébrique des potentiels d'action musculaires (Day and Hulliger 2001) et donne une représentation du nombre d'unités motrices activées et de leur fréquence de décharge (Figure 12). Cette réprésentation nécessite plusieurs précautions quant à son interprétation. En effet, certains facteurs physiologiques et non physiologiques peuvent influencer la forme du signal EMG recueilli (Farina, Merletti, and Enoka 2004).

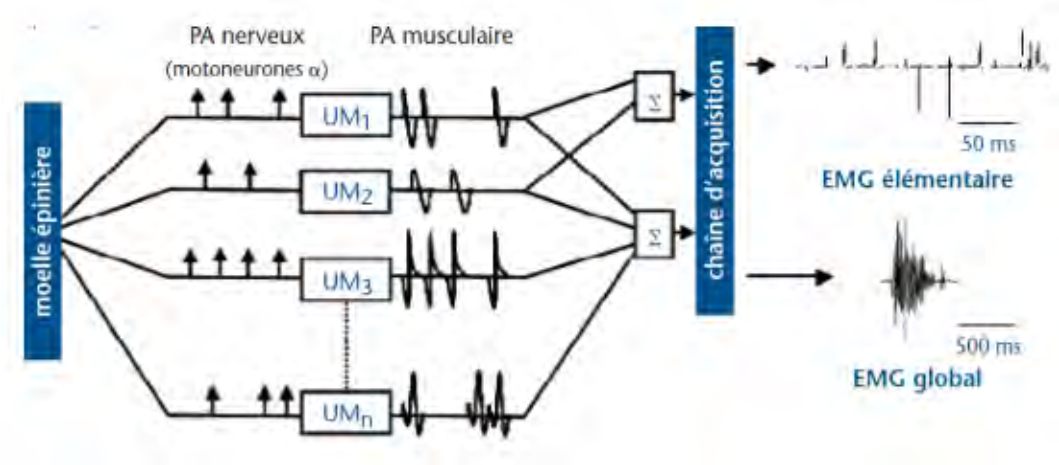

Figure 12 : correspondance physiologique du signal électromyographique. Les motonoeurones alpha issus de la moëlle épinière créent des potentiels d'action « nerveux », qui en retour créent des potentiels d'action « musculaires » au niveau de l'unité motrice. La sommation du signal enregistré sur quelques unités motrices (méthode par électrode-aiguille) donne un signal EMG « élémentaire », alors que la sommation du signal créé par un plus grand nombre d'unités motrices (méthode « EMG de surface ») donne un signal EMG « global ». (Adapté de Turpin, 2012).

Parmi ces limitations, le phénomène « d'amplitude cancellation » consiste en l'annulation des phases positives et négatives de potentiels d'action musculaires lorsqu'ils se superposent en raison d'un délai temporel d'enregistrement légèrement différent. Ceci peut causer une sous-estimation de l'amplitude du signal de 62% (Keenan et al. 2005). Ce phénomène semble majoré par la fatigue en raison de la diminution de la vitesse de conduction des fibres musculaires, induisant une augmentation de la durée des potentiels d'action, et donc à un chevauchement plus important. Certaines méthodes de normalisation permettent de remédier partiellement à ce problème, qui ne constitue cependant pas une limite pour l'interprétation des patterns d'activité musculaire en termes de temps d'activation et d'allure.

Une autre difficulté méthodologique est l'hétérogénéité du recrutement musculaire. En effet un muscle est constitué d'unités motrices ayant différentes propriétés physiologiques et mécaniques. Ces propriétés ne sont pas réparties de façon homogène dans le muscle : les unités motrices « lentes » sont plutôt situées en profondeur, tandis que les unités « rapides » sont plutôt périphériques (Dahmane et al. 2005; Knight and Kamen 2005). Notamment, et en raison du principe d'Henneman (1965), les unités motrices recrutées en début de contraction ou lors de contraction à faible intensité seraient essentiellement situées en profondeur du muscle, et donc à distance des électrodes. Cette propriété conduit à deux problèmes dans l'interprétation du signal : 1) le déplacement des électrodes par rapport au muscle peut conduire à ne pas mesurer l'activité des mêmes fibres musculaires au cours du mouvement, 2) la variation inter-individuelle dans le placement des électrodes peut induire une variabilité du volume musculaire étudié.

Le phénomène de « cross-talk » ou « diaphonie » désigne l'enregistrement non désirable de l'activité des muscles adjacents à celui visé (De Luca 1997; Farina, Merletti, and Enoka 2004). Son importance dépend principalement du volume musculaire étudié, de l'épaisseur de la couche sous-cutanée, et du système de détection utilisé. Ce phénomène étant difficilement quantifiable de façon non-invasive, des précautions doivent être prises pour sa réduction comme la minimisation de l'impédance de la peau (Hermens et al. 2000), et un choix judicieux du positionnement des électrodes sur le ventre du muscle et à distance de ses insertions (Mesin, Merletti, and Rainoldi 2009). En respectant ces principes, il a été montré que l'influence du cross-talk pouvait être limitée lors du pédalage (Chapman et al. 2010).

Enfin, il est à noter que le signal EMG peut aussi être influencé par le mouvement des électrodes et des câbles, par les sources électromagnétiques environnementales (e.g. signal électrique à 50 Hz), et l'activité électrique cardiaque. Pour y remédier, un traitement du signal est nécessaire (Figure 13).

Afin d'étudier la coordination, plusieurs études ont montré que l'activité musculaire peut être modélisée comme résultant d'une répartition en modules de l'activité de muscles fonctionnellement liés, aussi dénommées « synergies musculaires ». Ces dernières sont définies comme « un ensemble de muscles contrôlés comme une unité fonctionnelle » (Bizzi et al. 2008). Cette organisation permettrait la simplification de la commande centrale : un nombre réduit de synergies permettant de contrôler plusieurs ensembles musculaires (Figure 14). En collaboration avec Nicolas Turpin, les synergies musculaires mesurées au cours du pédalage en position assise et danseuse ont fait l'objet d'articles présentés en partie « Contributions Personnelles » (section III).

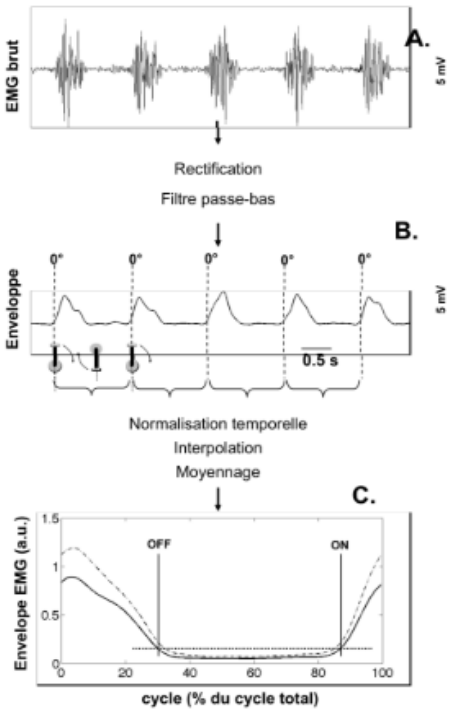

Figure 13 : A. le signal brut est rectifié et filtré pour en obtenir « l'enveloppe ». B. Le début et la fin de chaque cycle sont identifiés à partir d'un signal mécanique ou d'un « trigger ». C. Les cycles sont normalisés et interpolés pour obtenir un pattern représentatif, avec seuil permettant de déterminer si le muscle est considéré actif ou inactif. Exemple issu de données enregistrées sur un vastus lateralis lors du pédalage. (Adapté de Hug, 2011).

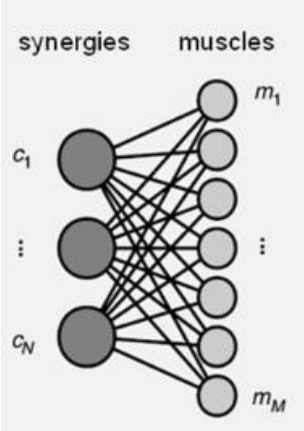

Figure 14 : modèle de génération d'activités musculaires par la combinaison de synergies musculaires. Des synergies indépendantes contrôlent chacune plusieurs muscles. (Adapté de Turpin, 2012).

II.1.6. Fonctions de Coût

En mécanique, l'intérêt de fonctions de coût est de synthétiser sous la forme d'une seule variable algébrique un indice représentatif du coût global d'une action et illustre donc le contrôle moteur humain. Pour l'étude du cyclisme, le premier indice proposé a été le « Moment Cost Function » (MCF), un indice basé sur le moment résultant des deux articulations principales du membre inférieur que sont le genou et la hanche (Redfield and Hull 1986; Hull and Gonzalez 1988; Gonzalez and Hull 1989) :

$$MCF_{Hull} = \sum(M_k^2 + M_h^2) \qquad \text{(Equation 5)}$$

Où M_k et M_h sont respectivement le moment articulaire résultant au niveau du genou et de la hanche, calculés par méthode de dynamique inverse et réalisée à l'origine en deux dimensions. Cette expression est généralement appliquée sur un cycle de pédalage complet. Cet indice représente un moyen non-invasif permettant l'estimation des efforts musculaires du membre inférieur de façon globale. Ses créateurs l'ont d'abord utilisé afin de modéliser des réglages optimaux par minimisation de ce critère en fonction de l'anthropométrie de cyclistes (Gonzalez and Hull 1989 / Figure 15).

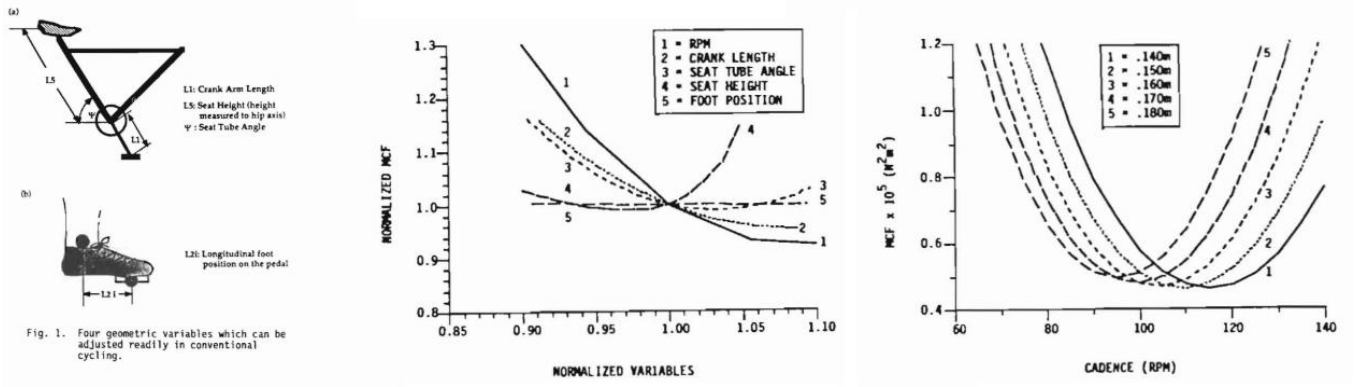

Figure 15 : (Gauche) Quatre variables géométriques utilisées par Gonzalez et Hull (1989). (Centre) Impact sur le « Moment Cost Function » de la variation de ces mesures, exprimées en valeur normalisée. (Droite) Variation du « Moment Cost Function » en fonction de la cadence de pédalage et de la longueur des manivelles. Données obtenues par modélisation. (Adapté de Gonzalez et Hull, 1989).

Suite à ces données obtenues par modélisation, une étude a vérifié expérimentalement l'effet de la variation de la cadence de pédalage sur une « Moment Cost Function » légèrement modifiée et incluant le couple articulaire résultant à la cheville dans son calcul (Marsh, Martin, and Sanderson 2000):

$$MCF_{Marsh} = |\bar{M}_A| + |\bar{M}_K| + |\bar{M}_H| \qquad \text{(Equation 6)}$$

Où $|\bar{M}_A|$, $|\bar{M}_K|$, et $|\bar{M}_H|$ sont respectivement les moments articulaires résultants exprimés dans un modèle saggital en deux dimensions au niveau de la cheville, du genou, et de la hanche, mis en valeur absolue et moyennés au cours d'un cycle de pédalage. Cette étude a démontré que la cadence de pédalage spontanément choisie n'est pas différente statistiquement de celle qui minimise le « moment cost function », ce qui n'est pas le cas pour d'autres indices physiologiques comme la consommation d'oxygène (Coast and Welch 1985; Marsh and Martin 1993), et que cette cadence augmente avec l'augmentation de la puissance de pédalage (Figure 16).

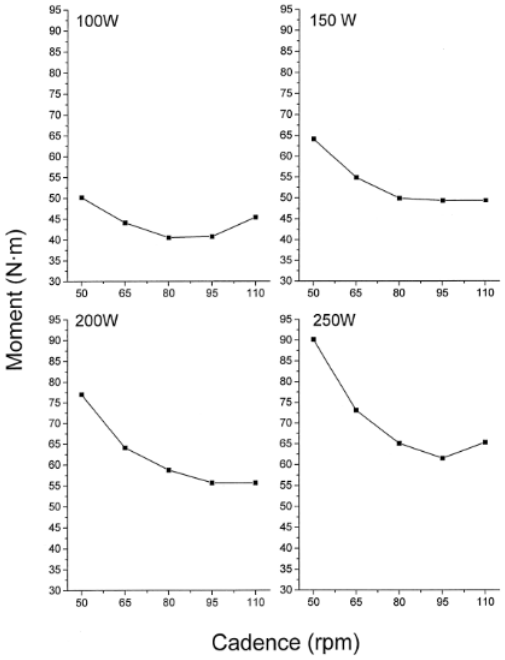

Figure 16 : influence de la cadence et de la puissance sur la « Moment Cost Function ». L'augmentation de la puissance de pédalage augmente la cadence de pédalage définie comme optimale par ce critère. (Adapté de Marsh et al., 2000).

Un dernier exemple de fonction de coût utilisée pour l'analyse du pédalage a été proposé par MacIntosh et al. (2000). Cette dernière est basée sur l'activité électromyographique de plusieurs muscles du membre inférieur :

$$ECF = EMG_{TA} + EMG_{SOL} + EMG_{GM} + EMG_{VM} + EMG_{RF} + EMG_{ST} + EMG_{BF} + EMG_{Gmax}$$

(Equation 7)

Où *ECF* est l'activité électromyographique représentative de l'activité globale du membre inférieur, et EMG_{TA}, EMG_{SOL}, EMG_{GM}, EMG_{VM}, EMG_{RF}, EMG_{ST}, EMG_{BF}, et EMG_{GMAX} sont respectivement les activités électromyographiques moyennées sur un cycle des muscles *tibialis anterior*, *soleus*, *gastrocnemius medialis*, *vastus medialis*, *rectus femoris*, *semi tendinosus*, *biceps femoris*, et *gluteus maximus*.

A l'aide de ce critère, ces auteurs ont eux aussi vérifié l'hypothèse de l'augmentation de la cadence de pédalage optimale en association avec l'augmentation de la puissance au pédalier (Figure 17).

L'utilisation de fonctions de coût a aussi été utilisée pour comparer le pédalage assis et celui en danseuse dans le cadre de ces travaux de thèse (section III.8).

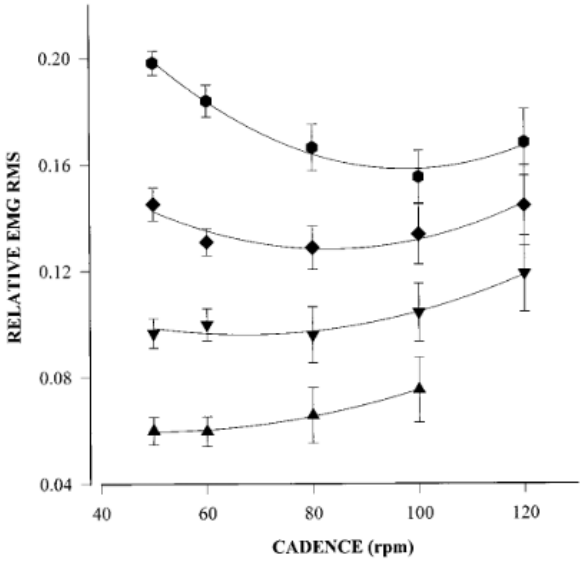

Figure 17 : activité électromyographique globale du membre inférieur en fonction de la cadence, et de la puissance de 100 à 400 W (de bas en haut, respectivement). (Adapté de MacIntosh et al., 2000).

II.2. Position assise versus Position danseuse

II.2.1. Introduction

Bien que moins richement étudiées que les différences entre la marche et la course, les différences entre les positions assis et danseuse en cyclisme ont fait l'objet de travaux. La revue de littérature qui va suivre est ainsi centrée vers l'effet de la position sur les principaux paramètres mécaniques et physiologiques mesurables lors du pédalage.

II.2.2. Effets de la position sur les variables mécaniques

Par analogie au fait que la course soit préférée à la marche pour les vitesses élevées de déplacement, la position en danseuse est souvent préférée à celle assise lorsqu'il est nécessaire de développer des puissances mécaniques élevées. Hansen et Waldeland (2008) ont testé sur tapis roulant motorisé le temps de soutien maximal dans les deux positions à différents pourcentages de la puissance correspondant à la consommation maximale d'oxygène déterminée lors d'un test incrémental (Figure 18).

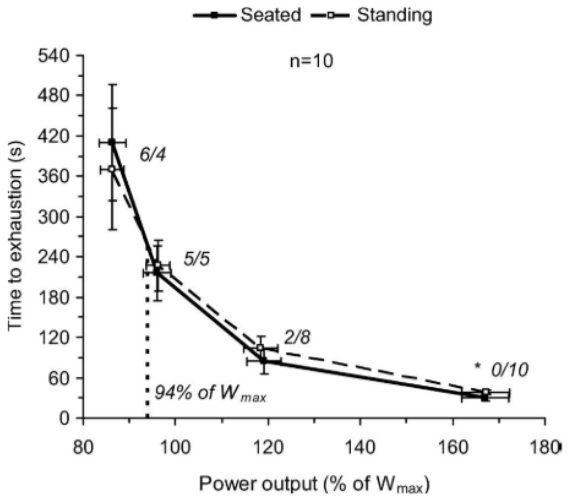

Figure 18 : temps de soutien à différents pourcentages de la puissance correspondant à la consommation maximale d'oxygène en position assise et danseuse. Trait plein : Assis. Trait pointillé : Danseuse. (Adapté de Hansen et Waldeland, 2008).

Cette étude montre que le temps de soutien est maximisé pour la plupart des participants à basse puissance en position assise, et à haute puissance en position danseuse. La puissance de transition théorique représentait en moyenne 94% de la puissance correspondant à la consommation maximale d'oxygène déterminée lors d'un test incrémental en position assise. D'autres études ont montré la supériorité de la position en danseuse pour la production de puissance mécanique. Reiser et al. (2002) ont montré que la puissance développée était supérieure au cours de plusieurs tests de Wingate (épreuve de pédalage maximale de 30 secondes) réalisés sur ergocycle, avec en moyenne 11 ± 0,4 $W.kg^{-1}$ en position danseuse contre 10,4 ± 0,6 $W.kg^{-1}$ en position assise. Millet et al. (2002) ont publié des résultats similaires sur 30 secondes (803 ± 103 W en danseuse vs 635 ± 123 W assis). McLester et al. (2004) ont quant à eux montré que la puissance développée au cours de 3 tests de Wingate répétés était améliorée lors de la 3ème répétition en raison d'une plus faible perte de puissance au cours des 30 secondes.

Plusieurs études ont montré que cette augmentation de puissance en danseuse s'accompagne généralement d'une diminution de la cadence de pédalage spontanément utilisée (Millet et al. 2002; Harnish, King, et Swensen 2007; Lucía, Hoyos, et Chicharro 2001).

Du point de vue des couples articulaires, le couple de flexion plantaire ainsi que celui d'extension du genou augmenteraient en danseuse (Li et Caldwell 1998; Caldwell et al. 1999 / Figure 19).

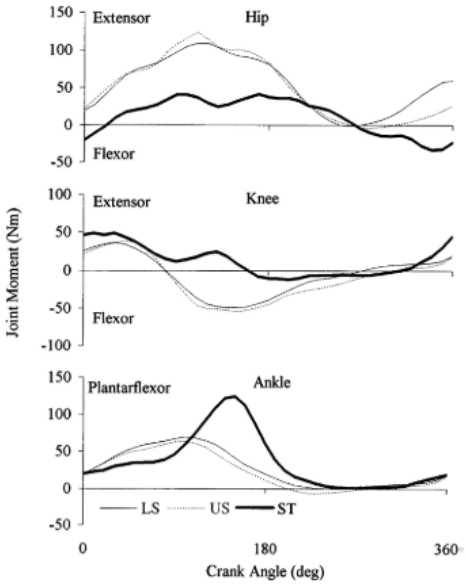

Figure 19 : patterns de moments articulaires en fonction de l'angle de la manivelle. LS : position assise sur terrain plat. US : position assise sur terrain en pente de 8%. ST : position danseuse sur pente de 8%. (Adapté de Li et Caldwell, 1998).

Une seule étude a testé l'effet de la position sur une fonction de coût (Gonzalez and Hull 1989) basée sur les moments articulaires (Poirier, Do, and Watier 2007 / Figure 20).

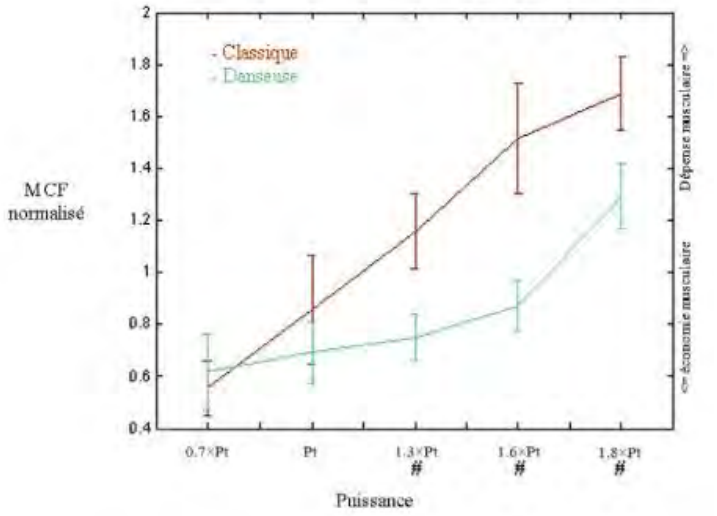

Figure 20 : Moment Cost Function en fonction de la puissance de pédalage (normalisée par la puissance spontanée de transition) en position assis (« Classique) et danseuse. (Adapté de Poirier et al., 2007).

Cette étude montre que la position choisie spontanément minimiserait la fonction de coût utilisée. Ces résultats ont été confirmés dans un contexte expérimental différent dans la section III.8 de cette de thèse. L'étude de Poirier et al. (2007) montre aussi un décalage des valeurs d'angle et de valeur du maximum de couple appliqué à l'axe médiolatéral du pédalier (Figure 21). Ce résultat est retrouvé dans d'autres études (Caldwell et al. 1998; Li and Caldwell 1998).

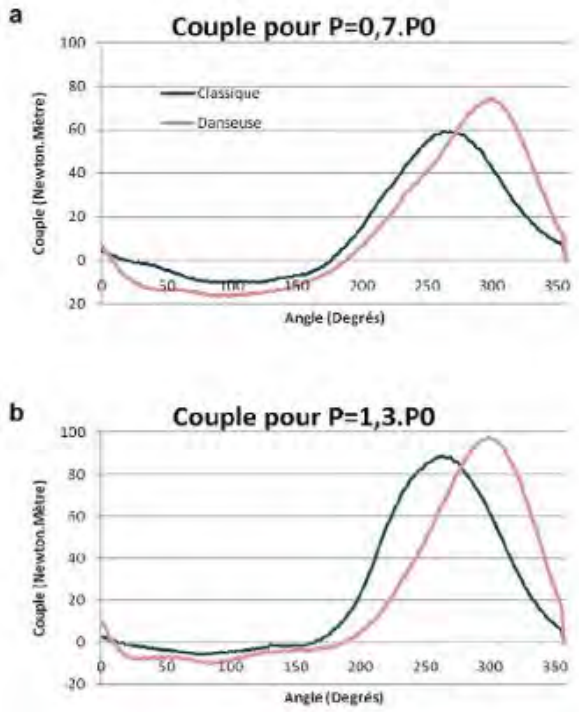

Figure 21 : patterns de couple appliqué au pédalier. Bleu : danseuse. Rouge : assis. (Haut) : à 70% de la puissance spontanée de transition. (Bas) : à 130% de la puissance spontanée de transition. Sont à noter les différences lors des parties négatives sur la gauche de figures (couple anti-propulsif), ainsi que le décalage temporel et de magnitude des valeurs maximales.(Adapté de Poirier, 2007).

Enfin, les efforts sur le cintre n'ont été que très peu étudiés et comparés entre les deux positions. Une des premières études sur le thème est à attribuer à Stone et Hull (1993), qui ont montré l'évolution des patterns de forces et moments appliqués sur les poignées du cintre (ou « cocottes ») pour trois sujets différents. Par la suite, Poirier (2009) a montré une diminution progressive des forces appliquées sur le cintre (mesurées à la potence), suivie d'une forte augmentation lors du passage en danseuse (Figure 22).

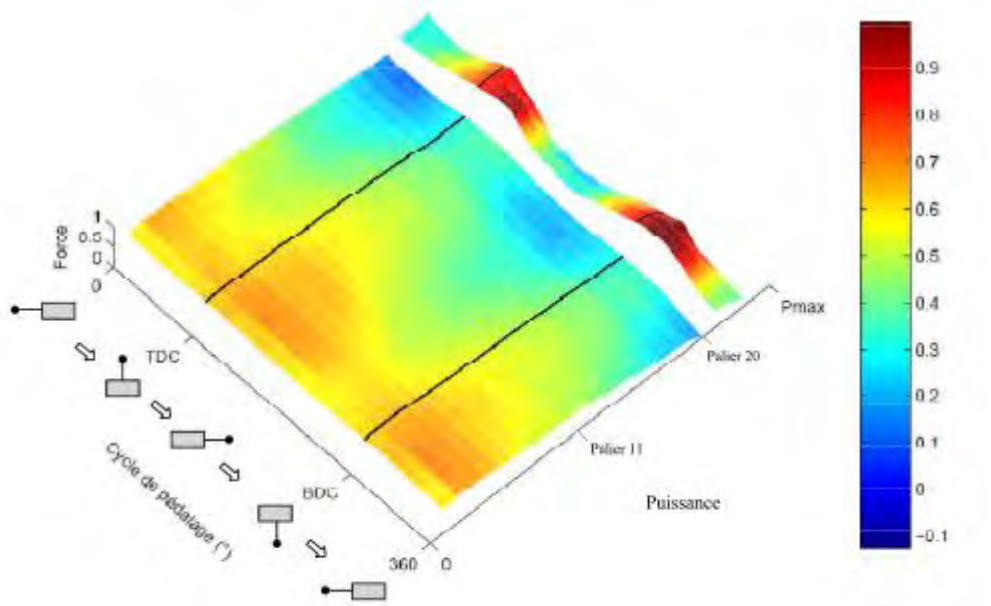

Figure 22 : résultante des forces exercées verticalement sur le cintre (au niveau de la potence). Un effort de poussée du haut vers le bas est représenté par une valeur positive, tandis qu'un effort de traction (du bas vers le haut) est représenté par une valeur négative. Est à noter la diminution des efforts avec l'augmentation de la puissance en position assise (palier 0 à 20), puis l'augmentation au palier 20 correspondant à la transition en danseuse. (Adapté de Poirier, 2009).

II.2.3. Effet de la position sur les variables physiologiques

D'un point de vue physiologique, de nombreuses études se sont intéressées à la distinction entre position assise et danseuse du point de vue de la consommation d'oxygène, de la fréquence cardiaque, de la perception de l'effort, du rendement et de l'activité électromyographique.

Au niveau de la consommation d'oxygène, la position assise a été montrée comme moins coûteuse à faible puissance de pédalage (Ryschon et Stray-Gundersen 1993; Tanaka et al. 1996), mais aucune différence n'a pu être observée entre les deux positions à haute puissance (Harnish, King, et Swensen 2007; Millet et al. 2002; Tanaka et al. 1996). Le rendement ne semble pas non plus différent entre les deux positions pour du pédalage sur le terrain à une puissance correspondant à 75% de celle correspondant à la consommation maximale d'oxygène déterminée lors d'un test incrémental en position assise (Millet et al., 2002). La fréquence cardiaque a été décrite comme plus élevée en danseuse (Millet et al., 2002 ; Tanaka, 1996). Poirier montre des résultats légèrements différents avec une fréquence cardiaque plus faible assis lors du pédalage à faible puissance, et une absence de différence à haute puissance (Figure 23).

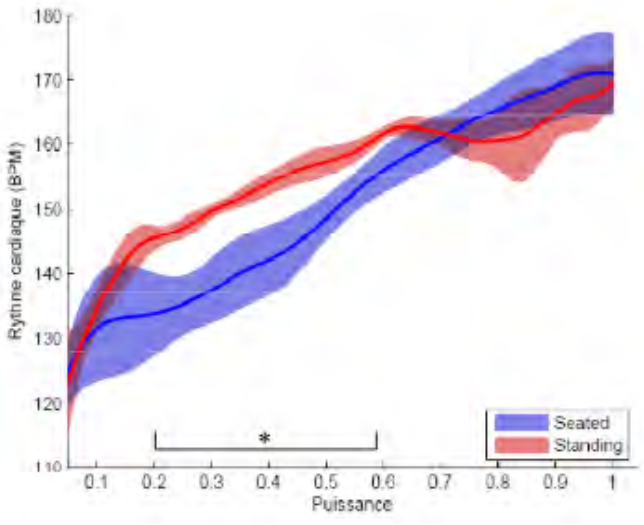

Figure 23 : fréquence cardiaque exprimée en battement par minute, en fonction de la puissance de pédalage exprimée en pourcentage de la puissance spontanée de transition assis-danseuse. (Adapté de Poirier, 2009).

Au niveau de la perception de l'effort, seulement deux études ont comparé les deux positions. Millet et al. (2002) n'ont pas montré de différence significative entre les deux positions pour deux niveaux de puissance, tandis que Poirier (2009) a confirmé ce résultat pour une plus large étendue de puissance.

Enfin, au niveau de l'activité électromyographique, la littérature suggère des différences dans les profils temporels et les niveaux d'activation de plusieurs muscles (Li and Caldwell 1998, Figure 24). Par exemple, Duc et al. (2008) ont montré une diminution du niveau de l'activité du *semimembranosus* en danseuse, ainsi qu'une importante augmentation du niveau d'activité des muscles du bras (*Triceps Brachii* et *Biceps Brachii*) et du tronc (*Rectus Abdominis* et *Ilio-Costalis*) dans cette position. Au contraire, Li et Caldwell (1998) ont montré des niveaux d'activation augmentés des muscles *gluteus maximus*, *tibialis anterior*, et *rectus femoris* en danseuse (Figure 24). Poirier (2009) montre quant à lui une diminution du temps d'activation du *biceps femoris* en danseuse. Du point de vue des synergies musculaires, aucun avantage d'une position sur l'autre n'a pû être démontré à ce jour (Hug et al. 2011) : les synergies musculaires des membres inférieurs semblent identiques dans les deux positions et seul un décalage temporel au cours du cycle permet de les distinguer.

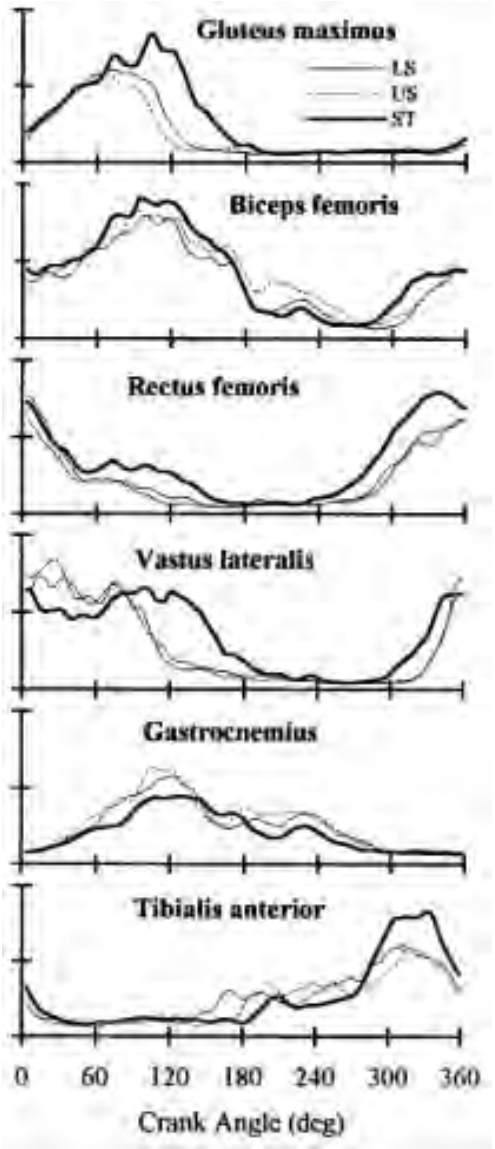

Figure 24 : enveloppes électromyographiques mesurées par Li et Caldwell (1998) sur 6 muscles. LS : position assise sur terrain plat. US : position assise sur terrain sur pente de 8%. ST : position danseuse sur pente de 8%. (Adapté de Li et Caldwell, 1998).

III) Contributions Personnelles

Illustration : peinture acrylique, auteur inconnu.

III.1. INTRODUCTION

Les contributions apportées par ces travaux de thèse sont centrées autour d'une étude portant à la fois sur les variables mécaniques des positions « assis » et « danseuse » mais aussi aux critères qui sous-tendent la transition d'une position vers l'autre. Celle-ci a été réalisée en conditions de laboratoire d'analyse biomécanique sur un ergocycle stationnaire Lode Excalibur (Groningen, Pays-Bas) à friction électromagnétique. La particularité de cet ergocycle réside dans son intrumentation permettant la mesure des efforts appliqués au niveau de chacun des appuis du cycliste (selle, partie gauche et droite du cintre, et pédale gauche et droite). L'analyse réalisée lors de ces études combine les nouvelles possibilités de mesure apportées par cet ergocycle entièrement instrumenté, en complément avec une mesure de la cinématique du corps complet et de l'activité electromyographique de 16 muscles. Ce dispositif est présenté dans la section III.2 « Plateau Expérimental ».

Dans une première partie des contributions scientifiques de ces travaux de thèse, pour la première fois l'effet de la position (assis vs danseuse) et de la puissance de pédalage sur la contribution mécanique des membres supérieurs en cyclisme a été analysé. Cette étude a été complétée par une analyse électromyographique de membres supérieurs lors du pédalage. Afin d'expliquer ces premiers résultats, une seconde partie centrée sur la mesure des efforts externes appliqués sur l'ergocycle a été réalisée, puis approfondie par méthode de dynamique inverse dans le cadre d'une troisième partie pour mettre en évidence un critère mécanique simple et explicatif de la transition en danseuse. Dans une quatrième partie, une analyse des synergies musculaires lors de la transition assis-danseuse a été effectuée. Enfin, dans une cinquième partie, l'effet de la puissance de pédalage sur des fonctions de coût représentatives des efforts musculaires du membre inférieur a été testé, et met en évidence d'autres explications à la transition spontanée d'un cycliste vers la position danseuse.

III.2. PLATEAU EXPERIMENTAL

Afin de procéder à l'analyse biomécanique la plus complète possible, les participants ont réalisé un protocole expérimental sur ergocycle Excalibur (Lode, Groningen, Pays-Bas / Figure 25). Ces derniers étaient équipés de marqueurs passifs dont les positions étaient enregistrées en instantané à une fréquence de 200 Hz par des caméras Vicon (Oxford Metrics, Oxford, Royaume-Uni).

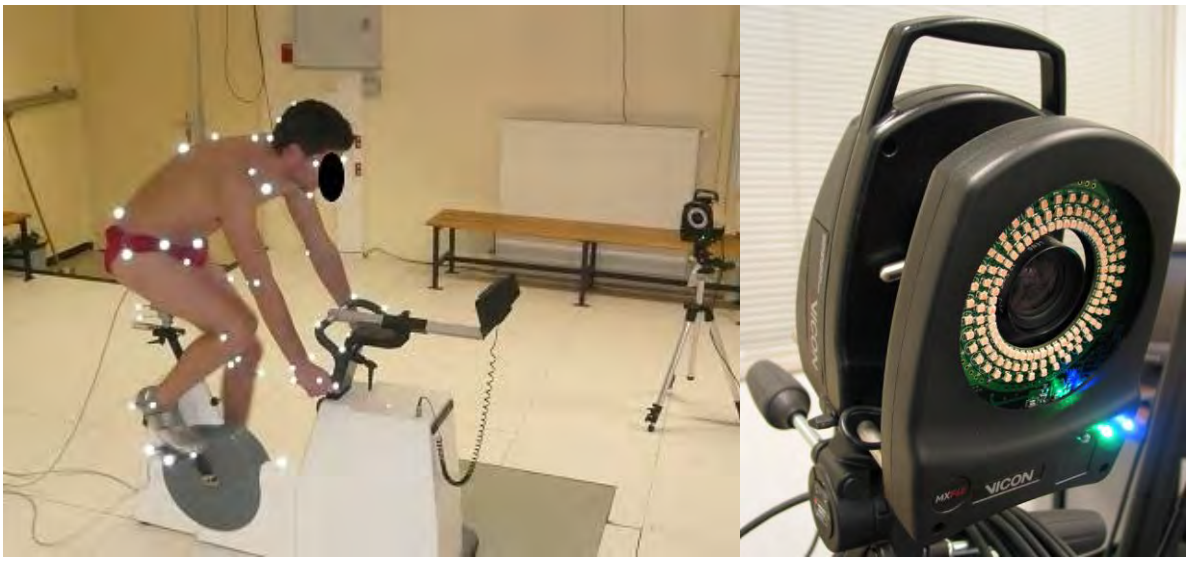

Figure 25 : (Gauche) Ergocycle Lode Excalibur en cours d'utilisation. (Droite) Caméra Vicon.

L'ergocycle utilisé est instrumenté de cinq capteurs 6 composantes Sensix (Poitiers, France). Ces derniers permettent la mesure en 3D des forces et moments appliqués, avec une précision annoncée par le fabricant à 1% sur chaque composante, et à 1,5% sur la combinaison des 6 composantes (Figure 26).

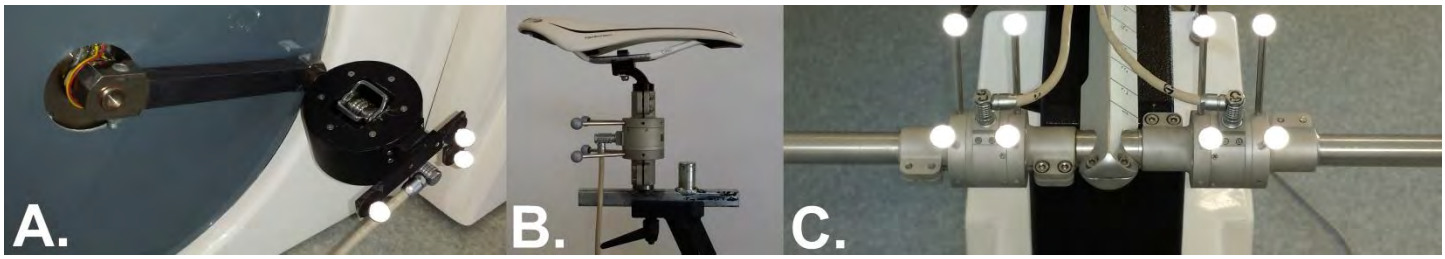

Figure 26 : capteurs Sensix 6 composantes utilisés dans le cadre de ces travaux de thèse. A. I-Crankset 1 pour la mesure aux pédales. B. Capteur au tube de selle. C. Capteur permettant la mesure des efforts sur les parties gauche et droite du cintre.

Afin d'enregistrer l'activité électromyographique des participants au cours du pédalage, deux dispositifs à 8 voies Bagnoli (Delsys, Boston, Etats-Unis) ont été utilisés (Figure 27).

Figure 27 : dispositif pour l'enregistrement d'électromyographie de surface Delsys Bagnoli.

Une fois les participants équipés avec les électrodes électromyographiques et les marqueurs passifs destinés à l'analyse cinématique, ces derniers effectuaient deux enregistrements. Le premier afin de permettre l'implémentation de la méthode SCoRE pour déterminer la position des centres articulaires des hanches et des épaules (Begon, 2007), et le second afin d'effectuer une pesée sur l'ergocycle en position statique mains sur le cintre et manivelles à l'horizontale.

A la suite de ces étapes, les participants réalisaient un protocole permettant la détermination de leur puissance de transition spontanée en danseuse. Enfin, et suite à un temps de repos de 5 minutes, ces derniers réalisaient 6 séquences de pédalages à 20, 40, 60, 80, 100 et 120% de leur puissance spontanée de transition, assis et en danseuse, dans un ordre aléatoire. Ce protocole expérimental est illustré sur la Figure 28).

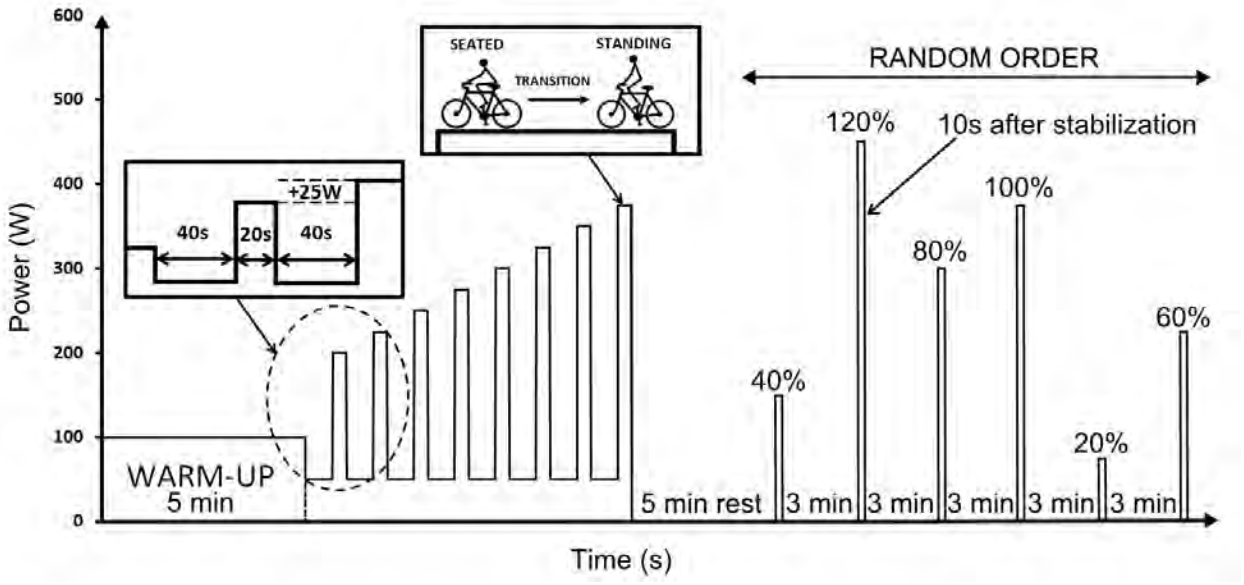

Figure 28 : protocole expérimental permettant la détermination de la puissance de transition spontanée assis-danseuse.

III.3. Etude 1 : Effet de la position et de la puissance sur la dynamique des membres superieurs

Ce premier article accepté dans la revue « Journal of Applied Biomechanics » est intitulé « Influence of Position and Power Output on Upper Limb Kinetics in Cycling ». Faisant le constat du faible nombre d'études consacrées à l'analyse du rôle du membre supérieur en cyclisme, et des quelques données indiquant un potentiel effet de la puissance et de la position (assis vs danseuse), notre objectif a été de présenter pour la première fois une analyse du rôle mécanique du membre supérieur en cyclisme. Basée sur une analyse de dynamique inverse des actions mécaniques effectuées au niveau du poignet, du coude et de l'épaule avec comme données d'entrée la cinématique du membre supérieur et les efforts résultant au niveau du cintre, l'étude a porté sur un échantillon préliminaire de 17 participants. Les résultats montrent que la puissance de pédalage et la position ont un effet sur 43 des 58 variables mécaniques étudiées. En position assise et à faible puissance, le membre supérieur semble n'avoir qu'un rôle équilibrateur et de support du tronc. A partir du niveau de puissance correspondant à la transition spontanée en danseuse, les actions mécaniques des articulations du membre supérieur associées à la traction sur le cintre apparaissent. Suite à cette analyse, une question s'est posée : pourquoi les participants tirent-ils sur le cintre à haute puissance ? Une hypothèse explicative serait que l'activation des membres supérieurs permettrait une activation plus importante des muscles du membre inférieur (Ebben, Leigh, et Geiser 2008; Turpin et al. 2014). Toutefois, cette action de traction pourrait-elle n'avoir qu'une explication mécanique ?

ORIGINAL RESEARCH

http://dx.doi.org/10.1123/jab.2014-0295

[AUQ1]Antony Costes and David Villeger are with PRISSMH-LAPMA, University Toulouse III Paul Sabatier, Toulouse, France. Nicolas A. Turpin is with PRISSMH-LAPMA, University Toulouse III Paul Sabatier, Toulouse, France; and CRIR, Institut de Réadaptation Gingras-Lindsay de Montréal and Jewish Rehabilitation Hospital, Laval, Quebec, Canada. Pierre Moretto is with the University of Toulouse, UPS, CRCA, Toulouse, France; and CRCA, CNRS, Toulouse, France. Bruno Watier is with LAAS, CNRS, Toulouse, France; and the University of Toulouse, UPS, LAAS, F-31400 Toulouse, France. Address author correspondence to Anthony Costes at antony.costes@univ-tlse3.fr.

Influence of Position and Power Output on Upper Limb Kinetics in Cycling

Antony Costes,[1] Nicolas A. Turpin,[1,2] David Villeger,[1] Pierre Moretto,[3,4] and Bruno Watier[3,5]

[1]University Toulouse III Paul Sabatier; [2]Institut de Réadaptation Gingras-Lindsay de Montréal and Jewish Rehabilitation Hospital; [3]University of Toulouse; [4]CRCA, CNRS; [5]LAAS, CNRS

Several suggestions on the upper limb involvement in cycling exist but, to date, no study has quantified upper limb kinetics in this task. The aim of this study was to determine how crank power and pedaling position (seated or standing) affect upper limb kinetics. Handlebar loadings and upper limb kinematics were collected from 17 participants performing seated or standing pedaling trials in a random order at 6 crank powers ranging from 20% (112 ± 19 W) to 120% (675 ± 113 W) of their spontaneous sit-to-stand transition power. An inverse dynamics approach was used to compute 3D moments, powers, and works at the wrist, elbow, and shoulder joints. Over 29 parameters investigated, increases in crank power were associated with increases in the magnitudes of 23 and 20 of the kinetic variables assessed in seated and standing positions, respectively. The standing position was associated with higher magnitudes of upper limb kinetics. These results suggest that both upper and lower limbs should be considered in future models to better understand whole body coordination in cycling.

Keywords: inverse dynamics, joint torques, powers, works, standing

Previous work dedicated to pedaling performance and injury prevention in cycling mainly focused on lower limb biomechanics.[1] However, because the upper limbs may provide significant contributions in trunk support, stabilization, or power transfer to the cranks,[2] knowledge in regard to upper limb kinetics in cycling could be useful for both performance improvement and clinical applications.

To date, only indirect insights into upper limb actions have been available. Previous studies assessed rider-induced forces and moments on the handlebar and showed that both pattern and magnitude of the crank power, and position (ie, seated or standing), influenced handlebar loadings. At crank power corresponding to 200 W, the handlebar forces were always oriented in both the forward and downward directions in a seated position, suggesting that the role of the arms is mainly to support the torso weight.[3] Conversely, at crank power higher than 200 W, alternation between pulling and pushing forces on the handlebar have been observed both in seated and standing positions, suggesting that the arms play a different role as crank power increases.[4,5]

Upper limb contribution to crank power has never been assessed directly but its role has been suggested by Baker and colleagues.[6] They showed that maximal crank power was lower without handgrip on the handlebar (1136 ± 88 W) in comparison with handgrip (1461 ± 94 W), suggesting that the upper limb may influence the crank power. Nevertheless, hand gripping could influence the lower limbs' performance by inducing greater muscular activations,[7,8] suggesting that muscular/mechanical upper limbs' contribution to the crank power needs further verification.

Further insights about the contribution of the upper limbs in cycling have been highlighted through the quantification of energy transfer through the hip joint. Indeed, inverse dynamics models of cycling have shown that crank power could be decomposed into the sum of ankles, knees, hip powers, and hip power transfer. This last term, calculated as the dot product between hip joint linear velocity and hip reaction force, is presumably partly generated by the upper limbs.[2] One study compared the seated and standing positions and showed higher magnitudes of hip power transfer in a standing position.[9] In a seated position, power transfer through the hip joint has been reported to represent 5% of the crank power at 540 W,[9,10] a percentage that could increase with power output (ie, from 3% at 250 W to 8% at about 1000W[11]), suggesting that the upper limbs may contribute to crank power.

These indirect evidences prove the importance of the upper limbs' involvement in the cycling movement, however knowledge of the level of upper limb joint moments or upper limb power production in cycling is still lacking. Therefore, the aim of this study was to test the effect of power output and position on the magnitudes of upper limb joint moments, powers, and works. Our hypothesis is that the magnitude of upper limb kinetics could be increased by an increase in crank power output and/or the use of a standing position instead of a seated one.

Methods

Seventeen male students (age: 23.2 ± 3.4 y, height: 1.77 ± 0.06 m, body mass: 73.7 ± 8.8 kg) volunteered to participate in the study. These participants were chosen to avoid expertise effects and were classified as category 4 (recreational) or 5 (athlete noncyclist) cyclists according to Ansley and Cangley's classification (category 1 would be professional cyclists riding more than 30000 km per year and category 6 would be sedentary noncyclists).[12] Each participant was informed of the experimental procedure and signed an informed consent form before the study. The experimental design of the study was conducted in accordance with the Declaration of Helsinki and approved by the University of Toulouse ethical committee. Participants were asked to avoid high-intensity or exhaustive exercise at least 72 hours before the laboratory trials.

Protocol

The cycling tests were performed using an electromagnetically braked Excalibur (LODE, Groningen, Netherlands). The rate of power output variation imposed by the ergometer was set to 1000 $W \cdot s^{-1}$. Participants first performed a cycling test to determine their spontaneous sit-to-stand transition power. This methodology was used in analogy with the walk-run transition to provide different percentages of power output according to a common biomechanical reference for the participants. In this test, phases of 40 seconds at a crank power of 50 W were alternated with phases of 20 seconds with an increment in power. In these 20-second phases, the starting crank power was 200 W, and was incremented by 25 W at each step. This protocol including intervals was chosen after preliminary trials showed that some participants may reach exhaustion before the sit-to-stand transition when using different protocols of crank power increased without recovery. The participants were instructed before the test to maintain a pedaling cadence of 90 revolutions per minute (rpm) provided by a visual feedback. During the test, the participants were encouraged to maintain 90 rpm as soon as their cadence was under or above 90 ± 5 rpm. The sit-to-stand transition power was considered as the crank power at which participants rose from the saddle during at least 10 seconds when they could not maintain 90 rpm in a seated position.

After a 5-minute rest period, participants performed 12 randomized trials in either a seated or standing position at crank power corresponding to 20%, 40%, 60%, 80%, 100%, or 120% of their sit-to-stand transition power. Each pedaling trial recording lasted 10 seconds and was started as soon as the participant was able to steadily pedal at the target crank power at 90 rpm. The pedaling cadence was standardized for all the participants because of its possible influence on the upper limb kinetics. Three minutes of passive rest were allowed between each trial.

Standardized Positioning

To limit bike positioning effects, standardized settings were established. The seat tube angle was set to 73° and the crank length was 0.17 m. The pedal cleat was positioned under the first metatarsal bone.[13] The saddle height was set to obtain a 150° knee angle during full leg extension. The handlebar was flat and positioned to standardize drop and reach lengths according to torso and arm lengths.[14] The positioning of the 2 hands on the handlebar was left up to the participant (handlebar width: 0.7 m, sweep angle: 0°).

Kinematics

Kinematic data from 18 passive markers on the upper limbs were recorded by 12 infrared cameras (VICON, Oxford, UK) at 200 Hz (Figure 1). The anatomical landmarks were selected according to de Leva.[15] The wrist and elbow joint centers were defined as the midpoints between the processus styloideus ulnae and radii, and between the lateral and medial epicondyles, respectively. The shoulder joint center was located using the SCoRE method.[16] For this method, a specific procedure previously suggested to locate the hip joint center was applied.[17] In a preliminary recording, the participants were asked to repeat shoulder flexion-extension, abduction-adduction, and circumduction. The SCoRE method then allowed the localization of the shoulder joint centers relative to a coordinate system attached to the thorax. Coordinate systems for each of the 3 segments were defined as recommended by the International Society of Biomechanics (ISB).[18] To provide upper limb loadings according to crank angle, 2 additional markers were added on the anterior and posterior part of a strip embedded externally to the pedals to determine the position of each pedal axis.

\insert Figure 1

Handlebar Sensors

The 3D force and moment vectors applied to the handlebar were recorded from 2 tubular sensors (SENSIX, Poitiers, France) positioned on each side of the handlebar (Figure 1C). These dynamometers had a maximum 1% error on each direction (combining linearity and hysteresis errors), and a maximum 1.5% error on the 6 component combination. All measures were given at the sensor reference point, which was localized by 4 reflective markers in the global reference frame. These markers also allowed the localization of the sensor orientation and were fixed to the sensors with a built-in interface.

Inverse Dynamic and Data Analysis

A Newton-Euler recursive algorithm was implemented to perform the bottom-up inverse dynamics protocol used to calculate the 3D joint moments, successively at the wrist, elbow, and shoulder joints (details of the equations in Winter[19]). Handlebar reaction forces and moments vectors were translated from the sensor reference point to the wrist joint center using Varignon's formula. Body segments' inertial parameters were derived from the scaling equations given in de Leva.[15] Handlebar loadings and upper limb kinematics were synchronized using Nexus 1.7.1 system (VICON, Oxford, UK) and marker position data were filtered using a fourth-order, zero-phase-shift, low-pass Butterworth with an 8-Hz cutoff frequency.[20]

To obtain the joint loadings in function of crank angle, data from a total of 15 pedaling cycles were averaged for each value of crank angle obtained during the pedaling trials of the second part of the study (from 2% to 120% of the sit-to-stand transition power in a random order). Moments applied to the upper limb were the net joint moments at the wrist, elbow, and shoulder, and the external forces were the handlebar reaction force and the joint force acting on the upper arm at the shoulder. Joint moment vectors were expressed according to the segment coordinate systems described in the Kinematics section earlier. External forces and moments developed mechanical energy if they produced or absorbed power during the movement.[21] Joint powers were calculated at each joint as the product of the joint moment and joint angular velocity, the power transferred across the shoulder joint was computed as the dot product between the shoulder reaction force and its linear velocity, and handlebar

power was considered to be zero given the fixed cycling ergometer.[2] The instantaneous power equation specific to the upper limbs in cycling was therefore:

$$P_t \quad \sum_{1}^{3} (P_j) \quad F_{sf} \cdot V_{sf} \quad \frac{dE_t}{dt}, \quad (1)$$

where P_t represents the total upper limb power, P_j represents the joint powers, F_{sf} represents the reaction force at the shoulder, V_{sf} represents the shoulder linear velocity, and $\frac{dE_t}{dt}$ represents the change in mechanical energy of the upper limbs. The upper limb network, $W_{UL(NET)}$, was defined as the mean over 15 complete crank revolutions of the time-integral of the total upper limb power as:

$$W_{UL\,(NET)} \quad \int_{1cycle} [P_t \; t \;]dt \quad \sum_{i\;1}^{1cycle\;6} \int [M_i \; t \; . \omega_i(t)]dt \quad \sum_{i\;1}^{1cycle\;2} \int [F_{sfi} \; t \; . V_{sf}(t)]dt \;, \quad (2)$$

where M_i and $_i$ were the i^{th} joint moment and joint angular velocity, respectively. These calculations were performed in the sagittal plane to allow direct comparisons with the power produced at the crank. To compare the total work of the upper limbs to the total work done at the crank, $W_{UL(NET)}$ was divided by the time-integral of the crank power over a crank revolution (W_{crank}) to obtain $W_{UL(RELATIVE)}$:[10,11,20]

$$W_{UL\,(RELATIVE)} \quad \frac{W_{UL\,(NET)}}{W_{crank}} \quad 100 \; . \quad (3)$$

The absolute work done by the upper limbs ($W_{UL(ABSOLUTE)}$) during 1 crank revolution was computed as the sum of the absolute value of the work done by the 2 arms and the shoulder transfers, and considers both eccentric and concentric work as positive[19,22] as:

$$W_{UL\,(ABSOLUTE)} \quad \sum_{i\;1}^{1cycle\;8} \int \left|P_i \; t \;\right| dt \quad \sum_{i\;1}^{1cycle\;6} \int \left|M_i \; t \; . \omega_i(t)\right| dt \quad \sum_{i\;1}^{1cycle\;2} \int \left|F_{STi} \; t \; . V_{Si}(t)\right| dt \;. \quad (4)$$

The entire data processing was performed using custom-made codes written in Scilab 5.4.0 (SCILAB, Scilab Enterprises, Versailles, France).

Data Reduction and Statistics

Results are reported as mean ± standard deviation. Moments, powers minima and maxima, and works were extracted at each joint for each pedaling condition and these variables were divided by the participant's body mass. Two-way repeated measure ANOVAs (position = seated and standing × crank power = 20%, 40%, 60%, 80%, 100%, and 120% of the sit-to-stand transition power) to test the effect of the position and of the crank power on the upper limb moment, power, and work magnitudes were performed after checking for data normality using Shapiro-Wilk tests and for variance homogeneity using Levene tests. Post hoc analyses were performed using Bonferroni's method. All statistical analyses were performed using the STATISTICA software (STATSOFT, Maisons-Alfort, France). An alpha value of .05 was defined as the level of statistical significance.

Results

The 6 power outputs corresponding from 20% to 120% of the sit-to-stand transition power were of 112 ± 19 W (1.6 ± 0.3 W·kg^{-1}) for 20%; 225 ± 38 W (3.2 ± 0.6 W·kg^{-1}) for 40%; 337 ± 56 W (4.7 ± 0.9 W·kg^{-1}) for 60%; 450 ± 75 W (6.3 ± 1.2 W·kg^{-1}) for 80%; 562 ± 94 W (7.9 ± 1.5 W·kg^{-1}) for 100%; and 675 ± 113 W (9.5 ± 1.8 W·kg^{-1}) for 120%. Because the participants could select their mediolateral hand position on the handlebar, which could have affected upper limb kinetics, their hand position across pedaling conditions has been checked. The pedaling condition had no effect on hand position (Table 1).

\insert Table 1\

A significant effect of crank power was observed in 16 out of 18 moments analyzed in the seated position and in 14 out of 18 in the standing position, showing that joint moments increased in magnitude with increasing crank power (Figure 2–4). A significant effect of position was observed, with most of the moments higher in magnitude in standing position in comparison with the seated position.

\insert Figure 2\
\insert Figure 3\
\insert Figure 4\

Normalized moments developed about the wrist, elbow, and shoulder joints across the pedaling cycle at each percentage of the sit-to-stand transition power in the frontal, sagittal, and transverse planes are presented in Figures 2, 3, and 4, respectively.

Maximum negative power in the seated position increased for all joints with increasing crank power (Figure 5), whereas maximum positive power increased only at the shoulder joint level. Both negative and positive power was higher in standing position compared with seated position. In standing position, crank power affected shoulder and elbow maximum negative powers, whereas only shoulder maximum positive power increased with increasing crank power.

\insert Figure 5\

Net joint work ($W_{UL\,(NET)}$) presented no significant effect of crank power in the seated position (Figure 6A). Conversely, $W_{UL(NET)}$ significantly increased in the standing position at 100% of the sit-to-stand transition power in comparison with 20%. $W_{UL(NET)}$ at 120% of the sit-to-stand transition power was significantly higher than all the other crank power conditions. $W_{UL(NET)}$ was significantly higher in the standing position compared with the seated position at 120% of the sit-to-stand transition power.

\insert Figure 6\

The total work done by the upper limbs expressed in proportion to the total work generated at the crank ($W_{UL(RELATIVE)}$) ranged from 0.5% to 2% in the seated position and from 1.5% to 2.5% in the standing position (Figure 6B). No significant effect of crank power on upper limbs' total work was observed either in the seated or in the standing position.

The amount of work in absolute value generated by the upper limbs ($W_{UL(ABSOLUTE)}$) increased with crank power in both seated and standing positions, with $W_{UL(ABSOLUTE)}$ at 120% of the sit-to-stand transition power different from all other crank powers (Figure 6C). $W_{UL(ABSOLUTE)}$ was higher in the standing position than in the seated position at all crank powers.

Discussion

The aim of the current study was to assess, for the first time, upper limb joint loadings in cycling, and to test if these variables were affected by crank powers and pedaling positions. Results showed that increase in crank power led to an increase in magnitude of the upper limb moments in both the seated and standing positions. The crank power value determined in this study was higher than the one of a previous study, reporting 419 ± 30 W as the power above which standing position should be chosen to maximize performance.[23] Because Hansen and Waldeland[23] compared times to exhaustion during cycling at different percentage of maximal oxygen uptakes, methodological differences in the criterion defining the optimal sit-to-stand transition power may explain this result.

The increase in upper limb joint moments with increasing power suggests new biomechanical constraints in these conditions. The common point between the variables affected by the crank power was that they were associated with handlebar pulling, whereas the variables not affected were mostly associated with handlebar pushing. Previous studies confirm this evolution of handlebar actions with increasing power.[3–5] However, why handlebar pulling magnitudes increase with increasing crank power, but not handlebar pushing, is still unclear. A first hypothesis could be that cyclists activate their upper limb muscles to better activate their lower limb muscles.[7,8] This could explain the increase in handlebar pulling, but not the stability in handlebar pushing. Another explanation could be found in the main goal of the cycling task: producing crank power. When this constraint increases, it is necessary for a given cadence to produce higher pedal force and thus more vertical force. At one point, these vertical pedal forces may counterbalance the body weight. This finding is consistent with the observation of a reduction of the saddle vertical force with increasing crank power.[5,24] The observed increase in handlebar pulling may be used to avoid body elevation when the pedal vertical forces exceed the body weight. Therefore, the increase in upper limb joint moments may allow the performance by trunk stabilization. Given the fact that experts develop higher crank power outputs[25] and that they have been observed to push more and pull less on the pedal than less-trained cyclists,[26] pedaling in a seated position for this population may imply higher levels of upper limb loadings, because of the necessary higher handlebar pulling to remain seated. Studies assessing maximal upper limb moments in isolated joint testing reported higher magnitudes than the one observed in our study.[27,28] This comparison suggests that, in cycling, upper limb joint moments may not reach the maximum magnitude possible. However, it cannot be ruled out that the upper limb muscles may face important demands in force given the specific context of pedaling and the likely nonoptimal position for each joint to produce moments, and because of the decrease in joint torque production associated with the increase in joint angular velocity.[29] In this sense, previous findings showed that myoelectrical activity of the forearm muscles is close to maximal during maximum power pedaling.[6] To improve performance by creating high pedal forces with limited trunk movements, and to avoid the standing position to decrease aerodynamic drag,[30] one implication of these results may be the use of strength conditioning programs involving the upper limbs and focusing on the muscular actions associated with handlebar pulling.

The mechanical energy cost of the upper limbs was represented in our study by measurement of $W_{UL\ (ABSOLUTE)}$, which cumulates values of work associated with both concentric and eccentric contractions. The increased $W_{UL\ (ABSOLUTE)}$ could be associated with an increase in metabolic cost with increasing crank power. This result is in line with one study which demonstrated a significant reduction in metabolic cost when the torso was stabilized to decrease upper limb actions in cycling.[31] The study by McDaniel and colleagues suggested that upper limbs represented about 2% of the pedaling energy cost. However, their study was limited in the crank power they could impose on their subjects (maximum 250 W). From the increase in joint moments and powers observed in our results for power outputs > 250 W, it could be expected that the absolute value of the metabolic cost due to the upper limbs would be higher for higher power outputs. Previous studies showed increasing magnitudes of hip transfer power in the standing position[9] and with increasing crank power from 3% of the pedal power at 250 W to 8% at about 1000 W.[10,11] However, the relative upper limb work generation, $W_{UL(RELATIVE)}$, remained low in both positions and lower than the reported data on hip power transfer. That could mean that other parts of the body such as the back and/or the contralateral leg could participate in the power transmitted through the hip joint force, and that the upper limb direct contribution to the crank power remains low. Further investigations using inverse dynamics with instrumented pedals and seats and lower limb kinematic reconstruction are needed to confirm that the upper limbs could only be partially responsible for the so-called hip transfer power in the literature. These considerations related to moments and works created by the upper limbs suggest that future models should consider both upper and lower limbs when modeling cycling biomechanics and energy expenditures, especially when the focus is on high crank power, elite athletes, and/or on the standing position.

It is important to note that pedaling on a cycling ergometer and cycling in the field are 2 different things.[32] Even if the former is a common practice for rehabilitation and training, it does not allow lateral bicycle oscillations, which are supposed to interfere with the pedaling technique. Thus, upper limb kinetics may presumably be modified in the field, particularly in the standing position in which roll angles up to 24° have been observed and may increase the upper limb moments specifically in the frontal plane.[33] Other factors such as slope or vibrations may have effects on the upper limb kinetics, in addition to other handlebar systems like road or time-trial, with other drop and reach settings. To test these effects, sensors recording full-body kinematics, and three-dimensional loads applied on each of the bicycle's supports are necessary to provide inverse dynamics analyses of cycling in field conditions. These methods often used to provide insights into the biomechanical causes of the observed movement are limited in accuracy by the combination of kinetic, kinematic, and anthropometric errors, however these sources of error should not change the conclusion about both position and crank power having an effect on upper limb kinetics. Further studies are necessary to fully understand which parameters are leading a cyclist to spontaneously transit from seated to the standing position.

In summary, this study measured three-dimensional moments, powers, and works done at the upper limb joints for various position and crank power conditions. We conclude that upper limb kinetics are affected by both crank power and the pedaling position. By providing a first reference of upper limb kinetic measurements, and by showing that these variables are affected by both the power output and the cycling position, these results have implications for clinicians, athletes, coaches, and sport scientists aiming to enhance performance and prevent injuries in cycling.

Acknowledgments

Antony Costes was funded by a PhD grant from the French Ministry of Education and Research (Ministère de l'Education et de la Recherche). The authors have no financial or personal relationships with other people or organizations that could have inappropriately influenced this research.

References

1. Bini RR, Diefenthaeler F. Mechanical work and coordinative pattern of cycling: a literature review. Kinesiology. 2009;41(1):25–39.
2. Kautz SA, Hull M, Neptune R. A comparison of muscular mechanical energy-expenditure and internal work. J Biomech. 1994;27(12):1459–1467 doi:10.1016/0021-9290(94)90195-3. PubMed
3. Bolourchi F, Hull MA. Measurement of rider induced loads during simulated bicycling. Int J Sport Biomech. 1985;1:308–329.
4. Stone C, Hull ML. The effect of rider weight on rider-induced loads during common cycling situations. J Biomech. 1995;28(4):365–375 doi:10.1016/0021-9290(94)00102-A. PubMed
5. Poirier E. Transition from the classical posture to the upright posture during cycling. Biomechanical criterion effects on the cyclist propulsion technique. [dissertation]. Toulouse: University of Toulouse; 2009
6. Baker J, Gal J, Davies B, Bailey D, Morgan R. Power output of legs during high intensity cycle ergometry: influence of hand grip. J Sci Med Sport. 2001;4(1):10–18 doi:10.1016/S1440-2440(01)80003-7. PubMed
7. Turpin NA, Costes A, Villeger D, Watier B. Selective muscle contraction during plantarflexion is incompatible with maximal voluntary torque assessment. Eur J Appl Physiol. 2014;114(8):1667–1677. PubMed
8. Ebben WP, Leigh DH, Geiser CF. The effect of remote voluntary contractions on knee extensor torque. Med Sci Sports Exerc. 2008;40(10):1805–1809 doi:10.1249/MSS.0b013e31817dc4ad. PubMed
9. Caldwell GE, van Emmerik REA. Movement proficiency: tasks, demands, and constraints. In W.A. Sparrow (Ed.). Energetics of Human Activity. Champaign, IL: Human Kinetics; 2000:66–95.
10. Martin JC, Brown NAT. Joint-specific power production and fatigue during maximal cycling. J Biomech. 2009;42(4):474–479 doi:10.1016/j.jbiomech.2008.11.015. PubMed
11. Elmer SJ, Barratt PR, Korff T, Martin JC. Joint-specific power production during submaximal and maximal cycling. Med Sci Sports Exerc. 2011;43(10):1940–1947 doi:10.1249/MSS.0b013e31821b00c5. PubMed
12. Ansley L, Cangley P. Determinants of "optimal" cadence during cycling. Eur J Sport Sci. 2009;9(2):61–85 doi:10.1080/17461390802684325.
13. Viker T, Richardson MX. Shoe cleat position during cycling and its effect on subsequent running performance in triathletes. J Sports Sci. 2013;31(9):1007–1014 doi:10.1080/02640414.2012.760748. PubMed
14. de Vey Mestdagh K. Personal perspective: in search of an optimum cycling posture. Appl Ergon. 1998;29(5):325–334 doi:10.1016/S0003-6870(97)00080-X. PubMed
15. de Leva P. Adjustments to Zatsiorsky-Seluyanov's segment inertia parameters. J Biomech. 1996;29(9):1223–1230 doi:10.1016/0021-9290(95)00178-6. PubMed
16. Ehrig RM, Taylor WR, Duda GN, Heller MO. A survey of formal methods for determining the centre of rotation of ball joints. J Biomech. 2006;39(15):2798–2809 doi:10.1016/j.jbiomech.2005.10.002. PubMed
17. Begon M, Monnet T, Lacouture P. Effects of movement for estimating the hip joint centre. Gait Posture. 2007;25(3):353–359 doi:10.1016/j.gaitpost.2006.04.010. PubMed
18. Wu G, van der Helm FC, Veeger HE, et al. ISB recommendation on definitions of joint coordinate systems of various joints for the reporting of human joint motion—Part II: shoulder, elbow, wrist and hand. J Biomech. 2005;38(5):981–992 doi:10.1016/j.jbiomech.2004.05.042. PubMed
19. Winter DA. Biomechanics and Motor Control of Human Movement. Hoboken, NJ: John Wiley & Sons; 1990:370.
20. McDaniel J, Behjani NS, Elmer SJ, Brown NA, Martin JC. Joint-specific power-pedaling rate relationships during maximal cycling. J Appl Biomech. 2014;30(3):423–430 doi:10.1123/jab.2013-0246. PubMed
21. Aleshinsky SY. An energy-sources and fractions approach to the mechanical energy-expenditure problem. 2. movement of the multilink chain model. J Biomech. 1986;19(4):295–300 doi:10.1016/0021-9290(86)90004-7. PubMed
22. van Ingen Schenau GJ, Cavanagh PR. Power equations in endurance sports. J Biomech. 1990;23(9):865–881 doi:10.1016/0021-9290(90)90352-4. PubMed
23. Hansen EA, Waldeland H. Seated versus standing position for maximization of performance during intense uphill cycling. J Sports Sci. 2008;26(9):977–984 doi:10.1080/02640410801910277. PubMed
24. Costes A, Turpin NA, Villeger V, Moretto P, Watier B. A reduction of the saddle vertical force triggers the sit–stand transition in cycling. J Biomech. 2015; in press doi:10.1016/j.jbiomech.2015.07.035. PubMed
25. Pinot J, Grappe F. The record power profile to assess performance in elite cyclists. Int J Sports Med. 2011;32(11):839–844. doi:10.1055/s-0031-1279773.
26. Coyle EF, Feltner ME, Kautz SA, et al. Physiological and biomechanical factors associated with elite endurance cycling performance. Med Sci Sports Exerc. 1991;23(1):93–107. PubMed doi:10.1249/00005768-199101000-00015
27. Holzbaur KRS, Delp SL, Gold GE, Murray WM. Moment-generating capacity of upper limb muscles in healthy adults. J Biomech. 2007;40(11):2442–2449 doi:10.1016/j.jbiomech.2006.11.013. PubMed
28. Delp SL, Grierson AE, Buchanan TS. Maximum isometric moments generated by the wrist muscles in flexion-extension and radial-ulnar deviation. J Biomech. 1996;29(10):1371–1375 doi:10.1016/0021-9290(96)00029-2. PubMed
29. Anderson DE, Madigan ML, Nussbaum MA. Maximum voluntary joint torque as a function of joint angle and angular velocity: Model development and application to the lower limb. J Biomech. 2007;40(14):3105–3113 doi:10.1016/j.jbiomech.2007.03.022. PubMed
30. Martin JC, Gardner AS, Barras M, Martin DT. Modeling sprint cycling using field-derived parameters and forward integration. Med Sci Sports Exerc. 2006;38(3):592–597 doi:10.1249/01.mss.0000193560.34022.04. PubMed
31. McDaniel J, Subudhi A, Martin JC. Torso stabilization reduces the metabolic cost of producing cycling power. Can J Appl Physiol. 2005;30(4):433–441. PubMed doi:10.1139/h05-132
32. Bertucci WM, Betik AC, Duc S, Grappe F. Gross efficiency and cycling economy are higher in the field as compared with on an axiom stationary ergometer. J Appl Biomech. 2012;28(6):636–644. PubMed
33. Bertucci W, Taiar R, Grappe F. Differences between sprint tests under laboratory and actual cycling conditions. J Sports Med Phys Fitness. 2005;45(3):277–283. PubMed
34. Delp SL, Anderson FC, Arnold AS, et al. OpenSim: open-source software to create and analyze dynamic Simulations of movement. IEEE Trans Biomed Eng. 2007;54(11):1940–1950 doi:10.1109/TBME.2007.901024. PubMed

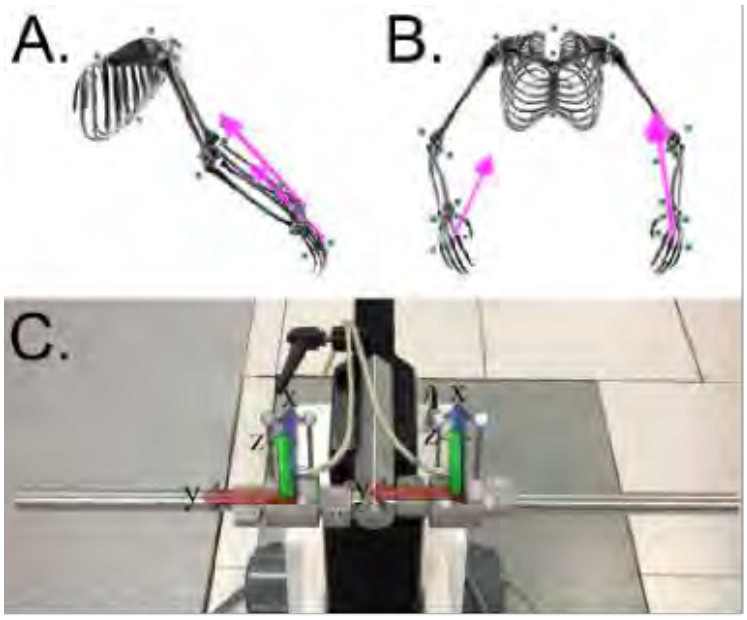

Figure 1 — (A) Sagittal view of the marker set used to reconstruct the upper limb kinematics. (B) Frontal view. The arrows represent the reaction forces recorded by the handlebar sensors and the dots represent the passive markers used to model the bone movements and orientations. (Figures made with Opensim 3.2 software.[34]) (C) Handlebar with 6-component sensors and the marker set used to locate the sensor origins and orientations; x, y, and z represent the anteroposterior, mediolateral, and vertical axis, respectively.

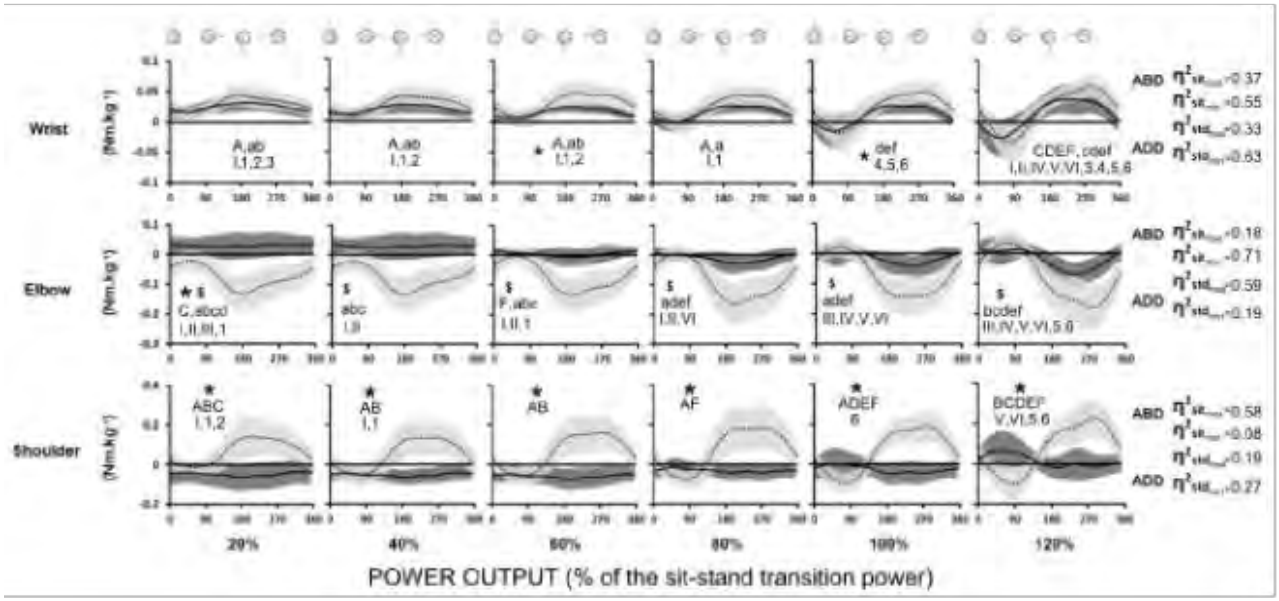

Figure 2 — Frontal plane moments in the joint coordinate systems for the left upper limb at the wrist, elbow, and shoulder in function of the right crank angle. Mean seated cycling (solid black line) and standing cycling (dotted black line) are represented ± one standard deviation (dark gray shading for seated/light gray shading for standing). Data are normalized by body mass over 15 pedaling cycles at 90 revolutions per minute (rpm). ABD = abduction; ADD = adduction. * Significant difference between maximum seated and standing position. $ Significant difference between minimum seated and standing position. ABCDEF indicate a significant difference compared with 120%, 100%, 80%, 60%, 40%, and 20% of the power output corresponding to the sit-to-stand transition for the maximum magnitude in the seated position; abcdef indicate a significant difference compared with the minimum magnitude in seated position; I,II,III,IV,V,VI indicate a significant difference compared with maximum magnitude in the standing position; and 1,2,3,4,5,6 indicate a significant difference compared with minimum magnitude in the standing position. $^2_{sit}$ = eta-squared in the seated position. $^2_{std}$ = eta-squared in the standing position.

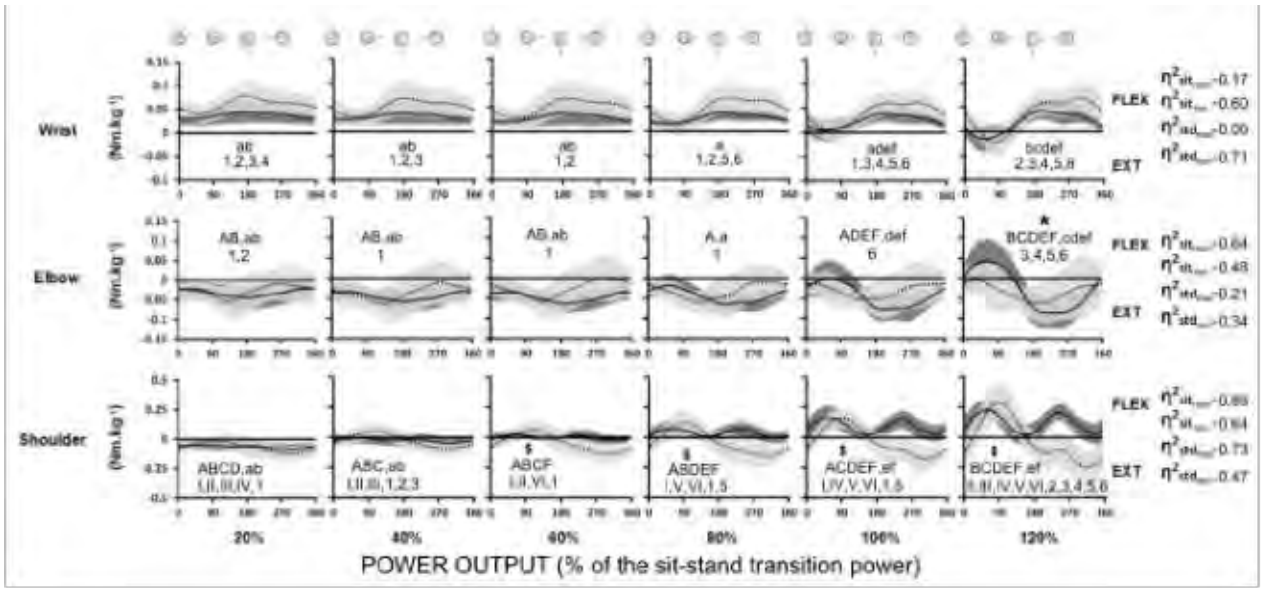

Figure 3 — Sagittal plane moments in the joint coordinate systems for the left upper limb at the wrist, elbow, and shoulder in function of the right crank angle. Mean seated cycling (solid black line) and standing cycling (dotted black line) are represented ± one standard deviation (dark gray shading for seated/light gray shading for standing). Data normalized by body mass over 15 pedaling cycles at 90 revolutions per minute (rpm). FLEX = flexion; EXT = extension. * Significant difference between maximum seated and standing position. $ Significant difference between minimum seated and standing position. ABCDEF indicate a significant difference compared with 120%, 100%, 80%, 60%, 40%, and 20% of the power output corresponding to the sit-to-stand transition for the maximum magnitude in the seated position; abcdef indicate a significant difference compared with the minimum magnitude in seated position; I,II,III,IV,V,VI indicate a significant difference compared with maximum magnitude in the standing position; and 1,2,3,4,5,6 indicate a significant difference compared with minimum magnitude in the standing position. $^2_{sit}$ = eta-squared in the seated position. $^2_{std}$ = eta-squared in the standing position.

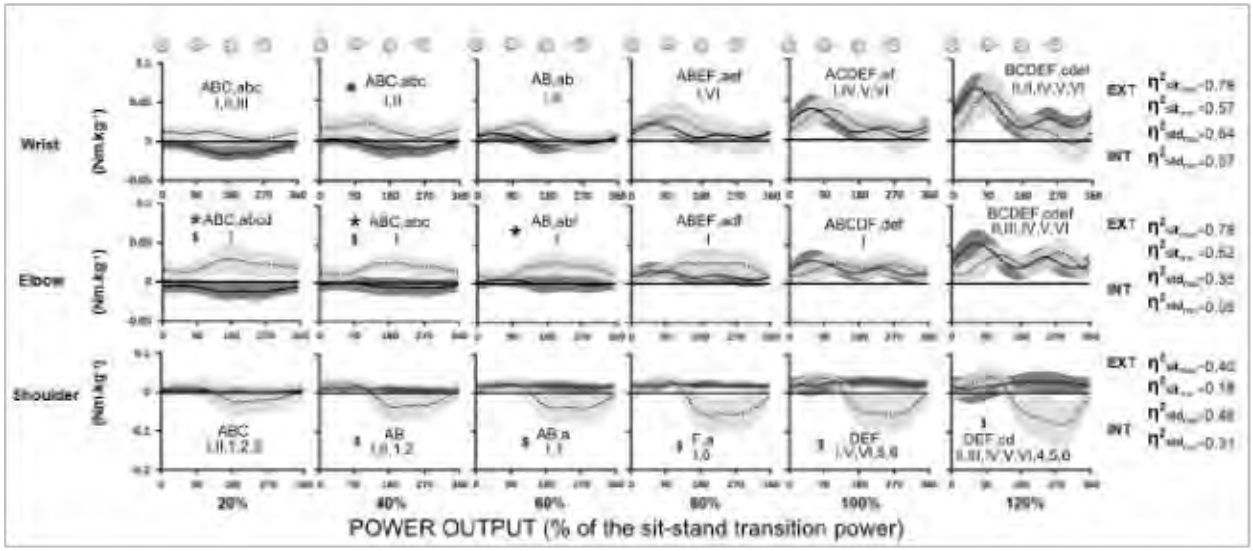

Figure 4 — Transverse plane moments in the joint coordinate systems for the left upper limb at the wrist, elbow, and shoulder in function of the right crank angle. Mean seated cycling (solid black line) and standing cycling (dotted black line) are represented ± one standard deviation (dark gray shading for seated/light gray shading for standing). Data normalized by body mass over 15 pedaling cycles at 90 revolutions per minute (rpm). EXT = external rotation; INT = internal rotation. * Significant difference between maximum seated and standing position. $ Significant difference between minimum seated and standing position. ABCDEF indicate a significant difference compared with 120%, 100%, 80%, 60%, 40%, and 20% of the power output corresponding to the sit-to-stand transition for the maximum magnitude in the seated position; abcdef indicate a significant difference compared with the minimum magnitude in seated position; I,II,III,IV,V,VI indicate a significant difference compared with maximum magnitude in the standing position; and 1,2,3,4,5,6 indicate a significant difference compared with minimum magnitude in the standing position. $^2_{sit}$ = eta-squared in the seated position. $^2_{std}$ = eta-squared in the standing position.

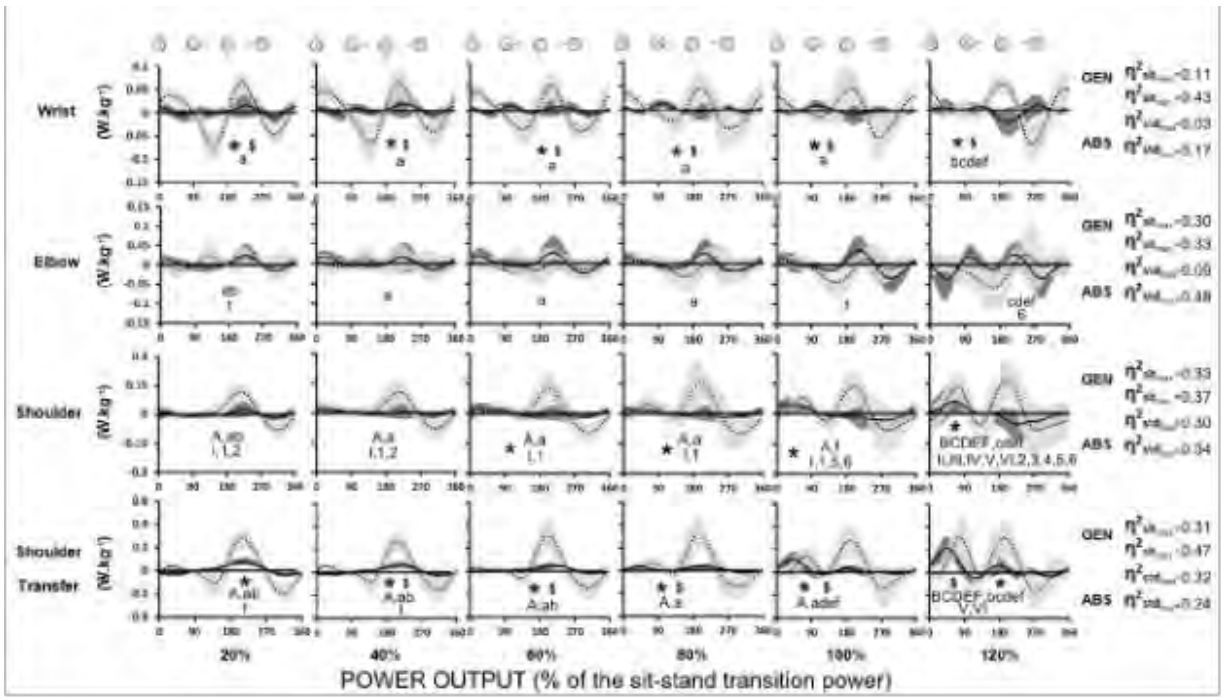

Figure 5 — Powers in the sagittal laboratory plane for the left upper limb at the wrist, elbow, and shoulder in function of the right crank angle. Mean seated cycling (solid black line) and standing cycling (dotted black line) are represented ± one standard deviation (dark gray shading for seated/light gray shading for standing). Data normalized by body mass over 15 pedaling cycles at 90 revolutions per minute (rpm). GEN = power generation; ABS = power absorption. * Significant difference between maximum seated and standing position. $ Significant difference between minimum seated and standing position. ABCDEF indicate a significant difference compared with 120%, 100%, 80%, 60%, 40%, and 20% of the power output corresponding to the sit-to-stand transition for the maximum magnitude in the seated position; abcdef indicate a significant difference compared with the minimum magnitude in seated position; I,II,III,IV,V,VI indicate a significant difference compared with maximum magnitude in the standing position; and 1,2,3,4,5,6 indicate a significant difference compared with minimum magnitude in the standing position. $^{2}_{sit}$ = eta-squared in the seated position. $^{2}_{std}$ = eta-squared in the standing position.

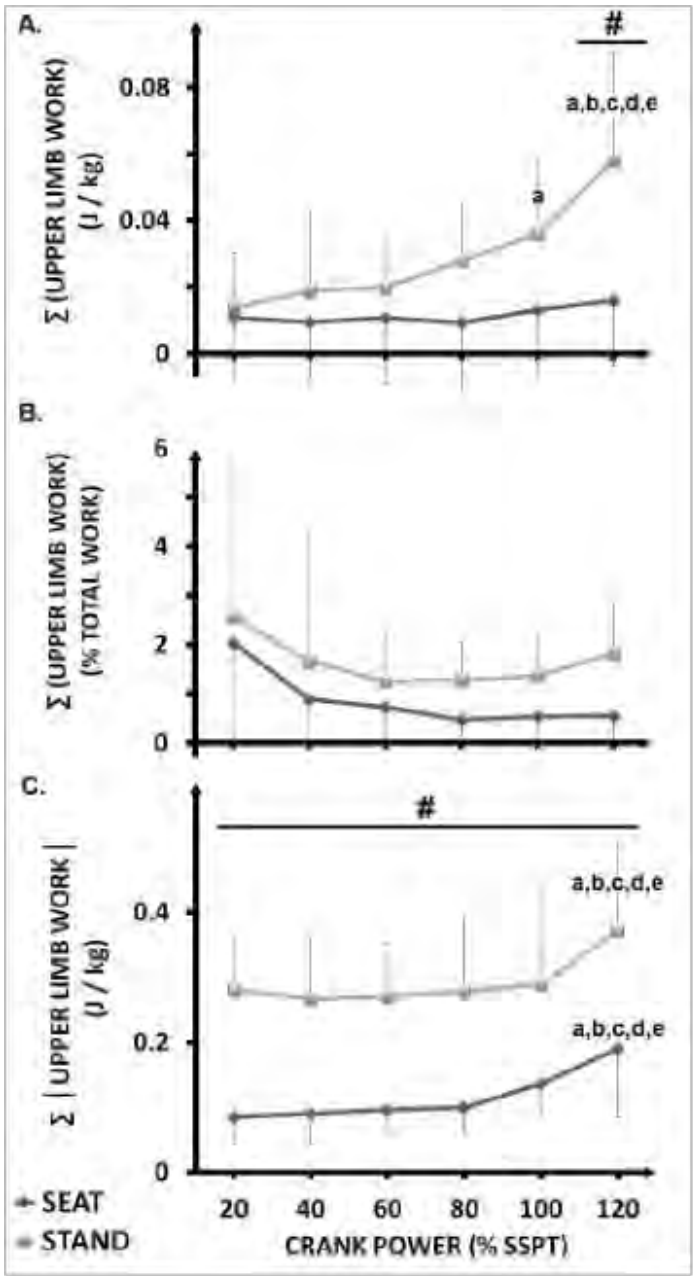

Figure 6 — Work done by the upper limbs. One dot represents the sum of the two wrists, elbows, shoulders, and shoulder transfer work for the given position (seated = dark gray squares; standing = gray squares) across crank power outputs. (A) $W_{UL(NET)}$. (B) $W_{UL(RELATIVE)}$. (C) $W_{UL(ABSOLUTE)}$. Power output from 20% to 120% of the sit-to-stand transition power correspond to 76 ± 13 J (1.1 ± 0.2 J·kg^{-1}), 151 ± 26 J (2.1 ± 0.4 J·kg^{-1}), 227 ± 39 J (3.2 ± 0.6 J·kg^{-1}), 302 ± 52 J (4.2 ± 0.8 J·kg^{-1}), 378 ± 65 J (5.3 ± 1 J J·kg^{-1}), and 453 ± 78 J (6.3 ± 1.2 J·kg^{-1}) works generated at the cranks by pedaling cycle, respectively. # Significant difference compared with seated cycling ($P < .05$). ^{a,b,c,d,e} Significant difference compared with 20%, 40%, 60%, 80%, and 100% of the sit-to-stand transition power, respectively.

Table 1 Hand position across pedaling conditions

	20%	40%	60%	80%	100%	120%
Seated						
Absolute	0.254 ± 0.031	0.256 ± 0.028	0.252 ± 0.028	0.253 ± 0.024	0.250 ± 0.027	0.251 ± 0.028
Relative	0 ± 0	0.002 ± 0.017	–0.002 ± 0.016	–0.001 ± 0.018	–0.003 ± 0.016	–0.003 ± 0.014
Standing						
Absolute	0.259 ± 0.021	0.258 ± 0.024	0.264 ± 0.023	0.259 ± 0.021	0.257 ± 0.026	0.262 ± 0.023
Relative	0.005 ± 0.026	0.004 ± 0.022	0.010 ± 0.022	0.005 ± 0.024	0.003 ± 0.023	0.008 ± 0.022

Note. Mean ± SD position of the center of the left hand on the mediolateral axis. "Absolute" represented the horizontal distance in m between the hand center (defined as the midpoint between the wrist joint center and the midpoint between the 2 metacarpal heads) and the handlebar center. "Relative" represented the difference in m between the hand center in the seated 20% condition and the hand center in the assessed condition. No significant difference was observed between pedaling conditions.

III.4. Etude 2 : Patterns d'Activite Musculaire des Membres Superieurs et du Tronc pendant le Pedalage Assis et en Danseuse

L'objectif de cet article accepté dans la revue « Journal of Sports Science » a été de clarifier le rôle fonctionnel des muscles du membre supérieur en cyclisme en position assis et danseuse lorsque la puissance de pédalage augmente.

L'activité électromyographique de 7 muscles du membre supérieur et du tronc a été étudiée assis et en danseuse pour des puissances d'environ 100 à 700 W. Les forces appliquées sur le cintre et les pédales ont été enregistrées simultanément. L'activité EMG intégrée, les patterns temporels des EMG et les synergies musculaires ont été analysés durant plusieurs séquences de 10 secondes réalisées à 90 rotations par minute.

La plupart des muscles observés avaient une activité tonique, devenant progressivement de plus en plus phasique avec l'augmentation de la puissance. Trois synergies musculaires ont été identifiées et associées à 1) la compensation des accélérations du tronc vers le haut par traction sur le cintre 2) au support du poids du tronc 3) à la stabilisation du corps. Le niveau d'activation des synergies 1 et 3 a été observé comme augmentant de manière importante avec l'augmentation de la puissance au pédalier, pendant les périodes de poussée de jambe ipsi- et contro-latérales, respectivement, suggérant un rôle important de ces synergies lors de l'augmentation de la production de puissance au pédalier.

En conclusion, cet article améliore notre compréhension de la biomécanique du cyclisme, et suggère que les muscles du membre supérieur ont un rôle important en cyclisme lorsque la production de puissance au pédalier est élevée.

JOURNAL OF SPORTS SCIENCES, 2016
http://dx.doi.org/10.1080/02640414.2016.1179777

Routledge
Taylor & Francis Group

Upper limb and trunk muscle activity patterns during seated and standing cycling

Nicolas A. Turpin[a,b], Antony Costes[c], Pierre Moretto[d] and Bruno Watier[e,f]

[a]Center for Interdisciplinary Research in Rehabilitation (CRIR), Institut de réadaptation Gingras-Lindsay de Montreal and Jewish Rehabilitation Hospital, Laval, Quebec, Canada; [b]Department of Neuroscience, University of Montréal, Quebec, Canada; [c]F2SMH, Université Paul Sabatier, Toulouse Cedex 9, France; [d]Centre de Biologie Intégrative, Centre de Recherches sur la Cognition Animale (UMR CNRS-UPS 5169), Université de Toulouse, UPS, Toulouse Cedex 9, France; [e]CNRS, LAAS, Toulouse, France; [f]University of Toulouse, UPS, LAAS, Toulouse Cedex 9, France

ABSTRACT

The objective of this study is to clarify the functional roles of upper limb muscles during standing and seated cycling when power output increases. We investigated the activity of seven upper limb and trunk muscles using surface electromyography (EMG). Power outputs ranged from ~100–700 W with a pedalling frequency of 90 revolution per minute. Three-dimensional handle and pedal forces were simultaneously recorded. Using non-negative matrix factorisation, we extracted muscle synergies and we analysed the integrated EMG and EMG temporal patterns. Most of the muscles showed tonic activity that became more phasic as power output increased. Three muscle synergies were identified, associated with (i) torso stabilisation, (ii) compensation/generation of trunk accelerations and (iii) upper body weight support. Synergies were similar for seated and standing positions (Pearson's $r > 0.7$), but synergy #2 (biceps brachii, deltoidus and brachioradialis) was shifted forward during the cycle (~7% of cycle). The activity levels of synergy #1 (latissimus dorsi and erector spinae) and synergy #2 increased markedly above ~500 W (i.e., ~+40–70% and +130–190%) and during periods corresponding to ipsi- and contralateral downstrokes, respectively. Our study results suggest that the upper limb and trunk muscles may play important roles in cycling when high power outputs are required.

ARTICLE HISTORY
Accepted 12 April 2016

KEYWORDS
Muscle synergy; pedalling performance; EMG; inter-limb coordination

Introduction

A cycle ergometer is routinely used in physical testing and rehabilitation procedures (Jones, Makrides, Hitchcock, Chypchar, & McCartney, 1985; Kautz & Brown, 1998). Previous studies have generally focused on lower limb biomechanics and scant attention has been paid to the upper limbs, although they may significantly contribute to cycling performance (Baker, Gal, Davies, Bailey, & Morgan, 2001; Baker & Davies, 2009; Elmer, Barratt, Korff, & Martin, 2011; Soden & Adeyefa, 1979; Stone & Hull, 1993). The coordination patterns of the arm and trunk muscles when cycling have not been extensively investigated nor their functional roles clearly established.

Apart from the roles of the trunk and arm muscles in steering the bicycle and supporting trunk weight, the upper limbs may be involved in stabilising the body (Duc, Bertucci, Pernin, & Grappe, 2008), particularly when riding on uneven surfaces like cobbles or on off-road terrains (Arpinar-Avsar, Birlik, Sezgin, & Soylu, 2013). Furthermore, they may either provide energy to the crank (Elmer et al., 2011; Martin & Brown, 2009) or facilitate maximal power output (Doré et al., 2006). Previous studies show that the arms are more activated while in the standing position (Duc et al., 2008) when they may be particularly involved in power production (Caldwell, van Emmerik, Hamill, & Sparrow, 2000; Stone & Hull, 1993; Tanaka, Bassett, Best, & Baker, 1996).

Stone and Hull (1993) reported that handlebar forces during standing cycling were roughly in phase with pedal forces (i.e., participants pulling up and back during the power stroke of the corresponding leg), highlighting their possible role in power production. In analyses of the power transferred across the hip joint, studies have shown that power contribution of the trunk and upper limbs increases almost linearly with power output, reaching about 13% at ~1000 W (Elmer et al., 2011). Moreover, when cycling without hand-gripping the handlebar, that is, in conditions in which upward forces on the handlebar cannot be produced, a decrease of 10–20% in the power produced can be observed, as compared to conventional conditions (Baker et al., 2001; Baker & Davies, 2009; Doré et al., 2006), which further suggests the active contribution of arms to cycling performance.

There is a scarcity of data on upper limb muscle activity during cycling (Arpinar-Avsar et al., 2013; Clarys, Cabri, & Antonis, 1989; Duc et al., 2008; Grant, Watson, & Baker, 2015; Padulo, Laffaye, Bertucci, Chaouachi, & Viggiano, 2014) and existing studies have reported divergent results (Duc et al., 2008; Padulo et al., 2014). For example, in Padulo et al. (2014), the biceps brachii muscle was active mainly during the downstroke phase, suggesting its role during power production, whereas in Duc et al. (2008), this muscle showed two peaks occurring at the downstroke ends of each leg, suggesting its role in upper body stabilisation. Therefore, the role and coordination patterns of arm muscles in cycling are not clear and require further investigation.

CONTACT Nicolas A. Turpin nicolas.turpin@umontreal.ca Center for Interdisciplinary Research in Rehabilitation (CRIR), Institut de réadaptation Gingras-Lindsay de Montreal, 6300 Avenue de Darlington, Montreal, Quebec, Canada H3S 2J4

Studies have shown that the activities of muscles involved in a task are temporally and spatially organised, such that functional muscle synergies can be identified (Ting & McKay, 2007; Turpin, Guevel, Durand, & Hug, 2011b). Synergies of the lower limb muscles during cycling have been identified by non-negative matrix factorisation (Barroso et al., 2014; Hug, Turpin, Couturier, & Dorel, 2011; Hug, Turpin, Guevel, & Dorel, 2010) and have revealed functionally significant groups consistent with those identified using biomechanical simulations (Raasch & Zajac, 1999). This approach may therefore be helpful in determining the functional roles of numerous muscles.

The upward and backward forces created at the handlebar (Stone & Hull, 1993) are likely to be generated by the shoulder muscles, by the elbow flexors and by the adductors of the arms (e.g., latissimus dorsi), but there is little if any data on this topic in the literature. The purpose of this paper is to describe the activation of these muscles during standing and seated cycling and to relate this activity to the handlebar forces. In particular, muscle synergies are identified to clarify the functional roles of these muscles. Since the contribution of the upper limbs appears to be related to power output (Elmer et al., 2011) and to the position used (Caldwell et al., 2000), this analysis pertains to tests performed in the seated and standing positions across a wide range of power outputs (~100–700 W).

Materials and methods

Participants

Seventeen males (23.3 ± 3.4 years; 1.78 ± 0.05 m, 72.6 ± 7.4 kg) volunteered and signed an informed consent to participate in this study. The participants were non-cyclists and belonged to category 4–5 of the Ansley and Cangley (2009) classification. The experimental design of this study was approved by the local ethics committee and was conducted in accordance with the Declaration of Helsinki. Participants were asked to avoid high-intensity or exhaustive exercise for at least 72 h before the laboratory trials.

Protocol

Participants exercised on a braked ergometer (Excalibur, LODE, Groningen, Netherlands) and using cleated cycling shoes, after being equipped with recording electrodes (see section "EMG recording"). After 5 min of warm up, they completed the first test to determine at which power output they would spontaneously transit to the standing position. This power output – the seat-stand transition power (SSTP, see also Costes, Turpin, Villeger, Moretto, and Watier (2015)) – was then used to normalise power across all participants in the second test. In the first test, the participants started in the seated position and exercised continuously at 50 W power. At regular 60 s intervals, the power was transiently raised for 20 s to a test power. The test power, initially 200 W, was incremented by 25 W until the subject adopted a standing position. The instructions were to maintain a stable pedalling frequency (i.e., 90 ± 5 revolution per minute (RPM)) and to feel free to adopt a more comfortable position to perform the task. SSTP was established when the participant cycled in the standing position for at least 10 s.

After a 5 min rest, the participants performed the second test, consisting of 10–12 s bouts of cycling in either the seated or standing position at 20%, 40%, 60%, 80%, 100% or 120% of SSTP (2 positions × 6 power-outputs = 12 trials) with 2–3 min of complete rest between bouts. These bouts were presented in random order. Once the participants reached the target pedalling frequency (i.e., typically after ~1–2 s), data were collected continuously for 10 s.

While cycling, the participants viewed their real-time RPM on a monitor and were instructed to maintain a 90-RPM pedalling frequency in both the first and second tests.

Participant positioning

The ergometer's saddle height was adjusted to obtain a knee angle of ~150° (180° = full extension) when the crank was at the lowest position while seated. The foot was positioned on the pedals so the axis of pedal rotation was vertically aligned with the metatarsophalangeal joint of the big toe. The seat tube angle was 73° and the crank length was 170 mm. The handlebars were flat (mountain bike type) and the position of the hands on the handlebars was left to the participants' discretion (handlebar width = 700 mm). The vertical and horizontal positions of the handlebars, which determined the drops and reaches, were adjusted for each participant according to de Vey Mestdagh (1998).

EMG recording

The electromyography (EMG) was recorded for seven muscles on the right side of the body: erector spinae L4–L5 (ES), latissimus dorsi (LD), anterior of the deltoïdus (Delt), tricep lateralis (TL), biceps brachii (BB), brachoradialis (Br) and flexor digitorum (FD). Prior to electrode application, the skin was shaved and cleaned with alcohol. The electrodes were active parallel bar sensors (Delsys DE 2.1 type, Delsys Inc, Boston, MA, USA; 1-cm interelectrode distance) and were placed in the middle of the muscle belly, longitudinally with respect to the underlying muscle fibres. Electrodes were secured with adhesive tape before recording. EMG signals were amplified (× 1000) and digitised (6–400 Hz bandwidth) at a 1-kHz sampling rate (Bagnoli 16, Delsys, Inc. Boston, USA).

Forces recording

The 3D forces were recorded at a 1-kHz sampling frequency from two instrumented pedals (I-Crankset-1, SENSIX, Poitiers, France) and from tubular sensors in place of the handlebars (SENSIX, Poitiers, France). These dynamometers had a maximum 1% error in each direction (combined linearity and hysteresis errors), and a maximum 1.5% error for the combined six components.

Data processing

All data were synchronised using a Nexus 1.7.1 system (VICON, Oxford, United Kingdom). Kinetics data were low-pass filtered using a low-pass Butterworth filter (2nd order, cut-off = 10 Hz).

EMG signals were band-pass filtered (4th order Butterworth) between 20–400 Hz. When necessary, electrical noise components were removed using band-stop filters (i.e., generally around 50, 100, 200, 300 and 400 Hz; band width = ± 0.3 Hz). Raw EMG signals were then demeaned to nullify possible bias in the EMG amplifiers.

Integrated EMG activity was obtained using a trapezoidal method applied to the rectified EMG. The EMG of the ~15 cycles of each condition was integrated to get a single value, which was normalised by the mean computed overall power output conditions and position in the second test (Yang & Winter, 1984).

Linear envelopes for each muscle were obtained by low-pass filtering fully rectified raw EMG signals with a 9 Hz low-pass filter (2nd order Butterworth, zero lag). For each participant and for each muscle, EMG envelopes were normalised in amplitude by the mean value computed for overall power conditions and positions in the second test.

The pedalling cycles were identified by trigger signalling of the lowest pedal position – bottom dead centre (BDC). A cycle corresponded to one pedal revolution, with 0% and 100% corresponding to the BDC.

Tonic activity was defined qualitatively as a stable activity level during the cycle, and phasic activity as a pattern with appreciable variations in amplitude.

Muscle synergy analysis

To facilitate the interpretation of the EMG data, we analysed muscle synergies using a non-negative matrix factorisation technique (Lee & Seung, 2001), in which the main features of the muscle coordination are extracted (i.e., to determine which muscles act together and their temporal organisation) (Hug, 2011). For each subject and each muscle, we averaged the EMG envelopes from each condition in the second test to obtain a representative pattern for one cycle. The data were then concatenated into a single matrix for factorisation, whereby each subject in a given position was represented in a matrix with 200 × 6 rows (i.e., 200 pts per cycle × 6 power levels) and seven columns (i.e., seven muscles). At each iteration, the synergy vectors were normalised by their Euclidian norm. Data for the seated and standing positions were analysed separately. The number of synergies extracted by the algorithm varied from one to seven and the variance accounted for (VAF) was computed each time. VAF is defined as 1-SSE/SST, SSE being the sum of the squared residuals and SST the total sum of the squared values. The number of synergies was defined as the first number at which the total VAF reached a value greater than 90% and a VAF for each muscle was greater than 75% (Hug et al., 2011).

Time lag, r-max and similarity

As in previous studies (Turpin, Guevel, Durand, & Hug, 2011a, Turpin et al., 2011b), we calculated timing differences between two activation patterns as the lag time at the maximum of their cross-correlation function. R-max is the maximum value of this function, taken as an index of shape similarity. To compare power-output patterns, we computed Pearson's r, lag, and r-max values between pairs of EMG patterns taken at powers p and p + 1, for p = [20%, 40%, 60%, 80% and 100%] of the SSTP, averaged to obtain a single value for each subject. Similarly, for comparisons across positions, we compared patterns in seated and standing positions at each power output and the similarity values were averaged for each subject.

Statistics

We assessed data normality using Shapiro–Wilk tests. We assessed the effect of the power output and position on the integrated EMG activity using Friedman tests. We used post hoc Wilcoxon matched pair tests with Bonferonni corrections and compared differences in the number of synergies and in individual synergy weightings with Wilcoxon matched pair tests. We used Pearson's r as a similarity measure between two activation patterns and to compare muscle synergies, and assessed the significance of the time lags using t-tests for a single mean (reference = 0). Data are presented as mean ± SD, with a level of significance at $P < 0.05$.

Results

In the first test, participants spontaneously transited to the standing position at a power (SSTP) of 582.4 ± 103.7 W, with 20%, 40%, 60%, 80% and 120% of SSTP corresponding to 116.5 ± 20.7, 232.9 ± 41.5, 349.4 ± 62.2, 465.9 ± 83.0 and 698.8 ± 124.5 W, respectively.

Muscle activity levels

Figure 1 shows the integrated EMG activity for each muscle in the second test as a function of the power output, which was associated with an increase in the integrated muscle activity for all muscles ($P < 0.002$). A global position effect was found for ES, LD and BR ($P < 0.007$). Figure 1 shows the seated and standing differences for each power output (for which all P values ≤ 0.004).

Muscle activation pattern

The upper limb muscles demonstrated tonic activities at the lowest powers and became more phasic with increasing power output (Figure 2), during which the muscle activity patterns were scaled in amplitude with few changes in their timing. This was evidenced by Pearson's r values greater than 0.8 when comparing pairs of EMG envelopes from adjacent powers (i.e., 0.803 ± 0.082 for seated and 0.834 ± 0.083 for standing on average for all muscles). With a change in position, the correlation values decreased (Table 1, first column). Seated and standing ES, Delt and Br activity patterns had similar shapes (Table 1, r-max values > 0.9) but were shifted in time. LD, TL and FD showed more marked shape changes with a change in position.

Muscle synergies

The VAF curve versus number of synergies extracted and the distribution of the number of synergies are depicted in Figure 3(a,b), respectively. The number of seated and standing synergies were similar (i.e., 3.4 ± 0.7 and 3.1 ± 0.8,

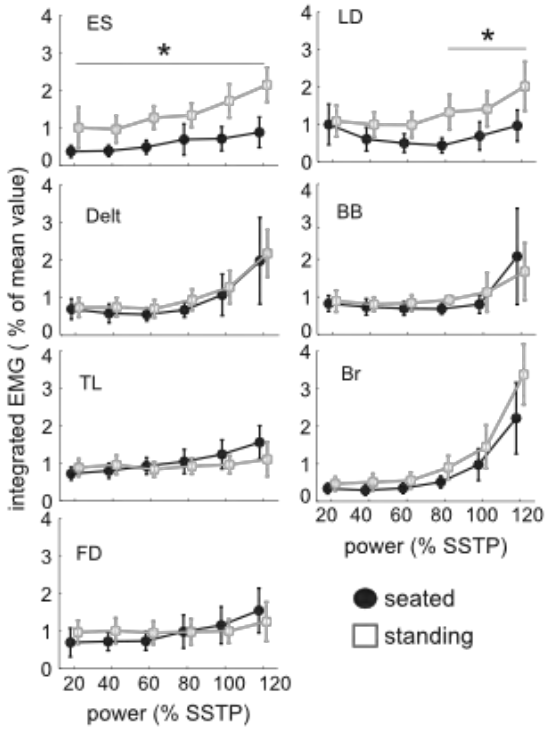

Figure 1. Integrated EMG activity. Power outputs are given in percentage of the seat-stand transition power (100% = 582 ± 103.7 Watts). Power outputs at which significant differences were found between seated and standing are indicated (*P < 0.05). ES: erector spinae-L4-L5 level; LD: latissimus dorsi; Delt: Anterior part of the deltoïdus; TL: tricep lateralis; BB: biceps brachii; Br: brachoradialis; FD: flexor digitorum.

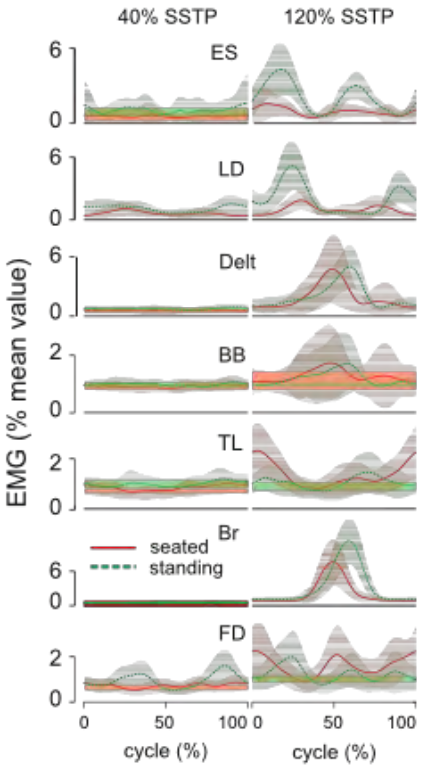

Figure 2. Averaged patterns of muscle activity. Patterns for all participants have been averaged (N = 17) at 40% and 120% of the seat-stand transition power (SSTP). The tick lines are the mean and the shaded areas represent ±1 SD. 0% and 100% of cycle correspond to the lowest position of the right pedal (or bottom dead centre). These two specific power outputs were chosen as they provide representative data at low and high power outputs. Note that BB, BR and Delt have very low levels of tonic activity at 40% of SSTP.

Table 1. Similarities and lags between the seated and standing activation patterns.

	Pearson's r	r-max	Lag (% cycle)	Peak occurrence (% cycle)	
				Seated	Standing
ES	0.313 ± 0.245	0.905 ± 0.043	1.8 ± 1.9*	41.9 ± 22.2	27.4 ± 17.1
LD	0.110 ± 0.401	0.840 ± 0.072	−2.1 ± 9.0	41.5 ± 18.7	39.0 ± 25.4
Delt	0.238 ± 0.308	0.956 ± 0.027	2.4 ± 4.1*	52.4 ± 15.1	58.1 ± 8.5
BB	0.039 ± 0.358	0.958 ± 0.017	2.3 ± 2.8	49.1 ± 8.1	55.6 ± 7.1
TL	0.412 ± 0.358	0.885 ± 0.000	1.2 ± 0.0	45.2 ± 40.9	60.7 ± 24.4
Br	0.415 ± 0.196	0.974 ± 0.010	3.5 ± 2.3*	51.7 ± 8.1	58.5 ± 6.7
FD	0.001 ± 0.290	0.884 ± 0.058	1.1 ± 5.4	58.4 ± 27.5	45.0 ± 23.1

Lag and r-max are defined in the section "Materials and methods". Peak occurrence is the percentage of cycle at which the maximum value of the EMG envelope is observed. Note that the differences between the occurrences of the peaks between seated and standing may differ from the lags because of the presence of several peaks in some muscle (e.g., ES, TL or FD). Significant lags are indicated with * (P < 0.05).

respectively; P = 0.142). Using this number, VAF was greater than 75% on average for all muscles in both positions. Seated VAF values ranged from 88.1 ± 12.5% (LD) to 97.3 ± 2.3% (FD) and standing values from 90.1 ± 11.5% (Br) to 98.2 ± 0.9% (BB), indicating good reconstruction rates. These synergies represent the relative balance between muscles that are activated simultaneously. The first synergy mainly activated LD, and to a lesser extent ES, Delt and BB (Figure 3(c)). Synergy #2 mainly activated Delt, BB and Br and synergy #3 TL, FD and ES. The correlation coefficients between the seated and standing synergies were 0.700 ± 0.226, 0.830 ± 0.170 and 0.727 ± 0.194 for synergies #1, #2 and #3, respectively, which is modest, and suggests differences in the weighting coefficients. These differences are indicated in Figure 3(c). The activation patterns of the synergies are depicted in Figure 3(d). Synergy #2 shifted forward in the cycle when standing, as compared to seated (Table 2, see also Figure 3 (d)). For synergies #1 and #3, changes in shape and timing occurred.

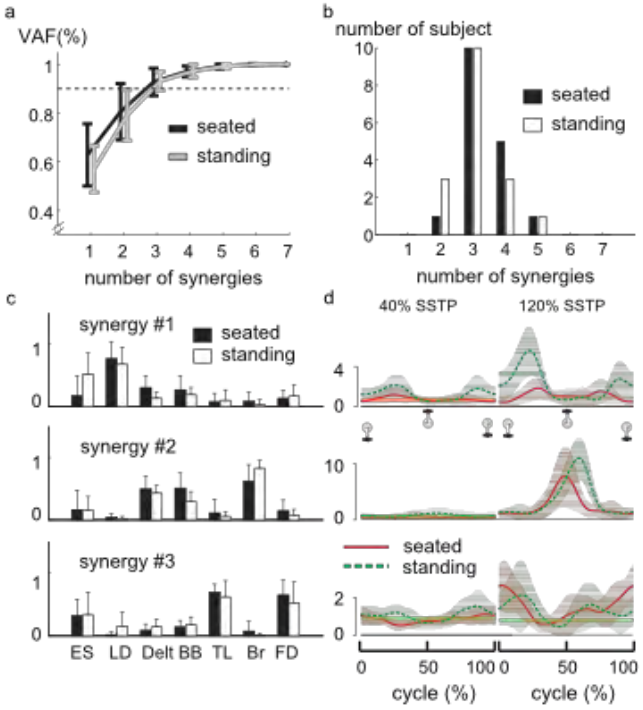

Figure 3. Muscle synergy analysis. (a) VAF versus number of synergies for the upper limbs (group data). The dashed line indicates 90% level. (b) Distribution of the number of synergies across participants. (c) Muscle synergies (group data). * indicates a significant difference between seated and standing ($P < 0.05$). (d) Averaged activation profiles of the three synergies at 40% and 120% of the seat-stand transition power (SSTP). The shaded areas represent ±1 SD. Dashed line: standing condition; solid line: seated condition.

Table 2. Similarities and lags for the synergies.

				Peak occurrence (% cycle)	
	Pearson's r	r-max	Lag (% cycle)	Seated	Standing
Synergy #1	0.084 ± 0.439	0.798 ± 0.086	−5.4 ± 16.1	42.8 ± 16.9	36.2 ± 26.0
Synergy #2	0.530 ± 0.249	0.919 ± 0.059	6.7 ± 5.0*	46.8 ± 11.2	55.5 ± 8.7
Synergy #3	0.241 ± 0.363	0.842 ± 0.086	1.1 ± 5.5	53.1 ± 29.2	51.8 ± 24.3

As in Table 1, the lags may differ from the occurrence of the peaks in some synergies (e.g., synergy #3) due to the presence of several peaks in their activation patterns. Significant lags are indicated with * ($P < 0.05$).

Discussion

One goal of this study was to clarify the roles of the upper limb and trunk muscles and to determine whether their activity patterns would be altered by power output or body position. The results revealed that most muscles had tonic activities at lower power outputs, which became more phasic as power increased. Change in position was associated with significant changes in the amplitude and timing of muscle activations. The analysis showed that the activity patterns of the upper limb muscles represent the combination of three muscle synergies, which were similar in both positions. Their functional roles are discussed below.

Synergy #1: stabilisation synergy

Duc et al. (2008) suggested that BB was involved in torso stabilisation and in controlling side-to-side leaning of the bicycle. This interpretation was confirmed by the observed reduction of arm muscle activation when bicycle tilts were constrained in their study. This assumption is reasonable, given the mechanical action of BB in such conditions (i.e., pulling the handlebar upward and backward) and given their particular timing, which corresponds to when the bicycle reaches maximum tilt angles (Soden & Adeyefa, 1979). The activation of BB at the ends of the downstrokes was also observed in our study before and after its main peak (i.e., ~30% and 80% of cycle while seated; Figure 2), but these bursts of activity were relatively small. Nevertheless, the same bursts could be observed in Delt and LD (mostly visible in the seated position) and these muscles then logically appeared in the same synergy (synergy #1). The absence of clear bursts in Delt and BB (compared with LD) while standing is consistent with their smaller weighting coefficients in this position (Figure 3). Synergy #1 may therefore represent a "stabilisation synergy". This interpretation is in agreement

with the mechanical actions of these muscles and with the observation that this synergy is more active in the standing position (Figure 3(d)) when stabilisation is more challenging. The need for stabilisation is reduced here but present as the application of uneven forces to both pedals tends to create a moment on the torso and to destabilise the upper body (Soden & Adeyefa, 1979).

Synergy #2: compensating for upward accelerations of the trunk and/or accelerating the trunk in the downward direction

The second synergy, involving the co-activation of BB, Br and Delt, was active during the activity of the knee extensors (i.e., 40–75% of cycle (Hug & Dorel, 2009; Hug et al., 2010)), which corresponds with the period in which Padulo et al. (2014) also observed BB activity. The activity of synergy #2 increased markedly after 80% of SSTP (~500 W) and was almost inactive at low power outputs. This likely explains why BB activity was observed during this period by Padulo et al. (2014), but not by Duc et al. (2008), whose study used respectively maximal and moderate power outputs.

In addition to being activated at similar moments in the cycle, we observed a similar temporal shift in the knee-extensor patterns and in the pattern of synergy #2 between the seated and standing positions (see Duc et al. (2008) or Hug et al. (2011) for comparison; see also the force patterns in Figure 4), which suggests (i) that they may indeed form a single synergy and (ii) that synergy #2 may play a role during power production. However, despite the high forces recorded at the pedal (~1000 N), Stone and Hull (1993) estimated the maximal arm muscle contribution to be about 15 W, which corresponds to less than 2% of the total power produced at the crank. The ~800 N value reported in Figure 4 suggests that this percentage may have been even lower in our study. Alternatively, Doré et al. (2006) proposed that "pulling upon the handle-bars, the center of mass of the whole body is maintained at a constant vertical level, so that leg extension can be directed to pushing down on the pedals". Interestingly, the large increase in the integrated EMG for the muscles of synergy #2 at high power output (Figure 1) is in agreement with this hypothesis, because it is likely linked to a trend to counteract the upward accelerations associated with upward pedal reaction forces. In other words, with increasing pedal forces, upward reaction forces acting on the trunk also

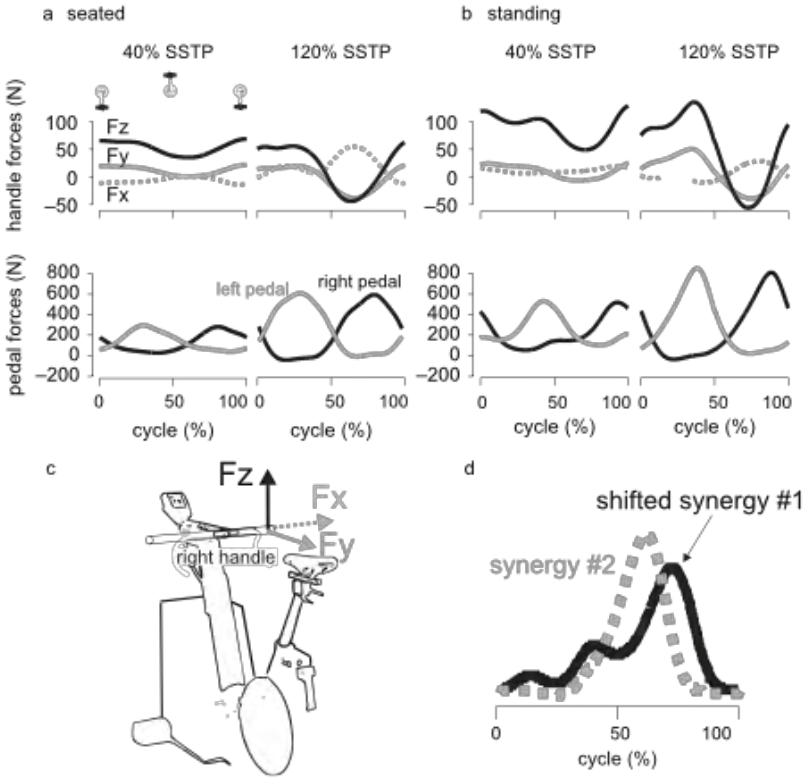

Figure 4. Handle and pedal forces. This figure depicts the forces of the right handle bar (on top) and of the right and left pedals (on the bottom) in the seated (a) and standing (b) positions. Data are in Newton and represent the averaged patterns over all participants (N = 17). The vertical components of the pedal forces are presented. The orientation of the three components of the handlebar forces is illustrated in panel (c). (d) Illustration of the difference between the timing of synergy #2 and the contralateral synergy #1 in the standing position at 120% of SSTP. The latter has been estimated as the temporal activation of synergy #1 (as in Figure 3 (d)) shifted by 50% of cycle. Because amplitudes of different synergy activations cannot be compared, these profiles are presented without dimension.

increase, and eventually tend to lift the upper body. This effect can be observed in the decrease of the baseline of the Fz component at the handlebar (Figure 4). At a certain point, the weight of the body may have been insufficient to counteract these forces, requiring additional forces from the arms. This interpretation may suggest that upper limb muscles do not necessarily produce power, but instead facilitate reaching the highest power outputs by providing stable support for leg actions. Nevertheless, the direct involvement of the arms muscle cannot be ruled out (Caldwell et al., 2000; Elmer et al., 2011). Because upper limb forces must be synchronised with those of the lower limbs, this also suggests that coordination between the muscles of synergy #2 and the knee-extensor muscles may be important in cycling performances, particularly when high power output is required.

In addition, we note that the activity of synergy #1 also markedly increased with power in the standing position, particularly during the downstroke of the contralateral leg (i.e., 0–45% of cycle, Figures 3(d) and 4(a,b). Other interesting observations were that (i) the pattern of this synergy at 120% represents a scaled version of the pattern at 40%, superimposed with a component occurring at 0–40% of the cycle and only when power was high. A simple interpretation would be that synergy #1 is a stabilisation synergy, acting at the end of downstrokes, and also contributes (directly or indirectly) to power production, particularly in the standing position and when high power is required. A recent study suggests that better performances in terms of bicycle acceleration are obtained when the arms are on the upper handlebar using a drop bar (Padulo et al., 2014). This difference in the position on the handlebar was associated with a marked increase in the LD activity level, especially during the downstroke of the contralateral leg (Padulo et al., 2014), which corresponds to the activity of synergy #1 in the present study. Although the number of muscles recorded was limited, these results suggest that this muscle (i.e., LD) may have contributed to the increase in acceleration. Synergy #1 may therefore act in cooperation with synergy #2 to either compensate for trunk accelerations in the upper direction or to accelerate the trunk in the downward direction (Figure 4(d)). Finally, as shown in Figure 4(d), the relative timing is distinct between synergy #1 and synergy #3 in the cycle.

Synergy #3: upper body weight support

The third synergy possessed a biphasic activity pattern and involved muscles that showed no larges variations with power output (i.e., TL and FD). This suggests that the muscles of this synergy were active at weak intensities. The muscles of this synergy tend to flex the wrist (FD), to push against the handlebar (TL) and to erect the trunk (ES), which points toward their role in supporting trunk weight. This interpretation is consistent with the fact that the major EMG burst occurred when the pedal was at its lowest point (i.e., at ~0% and 100% of cycle, Figure 3), when the body tended to be inclined toward the ipsilateral pedal.

Contrary to the study results of Duc et al. (2008), we found no significant differences in the activities of BB and TL between the seated and standing positions. It seems unlikely that the absence of differences is attributable to a limited sample size (i.e., N = 17). Other factors may explain these differences. For example, Duc et al. (2008) used a motorised treadmill, which allowed more significant lateral sways and imposed greater constraints on the upper limbs. They also used drop bars, which may have induced a more forward trunk position compared to the present study (see for example, Dorel, Couturier, and Hug (2009)). As such, greater body weight may have been supported by the arms in this particular position.

Conclusions

In this study, we identified three muscle synergies in upper limb and trunk muscles that are associated with (i) torso stabilisation, (ii) compensation/generation of trunk accelerations and (iii) upper body weight support. Large increases in the activities of synergy #1 and synergy #2 during critical power-production phases suggest that even if the arms do not produce substantial power output, their influence should not be neglected, particularly when the power output is high. Furthermore, in these conditions, coordination between the upper and lower limb muscles may play an important role in overall cycling performance.

Acknowledgements

AC was funded by a PhD grant from the French Ministry of Education and Research (Ministère de l'Education et de la Recherche). The authors are grateful to Dr Laurent Seitz for his help in language corrections.

Disclosure statement

No potential conflict of interest was reported by the authors.

Funding

AC was funded by a PhD grant from the French Ministry of Education and Research (Ministère de l'Education et de la Recherche).

References

Ansley, L., & Cangley, P. (2009). Determinants of "optimal" cadence during cycling. European Journal of Sport Science, 9(2), 61–85. doi:10.1080/17461390802684325

Arpinar-Avsar, P., Birlik, G., Sezgin, O. C., & Soylu, A. R. (2013). The effects of surface-induced loads on forearm muscle activity during steering a bicycle. Journal of Sports Science and Medicine, 12(3), 512–520.

Baker, J., Gal, J., Davies, B., Bailey, D., & Morgan, R. (2001). Power output of legs during high intensity cycle ergometry: Influence of hand grip. Journal of Science and Medicine in Sport, 4(1), 10–18. doi:10.1016/S1440-2440(01)80003-7

Baker, J. S., & Davies, B. (2009). Additional considerations and recommendations for the quantification of hand-grip strength in the measurement of leg power during high-intensity cycle ergometry. Research in Sports Medicine, 17(3), 145–155. doi:10.1080/15438620902897540

Barroso, F. O., Torricelli, D., Moreno, J. C., Taylor, J., Gomez-Soriano, J., Bravo-Esteban, E., … Pons, J. L. (2014). Shared muscle synergies in human walking and cycling. Journal of Neurophysiology, 112(8), 1984–1998. doi:10.1152/jn.00220.2014

Caldwell, G., van Emmerik, C., Hamill, J., & Sparrow, A. (2000). Movement proficiency: Incorporating task demands and constrains in assessing

human movement. In W. A. Sparrow (Ed.), Energetics of human activity (pp. 66–95). Champaign, IL: Human Kinetics.
Clarys, J. P., Cabri, J., & Antonis, J. (1989). EMG of up-hill racing — A new qualitative approach of cyclic movements. Journal of Biomechanics, 22 (10), 997. doi:10.1016/0021-9290(89)90153-X
Costes, A., Turpin, N. A., Villeger, D., Moretto, P., & Watier, B. (2015). A reduction of the saddle vertical force triggers the sit-stand transition in cycling. Journal of Biomechanics, 48(12), 2998–3003. doi:10.1016/j.jbiomech.2015.07.035
de Vey Mestdagh, K. (1998). Personal perspective: In search of an optimum cycling posture. Applied Ergonomics, 29(5), 325–334. doi:10.1016/S0003-6870(97)00080-X
Doré, E., Baker, J. S., Jammes, A., Graham, M., New, K., & Van Praagh, E. (2006). Upper body contribution during leg cycling peak power in teenage boys and girls. Research in Sports Medicine: An International Journal, 14(4), 245–257. doi:10.1080/15438620600985829
Dorel, S., Couturier, A., & Hug, F. (2009). Influence of different racing positions on mechanical and electromyographic patterns during pedalling. Scandinavian Journal of Medicine & Science in Sports, 19(1), 44–54. doi:10.1111/j.1600-0838.2007.00765.x
Duc, S., Bertucci, W., Pernin, J. N., & Grappe, F. (2008). Muscular activity during uphill cycling: Effect of slope, posture, hand grip position and constrained bicycle lateral sways. Journal of Electromyography and Kinesiology, 18(1), 116–127. doi:10.1016/j.jelekin.2006.09.007
Elmer, S. J., Barratt, P. R., Korff, T., & Martin, J. C. (2011). Joint-specific power production during submaximal and maximal cycling. Medicine & Science in Sports & Exercise, 43(10), 1940–1947. doi:10.1249/MSS.0b013e31821b00c5
Grant, M. C., Watson, H., & Baker, J. S. (2015). Assessment of the upper body contribution to multiple-sprint cycling in men and women. Clinical Physiology and Functional Imaging, 35(4), 258–266. doi:10.1111/cpf.12159
Hug, F. (2011). Can muscle coordination be precisely studied by surface electromyography? Journal of Electromyography and Kinesiology, 21(1), 1–12. doi:10.1016/j.jelekin.2010.08.009
Hug, F., & Dorel, S. (2009). Electromyographic analysis of pedaling: A review. Journal of Electromyography and Kinesiology, 19(2), 182–198. doi:10.1016/j.jelekin.2007.10.010
Hug, F., Turpin, N. A., Couturier, A., & Dorel, S. (2011). Consistency of muscle synergies during pedaling across different mechanical constraints. Journal of Neurophysiology, 106(1), 91–103. doi:10.1152/jn.01096.2010
Hug, F., Turpin, N. A., Guevel, A., & Dorel, S. (2010). Is interindividual variability of EMG patterns in trained cyclists related to different muscle synergies? Journal of Applied Physiology, 108, 1727–1736. doi:10.1152/japplphysiol.01305.2009
Jones, N. L., Makrides, L., Hitchcock, C., Chypchar, T., & McCartney, N. (1985). Normal standards for an incremental progressive cycle ergometer test. American Review of Respiratory Diseases, 131(5), 700–708.
Kautz, S. A., & Brown, D. A. (1998). Relationships between timing of muscle excitation and impaired motor performance during cyclical lower extremity movement in post-stroke hemiplegia. Brain, 121(3), 515–526. doi:10.1093/brain/121.3.515
Lee, D. D., & Seung, H. S. (2001). Algorithms for non-negative matrix factorization. Advances in Neural Information Processing Systems, 13, 556–562.
Martin, J. C., & Brown, N. A. (2009). Joint-specific power production and fatigue during maximal cycling. Journal of Biomechanics, 42(4), 474–479. doi:10.1016/j.jbiomech.2008.11.015
Padulo, J., Laffaye, G., Bertucci, W., Chaouachi, A., & Viggiano, D. (2014). Optimisation of starting conditions in track cycling. Sport Sciences for Health, 10(3), 189–198. doi:10.1007/s11332-014-0192-y
Raasch, C. C., & Zajac, F. E. (1999). Locomotor strategy for pedaling: muscle groups and biomechanical functions. Journal of Neurophysiology, 82(2), 515–525.
Soden, P. D., & Adeyefa, B. A. (1979). Forces applied to a bicycle during normal cycling. Journal of Biomechanics, 12(7), 527–541. doi:10.1016/0021-9290(79)90041-1
Stone, C., & Hull, M. L. (1993). Rider/bicycle interaction loads during standing treadmill cycling. Journal of Applied Biomechanics, 9, 202–202.
Tanaka, H., Bassett Jr., D. R, Jr., Best, S. K, & Baker Jr., K. R, Jr. (1996). Seated versus standing cycling in competitive road cyclists: Uphill climbing and maximal oxygen uptake. Canadian Journal of Applied Physiology, 21(2), 149–154. doi:10.1139/h96-013
Ting, L., & McKay, J. (2007). Neuromechanics of muscle synergies for posture and movement. Current Opinion in Neurobiology, 17(6), 622–628. doi:10.1016/j.conb.2008.01.002
Turpin, N. A., Guevel, A., Durand, S., & Hug, F. (2011a). Fatigue-related adaptations in muscle coordination during a cyclic exercise in humans. Journal of Experimental Biology, 214(19), 3305–3314. 214/19/3305 [pii]. doi:10.1242/jeb.057133
Turpin, N. A., Guével, A., Durand, S., & Hug, F. (2011b). No evidence of expertise-related changes in muscle synergies during rowing. Journal of Electromyography and Kinesiology, 21, 1030–1040. S1050-6411(11)00110-6 [pii]. doi:10.1016/j.jelekin.2011.07.013.
Yang, J. F., & Winter, D. A. (1984). Electromyographic amplitude normalization methods: Improving their sensitivity as diagnostic tools in gait analysis. Archives in Physical Medicine and Rehabilitation, 65(9), 517–521.

III.5. Etude 3 : Augmentation de puissance et Mesure des Efforts Appliques sur la Bicyclette

Ce deuxième article intitulé « Increasing Power Output and Movement Optimization in Cycling: Insights from a Fully Instrumented Cycling Ergometer » a été accepté et présenté lors du 33ème Congrès de la Société Internationale de Biomécanique du Sport le 30 Juin 2015 à Poitiers (France). A la suite de l'analyse des actions mécaniques effectuées par le membre supérieur et pour expliquer les tractions sur le cintre observées en position assise à partir du niveau de puissance correspondant à la transition spontanée en danseuse, l'hypothèse d'une explication mécanique a été évoquée. La première étape a été de définir les positions « assis » et « danseuse » d'un point de vue mécanique. De ce point de vue, la position assise est définie par la présence d'une force verticale sur la selle, et celle en « danseuse » par l'absence de cette force. L'hypothèse de recherche était donc « évidente » : la force verticale à la selle diminuerait lorsque la puissance de pédalage augmente. Pour compléter cette analyse, les efforts verticaux appliqués sur les pédales et le cintre ont aussi été mesurés. Les résultats montrent une diminution significative de la force verticale appliquée sur la selle (de $5,3 \pm 0,5$ N.kg^{-1} à $0,68 \pm 0,5$ N.kg^{-1}) lorsque la puissance de pédalage augmente (de $1,6 \pm 0,3$ W.kg^{-1} à $9,6 \pm 1,6$ W.kg^{-1}) pour une cadence de pédalage constante de 90 rotations par minute. D'autre part, il est à noter que des actions de traction sur le cintre et sur les pédales sont observées à partir du niveau de puissance correspondant à la transition spontanée en danseuse. En conclusion, il semble que le niveau de force verticale appliqué sur la selle soit un critère déterminant pour le déclenchement de la transition spontanée vers la position en danseuse. Les efforts de traction observés au niveau du cintre et des pédales indiquent des possibilités mécaniques pour continuer à pédaler assis malgré la baisse de la force appliquée sur la selle. Est-il possible d'établir un lien physique entre ces différentes forces ?

INCREASING POWER OUTPUT AND MOVEMENT OPTIMIZATION IN CYCLING: INSIGHTS FROM A FULLY INSTRUMENTED ERGOMETER

Antony Costes[1], Nicolas A. Turpin[1,2], David Villeger[1], Pierre Moretto[3,4] and Bruno Watier[5,6]

University of Toulouse, UPS, PRISSMH, Toulouse, France[1]
CRIR, Institut de Réadaptation Gingras-Lindsay de Montréal and Jewish Rehabilitation Hospital, Laval, Quebec, Canada[2]
University of Toulouse, UPS, CRCA, Toulouse, France[3]
CNRS, CRCA, Toulouse, France[4]
University of Toulouse, UPS, LAAS, Toulouse, France[5]
CNRS, LAAS, Toulouse, France[6]

We hypothesized that the saddle vertical force would be a critical parameter to explain the sit-to-stand transition during cycling. Twenty-five participants were required to pedal at six different powers ranging from 20 (1.6 ± 0.3 $W.kg^{-1}$) to 120% (9.6 ± 1.6 $W.kg^{-1}$) of their Sit-to-Stand Transition Power (SSTP) at 90 RPM. Five 6-component sensors recorded the loads applied on the saddle, pedals and handlebars. The results showed that the saddle vertical force decreased with increasing cycling power, from a static position on the bicycle (5.30 ± 0.50 $N.kg^{-1}$) to 120% of SSTP (0.68 ± 0.49 $N.kg^{-1}$). Pedal and handlebar force directions were reversed around SSTP, suggesting that the seated position may become constraining in these pedalling conditions. These results suggest that the saddle vertical reaction force may be predictive of the sit-to-stand transition in cycling, and that pedalling in the seated position at high crank forces add constraints on the cyclist, explaining the spontaneous change in coordination mode.

KEY WORDS: seated position, standing position, 6-component sensors.

INTRODUCTION: Most of the investigations in cycling biomechanics focused on the lower limb actions despite evidences that the whole body can be involved, and only a few studies reported the forces applied on the handlebar and/or on the saddle (Bolourchi & Hull, 1985; Wilson & Bush, 2007). However, the spontaneous full-body organisation in response to increasing pedalling power still needs to be described. The purpose of this study was to measure the force patterns applied by the cyclist on all his supports in order to explain why a spontaneous transition from the seated to the standing position is observed for a given cycling power. By using the simplest definitions of the seated (a vertical force applied on the saddle), and standing positions (lack of vertical force applied on the saddle), we hypothesized that the saddle vertical reaction force would be the critical parameter to explain this transition. Indeed, given the constraint of increasing pedal forces, the body weight may no longer be supported by the saddle, which may lead the cyclist to create additional forces on his supports in order to keep pedalling seated at a given level of efficient pedal forces (i.e. crank power for a given pedalling cadence).

METHODS: After a standardized bike positioning, 25 non-elite cyclists (23.2 ± 3.6 y, 1.77 ± 0.06 m, 71.5 ± 9.1 kg) were weighted on the ergocycle (LODE, Groningen, Netherlands) in order to measure a static level of saddle vertical force. This weight was determined with a horizontal crank position, and with 0.5 m between the two hands in prone position on the flat handlebar. Then, they performed an incremental test to determine their spontaneous Sit-to-Stand Transition Power (SSTP). In this protocol, active bouts of effort (20 s at 200 W + 25 W by increment) were alternated with recovery periods (40 s at 50 W), with a 90 RPM pedalling cadence. The power corresponding to SSTP was defined as the power at which the participant rose spontaneously from the saddle during 10 s. After five minutes of rest, 6 randomized trials of 10 s were performed in the seated position, with cycling powers ranging from 20 to 120% of SSTP, with 3 minutes of passive rest between each.
During these trials, the reaction forces applied on the handlebars, the saddle tube, and the pedals were recorded from three tubular sensors (SENSIX, Poitiers, France), and by two instrumented

pedals (I-Crankset-1, SENSIX, Poitiers, France) at a sampling frequency of 1 kHz. Three passive markers were positioned on each sensor, and their position recorded with twelve infrared cameras (VICON, Oxford, United-Kingdom) at 200 Hz. Kinetic and kinematic data were synchronized using Nexus 1.7.1 system (VICON, Oxford, United-Kingdom) and filtered using a 4th order, zero phase-shift, low-pass Butterworth with a 8 Hz cutoff frequency (McDaniel, Behjani, Elmer, Brown, & Martin 2014). Data analyses were performed using Scilab 5.4.0 (SCILAB, Scilab Enterprises). In the present study, only the vertical component of the 3D reaction forces expressed in the laboratory reference frame were considered. All statistical analyses were performed using the STATISTICA software (STATSOFT, Maisons-Alfort, France). A p-value of 0.05 was defined as the level of statistical significance.

RESULTS: The cycling power corresponding to the sit-to-stand transition was 568 ± 93 W (8.0 ± 1.4 W.kg^{-1}). Thus, cycling powers corresponding from 20 to 120% ranged from 114 ± 19 W (1.6 ± 0.3 W.kg^{-1}) to 682 ± 111W (9.6 ± 1.6 W.kg^{-1}). Because of the constant pedaling cadence imposed, increases in power output lead to equivalent increases in effective force production on the pedals.
The static vertical reaction force on the saddle was 5.30 ± 0.50 N.kg^{-1}.
The minimum and maximum saddle vertical reaction forces observed during one pedal revolution for each cycling power are presented in Figure 1A. The minimum reaction force decreased with increasing cycling power by 87% from a static position on the bicycle (5.30 ± 0.50 N.kg^{-1}) to 120% of SSTP (0.68 ± 0.49 N.kg^{-1}). SSTP corresponded to a minimum value of saddle vertical force of 0.99 ± 0.50 N.kg^{-1}. Saddle vertical reaction force patterns are represented in a descriptive purpose in Figure 1B.

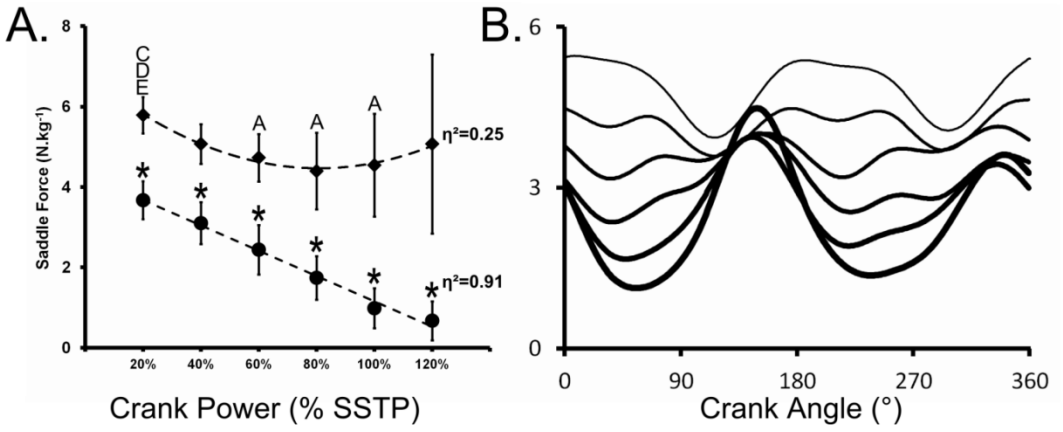

Figure 1: A. Maximum and minimum saddle vertical reaction force. *: difference with all other crank powers. A, B, C, D, E, and F: difference in comparison to 20, 40, 60, 80, 100, and 120% of SSTP, respectively. η²: partial eta-squared. B. Saddle vertical reaction force patterns along one right crank pedal cycle averaged for the participants. The wider line corresponds to the higher crank power.

The minimum and maximum pedal and handlebar vertical reaction forces during one pedal revolution are presented in Figure 2. Maximum pedal vertical reaction forces increased with cycling power (R^2 = 0.998 and 0.999 for the left, and right pedal, respectively), while minimum pedal vertical reaction forces decreased with cycling power and became negative above 80% of SSTP.
Minimum handlebar vertical reaction forces decreased with cycling power and became negative from SSTP.

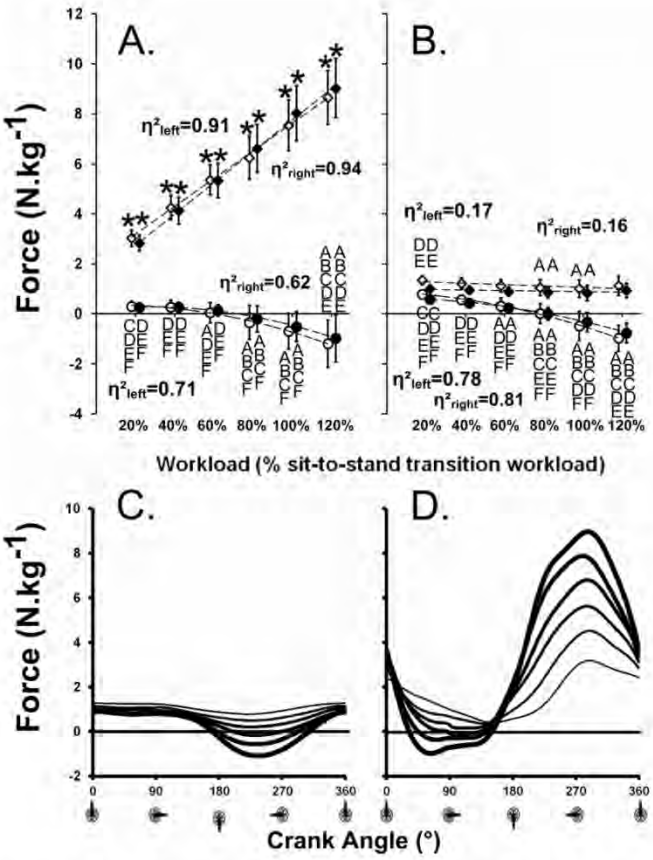

Figure 2: Minimum (dots) and maximum (diamonds) left (white), and right (black) vertical reaction forces. A. Pedals. B. Handlebars. *: difference with all other crank powers. A, B, C, D, E, and F: difference in comparison to 20, 40, 60, 80, 100, and 120% of SSTP, respectively. η^2: partial eta-squared. C. and D. Left handlebar and left pedal vertical reaction force patterns along one right crank pedal cycle averaged for the participants, respectively. The wider line corresponds to the higher crank power.

DISCUSSION: In the present investigation, we hypothesized that the saddle vertical force would decrease with increasing pedal forces and would predict the sit-to-stand transition in cycling. Our results support our hypothesis as a strongly linear relationship was observed between the saddle vertical reaction force and cycling power (Figure 1). The sit-to-stand transition occurred at minimum saddle vertical force of about 1 $N.kg^{-1}$. Handlebar and pedal reaction forces also showed interesting evolutions, with their minima tending to be negative around SSTP (Figure 2). A plausible explanation may be that the inversion in the direction of these forces corresponds to a trend to counteract the upward acceleration linked to upward pedal reaction forces (i.e. pulling on the pedal and on the handlebar to remain seated). Previous studies have shown that pulling on the pedals, although increasing the mechanical effectiveness of pedaling, was detrimental to the metabolic efficiency (Edwards, Jobson, George, Day, & Nevill, 2009; Korff, Romer, Mayhew, & Martin, 2007), and was a strategy opposite to the one employed by elite cyclists (Coyle et al., 1991).

Similarly to pedal traction, pulling on the handlebar is associated with an important metabolic cost, increasing with the pedal force (McDaniel, Subudhi, & Martin, 2005).

However, at the power output at which the part of the body weight supported by the saddle was compensated by the upward pedal reaction forces, both pedal and handlebar pulling forces shared a common interest in counterbalancing these pedal forces, and allowing to stay seated by adding

vertical force on the saddle. Given the length of the measurements in this study, the downward forces created on the pedals and handlebars allowed to temporarily keep pedaling in the seated position despite their metabolic cost, a strategy presumably impossible to hold for longer durations. These results suggest that the standing position may be preferred at a given level of pedal force due to an increase in the necessity to create these downward reaction forces and/or because of the fact that the saddle becomes useless to carry the body weight.

CONCLUSION: Because of the high vertical reaction forces applied by the pedals at high crank power, the saddle vertical force dramatically decreased, which may have triggered the sit-to-stand transition. This spontaneous transition occurred at minimum saddle vertical force of about 1 $N.kg^{-1}$. The strong relationship between saddle vertical force and cycling power for a given pedaling cadence suggests that SSTP can be predicted with this value of saddle vertical force. Behaviors counteracting the upward vertical pedal forces were observed around the power corresponding to SSTP by studying handlebar and pedal forces, suggesting that the spontaneous choice to rise in the standing position may be a solution to reduce these constraints. In addition, this study suggests that improving bike settings and considering the specificities imposed by high force pedaling on the whole body during training may improve cycling performance. Clinicians, researchers, and manufacturers trying to understand the etiology of groin injuries and erectile dysfunction associated with cycling (Lowe, Schrader, & Breitenstein, 2004; Carpes, Dagnese, Kleinpaul, Martins, & Mota, 2009) should also consider which factors can influence saddle forces.

REFERENCES:

Bolourchi, F. & Hull, M.A. (1985). Measurement of Rider Induced Loads During Simulated Bicycling. *Int. J.Sports Biomech*, 1, 308–329.

Carpes, F.P., Dagnese, F., Kleinpaul, J.F., Martins, E. & Mota, C.B. (2009). Bicycle Saddle Pressure: Effects of Trunk Position and Saddle Design on Healthy Subjects. *Urol. Int*, 82, 8–11.

Coyle, E.F., Feltner, M.E., Kautz, S.A., Hamilton, M.T., Montain, S.J., Baylor, A.M., Abraham, L.D. & Petrek, G.W. (1991). Physiological and biomechanical factors associated with elite endurance cycling performance. *Med. Sci. Sports Exerc*, 23, 93–107.

Edwards, L.M., Jobson, S.A., George, S.R., Day, S.H. & Nevill, A.M. (2009). Whole-body efficiency is negatively correlated with minimum torque per duty cycle in trained cyclists. *J. Sports Sci*, 27, 319–325.

Korff, T., Romer, L.M., Mayhew, I. & Martin, J.C. (2007). Effect of pedaling technique on mechanical effectiveness and efficiency in cyclists. *Med. Sci. Sports Exerc*, 39, 991–995.

Lowe, B.D., Schrader, S.M. & Breitenstein, M.J. (2004). Effect of bicycle saddle designs on the pressure to the perineum of the bicyclist. *Med. Sci. Sports Exerc*, 36, 1055–1062.

McDaniel, J., Behjani, N.S., Elmer, S.J., Brown, N.A. & Martin, J.C. (2014). Joint-specific power-pedaling rate relationships during maximal cycling. *J. Appl. Biomech*, 30, 423–430.

McDaniel, J., Subudhi, A. & Martin, J.C. (2005). Torso stabilization reduces the metabolic cost of producing cycling power. *Can. J. Appl. Physiol*, 30, 433–441.

Wilson, C. & Bush, T.R. (2007). Interface forces on the seat during a cycling activity. *Clin. Biomech*, 22, 1017–1023.

Acknowledgement

Antony Costes was funded by a PhD grant from the French Ministry of Education and Research (Ministère de l'Education et de la Recherche). The authors would like to thanks Dr. Laurent Seitz for his review of the manuscript.

III.6. ETUDE 4 : UNE DIMINUTION DE LA FORCE VERTICALE SUR LA SELLE DECLENCHE LA TRANSITION ASSIS-DANSEUSE

Ce troisième article intitulé « A Reduction of the Saddle Vertical Force Triggers the Sit-Stand Transition in Cycling » a été accepté et publié dans la revue « Journal of Biomechanics ». Afin d'approfondir l'analyse effectuée dans l'article précédent, l'objectif de cet article a été d'établir un lien entre la force verticale appliquée sur la selle et les autres forces appliquées par et sur un cycliste. Par une application de la 2nde loi de Newton sur le tronc d'un cycliste, rendue possible par l'application d'un procédé de dynamique inverse sur chacun de ses appuis, une équation simple a été proposée afin de rendre compte de l'état d'équilibre entre les différentes forces appliquées sur le cycliste. Cette équation (Equation 1 dans l'article ci-après) a aussi fourni une possibilité de vérification de la précision du procédé de dynamique inverse utilisé pour ces travaux de thèse. Les résultats de cette étude ont montré une réduction de la force verticale appliquée sur la selle en association avec l'augmentation du niveau de puissance au pédalier (pour une cadence fixée à 90 rotations par minute). D'après le modèle utilisé, cette diminution de la force verticale à la selle est principalement expliquée par une augmentation des forces verticales appliquées sur les pédales, qui par réaction tend à créer une force verticale sur les hanches, provoquant elle-même une tendance à élever le tronc. Pour éviter une élévation du tronc par des forces dépassant son poids, des stratégies compensatoires sont nécessaires. Comme montré dans l'article précédent, ces dernières consistent en une traction sur les pédales et le cintre, et par des accélérations du tronc vers le bas en synchronisation avec les efforts sur les pédales. En conclusion, ces données suggèrent que la diminution de la force verticale appliquée sur la selle pourrait être un déclencheur de la transition spontanée en danseuse, et que pédaler à haut niveau de force en position assise implique de nouvelles contraintes mécaniques associées au maintien d'un niveau de force verticale minimal sur la selle. Par ailleurs, cet article a permis une quantification et une forme de validation de la précision du procédé de dynamique inverse utilisé dans ces travaux.

Journal of Biomechanics ∎ (∎∎∎∎) ∎∎∎–∎∎∎

Contents lists available at ScienceDirect

Journal of Biomechanics

journal homepage: www.elsevier.com/locate/jbiomech
www.JBiomech.com

A reduction of the saddle vertical force triggers the sit–stand transition in cycling

Antony Costes [a,*], Nicolas A. Turpin [a,b], David Villeger [a], Pierre Moretto [c,d], Bruno Watier [e,f]

[a] University of Toulouse, UPS, PRISSMH, 118 Route de Narbonne, 31062 Toulouse Cedex 9, France
[b] Center for Interdisciplinary Research in Rehabilitation (CRIR), Institut de Réadaptation Gingras-Lindsay de Montréal and Jewish Rehabilitation Hospital, Laval, Quebec, Canada
[c] University of Toulouse, UPS, CRCA, 118 route de Narbonne, F-31062 Toulouse Cedex 9, France
[d] CNRS, CRCA, 118 route de Narbonne, F-31062 Toulouse Cedex 9, France
[e] CNRS, LAAS, 7 Avenue du Colonel Roche, F-31400 Toulouse, France
[f] University of Toulouse, UPS, LAAS, F-31400 Toulouse, France

ARTICLE INFO

Article history:
Accepted 30 July 2015

Keywords:
Inverse dynamics
Pedaling
SEAT
STAND

ABSTRACT

The purpose of the study was to establish the link between the saddle vertical force and its determinants in order to establish the strategies that could trigger the sit–stand transition. We hypothesized that the minimum saddle vertical force would be a critical parameter influencing the sit–stand transition during cycling. Twenty-five non-cyclists were asked to pedal at six different power outputs from 20% (1.6 ± 0.3 W kg^{-1}) to 120% (9.6 ± 1.6 W kg^{-1}) of their spontaneous sit–stand transition power obtained at 90 rpm. Five 6-component sensors (saddle tube, pedals and handlebars) and a full-body kinematic reconstruction were used to provide the saddle vertical force and other force components (trunk inertial force, hips and shoulders reaction forces, and trunk weight) linked to the saddle vertical force. Minimum saddle vertical force linearly decreased with power output by 87% from a static position on the bicycle (5.30 ± 0.50 N kg^{-1}) to power output = 120% of the sit–stand transition power (0.68 ± 0.49 N kg^{-1}). This decrease was mainly explained by the increase in instantaneous pedal forces from 2.84 ± 0.58 N kg^{-1} to 6.57 ± 1.02 N kg^{-1} from 20% to 120% of the power output corresponding to the sit–stand transition, causing an increase in hip vertical forces from -0.17 N kg^{-1} to 3.29 N kg^{-1}. The emergence of strategies aiming at counteracting the elevation of the trunk (handlebars and pedals pulling) coincided with the spontaneous sit–stand transition power. The present data suggest that the large decrease in minimum saddle vertical force observed at high pedal reaction forces might trigger the sit–stand transition in cycling.

1. Introduction

Seated (SEAT) and Standing (STAND) are the two common positions chosen during bicycle locomotion. Several studies comparing the two positions have shown that spontaneous pedaling cadences are slower in STAND than in SEAT position (Harnish et al., 2007; Lucía et al., 2001), and that the STAND position is associated with the highest power outputs (McLester et al., 2004; Millet et al., 2002; Reiser et al., 2002). Furthermore, the fact that cyclists tend to spontaneously switch from SEAT to STAND when high force applied to the pedals are needed (i.e. during fast accelerations or steep climb ascensions) suggests that the change in position favors a maximization of the pedal reaction forces (Hansen and Waldeland, 2008). However, the parameters leading to select one position over the other one in order to produce a given combination of pedal reaction force and power output need to be clarified.

Many attempts have been made to understand the mechanisms underlying these positions, particularly to determine the superiority of the STAND position to produce higher power outputs and pedal reaction forces. From a joint torque perspective, a study using the moment cost function defined by Gonzalez and Hull (1989) presented a slight reduction of this cost function above the sit–stand transition power (Poirier et al., 2007), whereas lower limbs net joint torques have been described by others as increasing in STAND position for both the ankle plantarflexion and the knee extension (Caldwell et al., 1999; Li and Caldwell, 1998). From a metabolic energy consumption perspective, the SEAT position has been shown to be more efficient to produce lower power outputs (Ryschon and Stray-Gundersen, 1991; Tanaka et al., 1996), and equally efficient as the STAND one to produce high power

* Corresponding author. Tel.: +33 5 61 55 64 40; fax: +33 5 61 55 82 80.
E-mail address: antony.costes@univ-tlse3.fr (A. Costes).

http://dx.doi.org/10.1016/j.jbiomech.2015.07.035
0021-9290/

outputs (Harnish et al., 2007; Millet et al., 2002; Tanaka et al., 1996). Regarding studies using electromyography, the literature suggests that differences in the temporal profiles and in the level of activation of the muscles could be expected between SEAT and STAND (Li and Caldwell, 1998; Hug et al., 2011). For example, Duc et al. (2008) reported a slight decrease for the *semimembranosus* activation from SEAT to STAND, whereas Li and Caldwell (1998) reported increased activations of the *gluteus maximus, tibialis anterior* and *rectus femoris* muscles in STAND position. These differences may influence the coordination patterns in both positions (De Marchis et al., 2013). Nonetheless, the muscle synergies activated in the two positions may remain similar (Hug et al., 2011) and the literature does not provide evidences of an advantage of one position against the other at this level.

Since there is no obvious reason to prefer the STAND rather than the SEAT position to produce one given power output, we propose in this study to reverse the questioning and to wonder why the SEAT position is no longer chosen, instead of why the STAND position may become optimal beyond a given level of crank power. To test our hypotheses, we first propose a criterion that could clearly distinguish the two positions: the SEAT position is characterized by a contact between the cyclist and the saddle (i.e. a vertical force is applied by the cyclist on the saddle) whereas the STAND position is characterized by the absence of this vertical force. In this definition, the force applied by the cyclist on the saddle (and reciprocally) is of central interest, and the sit–stand transition is defined by the disappearance of this force.

To the best of our knowledge, only three studies measured saddle forces in cycling. The first one presented saddle force at three pedaling cadences and described a double period pattern with maximum magnitudes decreasing as cadence decreases (Bolourchi and Hull, 1985). However, the second study did not found this double period pattern (Stone and Hull, 1995) while the third one observed both of these patterns (Wilson and Bush, 2007). To better understand this phenomenon, we propose to investigate the saddle force patterns. According to Newton's second law, this force is the result of a simple mechanical interaction between the cyclist's body weight and the other forces applied on his bicycle. Consequently, a downward vertical force applied on the pedal would result by reaction in an upward force on the hip, accelerating the trunk in an upward direction, and decreasing the force applied on the saddle by the cyclist. Therefore, we propose to measure vertical forces applied on the saddle, in complement with the other forces acting on the trunk of the cyclist (i.e. hips and shoulders reaction forces, trunk weight, and acceleration of the trunk's center-of-mass) at different pedal reaction forces. The aims of this study are to validate a full-body inverse dynamics model of cycling and to test the hypothesis that saddle vertical force would decrease and reach values close to zero with increasing pedal forces, making the SEAT position irrelevant given its definition and leading the cyclist to spontaneously adopt the STAND position.

2. Methods

2.1. Participants

Twenty five male sport science students (23.2 ± 3.6 y, height 1.77 ± 0.06 m, body mass 71.5 ± 9.1 kg) volunteered for this investigation. The participants were non-cyclists and belonged to category 4–5 according to Ansley and Cangley (2009) classification. Each participant was informed of the experimental procedure and signed an informed consent form prior to the study. The study was conducted in accordance with the declaration of Helsinki and was approved by the University of Toulouse ethical committee. Participants were asked to avoid high-intensity or exhaustive exercise at least 72 h before the laboratory trials.

2.2. Experimental protocol

The cycling tests were performed using an electromagnetically braked cycle ergometer Excalibur (LODE, Groningen, Netherlands). To limit bike positioning effects, standardized settings were adopted. Briefly, pedal cleats were positioned under the first metatarsal bone (Viker and Richardson, 2013), the saddle height was set at a 150° knee angle during maximum leg extension, the seat tube angle was set to 73°, the crank length was 0.17 m in length and the handlebar was flat. The latter was positioned to standardize drop (the vertical distance between the top of the saddle and the handlebar mediolateral axis) and reach (the horizontal distance between the back of the saddle and the handlebar mediolateral axis) lengths according to torso and arm lengths (De Vey Mestdagh, 1998). The mediolateral positioning of the two hands on the handlebar was left up to the participant (handlebar width: 0.7 m).

After bike positioning, participants were first weighed on the cycle ergometer in order to measure a static level of saddle vertical force (representing 0% of the sit–stand transition power). This weighing was made with the shoes fixed on the pedals, the hands on the handlebars, and the cranks in horizontal position. Then, after a five-minute warm-up at 100 W, they performed a cycling test to determine their spontaneous sit–stand transition power (Fig. 1). In this test, phases of 20 s with a starting power output of 200 W incremented by 25 W at each step rest were alternated with rest phases of 40 s at a power output of 50 W. The sit–stand transition power was considered as the power output at which participants rose from the saddle during at least 10 s. A visual feedback of the pedaling cadence was provided to the participants who were instructed to maintain it at 90 ± 5 rpm.

Then, after a five-minute rest period, participants performed six randomized trials at power output corresponding to 20%, 40%, 60%, 80%, 100% or 120% of their sit–stand transition power and were asked to remain seated throughout these sequences. Each pedaling trial began with a minimum stabilization time of 10 s at the target power output at 90 rpm, followed by 10 s of data recording. Three minutes of passive rest were given between each of these six trials.

2.3. Data acquisition

The 3D force and moment components applied to the handlebar, saddle tube and pedals were recorded from three tubular sensors (SENSIX, Poitiers, France), and by two instrumented pedals (I-Crankset-1, SENSIX, Poitiers, France) at 1 kHz (Fig. 2). According to the manufacturer, these dynamometers had a maximum 1% error on each direction (combining linearity and hysteresis errors), and a maximum 1.5% error on the 6 components combination.

Kinematics data were collected from 56 passive markers recorded by twelve infrared cameras (VICON, Oxford, United-Kingdom) at 200 Hz. The kinetics sensors' reference points were defined as shown in Fig. 2. The ankle (because of the impossibility to stick one kinematic marker on the *medial malleollus* in reason of the crank proximity), shoulder and hip joint centers were located using the SCoRE method (Ehrig et al., 2006). For this method, a preliminary recording asking the participants to repeat flexion–extension, abduction–adduction and circumduction of the tested joint allowed the localization of their centers-of-rotation (Begon et al., 2007). Body segments masses, center-of-mass positions, and radii of gyration were defined in accordance with De Leva's (1996) anthropometric charts. All kinetics and kinematics data were recorded in three-dimensions.

2.4. Data reduction and analysis

Kinetics and kinematics data were synchronized using Nexus 1.7.1 system (VICON, Oxford, United-Kingdom) and filtered using a 4th order, zero phase-shift, low-pass Butterworth with a 8 Hz cutoff frequency (McDaniel et al., 2014). In order to determine the factors affecting the saddle vertical force, the trunk was represented (comprising the head and the pelvis) as being submitted to external forces applied on the shoulders, hips, and saddle contact. The following equality has been computed by isolating the head and trunk solid according to Newton's second law:

$$F_s = m_t a_t - (W_t + F_h + F_{sh}) \quad (1)$$

where m_t is the mass of the head and trunk solid according to De Leva's anthropometric chart, a_t is the linear acceleration of the head and trunk center-of-mass, W_t is the sum of the head and trunk weights, F_s is the saddle reaction force obtained from the saddle tube sensor, F_{sh} is the shoulder reaction force calculated by a inverse dynamics method from the handlebar sensors, and F_h the hip reaction force calculated by the inverse dynamics method from the pedal sensors. To compute F_h and F_{sh}, a classic inverse dynamic process was used (Winter, 1990). In this method, body-segments from upper and lower limbs were considered rigid and interconnected by frictionless joints and their inertial parameters were derived from the scaling equations (De Leva, 1996). Given the aims of the study, only the vertical components in Eq. (1) were considered. This model is illustrated in Fig. 3. Pedal forces were converted from the local to the global coordinate system by using a rotation matrix based on three kinematic markers placed on a strip embedded externally to the pedals. The entire data processing was performed using custom-made codes written in Scilab 5.4.0 (SCILAB, Scilab Enterprises). All the data were normalized to the subject's body mass. During the crank cycle corresponding to the minimum saddle vertical force observed

Please cite this article as: Costes, A., et al., A reduction of the saddle vertical force triggers the sit–stand transition in cycling. Journal of Biomechanics (2015), http://dx.doi.org/10.1016/j.jbiomech.2015.07.035

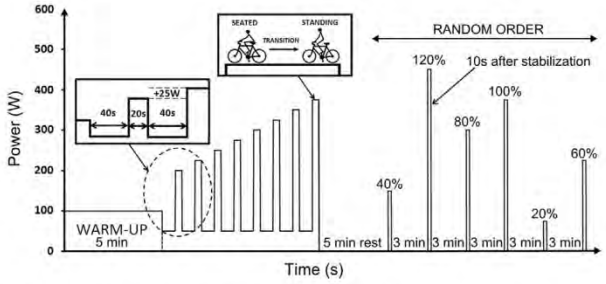

Fig. 1. Experimental protocol. The first part of the test determined the spontaneous sit–stand transition power. After 5 min of rest, the following phase was proposed in a random order from 20% to 120% of this sit–stand transition power at 90 rpm.

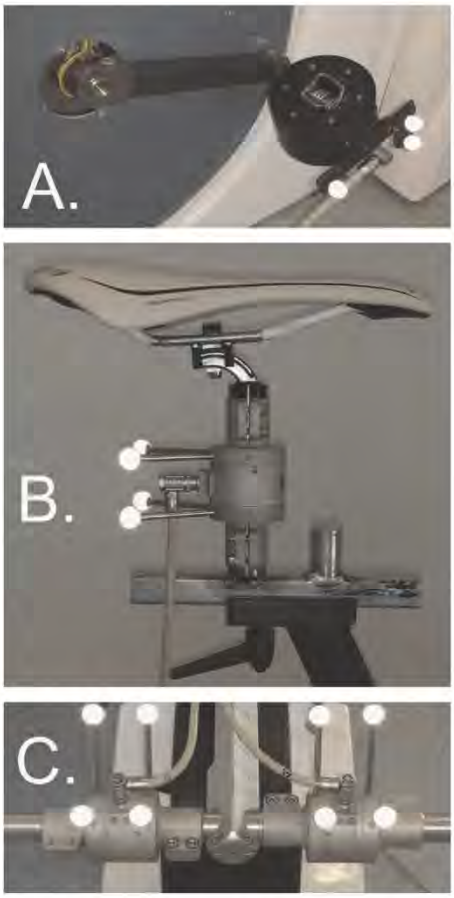

Fig. 2. 3D force and moment sensors. (A) Pedal. (B) Saddle tube. (C) Handlebars.

among the 10 s of recording for each power output, vertical forces presented in Eq. (1) and the sum of the instantaneous vertical pedal forces were extracted. In this crank cycle and at the instant corresponding to the minimum saddle vertical force, vertical force values were retained for further analyzes.

2.5. Statistics

Before each statistical test, data normality and variance homogeneity were assessed using Shapiro–Wilk's, and Levene's tests, respectively. A one-way repeated measures ANOVA (power output = 20%, 40%, 60%, 80%, 100% and 120% of sit–stand transition power) was performed to compare saddle force levels across power outputs. Post-hoc analyses were performed using Bonferroni's method. To check the accuracy of the experimental model represented by the equality computed in Eq. (1), the difference between saddle vertical reaction force and the equivalent sum of forces was quantified for each power output condition using the root-mean-square error (RMSE). In addition, Pearson's coefficients (R) were used to determine

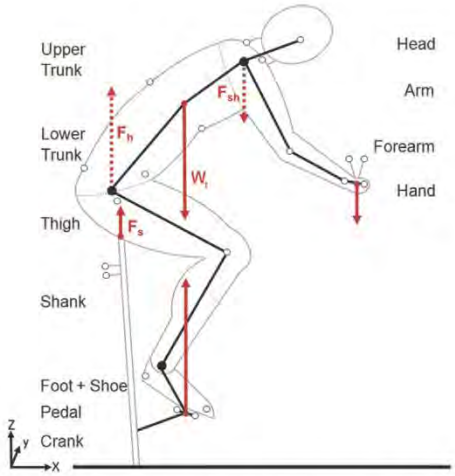

Fig. 3. Theoretical model of the cyclist. For clarity only one side of the body is represented. Arrows represent external forces (saddle, pedals, handlebars, and weight of the trunk and head solid), and dashed arrows represent reaction forces applied on the trunk at the hip and shoulder levels calculated by inverse dynamics. Only the vertical components of these forces are represented. White dots represent kinematic markers. Black dots represent joint centers calculated using the SCoRE method.

the correlation between the two patterns. Partial eta-squared (η^2) was used to quantify the size of the effect of power output on vertical forces. All statistical analyzes were performed using STATISTICA (STATSOFT, Maisons-Alfort, France). A p-value of 0.05 was defined as the level of statistical significance.

3. Results

The sit–stand transition power reached during a pedaling phase of 20 s at 90 rpm (i.e. during the first test, see Section 2) was 568 ± 93 W (8.0 ± 1.4 W kg^{-1}) and the power outputs corresponding to 20%, 40%, 60%, 80%, 100% and 120% of sit–stand transition power were 114 ± 19 W (1.6 ± 0.3 W kg^{-1}), 227 ± 37 W (3.2 ± 0.5 W kg^{-1}), 341 ± 56 W (4.8 ± 0.8 W kg^{-1}), 454 ± 74 W (6.4 ± 1.1 W kg^{-1}), 568 ± 93 W (8.0 ± 1.4 W kg^{-1}) and 682 ± 111 W (9.6 ± 1.6 W kg^{-1}), respectively.

The static vertical force on the saddle (0% of sit–stand transition power) was 5.30 ± 0.50 N kg^{-1}.

Descriptive statistics about saddle vertical force are shown in Table 1. A significant main effect ($p < 0.001$) of power output was found, showing that the magnitudes of minimum saddle vertical forces decreased with increasing power output. Post-hoc tests indicated that the saddle vertical force decreased significantly between each power output condition.

Accuracy of the model was assessed and the results of the saddle vertical force pattern reconstruction using the equality described in Eq. (1) are presented in Table 2. An illustration of this reconstruction is presented in Fig. 4.

Vertical saddle, trunk inertial force, shoulders and hips reaction force patterns are presented in Fig. 5.

The variation with power output of each term detailed in Eq. (1) at the instantaneous minimum saddle vertical force in the cycle is presented in Fig. 6. In addition, the sum of the instantaneous vertical pedal forces is represented in a descriptive purpose.

4. Discussion

The primary purpose of this investigation was to test the hypothesis that the saddle vertical forces would decrease with increasing power output. Our findings supported our hypothesis

Please cite this article as: Costes, A., et al., A reduction of the saddle vertical force triggers the sit–stand transition in cycling. Journal of Biomechanics (2015), http://dx.doi.org/10.1016/j.jbiomech.2015.07.035

with a linear decrease of 87.4% of the saddle vertical reaction force, from 5.30 ± 0.50 N kg^{-1} to 0.68 ± 0.49 N kg^{-1}, between a static position on the bicycle and the minimum instantaneous value obtained while pedaling at 120% of the sit–stand transition power (Table 1). Another purpose of the study was to determine the forces applied on the trunk during cycling at different pedal reaction forces in order to interpret the decrease in saddle vertical force. The results showed that the model presented in Eq. (1) provided an accurate examination of the forces associated with the saddle vertical force (Table 2 and Fig. 4). These data suggest that the vertical saddle force decreased mainly in response to the increase in hip vertical reaction forces (Figs. 5 and 6). Consequently, with increasing pedal reaction forces, the body weight was less and less supported by the saddle. The results indicated that when the saddle force approached 1 N kg^{-1}, the participants tended to spontaneously transit to the STAND position, suggesting that the saddle force could be a predictor of the sit–stand transition power.

A combination of several strategies was observed to limit the decrease in saddle vertical force in response to the increasing demand in pedal force, potentially increasing both the sit–stand transition power and the delay before the occurrence of the sit–stand transition. These strategies are likely to help maintaining the SEAT position when high level of pedal reaction forces is created and may also explain why the saddle vertical force did not reach zero (Fig. 6). However, these strategies have been previously reported as particularly metabolically costly (Korff et al., 2007; Edwards et al., 2009; McDaniel et al., 2005). The first strategy observed was to pull on the pedal to create downward reaction forces at the hip level (Fig. 5). This pedal pulling may be associated with the advantage of increasing the mechanical effectiveness of pedaling (Korff et al., 2007), and explains the non-linear increase in the sum of pedal vertical forces during with increasing crank power (Fig. 6). However, and probably because human's lower limb is far stronger to produce force in extension than in flexion (Anderson et al., 2007), increasing the mechanical effectiveness by training cyclists to pull more on the pedals has been reported to decrease their metabolic efficiency (Korff et al., 2007; Edwards et al., 2009). Because experts in cycling have been reported to push more on the pedals at equivalent power output (Coyle et al., 1991) it could be expected that they would have to create downward forces by pulling their handlebars and/or pedals and/or accelerating their trunk downward simultaneously to the decrease in vertical saddle force at lower power outputs than the non-cyclists from our study, and more frequently in their daily practice because of the higher power output that they develop. Further investigations are needed to confirm this hypothesis which could lead to improvement in cycling performance. A second strategy observed to limit the reduction of the saddle vertical force was to accelerate the trunk's center-of-mass downward (Fig. 5). It is worth noting that the pattern of these accelerations is synchronized with the pattern of saddle vertical force from 100% of the sit–stand transition power: when the saddle force was at its minimum, the trunk's center-of-mass was accelerated downward, and reciprocally, the upward acceleration of the trunk's center-of-mass occurred while the saddle vertical force was at its maximum, the whole occurring twice by pedaling cycle. A third strategy was to create a downward reaction force at the shoulders by pulling on the handlebar, this last strategy was mainly observed above the sit–stand transition power (Fig. 6). Both of these strategies involve additional muscular efforts from the upper limbs. As highlighted by McDaniel et al. (2005), the upper limbs' metabolic cost is important in cycling. These authors showed that the use of a modified saddle allowing the stabilization of the trunk and a potential decrease in upper limb muscular efforts decreased the metabolic cost of pedaling for a fixed power output. The reductions were of 1.6%, 1.2%, and 0.2% at 40, 60, and 80 rpm, respectively and they showed that the best improvement in metabolic cost was obtained at the highest level of pedal forces (for a fixed power output), i.e. in the conditions corresponding to the highest handlebars and pedals pulling and trunk inertial forces observed in our study. The present data are in agreement with the interpretation that with increasing pedal forces, the body weight was less and less supported by the saddle, and that downward forces acting on the trunk were required to maintain the SEAT position above one level of crank power (for a given pedaling cadence of 90 rpm). The fact that costly strategies to counteract the elevation of the trunk emerged at the power at which the participants spontaneously switched to the STAND position suggests that this position could have been chosen in order to avoid these strategies. It is worth mentioning that several other factors may influence the choice of the cycling position in the field such as aerodynamics (Debraux et al., 2011; Millet et al., 2014), or slope gradient (Bertucci et al., 2005; Duc et al., 2008). However, the difficulty to keep force on the saddle during high pedal reaction force production observed in this study is making the SEAT position less attractive in these conditions, giving a mechanical reason to trigger the sit–stand transition. Our study is the first to present saddle force patterns at different levels of pedal reaction force as a justification to trigger the sit–stand transition, and to explain these patterns by a mechanical decomposition of the forces applied on the trunk during cycling. In order to further confirm the present results, experimental designs manipulating the body weight, and/or testing pedaling cadence effects on the magnitude of saddle vertical force and the occurrence of the sit–stand transition are warranted. Additionally, Hansen and Waldeland (2008) implemented repeated cycling bouts to exhaustion with experimented cyclists and reported smaller sit–stand transition power output than the one observed in this study with non-cyclists. This difference illustrates a potential protocol-dependence of the sit–stand transition power, which may therefore also be affected by the duration of the cycling trial. Altogether, further investigations on the sit–stand transition paradigm in cycling may lead to improvements in pedaling efficiency by potentially decreasing the mechanical cost of pedaling in SEAT position at high pedal reaction forces, and by determining the precise pedal reaction force level at which the sit–stand transition is necessary to maximize performance for different cadences, weights and durations conditions.

By determining the parameters involved in saddle force patterns, the present study also has implication for clinicians, researchers, and manufacturers trying to understand the etiology of groin injuries and

Table 1
Minimum saddle vertical reaction forces across power outputs.

	20%	40%	60%	80%	100%	120%	η^2
Minimum (N kg^{-1})	3.68 ± 0.47 [2.58–4.60]$^{\$}$	3.12 ± 0.50 [2.15–4.15]$^{\$}$	2.51 ± 0.58 [1.30–3.69]$^{\$}$	1.78 ± 0.57 [0.67–2.96]$^{\$}$	1.09 ± 0.51 [0.13–2.17]$^{\$}$	0.68 ± 0.49 [0.02–1.68]$^{\$}$	0.91

Data are expressed in N kg^{-1} as mean ± standard deviation [range]. η^2: partial eta-squared (effect size).

$^{\$}$ Difference with all other pedaling conditions ($p < 0.001$).

Please cite this article as: Costes, A., et al., A reduction of the saddle vertical force triggers the sit–stand transition in cycling. Journal of Biomechanics (2015), http://dx.doi.org/10.1016/j.jbiomech.2015.07.035

Table 2
Accuracy of the mechanical decomposition.

	20%	40%	60%	80%	100%	120%	Mean (all conditions)
RMSE	0.36 (± 0.18)	0.44 (± 0.19)	0.57 (± 0.26)	0.65 (± 0.27)	0.73 (± 0.25)	0.80 (± 0.20)	0.59 (± 0.22)
R	0.90 (± 0.08)*	0.81 (± 0.12)*	0.78 (± 0.12)*	0.75 (± 0.15)*	0.80 (± 0.14)*	0.84 (± 0.13)*	0.81 (± 0.12)*

Root-mean-square-error (RMSE) expressed in N kg^{-1} and coefficients of correlation (R) between the pattern of vertical saddle force and the pattern of the sum of forces applied on the trunk (terms described in Eq. (1)) presented as mean (± SD).

* Significant coefficient of correlation ($p < 0.001$).

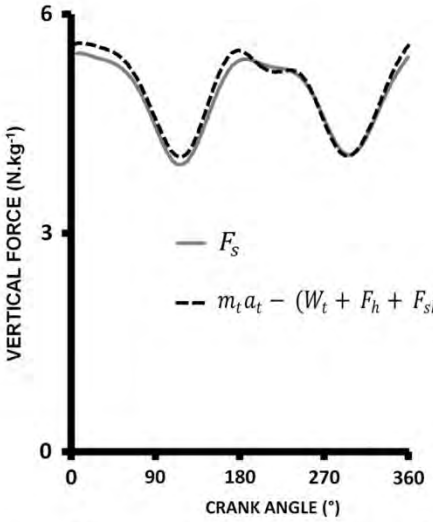

Fig. 4. Illustration of the mean saddle vertical reaction force and mean sum of forces applied on the trunk (presented in Eq. (1)) patterns for all participants (n=25) for power output=20% of the sit–stand transition power.

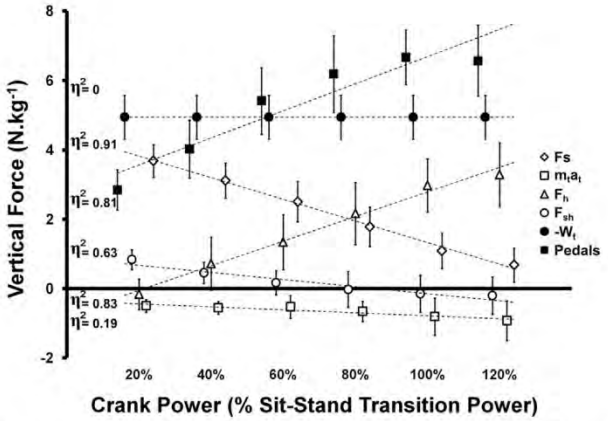

Fig. 6. Evolution of the vertical reaction forces across power outputs at the crank angle corresponding to the instantaneous minimum saddle vertical force among the 10 s of recording. Positive values indicate upward reaction forces (except for the trunk's weight, reverted in a purpose of readability). Diamonds: saddle vertical reaction forces. Squares: product between the mass of the trunk and the acceleration of its center of mass. Triangles: sum of the two hip vertical reaction forces. White circles: sum of the two shoulder vertical reaction forces. Black dots: weight of the head and trunk. Black squares: sum of the two pedal vertical reaction forces. η^2: partial eta-squared (effect size).

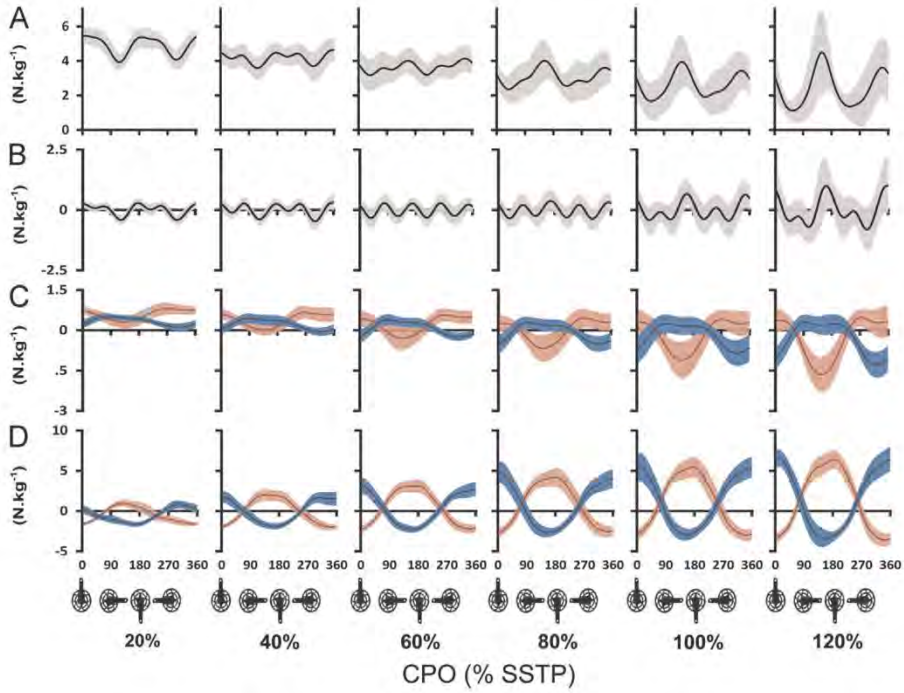

Fig. 5. Vertical reaction force patterns presented along the crank cycle corresponding to the minimum saddle vertical reaction force recorded for each power output. Mean lefts (red line) and rights (blue line) are presented ± one standard deviation. Data normalized by body-mass. (A) Saddle. (B) Mass time acceleration of the trunk's center-of-mass. (C) Shoulders. (D) Hips. (For interpretation of the references to color in this figure legend, the reader is referred to the web version of this article.)

Please cite this article as: Costes, A., et al., A reduction of the saddle vertical force triggers the sit–stand transition in cycling. Journal of Biomechanics (2015), http://dx.doi.org/10.1016/j.jbiomech.2015.07.035

erectile dysfunction associated with cycling (Bressel et al., 2010; Bressel and Larson, 2003; Carpes et al., 2009; Lowe et al., 2004). Indeed, the inconsistency of the patterns of saddle force observed previously (Bolourchi and Hull, 1985; Stone and Hull, 1995; Wilson and Bush, 2007) can be explained by the different pedaling conditions used in these studies. Due to the sensitiveness of saddle forces (and thus saddle pressures) to pedal reaction forces, cyclists suffering from these pathologies should decrease their pedaling cadence for the same workload, as this is supposed to increase hip upward reaction force in order to decrease the saddle reaction force.

It is important to note some limitations of the present study. The use of a cycling ergometer is a common practice for testing, rehabilitation and training, and as stated above differs with cycling in the field (Bertucci et al., 2012). Reproducing this protocol during field cycling may therefore be aimed in future investigations. Likewise, the potential protocol-dependence of the spontaneous sit–stand transition power determination needs further investigations, in addition with pedaling cadence and/or bike settings effects.

5. Conclusion

The body weight is gradually less supported by the saddle as pedal reaction forces increase, thus decreasing the mechanical advantage of pedaling in the SEAT position. Strategies counteracting the upward vertical pedal forces were observed around the power corresponding to the sit–stand transition, suggesting that the spontaneous choice to rise in the STAND position may be a solution to reduce the need to overcome these constraints. The spontaneous sit–stand transition occurred at minimum saddle vertical force about 1 N kg^{-1}; the high linearity of the relationship between saddle vertical force and power output for a given cadence suggests an ability of prediction of the sit–stand transition.

Conflict of interest

The authors have no financial or personal relationships with other people or organizations that could have inappropriately influenced this research.

Acknowledgments

Antony Costes was funded by a PhD grant from the French Ministry of Education and Research (Ministère de l'Education et de la Recherche). The authors would like to thank Dr. Laurent Seitz for his review of the manuscript.

References

Anderson, D.E., Madigan, M.L., Nussbaum, M.A., 2007. Maximum voluntary joint torque as a function of joint angle and angular velocity: model development and application to the lower limb. J. Biomech. 40, 3105–3113.
Ansley, L., Cangley, P., 2009. Determinants of "optimal" cadence during cycling. Eur. J. Sport Sci. 9, 61–85.
Begon, M., Monnet, T., Lacouture, P., 2007. Effects of movement for estimating the hip joint centre. Gait Posture 25, 353–359.
Bertucci, W., Betik, A., Duc, S., Grappe, F., 2012. Gross efficiency and cycling economy are higher in the field as compared with on an axiom stationary ergometer. J. Appl. Biomech. 28, 636–644.
Bertucci, W., Grappe, F., Girard, A., Betik, A., Rouillon, J.D., 2005. Effects on the crank torque profile when changing pedalling cadence in level ground and uphill road cycling. J. Biomech. 38, 1003–1010.
Bolourchi, F., Hull, M.A., 1985. Measurement of rider induced loads during simulated bicycling. Int. J. Sports Biomech. 1, 308–329.
Bressel, E., Larson, B.J., 2003. Bicycle seat designs and their effect on pelvic angle, trunk angle, and comfort. Med. Sci. Sports Exerc. 35, 327–332.
Bressel, E., Nash, D., Dolny, D., 2010. Association between attributes of a cyclist and bicycle seat pressure. J. Sex. Med. 7, 3424–3433.
Caldwell, G.E., Hagberg, J.M., McCole, S.D., Li, L., 1999. Lower extremity joint moments during uphill cycling. J. Appl. Biomech. 15, 166–181.
Carpes, F.P., Dagnese, F., Kleinpaul, J.F., Martins, E., de, A., Mota, C.B., 2009. Bicycle saddle pressure: effects of trunk position and saddle design on healthy subjects. Urol. Int. 82, 8–11.
Coyle, E.F., Feltner, M.E., Kautz, S.A., Hamilton, M.T., Montain, S.J., Baylor, A.M., Abraham, L.D., Petrek, G.W., 1991. Physiological and biomechanical factors associated with elite endurance cycling performance. Med. Sci. Sports Exerc. 23, 93–107.
Debraux, P., Grappe, F., Manolova, A.V., Bertucci, W., 2011. Aerodynamic drag in cycling: methods of assessment. Sports Biomech. 10, 197–218.
De Marchis, C., Schmid, M., Bibbo, D., Castronovo, A.M., D'Alessio, T., Conforto, S., 2013. Feedback of mechanical effectiveness induces adaptations in motor modules during cycling. Front. Comput. Neurosci. 17, 7–35.
De Leva, P., 1996. Adjustments to Zatsiorsky–Seluyanov's segment inertia parameters. J. Biomech. 29, 1223–1230.
De Vey Mestdagh, K., 1998. Personal perspective: in search of an optimum cycling posture. Appl. Ergon. 29, 325–334.
Duc, S., Bertucci, W., Pernin, J.N., Grappe, F., 2008. Muscular activity during uphill cycling: effect of slope, posture, hand grip position and constrained bicycle lateral sways. J. Electromyogr. Kinesiol. 18, 116–127.
Edwards, L.M., Jobson, S.A., George, S.R., Day, S.H., Nevill, A.M., 2009. Whole-body efficiency is negatively correlated with minimum torque per duty cycle in trained cyclists. J. Sports Sci. 27, 319–325.
Ehrig, R.M., Taylor, W.R., Duda, G.N., Heller, M.O., 2006. A survey of formal methods for determining the centre of rotation of ball joints. J. Biomech. 39, 2798–2809.
Gonzalez, H., Hull, M.L., 1989. Multivariable optimization of cycling biomechanics. J. Biomech. 22, 1151–1161.
Hansen, E.A., Waldeland, H., 2008. Seated versus standing position for maximization of performance during intense uphill cycling. J. Sports Sci. 26, 977–984.
Harnish, C., King, D., Swensen, T., 2007. Effect of cycling position on oxygen uptake and preferred cadence in trained cyclists during hill climbing at various power outputs. Eur. J. Appl. Physiol. 99, 387–391.
Hug, F., Turpin, N.A., Couturier, A., Dorel, S., 2011. Consistency of muscle synergies during pedaling across different mechanical constraints. J. Neurophysiol. 106, 91–103.
Korff, T., Romer, L.M., Mayhew, I., Martin, J.C., 2007. Effect of pedaling technique on mechanical effectiveness and efficiency in cyclists. Med. Sci. Sports Exerc. 39, 991–995.
Li, L., Caldwell, G.E., 1998. Muscle coordination in cycling: effect of surface incline and posture. J. Appl. Physiol. 85, 927–934.
Lowe, B.D., Schrader, S.M., Breitenstein, M.J., 2004. Effect of bicycle saddle designs on the pressure to the perineum of the bicyclist. Med. Sci. Sports Exerc. 36, 1055–1062.
Lucía, A., Hoyos, J., Chicharro, J.L., 2001. Preferred pedalling cadence in professional cycling. Med. Sci. Sports Exerc. 33, 1361–1366.
McDaniel, J., Behjani, N.S., Elmer, S.J., Brown, N.A., Martin, J.C., 2014. Joint-specific power–pedaling rate relationships during maximal cycling. J. Appl. Biomech. 30, 423–430.
McDaniel, J., Subudhi, A., Martin, J.C., 2005. Torso stabilization reduces the metabolic cost of producing cycling power. Can. J. Appl. Physiol. 30, 433–441.
McLester, J.R., Green, J.M., Chouinard, J.L., 2004. Effects of standing vs. seated posture on repeated Wingate performance. J. Strength Cond. Res. 18, 816–820.
Millet, G.P., Tronche, C., Fuster, N., Candau, R., 2002. Level ground and uphill cycling efficiency in seated and standing positions. Med. Sci. Sports Exerc. 34, 1645–1652.
Millet, G.P., Tronche, C., Grappe, F., 2014. Accuracy of indirect estimation of power output from uphill performance in cycling. Int. J. Sports Physiol. Perform. 9, 777–782.
Poirier, E., Do, M., Watier, B., 2007. Transition from seated to standing position in cycling allows joint moment minimization. Sci. Sports 22, 190–195.
Reiser 2nd, R.F., Maines, J.M., Eisenmann, J.C., Wilkinson, J.G., 2002. Standing and seated Wingate protocols in human cycling. A comparison of standard parameters. Eur. J. Appl. Physiol. 88, 152–157.
Ryschon, T.W., Stray-Gundersen, J., 1991. The effect of body position on the energy cost of cycling. Med. Sci. Sports Exerc. 23, 949–953.
Stone, C., Hull, M.L., 1995. The effect of rider weight on rider-induced loads during common cycling situations. J. Biomech. 28, 365–375.
Tanaka, H., Bassett Jr, D.R., Best, S.K., Baker Jr, K.R., 1996. Seated versus standing cycling in competitive road cyclists: uphill climbing and maximal oxygen uptake. Can. J. Appl. Physiol. 21, 149–154.
Viker, T., Richardson, M.X., 2013. Shoe cleat position during cycling and its effect on subsequent running performance in triathletes. J. Sports Sci. 31, 1007–1014.
Wilson, C., Bush, T.R., 2007. Interface forces on the seat during a cycling activity. Clin. Biomech. 22, 1017–1023.
Winter, D.A., 1990. Biomechanics and Motor Control of Human Movement. Wiley-Interscience, New York, p. 370.

Please cite this article as: Costes, A., et al., A reduction of the saddle vertical force triggers the sit–stand transition in cycling. Journal of Biomechanics (2015), http://dx.doi.org/10.1016/j.jbiomech.2015.07.035

III.7. Etude 5 : Patterns d'Activite Musculaire associes avec la Transition Assis-Danseuse en Cyclisme : Modularite et Preuves d'une Transition Optimale

La transition de la position assise vers celle en danseuse en cyclisme semble favoriser la performance pendant la pratique du cyclisme à haut niveau de puissance. L'hypothèse testée dans cet article a été que les stratégies d'activation musculaire utilisées pourraient expliquer l'avantage de la position en danseuse à puissance de pédalage élevée.

Neuf muscles du membre inférieur ont été étudiés sur 17 participants novices pendant des séquences de pédalage assis et en danseuse réalisées de 20 à 120% de leur puissance spontanée de transition en danseuse déterminée lors d'un test préalable. L'activité EMG intégrée, les patterns temporels EMG, ainsi que les synergies musculaires ont été analysées.

Des synergies musclaires similaires ont été trouvées dans les deux positions. En comparaison avec la position assise, celle en danseuse a été observée comme temporairement décalée pour deux synergies associées à l'extension de genou et de cheville. L'activité EMG intégrée a augmenté de façon différente entre les positions, et était inférieure en position assise en-dessous de la puissance spontanée de transition, à partir et au-dessus de cette position en danseuse.

En conclusion, les positions « assis » et « danseuse » sont associées à des stratégies différentes d'activation musculaire pour produire de la puissance au pédalier, résultant en un avantage de la position en danseuse en termes d'activité EMG intégrée aux puissances de pédalage supérieures au niveau spontané de transition assis-danseuse.

Muscles activity patterns associated with the seated and standing positions in pedaling: evidences for an optimal transition

Nicolas A. Turpin[1,2 *], Antony Costes[2], Pierre Moretto[3,6] and Bruno Watier[4,5]

[1]*Center for Interdisciplinary Research in Rehabilitation (CRIR), Institut de réadaptation Gingras-Lindsay de Montreal and Jewish Rehabilitation Hospital, Laval, Quebec, Canada*

[2]*University of Toulouse, UPS, PRISSMH, 118 Route de Narbonne, 31062 Toulouse Cedex 9, France*

[3]*University of Toulouse; UPS; Centre de Recherches sur la Cognition Animale; 118 route de Narbonne, F-31062 Toulouse Cedex 9, France*

[4] *CNRS ; LAAS ; 7 avenue du colonel Roche, F-31077 Toulouse, France*

[5] *University of Toulouse; UPS; LAAS; 118 route de Narbonne, F-31062 Toulouse Cedex 9, France*

[6]*CNRS; CRCA; 118 route de Narbonne, F-31062 Toulouse Cedex 9, France*

Running head: Lower limbs muscle activity during cycling

[*]**Corresponding author:**

Nicolas A. Turpin

Center for Interdisciplinary Research in Rehabilitation (CRIR), Institut de réadaptation Gingras-Lindsay de Montreal, 6300 Avenue de Darlington, Montreal H3S 2J4, QC, Canada

email: nicolas.turpin@umontreal.ca

phone: (514) 340 3155

Abstract

Transiting from the seated to the standing position in pedaling may favor performance during intensive cycling. It was hypothesized that the muscle activation strategies used to produce power-output would enable to explain the advantage of the standing position at high power-output.

Nine muscles of the lower limb were investigated in 17 untrained man during seated and standing cycling sequences performed at power-outputs ranging from 20 to 120% of their spontaneous seat to stand transition power (SSTP), determined in a specific test. Integrated EMG activity, temporal patterns of the EMGs and muscles synergies were analyzed.

Similar muscles synergies were found in both positions (scalar products >0.957± 0.077). Compared to seated, the standing position was associated with a marked temporal shift in the activation pattern of two synergies associated with knee and ankle extensor muscles. Integrated muscle activity increased in specific fashions in seated and standing and was found to be lower below SSTP (i.e., 562±94 Watts) in the seated position for most of the recorded muscles and lower or equal above SSTP in the standing position.

In conclusions, seated and standing positions are subserved by distinct activation strategies to produce power-output resulting in an advantage of the standing position in terms of integrated muscle activity at power-outputs greater than SSTP.

KEYWORDS: locomotion, modules, muscle synergy, cycling

Introduction

Bicycling can be performed in either seated or standing position. However, the reasons that lead to adopt one over the other position are still unclear.

The transition from a seated to a standing position generally occur during steep climb ascensions or when fast accelerations are needed, suggesting that the standing position favors high power outputs (Hansen & Waldeland 2008; Millet et al. 2002; Padulo et al. 2014). The more forward position of the hip which may provide different leverage over the crank arm and the greater contribution of the upper limbs have been suggested as explanations to the advantages provided to the standing position (Caldwell et al. 1999; Stone & Hull 1993). Such hypotheses have predictable consequences. For instance a favorable leverage over the crank arm would likely be associated with less activity of the lower limb muscles or with greater efficiency of the standing position to produce power-output. Moreover, a greater contribution of the upper limbs would be logically associated with greater activation of the related muscles or with greater joint torque. Conversely, most of the previous studies did not show any obvious advantage of the standing position in terms of lower limbs joint torque (Caldwell, Hagberg 1999; Li & Caldwell 1998), lower limbs muscle activity (Duc et al. 2008; Li & Caldwell 1998) and energetic efficiency (i.e., defined as work over energy expended) (Harnish et al. 2007; Millet, Tronche 2002; Tanaka et al. 1996). The greater contribution of the upper limbs in standing cycling has been highlighted through analysis of muscle activation (Duc, Bertucci 2008), forces applied to the handle (Soden & Adeyefa 1979; Stone & Hull 1993) and power transferred across the hip joint (Elmer et al. 2011; van Ingen Schenau et al. 1990). However, the actual contribution of the upper limbs to crank power-output appears to be limited (Dore et al. 2006; Stone & Hull 1993) and may not fully explain the gain in power production associated with the standing position (Dore, Baker 2006; Millet, Tronche 2002; Stone & Hull 1993).

The advantage of the standing position may also bear on muscle coordination which is thought to represent a critical determinant of mechanical efficiency and power output in cycling (Wakeling et al. 2010). The change from a seated to a standing position is associated with significant changes in the intensity and timing of EMG activity (Duc, Bertucci 2008; Li & Caldwell 1998) but these changes have not been clearly related to a greater ability to produce power-output in the standing position. The postural change results in different relative moment arms and length at which the muscles are contracting, thus changing the relative advantages of the muscles to create joint torque (Caldwell, Hagberg 1999; Li & Caldwell 1998). These may result in changes in the structure of muscle synergies (Wakeling et al. 2011), here defined as groups of muscles activated together in a specific balance (Hug et al. 2011). The muscle synergies have been studied from a handful of studies in cycling and mainly in the seated position. A recent report found no change in the number or in the structure of the muscle synergies between the seated and standing positions (Hug, Turpin 2011). Yet, this study investigated a very specific population (i.e., experts in cycling) and obtained results that differed from studies examining untrained participants (Barroso, Torricelli 2014; De Marchis, Schmid 2013). This aspect requires therefore further investigations.

Actually, evidences can be found showing that the standing position could be advantageous over the seated position in terms of energy expended or in terms of effort, but only when power output is high. For example, Hansen *et al.* (2008) recently showed in trained cyclists that the standing position is associated with greater time to exhaustion at power-outputs greater that 94% of their maximum power-output. Additionally, Tanaka *et al.* (1996) reported that their subjects felt less sensation of effort in the leg in the standing position compared to the seated position, but solely during steep hill climbing and not during moderate hill climbing. These studies suggest therefore that the standing position could be favorable when exercising at high power-output but not at moderate power-output.

Given the above, the goal of the present study was to identify the coordination patterns of the lower limb muscles in the seated and standing positions across a wide range of power-outputs (~100-700 Watts) in order to determine how muscle activity is distributed spatially (i.e., in terms of muscle synergies), temporally and in terms of their intensities in these two positions. It was hypothesized that the muscle activation strategies used to produce power-output would be distinct between the seated and the standing positions and would allow to understand why the standing position is adopted mainly when high power-output is required.

MATERIALS AND METHODS

Participants

Seventeen males (23.3±3.4 years; 1.78±0.05m, 72.6+67.4kg) unexperienced in cycling volunteered to the study after signing an informed consent form. The experimental design of the study was approved by the local ethical committee and was conducted in accordance with the declaration of Helsinki.

Experimental procedure

Participants were first instrumented with the recording electrodes and with the position markers (see section *electromyography* and section *kinematics recordings*). Participants performed all tests on an electromagnetically braked ergometer (Excalibur, LODE, Groningen, The Netherlands) and used cleated cycling shoes.

After 5 min of warm-up on the ergometer at ~100 Watts, the participants performed the sit-to-stand transition test consisting in an incremental pedaling exercise to determine the *seat-to-stand transition power* (SSTP). STTP corresponds to the power at which the participants would spontaneously switch from the seated to the standing position and this particular power output was used to normalize the power across participants. For this test, the participants started in the seated position and the ergometer was programmed so they exercised continuously at a power output of 50 Watts interrupted each 60s with transient sequences of 20 s during which power-output was rapidly set to the "test power". The test power was initially set to 200 Watts and was increased by 25 Watts until the subject choose to adopt the standing position. The participants were instructed to maintain the pedaling frequency as stable as possible (i.e., 90 RPM), and to feel free to adopt the more comfortable position (the seated or the standing position). SSTP was established when the participant cycled in the standing position for at least 10 s.

The second test, from which the EMG and kinematic data were analyzed consisted in twelve 10 s randomized trials, in which participants were placed in either the standing or the seated position and were required to exercise at power-outputs corresponding to 20, 40, 60, 80, 100, or 120% of SSTP at 90 RPM with 2-3 min between trials. This test resulted in a total of 12 trials per participant (i.e., = 2 positions × 6 power-outputs).

The participants were presented with their instantaneous RPM on a screen and were instructed to maintain a pedaling frequency of 90 RPM in both the first and the second test.

Electromyography

Surface EMG were recorded from 9 muscles of the right side of the body (i.e., *tibialis anterior*: TA, *soleus:* Sol, *gastrocnemuis lateralis:* GL, *vastus lateralis*: VL*, vastus medialis*: VM, *rectus femoris*: RF, *biceps femoris*: BF, *semitendinosus*: ST, and *gluteus maximus*: Gmax). Prior to electrode application, the skin was shaved and cleaned with alcohol to minimize impedance. Each electrode (Delsys DE 2.1, Delsys Inc, Boston, MA, USA; 1 cm interelectrode distance) was placed longitudinally with respect to the underlying muscle fibers arrangement and were located according to the recommendations of Surface EMG for Non-Invasive Assessment of Muscles (SENIAM). The quality of the EMG signal was assessed visually and the electrodes

were secured with adhesive tapes before recording. The EMG signal was amplified (× 1000), digitized (6-400 Hz bandwidth) at a sampling rate of 1 kHz (Bagnoli 16, Delsys, Inc. Boston, USA).

Participant positioning

The saddle height of the ergometer was adjusted such that a knee angle of ~150° (180° = full extension) was obtained with the crank at the lowest position while seated. The foot was positioned on the pedals so the rotation axis of the pedals was vertically aligned with the metatarsophalangeal joint of the big toe. The angle of the seat tube was of 73° and the length of the cranks of 0.17m. The handlebars were flat (mountain bike type) and the position of the hands on the handlebars was left free to the participants (handlebar width = 0.7m).

EMG signal processing

EMG signals were bandpass filtered (zero lag, 4th order Butterworth) between 20 and 400 Hz. Because components at 50Hz and its harmonics were found in the spectrum of the signal, band-stop filters around 50, 100, 150, 200, 250, and 300 Hz (band width = ± 0.3 Hz) were successively applied (zero lag, 4th order Butterworth). Linear envelope for each muscle was obtained by first subtracting the mean and then by low-pass filtering the fully rectified raw EMG signals with a 9 Hz low-pass filter (2nd order Butterworth, zero lag).

For each participant and for each muscle, EMG envelopes were normalized in amplitude by their mean value computed across all conditions (Yang & Winter 1984).

The integrated muscle activity was obtained by integrating the EMG envelopes over the ~15 cycles of each trial of the second test. For each muscle and each subject these values were normalized by the mean value computed across all conditions of power-output.

Cycles were identify by a trigger signal that indicated the lowest position of the right crank (bottom dead center; BDC). A cycle corresponded to one pedal revolution, with 0 and 100% corresponding to the BDC, a representation consistent with previous studies (Hug, Turpin 2010; Sarabon et al. 2012). EMG patterns were time-interpolated such that each cycle corresponded to a 200 points vector.

Times lags and patterns similarity

Similarity in the shape of the EMG and synergy patterns as well as of the muscle synergies were assessed using normalized scalar product (NSP), computed as:

$$\mathrm{NSP} = \frac{\mathbf{x}^T\mathbf{y}}{\sqrt{\mathbf{x}^T\mathbf{x}}\sqrt{\mathbf{y}^T\mathbf{y}}} \qquad \text{Equation 1}$$

With **x** and **y**, two vectors of the same dimension and superscript *T* denoting vector transposition.

To quantify the changes in timing, lag times were computed using an analogous to the cross correlation function. This function was obtained by iteratively computing the NSP between two waveforms, with one of

the two shifted by lags of -100 up to 100 time bins. The phase shift between the two EMG patterns was calculated as the lag time at the maximum of this function, and the corresponding NSP value defined NSP_{max}..

The NSP values expected by chance have been computed by comparing random synergy vectors (Roh et al. 2012). For each participant and each synergy, random synergy vectors were constructed by randomly sampling weightings from the ensemble of weightings of all (all conditions) original vectors.

Muscle synergies extraction

Muscle synergies extractions were performed by non-negative matrix factorization using an implementation of the Lee and Seung algorithm (Lee & Seung 1999; Lee & Seung 2001). In the algorithm, the synergy vectors were forced to have unit length at each iteration. The maximum number of iteration was set to 1E6. The stopping rule was a cost that decreased by less than 1E-6%.

Determining the number of synergies

The variance accounted for (VAF) was computed as follow:

$$VAF = 1 - SSE / SST \qquad \text{Equation 3}$$

Where SSE is the sum of squared residuals between the actual EMG data and its decomposition, and SST the total sum of square (i.e., of the original EMG data). VAF was iteratively computed by varying the number of synergies between 1 and the number of muscle in the EMG data to obtain the 'VAF' *vs.* 'number of synergies' curve. The number of synergies was defined as the smallest number explaining at least 90% of the total data variance and at least 75% of each muscle VAF.

Statistics

Normality of the data has been checked using Shapiro-Wilk's tests. Repeated measures ANOVAs (with position=[seated;standed] and power-output=[20 40 60 80 100 120]% as repeated measures) were used to analyze integrated muscle activity. Post-hoc analyses were then performed using Bonferroni's method. Significance of the time lags were analyzed using t-tests for single mean (references values = 0). Comparisons between random and actual synergy vectors were performed using paired t-test on Z-transformed NSP values. Values are reported as mean ± SD. A *p*-value below .05 was considered statistically significant.

RESULTS

The first test allowed to determine that participants spontaneously raised from the seated to the standing position at a power output of 562±94 Watts (i.e., the seat-to-stand transition power; STTP).

Muscle activation profile

EMG envelopes are depicted in Figure 1. Table 1 presents the maximum of the normalized scalar product ($NSP_{max)}$, time lags and percentages of cycle at which peak activity occurred for each muscle. NSP_{max} represents a measure of similarity of two patterns without any phase shift between them. Despite large similarities, the change in position was associated with changes in the timing of activation in 8 out-of 9 muscles, which were shifted forward in the cycle in standing compared to seated position (Table 1). EMG patterns were mainly scaled in amplitude with power-output in each position with slight changes in the timing or in the form of their activation patterns (i.e., NSP_{max}>0.972 and lags lower than 1.4% were found on average over all muscles; Table 1). Table 1 shows that the lags tended to be positive in seated and negative in standing indicating specific adaptations to power-output.

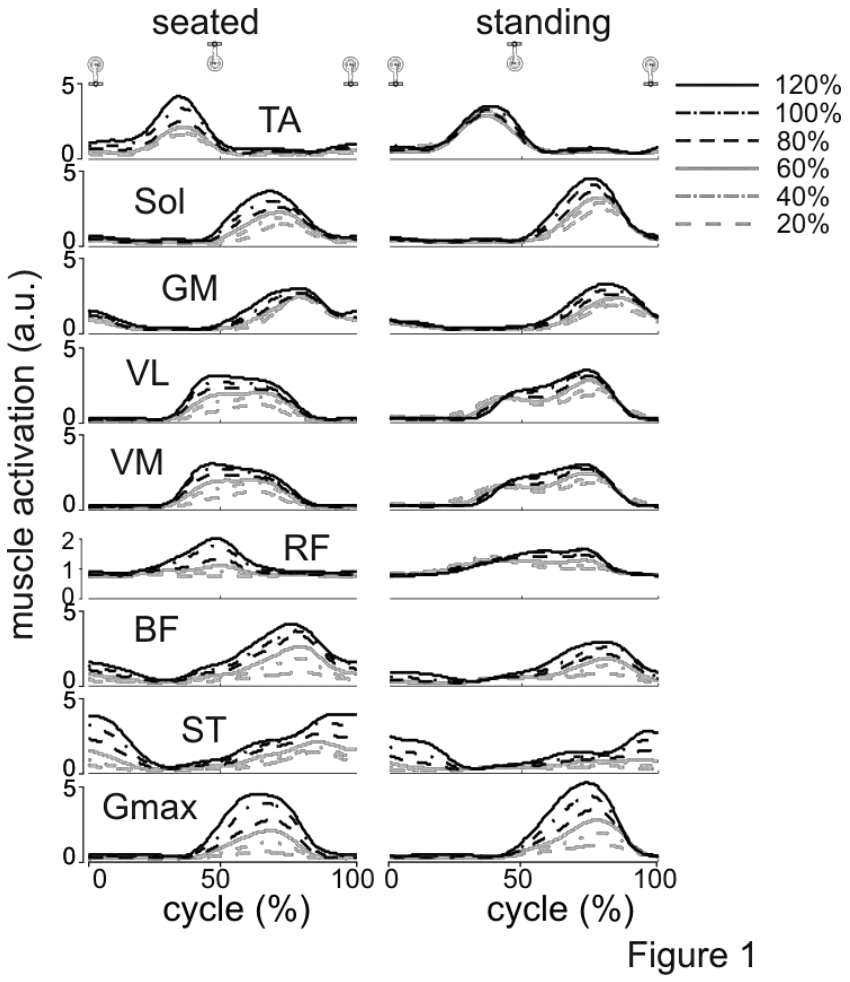

Figure 1. Ensemble averaged patterns of muscle activity. Each waveform represents the patterns averaged over all participants. EMG envelopes for each participant were normalized by the average EMG activity computed overall conditions.

Seated *vs.* Standing

	NSP max	lag	Seated peak (%)	Standing peak (%)
TA	0.965 ± 0.027	**2.2 ± 2.3**	37.6 ± 7.1	39.5 ± 8.8
SOL	0.988 ± 0.007	**6.5 ± 1.7**	70.6 ± 4.5	77.7 ± 3.4
GM	0.974 ± 0.021	**2.6 ± 4.0**	75.9 ± 9.7	83.0 ± 4.0
VL	0.930 ± 0.024	**8.1 ± 3.8**	56.8 ± 5.2	72.4 ± 5.3
VM	0.942 ± 0.025	**8.2 ± 3.3**	55.8 ± 5.0	71.0 ± 6.4
RF	0.943 ± 0.036	**6.6 ± 9.0**	45.8 ± 8.8	52.1 ± 13.4
BF	0.965 ± 0.023	**2.8 ± 4.3**	76.4 ± 5.3	80.9 ± 5.1
ST	0.947 ± 0.025	1.2 ± 8.0	75.2 ± 14.7	73.6 ± 16.9
Gmax	0.985 ± 0.018	**8.9 ± 1.9**	67.5 ± 2.1	77.4 ± 2.6

			Seated peak (%)	
Seated			power p	power p+1
TA	0.988 ± 0.012	-0.3 ± 0.7	38.4 ± 8.7	38.0 ± 6.5
SOL	0.994 ± 0.003	**-0.7 ± 0.6**	71.4 ± 4.3	70.3 ± 4.8
GM	0.993 ± 0.004	-0.3 ± 1.0	76.7 ± 8.0	75.0 ± 11.8
VL	0.996 ± 0.002	**-0.3 ± 0.4**	57.6 ± 5.4	55.8 ± 5.6
VM	0.995 ± 0.005	-0.3 ± 0.9	57.3 ± 4.8	55.3 ± 5.1
RF	0.991 ± 0.004	-1.4 ± 5.8	46.3 ± 10.1	45.2 ± 8.0
BF	0.989 ± 0.008	-0.1 ± 1.2	76.3 ± 5.7	76.1 ± 6.2
ST	0.987 ± 0.012	0.4 ± 2.5	77.1 ± 13.4	73.5 ± 18.2
Gmax	0.989 ± 0.019	-0.1 ± 1.0	67.5 ± 1.8	67.6 ± 2.1

Standing			Standing peak (%)	
			power p	power p+1
TA	0.989 ± 0.008	**1.1 ± 1.6**	38.9 ± 8.9	39.5 ± 8.8
SOL	0.996 ± 0.002	**1.1 ± 0.4**	76.2 ± 3.5	77.7 ± 3.4
GM	0.993 ± 0.005	**0.5 ± 0.8**	81.1 ± 6.6	83.0 ± 4.0
VL	0.986 ± 0.004	**1.1 ± 1.1**	69.5 ± 4.5	72.7 ± 5.2
VM	0.987 ± 0.005	**1.3 ± 1.1**	67.7 ± 5.2	71.0 ± 6.4
RF	0.982 ± 0.009	1.3 ± 2.6	49.9 ± 11.9	52.1 ± 13.4
BF	0.983 ± 0.010	-0.3 ± 1.9	80.2 ± 4.7	80.7 ± 5.1
ST	0.972 ± 0.009	0.7 ± 6.1	72.9 ± 16.7	73.6 ± 16.9
Gmax	0.991 ± 0.011	**1.2 ± 0.6**	76.3 ± 3.7	77.4 ± 2.6

Table 1. Maximum NSP, lags and occurrence of the peak activity for each muscle. Significant lags appears in bold (t-tests for single mean; reference values= 0). Seated *vs.* Standing corresponds to comparisons between waveforms taken at the same power output. In the 2nd and 3rd parts of the table, comparisons were made between the power p and power p+1 (p= [20, 40 , 60, 80 and 100 %]), e.g. if p= 100%, p+1= 120%. Occurrence of the peak activity and the lags are given in percentage of cycle.

Integrated muscle activity

There was significant increases in the integrated muscle activity in all muscles with power output (global effect, $p<.001$; Figure 2). Integrated muscle activity of all muscles was affected by the position (main effect p-values ranged from $p=.037$ to $p<.001$) except in GM ($p=.091$). There were significant interactions between power and position for all muscles expect GM and the post-hoc results showed that position affected global muscle activity at specific power-outputs only (indicated in Figure 2). Power-output was associated with increases integrated muscle activity in all muscles in the two positions, with $p<.05$ overall post-hoc comparisons except for RF and TA in the standing position (i.e., in this position the integrated activity of TA showed differences only between 120% and 60%, and RF between 120% and [20, 40, and 60 %]).

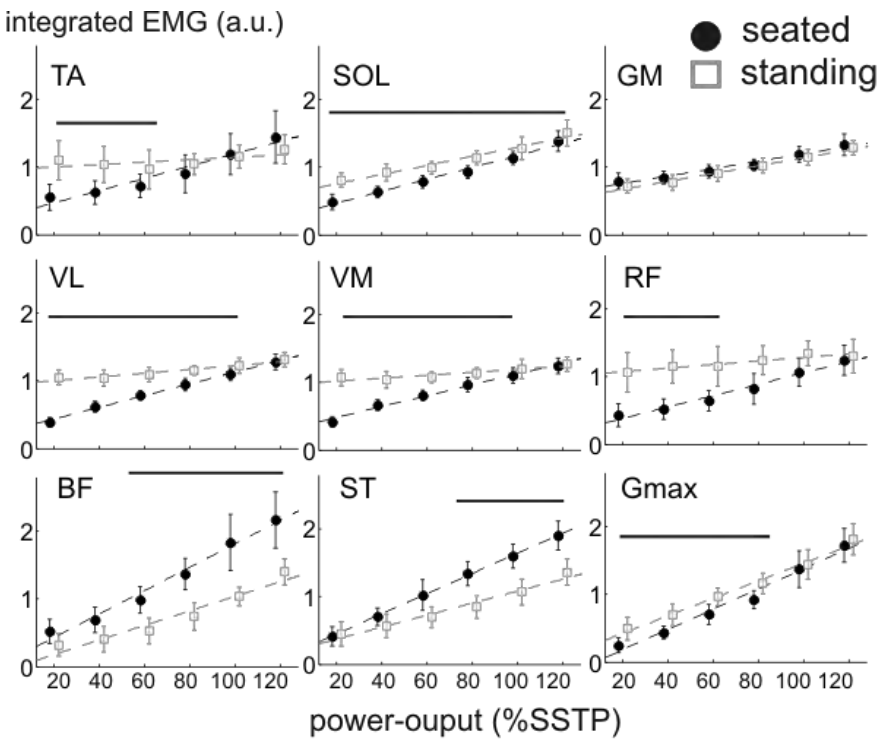

Figure 2. Integrated muscle activity. Values are given in percentage of the mean integrated activity obtained overall conditions and represented as mean ± SD. The lines above data indicate the powers at which significant differences were found between the values in seated and standing positions (p<.05). Power-output is given in percentage of the seat-to-stand transition power (SSTP).

Analysis of the muscle synergies

The variance accounted for (VAF) in function of the number of synergies extracted is presented in Figure 3A. The similarity of the two curves suggests similar dimensionalities in seated and standing. The synergies were extracted separately for each position and included all conditions of power-output. The large variation in power-outputs ensured that substantial motor variability was present, which is known to improve the identification of the synergies (Steele et al. 2015). The number of synergies was 4 using the criterion [VAF>0.9 & VAF_{muscle} >0.75]. VAF *per* muscle ranged from 85.1 ± 6.2% (Gmax) to 97.9 ± 0.7% (VM) in seated and from 86.9 ± 5.9% (Gmax) to 97.9 ± 0.5% (VM) in standing, which demonstrates very good reconstruction rates.

Muscle vectors are depicted in Figure 3B. The first synergy mainly co-activated the *rectus femoris* and *tibialis anterior* muscles (*RF/TA synergy),* the second synergy was associated with extensor muscles (EXT synergy), the third synergy was associated with ankle and hip extensors muscles (EXT2 synergy) and the fourth synergy was associated with knee flexors (FLEX synergy). Muscle synergies appeared to be very similar in the two positions, with an average NSP value of 0.957± 0.077 over all synergies between seated and standing. Z-transformed values for individual comparisons are reported in Figure 3C. These values were higher than chance level for all the synergies (p<0.001; Figure 4C) indicating significant similarities.

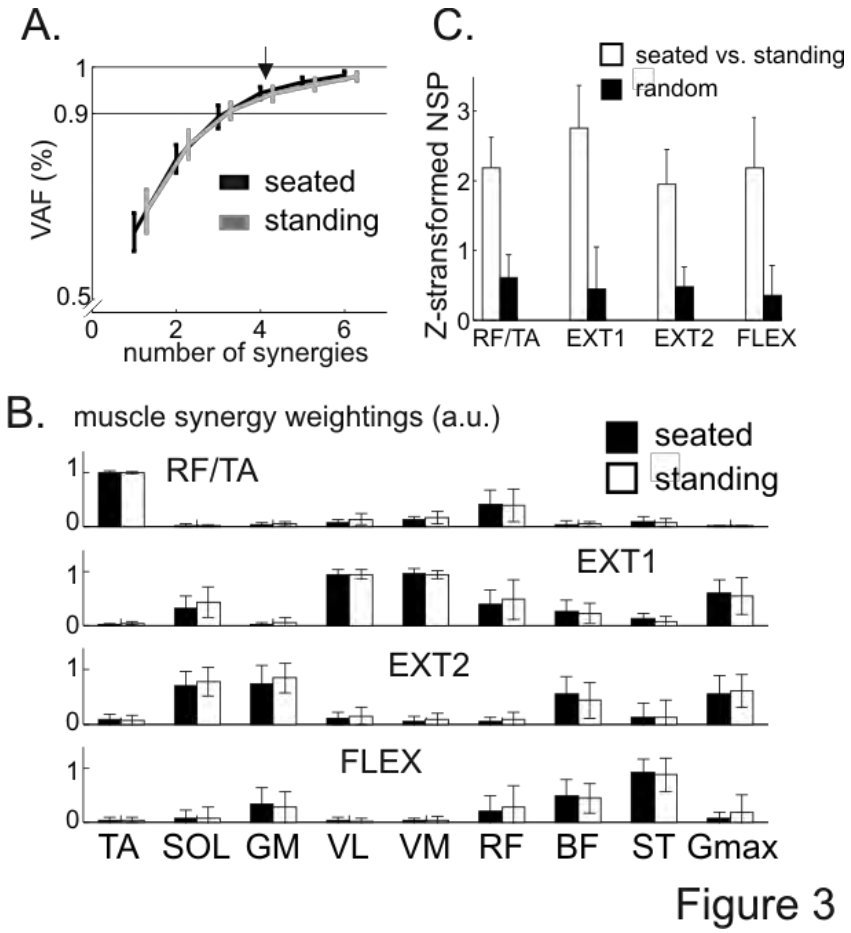

Figure 3. Dimensionality analysis and the muscle synergies. A. Cumulated variance accounted for in function of the number of synergies extracted in the seated and standing positions. Values are the averages computed over all participants. The arrow indicates the number of synergies determined for all subjects. **B.** Muscle synergy weightings. **C.** Z-transformed NSP values for comparisons between the muscle synergies in seated and standing (white bars). Black bars are the chance level NSP (i.e., obtained from comparisons between synergies composed of randomly shuffled weightings). For indication Z-transformed values of 1, 2 and 3 correspond to NSP values of 0.761, 0.964 and 0.995 respectively.

The synergy activation profiles are depicted in Figure 4 and the percentage of cycle at which their peak activity occurred as well as their similarity across power-outputs and positions are reported in Table 2. Timings of activation of RF/TA, EXT and EXT2 were significantly shifted forward in standing compared to seated. The change in power-output was associated with smaller but significant time shifts, mostly positive in seated and negative in standing.

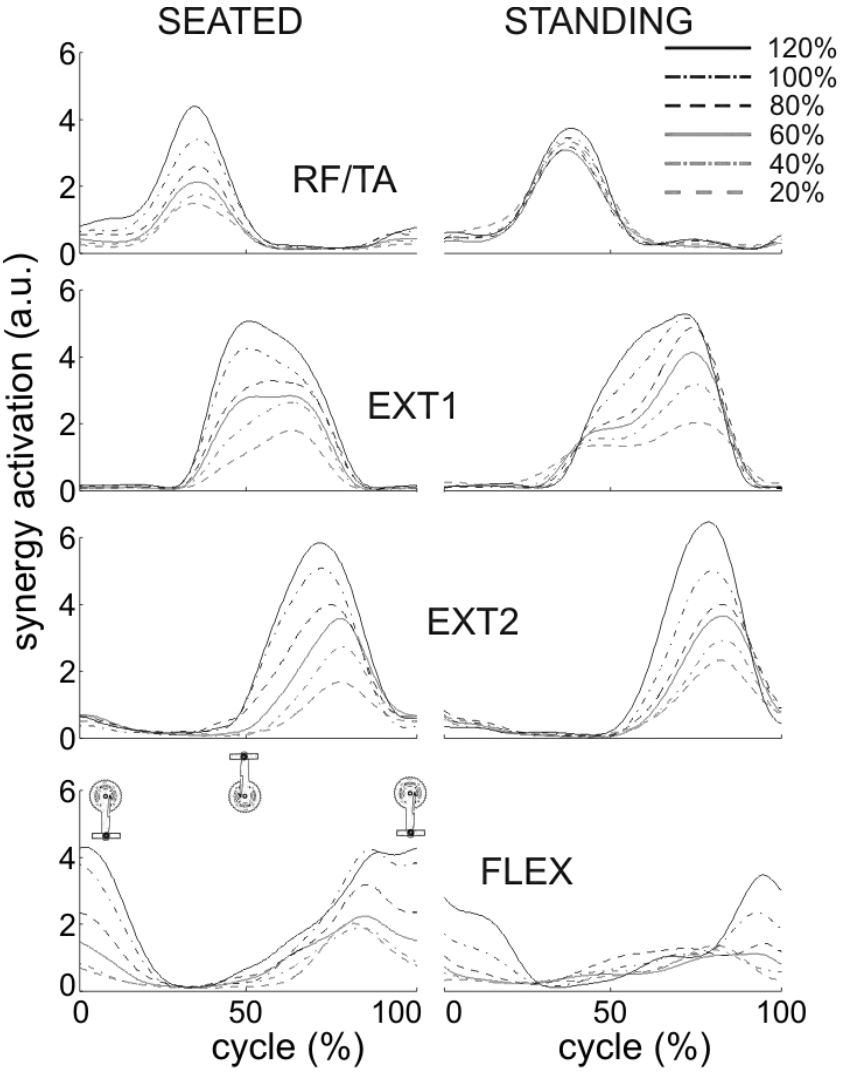

Figure 4

Figure 4. Synergy activation profiles. Synergy activations profiles are given in arbitrary unit (**a.u.**). Waveforms have been averaged over all participants.

seated vs. standing

	NSP max	Lag	seated peak (%)	standing peak (%)
RF/TA	0.967 ± 0.019	**2.7 ± 2.8**	37.1 ± 5.4	38.5 ± 4.1
EXT	0.953 ± 0.027	**8.9 ± 4.3**	57.4 ± 5.2	69.2 ± 6.8
EXT 2	0.979 ± 0.016	**7.0 ± 5.4**	71.8 ± 9.6	82.3 ± 3.3
FLEX	0.935 ± 0.034	-0.4 ± 11.7	73.2 ± 14.9	73.5 ± 11.8
			seated peak (%)	
seated			power p	power p+1
RF/TA	0.979 ± 0.016	0.2 ± 3.3	37.7 ± 8.5	36.5 ± 3.3
EXT	0.987 ± 0.006	**-1.8 ± 2.7**	59.8 ± 5.2	55.1 ± 5.7
EXT 2	0.977 ± 0.016	-2.4 ± 8.0	71.6 ± 12.8	71.9 ± 7.5
FLEX	0.954 ± 0.028	3.8 ± 4.8	76.7 ± 10.7	69.6 ± 22.3
			standing peak (%)	
standing			power p	power p+1
RF/TA	0.977 ± 0.022	**1.6 ± 1.7**	37.1 ± 2.9	38.9 ± 4.6
EXT	0.968 ± 0.015	**2.2 ± 1.8**	64.5 ± 6.7	69.1 ± 6.4
EXT 2	0.984 ± 0.009	1.4 ± 2.9	79.7 ± 3.3	81.7 ± 3.2
FLEX	0.944 ± 0.018	3.9 ± 6.8	70.2 ± 14.7	74.0 ± 15.8

Table 2. Maximum NSP, lags and occurrence of the peak activity for each synergy activation profiles. Significant lags appear in bold (t-tests for single mean; reference values= 0).

DISCUSSION

The results of the present study showed that the seated and standing coordination patterns in cycling both rely on 4 similar muscle synergies. The two positions were however distinct in terms of their activation patterns and how muscle activity was increased with power-output.

Optimality and the sit-to-stand transition

The results demonstrated distinct and power-output dependent patterns of muscle activation between the seated and the standing positions (Figure 1 and 2, Table 1). The activity of the knee flexors (i.e., ST, and BF) was lower in the standing position compared to the seated position at all tested power-outputs except the lowest ones (i.e., 20 and 40 %). Conversely, the activity of the extensors (i.e., Sol, VL, VM, RF and Gmax) and TA were lower in the seated position below SSTP (i.e., below 562±94 Watts) but were similar above SSTP. Thus, when considering the recorded muscles, these results suggest there is a net advantage in term of integrated muscle activity in the seated position below SSTP and in the standing position above SSTP.

Previous studies reported that metabolic economy and gross efficiency were similar between the standing and seated positions (Harnish, King 2007; Millet, Tronche 2002; Tanaka, Bassett 1996). However, in line with the present results, there are evidences that the differences in the cost of the two positions is power-dependent and that the narrow range of power-output previously investigated obscured the differences. For example, Ryschon et al. (1991) showed that energy expenditure was higher in standing *vs*. seated position, but investigated only low power-outputs (i.e., subjects exercised at 60-80RPM without resistive torques). Whereas, Tanaka et al. (1996) reported that subjects felt lesser sensations of effort in the legs in the standing position with a 10 % grade in comparison to a seated position but fail to find differences in heart rate or energy expenditure. The authors indeed suggested that upper body energy expenditures may have been higher in the standing position, masking the probable saving of energy associated with the standing position for the lower limbs. The absence of differences in terms of energy expenditure between the two positions may be related to the higher cost associated with the activity of upper limbs muscles in standing. Likewise, a recent study showed that the standing position was associated with longer time to exhaustion at high power-output (i.e., 94% of the participants maximum aerobic power) in comparison to the seated position (Hansen and Waldeland, 2008). It is therefore very likely that the standing position corresponds to an optimal behavior only at high power-output. An assumption that is in line with the present results and with the fact that the standing position is typically adopted at high power output or when high forces on the pedals are required. This is also in agreement with a previous study of our group reporting that the seated and standing positions allows for joint moment minimization depending on power-outputs (Poirier, Do 2007). Specifically, a cost function based on the torque produced by the hip and the knee joints was calculated as a function of power-output. The results demonstrated that below 80-85 % of the participant's maximum power output, the seated position was the most favorable position in term of this cost function and that this tendency was inverted above 80-85 %. Based upon the present data and those of previous studies, it appears that there is a critical power output beyond which the standing position becomes more favorable than the seated position in terms of lower limbs muscle activation.

Additionally, higher slopes were observed in the relationship between power output and integrated EMG in seated compared to standing position and higher y-intercepts were observed in standing for most of the recorded muscles (Figure 2). Integrated EMG reflects the metabolic costs of cycling (Bigland-Ritchie & Woods 1976; Blake & Wakeling 2013). It is also related to the neural drive to the muscles and could be viewed as a measure of effort (Cafarelli 1977; Noakes et al. 2005). The y-intercept is the cost in terms of integrated EMG when power-output is zero and can be interpreted as the cost of moving the limbs (McDaniel et al. 2002). Conversely, the slope of this relationship can be associated with the cost of producing mechanical power. In seated the y-intercept was close to zero whereas in standing the y-intercept was much greater (Figure 2). The fact that in standing subjects have to compensate for the weight of their upper body may account for this observation (Caldwell, Hagberg 1999). The lower slopes observed in the standing position indicates that a given increase in power output is associated with less increase in the cost in this position compared to seated, which may be interpreted as a form of efficiency. The standing position is associated with a superior contribution of the upper limbs (Stone & Hull 1993; Tanaka, Bassett 1996) which may take over part of the efforts from the lower limbs and explain this observation. However, the actual contribution of the upper limbs to crank power-output have been shown to be limited (Dore, Baker 2006; Stone & Hull 1993) and this might not fully explain the higher efficiency observed in the standing position. It could be hypothesized that differences in the relative moment arms and the length at which the muscles were contracting (Caldwell, Hagberg 1999), or that a different leverage over the crank arm for the knee and hip joints (Caldwell, Hagberg 1999; Stone & Hull 1993) changed the advantages of the muscles to produce power-output and account for the differences.

Similarity with the gait transition

Interestingly, similarities can be drawn between the cycling and gait patterns (Barroso, Torricelli 2014; Raasch & Zajac 1999). A transition could be defined as a discontinuous change in gait parameters leading to a different "mode" (Alexander 1989; Diedrich & Warren Jr 1995) with each mode characterized by distinct, stable and efficient coordination patterns (Diedrich & Warren Jr 1995).

When transiting from the walking to the running mode, at least 3 distinct features can be exposed. First, both modes are subserved by the same number of synergies namely, 5 in gait, and which appears to be very similar in the two modes (Cappellini et al. 2006; Ivanenko et al. 2004). This feature can also be found in other mammals where the same modules, i.e., the muscle synergies plus their associated activation patterns (Lacquaniti et al. 2012), tend to cooperate to give rise to a template of stable interlimb coordination patterns, namely, walk, trot or gallop (Maes & Abourachid 2013). Second, the two modes of coordination possess distinct temporal structures (Cappellini, Ivanenko 2006). This difference is significant since the temporal organization of the synergy activation patterns has been shown to be robust to changes in both velocity and body weight unloading during walking (Ivanenko, Poppele 2004). And third, the choice of a given mode of coordination could be associated with a form of optimization of the neural resources (Ivanenko et al. 2008). It is worth noting that the number and the structure of the synergies found in the present study were similar to that found in previous studies (Barroso, Torricelli 2014; De Marchis, Schmid 2013). The three

characteristics, namely similar modular organizations (Figure 3 and 4), distinct temporal structures (Figure 4, Table 1 and 2) and optimality (Figure 2) were also observed in the present study suggesting that seated and standing cycling also represent distinct and efficient modes of locomotion, comparable to the walking and running modes in gait.

Possible limitations

One possible limitation of this study is that the workload and not the pedaling frequency was modified to increase power output. Increasing the cycling frequency while maintaining the same load will increase power-output and the cost of the movement depending on the contraction velocity of each muscle (MacIntosh et al. 2000; McDaniel, Durstine 2002) . This may affect the cost of the movement very differently in seated *vs.* standing position. Therefore, it is possible that the power at which the spontaneous transition occurs could be different by changing the frequency of pedaling, a point which deserves future studies.

In the present study the mean has been used to normalize the EMG data whereas the maximum is a more common normalization. However, all conditions could be compared in terms of muscle activation patterns, or muscle synergies since the same normalization is used for each of them. Moreover, Yang and Winter proved that normalizing by the peak or the mean are equally suited to reduce inter-subject variability. Therefore, it is not likely that the normalization chosen have affected the conclusions of the present study.

Conclusion

This study demonstrated that despite similar synergies, the seated and standing positions in cycling are subserved by distinct activation patterns and distinct activation strategies to produce power-output resulting in an advantage of the standing position in terms of integrated muscle activity at power-outputs greater than ~500-600 Watts. This suggests that subjects may shift between the seated and standing coordination patterns in order to minimize neural resources.

PERSPECTIVES

The standing position is more economical in terms of muscle activity at high power-output but not at low power-output. This results from a combination of a higher efficiency of the muscles to produce power-output (here defined as the slope of the relationships between power-output an integrated EMG) and a higher initial cost. Energetic cost and efficiencies are in general studied through global measures influenced by upper and lower limbs. It would be interesting then to understand how these values change in different pedaling conditions (uphill slope, pedaling frequency etc.) The relationship between the spontaneous transition power (SSTP) and the amount of muscle activity suggests that transition is guided by intuition, or more likely by the sense of effort. The study suggested that the determination of an optimal transition power is possible by studying how lower-limbs muscle activity changes with power-output. We studied only untrained participants, but this study paves the way to future interesting studies on trained cyclists to better understand when it would be advantageous to shift from one position to the other.

Acknowledgements

The authors would like to thank PG Zanone and LB Seitz for their corrections of the manuscript. Antony Costes was funded by the French Education and Research Ministry (Ministère de l'éducation et de la recherche).

Conflict of interests

The authors declare no conflict of interests.

REFERENCES

Alexander RM. Optimization and gaits in the locomotion of vertebrates. *Physiol Rev*. 1989: **69**: 1199-1227.

Barroso FO, Torricelli D, Moreno JC, Taylor J, Gomez-Soriano J, Bravo-Esteban E, Piazza S, Santos C, Pons JL. Shared muscle synergies in human walking and cycling. *J Neurophysiol*. 2014: **112**: 1984-1998.

Bigland-Ritchie B, Woods JJ. Integrated electromyogram and oxygen uptake during positive and negative work. *J Physiol*. 1976: **260**: 267-277.

Blake OM, Wakeling JM. Estimating changes in metabolic power from EMG. *Springerplus*. 2013: **2**: 229.

Cafarelli E. Peripheral and central inputs to the effort sense during cycling exercise. *Eur J Appl Physiol Occup Physiol*. 1977: **37**: 181-189.

Caldwell GE, Hagberg JM, McCole SD, Li L. Lower extremity joint moments during uphill cycling. *Journal of Applied Biomechanics*. 1999: **15**: 166-181.

Cappellini G, Ivanenko YP, Poppele RE, Lacquaniti F. Motor Patterns in Human Walking and Running. *J Neurophysiol*. 2006: **95**: 3426-3437.

De Marchis C, Schmid M, Bibbo D, Bernabucci I, Conforto S. Inter-individual variability of forces and modular muscle coordination in cycling: A study on untrained subjects. *Human Movement Science*. 2013: **32**: 1480-1494.

De Marchis C, Schmid M, Bibbo D, Castronovo AM, D'Alessio T, Conforto S. Feedback of mechanical effectiveness induces adaptations in motor modules during cycling. *Front Comput Neurosci*. 2013: **7**: 35.

Diedrich FJ, Warren Jr WH. Why change gaits? Dynamics of the walk-run transition. *Journal of Experimental Psychology: Human Perception and Performance*. 1995: **21**: 183.

Dore E, Baker JS, Jammes A, Graham M, New K, Van Praagh E. Upper body contribution during leg cycling peak power in teenage boys and girls. *Res Sports Med*. 2006: **14**: 245-257.

Duc S, Bertucci W, Pernin JN, Grappe F. Muscular activity during uphill cycling: effect of slope, posture, hand grip position and constrained bicycle lateral sways. *J Electromyogr Kinesiol*. 2008: **18**: 116-127.

Dumas R, Cheze L, Verriest JP. Adjustments to McConville et al. and Young et al. body segment inertial parameters. *J Biomech*. 2007: **40**: 543-553.

Elmer SJ, Barratt PR, Korff T, Martin JC. Joint-specific power production during submaximal and maximal cycling. *Med Sci Sports Exerc*. 2011: **43**: 1940-1947.

Hansen EA, Waldeland H. Seated versus standing position for maximization of performance during intense uphill cycling. *Journal of sports sciences*. 2008: **26**: 977-984.

Harnish C, King D, Swensen T. Effect of cycling position on oxygen uptake and preferred cadence in trained cyclists during hill climbing at various power outputs. *European Journal of Applied Physiology*. 2007: **99**: 387-391.

Hug F, Turpin NA, Couturier A, Dorel S. Consistency of muscle synergies during pedaling across different mechanical constraints. *J Neurophysiol*. 2011: **106**: 91-103.

Hug F, Turpin NA, Guevel A, Dorel S. Is interindividual variability of EMG patterns in trained cyclists related to different muscle synergies? *J Appl Physiol*. 2010: **108**: 1727–1736.

Ivanenko YP, Cappellini G, Poppele RE, Lacquaniti F. Spatiotemporal organization of alpha-motoneuron activity in the human spinal cord during different gaits and gait transitions. *Eur J Neurosci*. 2008: **27**: 3351-3368.

Ivanenko YP, Poppele RE, Lacquaniti F. Five basic muscle activation patterns account for muscle activity during human locomotion. *J Physiol*. 2004: **556**: 267-282.

Lacquaniti F, Ivanenko YP, Zago M. Patterned control of human locomotion. *J Physiol*. 2012: **590**: 2189-2199.

Lee DD, Seung HS. Learning the parts of objects by non-negative matrix factorization. *Nature*. 1999: **401**: 788-791.

Lee DD, Seung HS. Algorithms for Non-negative Matrix Factorization. *Adv Neural Info Proc Syst*. 2001: **13**: 556-562.

Li L, Caldwell GE. Muscle coordination in cycling: effect of surface incline and posture. *J Appl Physiol (1985)*. 1998: **85**: 927-934.

MacIntosh BR, Neptune RR, Horton JF. Cadence, power, and muscle activation in cycle ergometry. *Med Sci Sports Exerc*. 2000: **32**: 1281-1287.

Maes L, Abourachid A. Gait transitions and modular organization of mammal locomotion. *J Exp Biol*. 2013: **216**: 2257-2265.

McDaniel J, Durstine JL, Hand GA, Martin JC. Determinants of metabolic cost during submaximal cycling. *J Appl Physiol (1985)*. 2002: **93**: 823-828.

Millet GP, Tronche C, Fuster N, Candau R. Level ground and uphill cycling efficiency in seated and standing positions. *Med Sci Sports Exerc*. 2002: **34**: 1645-1652.

Noakes TD, St Clair Gibson A, Lambert EV. From catastrophe to complexity: a novel model of integrative central neural regulation of effort and fatigue during exercise in humans: summary and conclusions. *Br J Sports Med*. 2005: **39**: 120-124.

Padulo J, Laffaye G, Bertucci W, Chaouachi A, Viggiano D. Optimisation of starting conditions in track cycling. *Sport Sci Health*. 2014: **10**: 189-198.

Poirier E, Do M, Watier B. Transition from seated to standing position in cycling allows joint moment minimization. *Science & Sports*. 2007: **22**: 190-195.

Raasch CC, Zajac FE. Locomotor Strategy for Pedaling: Muscle Groups and Biomechanical Functions. *J Neurophysiol*. 1999: **82**: 515-525.

Roh J, Rymer WZ, Beer RF. Robustness of muscle synergies underlying three-dimensional force generation at the hand in healthy humans. *J Neurophysiol*. 2012: **107**: 2123-2142.

Sarabon N, Fonda B, Markovic G. Change of muscle activation patterns in uphill cycling of varying slope. *Eur J Appl Physiol*. 2012: **112**: 2615-2623.

Soden PD, Adeyefa BA. Forces applied to a bicycle during normal cycling. *J Biomech*. 1979: **12**: 527-541.

Steele KM, Tresch MC, Perreault EJ. Consequences of biomechanically constrained tasks in the design and interpretation of synergy analyses. *J Neurophysiol*. 2015: jn 00769 02013.

Stone C, Hull ML. Rider/bicycle interaction loads during standing treadmill cycling. *Journal of applied biomechanics*. 1993: **9**: 202-202.

Tanaka H, Bassett DR, Jr., Best SK, Baker KR, Jr. Seated versus standing cycling in competitive road cyclists: uphill climbing and maximal oxygen uptake. *Can J Appl Physiol*. 1996: **21**: 149-154.

van Ingen Schenau GJ, van Woensel WW, Boots PJ, Snackers RW, de Groot G. Determination and interpretation of mechanical power in human movement: application to ergometer cycling. *Eur J Appl Physiol Occup Physiol*. 1990: **61**: 11-19.

Wakeling JM, Blake OM, Chan HK. Muscle coordination is key to the power output and mechanical efficiency of limb movements. *J Exp Biol*. 2010: **213**: 487-492.

Wakeling JM, Blake OM, Wong I, Rana M, Lee SSM. Movement mechanics as a determinate of muscle structure, recruitment and coordination. *Philosophical Transactions of the Royal Society B: Biological Sciences*. 2011: **366**: 1554-1564.

Wakeling JM, Horn T. Neuromechanics of muscle synergies during cycling. *J Neurophysiol*. 2009: **101**: 843-854.

Yang JF, Winter DA. Electromyographic amplitude normalization methods: improving their sensitivity as diagnostic tools in gait analysis. *Arch Phys Med Rehabil*. 1984: **65**: 517-521

III.8. ETUDE 6 : LA TRANSITION ASSIS-DANSEUSE EST ASSOCIEE A UNE MINIMISATION DE FONCTIONS DE COUT

Ce quatrième article intitulé « Minimization Of Cost Functions Is Associated With The Sit-Stand Transition In Cycling » est en révision pour la revue « Journal of Biomechanics ». A l'image de la transition de la marche vers la course, largement étudiée chez l'humain, notre hypothèse est que la transition assis-danseuse pourrait elle aussi avoir une explication multifactorielle (Raynor et al. 2002). A la suite des travaux précurseurs de Gonzalez and Hull (1989) sur l'usage de fonctions de coût mécanique adaptées à l'étude du pédalage, et des travaux de thèse de Poirier (2009) ayant montré une minimisation d'une « Moment Cost Function » dans la position spontanément choisie en cyclisme, différents objectifs ont été proposés. Le premier a été de tester à nouveau l'effet de la puissance de pédalage sur une fonction de coût basée sur les moments articulaires afin de confirmer les résultats de Poirier en utilisant un autre protocole incrémental conduisant à la transition assis-danseuse. En profitant d'avancées techniques, cette fonction de coût a été actualisée par l'utilisation d'un procédé de dynamique inverse en 3 dimensions au lieu de 2, et par l'utilisation d'une méthode d'adimensionnalisation des résultats (Hof 1996). Un second objectif a été de tester une autre fonction de coût basée sur l'activité électromyographiques de plusieurs chefs du membre inférieur (MacIntosh, Neptune, and Horton 2000). Enfin, un troisième objectif a été de tester la corrélation entre ces deux fonctions. En effet, si cette dernière paraît évidente en théorie, de nombreuses limitations pratiques (participation d'efforts non musculaires dans les couples articulaires, précision relative de la dynamique inverse, non-linéarité de la relation EMG-force, non exhaustivité des chefs musculaires étudiés, pondération des données de chaque muscle dans la fonction de coût EMG...) pourraient limiter cette association entre les données électrophysiologiques et mécaniques. Les résultats de cette étude ont montré que les deux fonctions sont hautement corrélées et minimisées dans la position spontanément choisie par les participants. Ces résultats confirment ceux de Poirier (2009) et apportent de nouvelles pistes pour améliorer la sensibilité de fonctions de coût représentatives des efforts musculaires du membre inférieur, ces dernières étant minimisées dans la position spontanément choisie par le cycliste, et proposant donc un nouveau critère explicatif de la transition assis-danseuse en cyclisme.

Original Article

SPONTANEOUS CHANGE FROM SEATED TO STANDING CYCLING POSITION WITH INCREASING WORKLOAD IS ASSOCIATED WITH A MINIMIZATION OF COST FUNCTIONS

ANTONY COSTES[a,*], NICOLAS A. TURPIN[a,b], DAVID VILLEGER[a], PIERRE MORETTO[c,d], BRUNO WATIER[e,f]

[a] *University of Toulouse, UPS, PRISSMH, 118 Route de Narbonne, 31062 Toulouse Cedex 9, France*

[b] *Center for Interdisciplinary Research in Rehabilitation (CRIR), Institut de Réadaptation Gingras-Lindsay de Montréal and Jewish Rehabilitation Hospital, Laval, Quebec, Canada*

[c] *University of Toulouse; UPS; Centre de Recherches sur la Cognition Animale; 118 route de Narbonne, F-31062 Toulouse Cedex 9, France*

[d] *Research Center on Animal Cognition (CRCA), Center for Integrative Biology (CBI), Toulouse University, CNRS, UPS, France*

[e] *CNRS, LAAS, 7 Avenue du Colonel Roche, F-31077 Toulouse, France*

[f] *University of Toulouse, UPS, LAAS, F-31400 Toulouse, France*

[*] Corresponding author. Tel.: +33 (0) 5 61 55 64 40; Fax: +33 (0) 5 61 55 82 80

E-mail address: antony.costes@univ-tlse3.fr (A. Costes).

Running Title: “Cost Functions in Cycling”

Word count: 3383 (abstract: 209).

Abstract

Spontaneous changes of position are useful to understand which criteria influence humans in their coordination to perform a given task. However, the factors explaining the sit-stand transition in cycling are still unclear. This study was designed to test the effects of position (seated or standing) during cycling at increasing crank power on cost functions representative of the lower limbs muscular efforts. Twenty-five participants performed an incremental test leading to the sit-to-stand transition, and subsequent randomized pedaling trials at powers ranging from 20 to 120% of the power corresponding to this transition in seated and standing position. Lower limbs net joint moments were used to define a Moment Cost Function (MCF) and EMG data defined an Electromyographic Cost Function (ECF). MCF and ECF increased with increasing crank power and were correlated to each other ($r = 0.93$, $p < 0.01$). Both cost-functions values were lower in seated below the sit-stand transition power and higher from this power in standing position. The results suggest that the spontaneous change of position observed in cycling with increasing crank power may represent an optimal choice regarding the increase in muscular efforts. These results support the use of such simple cost functions to define optimal settings in cycling and may provide applications for other tasks.

Key Words: INVERSE DYNAMICS, ELECTROMYOGRAPHY, PEDALING, JOINT MOMENTS.

1. Introduction

It is postulated that spontaneous changes of position are useful to understand which criteria are optimized in the movement given their relatively abrupt nature (Alexander, 1989; Diedrich and Warren, 1995). During gait, a transition from walking to running or vice versa occurs at around 2 $m.s^{-1}$ (Raynor et al., 2002) in association with the need of increasing or decreasing joint powers (Pires et al., 2014). Similarly, during cycling, a spontaneous transition from the seated to the standing position occurs during steep climb ascensions or when fast accelerations are needed, hence with the need of an increased power output and increased joint powers (Kautz et al., 1994). Despite large similarities between gait and cycling (Barroso et al., 2014; Raasch and Zajac, 1999), the presence of a transition in position in cycling still remains elusive. Previous studies suggested that the sit-stand transition may favor performance depending on the required power output (Hansen and Waldeland, 2008; Poirier et al., 2007). Therefore, it could be hypothesized that the spontaneous change of position observed in cycling could rely on an optimization strategy (Jackson et al., 2012).

Optimization criteria like minimum jerk (Flash and Hogan, 1985), minimum kinetic energy (Biess et al., 2007) or minimum muscular efforts (van den Bogert et al., 2012) may predict several features of human movement like kinematics, joint moments or muscles activations. In cycling, net joint moments computed by inverse dynamics have been proposed as indirect markers of the muscular efforts (Hull and Jorge, 1985). Gonzalez and Hull (1989) proposed that the sum of the absolute or squared lower limb net joint moments may be a criterion to optimize bicycle settings and pedaling cadence. This assumption about pedaling cadence has been tested experimentally, showing no statistical difference between the spontaneously chosen pedaling cadence and that minimizing a Moment Cost

Function (MCF) at different crank powers (Marsh et al., 2000). However, no previous researches have investigated the association between this criterion and the spontaneous change of position in cycling. Additionally, muscle activations have been proposed as criteria associated with pedaling optimization (Hug and Dorel, 2009). MacIntosh et al. (2000) proposed an estimate of general muscle activity by computing the mean activation of seven lower limb muscles, and reported that this cost function was the lowest at the cadence preferred by the participants in various crank power conditions. Others studies showed that the pedaling posture affects the EMG patterns of the lower limb muscles in pedaling (Duc et al., 2008; Li and Caldwell, 1998), but none investigated the relationship between an Electromyographic Cost Function (ECF) and the spontaneous change of position observed in cycling with increasing crank power.

Therefore, the first purpose of the study was to determine the relation between a moment-based (MCF) and an electromyography-based (ECF) cost functions. To explain the spontaneous change of position observed in cycling with increasing crank power, the secondary aim of the study was to test the effect of different crank powers conditions on these cost functions in seated and standing positions. Our hypotheses are that MCF and ECF would be correlated, and would be lower in seated and standing position below and from the spontaneous sit-stand transition power, respectively.

2. Methods

2.1. Participants

Twenty five male sport science students (age: 23.2 ± 3.6 y, height: 1.77 ± 0.06 m, body mass: 71.5 ± 9.1 kg) volunteered for this investigation. The participants were category 4-5

according to Ansley and Cangley (2009) classification. These participants were chosen with the assumption that novices would act more spontaneously than experts. Each participant was informed of the experimental procedure and signed an informed consent form prior to the study. The study was conducted in accordance with the declaration of Helsinki and was approved by the University of Toulouse ethical committee. Participants were asked to avoid high-intensity or exhaustive exercise at least 72 hours before the laboratory trials.

2.2. Experimental Protocol

After a standardized bike positioning, participants performed a cycling test to determine their spontaneous sit-stand transition power on an electromagnetically braked Excalibur (LODE, Groningen, Netherlands). The test started with a five-minute warm-up at 100 W. Then, sequences of 40 s at 50 W were alternated with sequences of 20 s with a starting power of 200 W, incremented by 25 W at each step. The sit-stand transition power was considered as the power at which participants rose from the saddle during at least 10 s. A visual feedback of the pedaling cadence was provided to the participants who were encouraged to maintain it as close as possible to 90 RPM throughout the whole test. After the end of the sit-stand transition test and a five-minute rest period, participants performed twelve randomized trials at crank powers corresponding to 20, 40, 60, 80, 100 or 120% of their sit-stand transition power in seated and standing positions. Each pedaling trial began with a stabilization of about 10 s at the target power output at 90 RPM, followed by 10 s of data recording. Three minutes of passive rest were given between each trial.

2.3. Data acquisition

The force and moment applied to the pedals were recorded from two instrumented pedals (I-Crankset-1, SENSIX, Poitiers, France) at 1 kHz. Kinematics data were collected from 22 passive markers on anatomical landmarks of the lower limbs selected according to De Leva's anthropometric charts (de Leva, 1996) and recorded by twelve infrared cameras (VICON, Oxford, United-Kingdom) at 200 Hz. Surface EMG recorded from 9 muscles of the right side of the body was used for this study i.e., *tibialis anterior* (TA), *soleus* (SOL), *gastrocnemius lateralis* (GL), *vastus lateralis* (VL), *vastus medialis* (VM), *rectus femoris* (RF), *biceps femoris* (BF), *semitendinosus* (ST), and *gluteus maximus* (Gmax). Prior to electrode application, the skin was shaved and cleaned with alcohol to minimize impedance. Each electrode (Delsys DE 2.1, Delsys Inc, Boston, MA, USA; 1 cm inter-electrode distance) was placed according to the recommendations of Surface EMG for Non-Invasive Assessment of Muscles (SENIAM). Electrodes were secured with adhesives tapes before recordings. EMG signals were amplified (×1000), digitized (6-400 Hz bandwidth) at a sampling rate of 1 kHz (Bagnoli 16, Delsys, Inc. Boston, USA). Kinetics, kinematics and muscle activation data were synchronized using Nexus 1.7.1 system (VICON, Oxford, United-Kingdom).

2.4. Data reduction and analysis

To compute ankle, knee and hip net joint moments, a classic inverse dynamic process was used (Winter, 1990). In this method, lower limbs' body-segments were considered rigid and interconnected by frictionless joints. Because of the impossibility to stick one marker on the *medial malleollus* in reason of the crank proximity, and because of

the lack of accuracy of one marker on the great trochanter to represent the hip joint center (Neptune and Hull, 1995), ankle and hip joint centers were located using the SCoRE method (Ehrig et al., 2006). For this method, a preliminary recording asking the participants to repeat flexion-extension, abduction-adduction and circumduction of the tested joint allowed the localization of their centers-of-rotation (Begon et al., 2007). The knee joint center was defined as the midpoint between the medial and lateral femoral condyles. The remaining body segments characteristics were defined in accordance with De Leva's anthropometric charts (de Leva, 1996). The Moment Cost Function (Marsh et al., 2000) was defined as:

$$MCF = M_A + M_K + M_H \quad \text{(Equation 1)}$$

where M_A, M_K, and M_H are the mean values on one cycle of the three-dimensional ankle, knee, and hip joint moment euclidian norms, respectively. MCF were computed in a dimensionless form by dividing them by the participant's body weight and his maximum leg length during the cycle (from the hip joint center to the center of the pedal axis) in order to reduce the variability associated with anthropometry (Hof, 1996). Kinetics and kinematics data were recorded in three-dimensions and filtered using a 4^{th} order, zero phase-shift, low-pass Butterworth with a 8 Hz cutoff frequency (McDaniel et al., 2014). EMG signals were bandpass filtered (zero lag, 4^{th} order Butterworth) between 20 and 400 Hz. Linear envelope for each muscle was obtained by first subtracting the mean and then by low-pass filtering the fully rectified raw EMG signals with a 4^{th} order, zero phase-shift,

low-pass Butterworth with a 8 Hz cutoff frequency. The Electromyographic Cost Function (ECF) was defined as (MacIntosh et al., 2000):

$$ECF = EMG_{TA} + EMG_{SOL} + EMG_{GM} + EMG_{VM} + EMG_{VL} + EMG_{RF} + EMG_{ST} + EMG_{BF} + EMG_{Gmax}$$

(Equation 2)

where EMG_i represents the mean value of the EMG envelope computed over the 15 cycles of each pedaling condition for the i^{th} muscle.

MCF and ECF for each pedaling condition were averaged on 15 pedaling cycles and then normalized by their mean value computed across all pedaling conditions (Yang and Winter, 1984). The entire data processing was performed using custom-made codes written in Scilab 5.4.0 (SCILAB, Scilab Enterprises).

2.5. Statistics

Before each statistical test, data normality and variance homogeneity were assessed using Shapiro-Wilk's, and Levene's tests, respectively. Pearson's correlation coefficients (r) were used to determine the correlation between the two cost functions. Two ways repeated measures ANOVAs with factors position = [seated; standing] and power output = [20; 40; 60; 80; 100; 120% of the sit-stand transition power] were performed to compare MCF and ECF across power outputs and positions. Post-hoc analyses were performed using Fisher's method. Partial eta-squared (η^2) were used to quantify the size of the effect

of power-output on the cost functions. All statistical analyses were performed using STATISTICA (STATSOFT, Maisons-Alfort, France). An alpha-value of 0.05 was defined as the level of statistical significance.

3. Results

The sit-stand transition power was 568 ± 93 W (8.0 ± 1.4 W.kg^{-1}) and the power outputs corresponding from 20 to 120% of the sit-stand transition power ranged from 114 ± 19 W (1.6 ± 0.3 W.kg^{-1}) at 20% to 682 ± 111W (9.6 ± 1.6 W.kg^{-1}) at 120%.

MCF and ECF were strongly correlated in seated ($r = 0.95$; $p < 0.01$), standing ($r = 0.86$; $p < 0.01$), and when combining both conditions ($r = 0.93$; $p < 0.01$) (Figure 1).

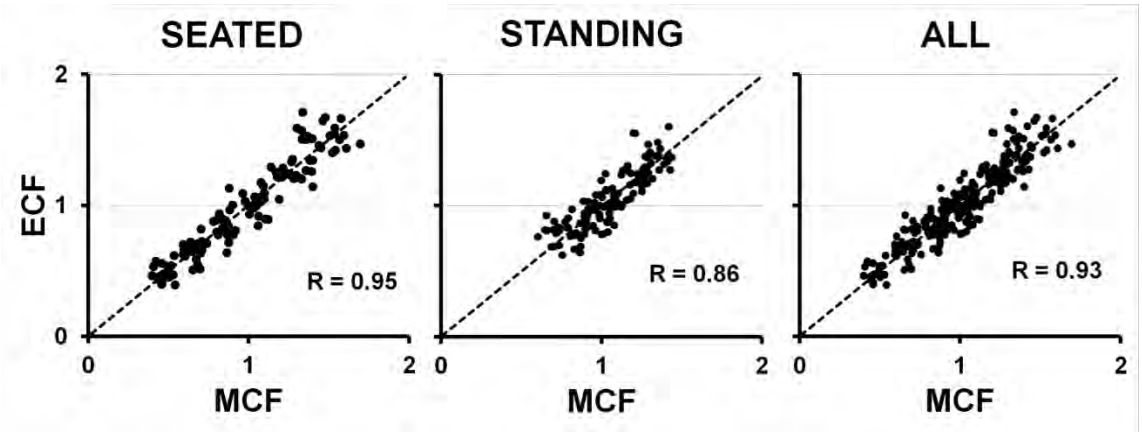

FIGURE 1 *– Correlation between the Moment Cost Function (MCF) and the Electromyographic Cost Function (ECF).*

MCF and ECF were strongly affected by the power output in both seated and standing positions ($p < 0.001$; Figure 2), as evidenced by partial η^2 of 0.98 and 0.89, and 0.96 and 0.89, respectively. The interaction was significant between position and power

output for both MCF and ECF ($p < 0.001$). Post-hoc results showed that MCF and ECF

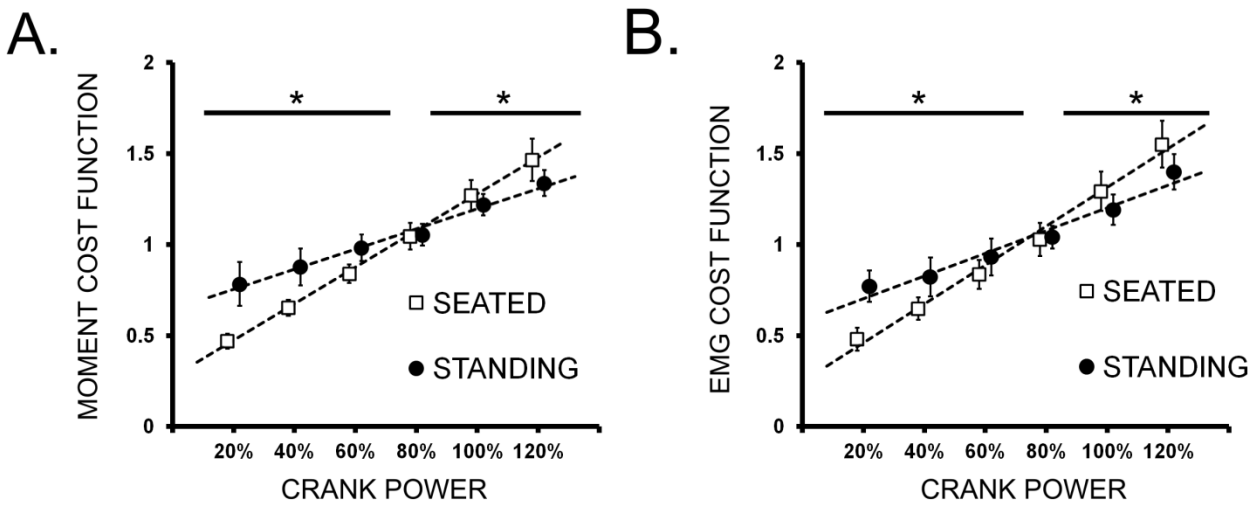

FIGURE 2 – Cost functions across power outputs. A. Moment-based Cost Function (MCF). B. EMG-based Cost Function (ECF).

*: significant difference between seated and standing positions ($p < 0.05$).

4. Discussion

The first purpose of this study was to test the relationship between a moment-based (MCF) and an electromyography-based cost function (ECF). This study was the first to investigate the sit-stand transition in cycling through the combined analysis of kinetics and electromyographics data. In accordance with our hypothesis, these cost functions presented a strong correlation between each other and had lower values in the spontaneously chosen cycling position.

The strong relationships we found between ECF and MCF was not obvious at first as many factors may have limited the correlation between these two cost functions. For example, the relation between muscle force and muscle activation as measured by surface electromyography is not always linear (Perry and Bekey, 1981). Moreover, joint moments are the product of individual muscle forces and of their lever arm across joints, which

change during the cycles. Their interpretation in regard to muscle forces is complex because of the existence of polyarticular muscles (Van Ingen Schenau et al., 1987). Additionally, the relationship between EMG and force in monoarticular muscles is not direct because muscle force arises from both contractile and non-contractile elements and the former cannot be taken into account by the EMG. Nevertheless, we found that the two cost functions carried similar information, given the high correlation coefficients between them. From this standpoint, both cost functions used in this study have the benefit to combine joint moments (MCF) or muscle activations (ECF) in a single variable the whole lower limbs. Their agreement to explain the spontaneous change of position in cycling indicates that both could be relevant to represent the total effort made by the lower limb muscles in cycling. Marsh et al. (2000) reported that the association between MCF and the preferred pedaling cadence was only moderate in two dimensions. However, the inclusion of 3D analyses, the scaling factors and the normalization used here may have improved the sensitivity of this cost function. Further experiments are needed to verify if improvements can be observed by adding upper limb kinetics and/or muscles data to these cost functions in order to get a full body representation. Our result suggests that both cost functions are equivalent and imply coherence between mechanical and electrophysiological measurements to provide a simple representation of the global lower limb muscular effort.

The second purpose of the study was to test the combined effect of power output and position on these cost functions. We hypothesized that cost functions would be lower in seated position before the power output corresponding to the spontaneous sit-stand transition, and in standing position from and above this power output. Our findings supported our hypothesis, and both MCF and ECF showed lower values at power-outputs corresponding to the spontaneously chosen positions. Based on these cost functions, these

results suggest that it is optimal to pedal in seated position below the power output corresponding to the spontaneous sit-stand transition, and *vice versa* in standing position from and above this power output. One interesting observation of this study was the occurrence of the intersection between seated and standing cost functions at around 80% of the sit-stand transition power. Indeed, the incremental nature of the protocol used to determine the spontaneous sit-stand transition power in this study may have induced a transition for the participants when the standing position enabled a significant decrease of the cost-function values. It may be verified in future studies if a lower sit-stand transition power would be observed if the protocol was decremental instead of incremental. For example, hysteresis in the speed at which the transition occurs have been observed in the walk-run versus run-walk transition speed (Thorstensson and Roberthson, 1987). The presence of a similar hysteresis in cycling may therefore be hypothesized and could be the focus of further research.

The ability to identify the cross-point of seated and standing cost functions relies on the different slopes and the different y-intercepts of these two lines. The lower slope in the relationship between cost functions and power-output in standing position in comparison to the seated position was a robust finding. The difference in slope and in y-intercept may have mechanical interpretations. The higher y-intercept value in standing position may be linked with the need for the legs to support a larger part of the body weight even without producing any power-output at the crank whereas a part of this weight is supported by the saddle in seated position. Conversely, the lower slope in standing position represents a smaller rate of increase in the cost per unit of power-output, which means that the standing position becomes more efficient than the seated position in terms of joint torque and integrated EMG to produce higher power-outputs. This advantage of the standing position

above one level of crank power is consistent with practitioners' habits, using the standing position in pedaling conditions (sprinting, climbing) in which high power-outputs are necessary. This last finding is important given that most previous studies failed to explain why the standing position often provides an advantage to produce high power-outputs.

Previous studies used oxygen consumption criteria to compare seated and standing positions in cycling. At low crank powers, the seated position has been shown to be more efficient (Ryschon and Stray-Gundersen, 1991; Tanaka et al., 1996). However, this approach failed to find any efficiency advantage of the standing position for high power outputs (Harnish et al., 2007; Millet et al., 2002; Tanaka et al., 1996). Only one recent study suggested an increase in gross efficiency in standing position (Bouillod et al., 2014). However, in this study, the increase in gross efficiency was caused by an increase in the crank power necessary to reach a given speed on a treadmill due to mechanical losses in the standing position, and the oxygen consumption was not different between the two positions at the same speed. Because the power at which the transition should occur has been reported to correspond to times to exhaustion around 210 s (Hansen and Waldeland, 2008), an important part of the energy production may come from anaerobic pathways (Medbø and Tabata, 1989). Therefore, the sustainability of the standing position to increase crank power may be too short to be highlighted with an oxygen consumption criterion. The cost functions proposed in this study may therefore offer an alternative to investigate bouts of exercise of such short duration. The fact that the minimization of these cost function was associated with the spontaneous choice of the participants suggest that they may be relevant to define individualized bike settings for cyclists. These results are in line with Gonzalez and Hull (1989) who used a moment cost function to define optimal settings (saddle height, anteroposterior cleat placement, cadence…) in a modelization of theoretical

cyclists. Further investigations are necessary to determine if such cost function would be useful to monitor the evolution of the cost of cycling, or other tasks, with training, fatigue and during rehabilitation.

Other mechanical factors may also influence the spontaneous change from the seated to the standing position. It has been previously suggested that the standing position could be used in order to increase the minimum crank torque, described as a weak point in the pedaling cycle (Caldwell, 2000). Indeed, the pattern of crank torque application may be shifted in this position, probably because of an increased gravitational component (Caldwell et al., 1998). Another mechanical factor influencing the sit-stand transition power may be a decrease in saddle vertical force (Costes et al., 2015). In a previous study (Costes et al., 2015), according to Newton's third law we proposed that equilibrium between the vertical component of pedals, handlebars, saddle, trunk's weight and trunk's inertial forces is fundamental. In this study, we showed that an increase in pedal forces is necessary to create higher crank powers for a given pedaling cadence. As a consequence, the saddle vertical force has been observed to decrease, which may be determinant in the triggering of the sit-stand transition.

In addition to the metabolic energy consumption, several other parameters have proven their influence on the walk-to-run transition such as mechanical, perceptual factors (Farris and Sawicki, 2012; Mohler et al., 2007) or optimization criteria (Alexander, 1989; Diedrich and Warren, 1995; Ivanenko et al., 2008). Gait and cycling are similar in many aspects and they have a common need to increase muscle powers in response to increasing speed for a given movement frequency. Therefore, by analogy it could be suspected that the same influences may also be found in cycling. One hypothesis to cope with the

diversity of factors influencing the transition during gait would be to consider the sense of effort as a determinant of the change in coordination mode. Integrative models such as the central governor model (Noakes et al., 2005) or the flush model (Millet, 2011) may explain how motor strategies (i.e., pace, or here coordination mode) are spontaneously selected in humans by taking into account several potential stressors perceived by the central nervous system.

In conclusion the present study suggested that moment or electromyography-based cost functions are correlated and smaller in the spontaneously chosen cycling position compared to the other position across a wide range of power-output. The cost functions defined in this study may provide a simple quantification of the muscular efforts in cycling and could be useful to define optimal settings such as saddle height, anteroposterior cleat placement or cadence. Future work may focus on other tasks to study the relevance of moment-based and/or electromyography-based cost functions to evaluate muscle effort.

Acknowledgements

Antony Costes was funded by a PhD grant from the French Ministry of Education and Research (Ministère de l'Education et de la Recherche). The authors would like to thank Dr. Laurent Seitz for his review of the manuscript.

Conflict of Interest

The authors have no financial or personal relationships with other people or organizations that could have inappropriately influenced this research.

References

Alexander, R.M., 1989. Optimization and gaits in the locomotion of vertebrates. Physiological Review 69, 1199–1227.

Ansley, L., Cangley, P., 2009. Determinants of "optimal" cadence during cycling. European Journal of Sport Science 9, 61–85.

Barroso, F.O., Torricelli, D., Moreno, J.C., Taylor, J., Gomez-Soriano, J., Bravo-Esteban, E., Piazza, S., Santos, C., Pons, J.L., 2014. Shared muscle synergies in human walking and cycling. Journal of Neurophysiology 112, 1984–1998.

Begon, M., Monnet, T., Lacouture, P., 2007. Effects of movement for estimating the hip joint centre. Gait and Posture 25, 353–359.

Biess, A., Liebermann, D.G., Flash, T., 2007. A computational model for redundant human three-dimensional pointing movements: Integration of independent spatial and temporal motor plans simplifies movement dynamics. Journal of Neuroscience 27, 13045–13064.

Bouillod, A., Pinot, J., Valade, A., Cassirame, J., Soto-Romero, G., Grappe, F., 2014. Gross efficiency is improved in standing position with an increase of the power output. Journal of Science and Cycling 3, 6.

Caldwell, G.E., Li, L., McCole, S.D., Hagberg, J.M., 1998. Pedal and Crank Kinetics in Uphill Cycling. Journal of Applied Biomechanics 14: 245-259.

Caldwell, G.E., van Emmerik, R.E.A., Hamill, J., 2000. Movement proficiency: incorporating task demands and constraints in assessing human movement. In: Energetics of Human Activity. Sparrow, W.A., Human Kinetics, Champaign, IL, USA, pp 66-95.

Costes, A., Turpin, N.A., Villeger, D., Moretto, P., Watier, B., 2015. A reduction of the saddle vertical force triggers the sit-stand transition in cycling. Journal of Biomechanics 48: 2998-3003.

De Leva, P., 1996. Adjustments to Zatsiorsky-Seluyanov's segment inertia parameters. Journal of Biomechanics 29, 1223–1230.

Diedrich, F., Warren, W., 1995. Why Change Gaits - Dynamics of the Walk Run Transition. Journal of Experimental Psychology: Human Perception and Performance 21, 183–202.

Duc, S., Bertucei, W., Pernin, J.N., Grappe, F., 2008. Muscular activity during uphill cycling: Effect of slope, posture, hand grip position and constrained bicycle lateral sways. Journal of Electromyography and Kinesiology 18, 116–127.

Ehrig, R.M., Taylor, W.R., Duda, G.N., Heller, M.O., 2006. A survey of formal methods for determining the centre of rotation of ball joints. Journal of Biomechanics 39, 2798–2809.

Farris, D.J., Sawicki, G.S., 2012. The mechanics and energetics of human walking and running: a joint level perspective. Journal of the Royal Society Interface 9, 110–118.

Flash, T., Hogan, N., 1985. The Coordination of Arm Movements - an Experimentally Confirmed Mathematical-Model. Journal of Neuroscience 5, 1688–1703.

Gonzalez, H., Hull, M.L., 1989. Multivariable optimization of cycling biomechanics. Journal of Biomechanics 22, 1151–1161.

Hansen, E.A., Waldeland, H., 2008. Seated versus standing position for maximization of performance during intense uphill cycling. Journal of Sports Science 26, 977–984.

Hof, A.L., 1996. Scaling gait data to body size. Gait and Posture 4, 222–223.

Hug, F., Dorel, S., 2009. Electromyographic analysis of pedaling: a review. Journal of Electromyography and Kinesiology 19, 182–198.

Hull, M.L., Jorge, M., 1985. A method for biomechanical analysis of bicycle pedalling. Journal of Biomechanics 18, 631–644.

Ivanenko, Y.P., Cappellini, G., Poppele, R.E., Lacquaniti, F., 2008. Spatiotemporal organization of alpha-motoneuron activity in the human spinal cord during different gaits and gait transitions. European Journal of Neuroscience 27, 3351–3368.

Jackson, M., Benkhemis, I., Begon, M., Sardain, P., Vallée, C., Lacouture, P., 2012. Identifying the criterion spontaneously minimized during the take-off phase of a sub-maximal long jump through optimal synthesis. Multibody System Dynamics 28 : 225-237.

Kautz, S.A., Hull, M.L., Neptune, R.R., 1994. A comparison of muscular mechanical energy expenditure and internal work in cycling. Journal of Biomechanics 27: 1459-1467.

Li, L., Caldwell, G.E., 1998. Muscle coordination in cycling: effect of surface incline and posture. Journal of Applied Physiology 85, 927–934.

MacIntosh, B.R., Neptune, R.R., Horton, J.F., 2000. Cadence, power, and muscle activation in cycle ergometry. Medicine Science in Sports and Exercise 32, 1281–1287.

Marsh, A.P., Martin, P.E., Sanderson, D.J., 2000. Is a joint moment-based cost function associated with preferred cycling cadence? Journal of Biomechanics 33, 173–180.

McDaniel, J., Behjani, N.S., Elmer, S.J., Brown, N.A., Martin, J.C., 2014. Joint-specific power-pedaling rate relationships during maximal cycling. Journal of Applied Biomechanics 30, 423–430.

Medbø, J.I., Tabata, I., 1989. Relative importance of aerobic and anaerobic energy release during short-lasting exhausting bicycle exercise. Journal of Applied Physiology 67, 1881–1886.

Millet, G.Y., 2011. Can Neuromuscular Fatigue Explain Running Strategies and Performance in Ultra-Marathons? The Flush Model. Sports Medicine 41, 489–506.

Mohler, B.J., Thompson, W.B., Creem-Regehr, S.H., Pick, H.L., Warren, W.H., 2007. Visual flow influences gait transition speed and preferred walking speed. Experimental Brain Research 181, 221–228.

Neptune, R.R., Hull, M.L., 1995. Accuracy assessment of methods for determining hip movement in seated cycling. Journal of Biomechanics 28, 423–437.

Noakes, T.D., Gibson, A.S., Lambert, E.V., 2005. From catastrophe to complexity: a novel model of integrative central neural regulation of effort and fatigue during exercise in humans: summary and conclusions. British Journal of Sports Medicine 39, 120–124.

Perry, J., Bekey, G.A., 1981. EMG-force relationships in skeletal muscle. Critical Reviews in Biomedical Engineering 7: 1-22.

Pires, N.J., Lay, B.S., Rubenson, J., 2014. Joint-level mechanics of the walk-to-run transition in humans. Journal of Experimental Biology 217, 3519-3527.

Poirier, E., Do, M., Watier, B., 2007. Transition from seated to standing position in cycling allows joint moment minimization. Science and Sports 22, 190-195.

Raasch, C.C., Zajac, F.E., 1999. Locomotor Strategy for Pedaling: Muscle Groups and Biomechanical Functions. Journal of Neurophysiology 82, 515–525.

Raynor, A.J., Yi, C.J., Abernethy, B., Jong, Q.J., 2002. Are transitions in human gait determined by mechanical, kinetic or energetic factors? Human Movement Science 21, 785–805.

Thorstensson, A., Roberthson, H., 1987. Adaptations to changing speed in human locomotion: speed of transition between walking and running. Acta Physiologica Scandinavica 131 : 211-214.

Van den Bogert, A.J., Hupperets, M., Schlarb, H., Krabbe, B., 2012. Predictive musculoskeletal simulation using optimal control: effects of added limb mass on energy cost and kinematics of walking and running. Proceedings of the Institution of Mechanical Engineers, Part P: Journal of Sports Engineering and Technology 226, 123–133.

Van Ingen Schenau, G.J., Bobbert, M.F., Rozendal, R.H., 1987. The unique action of bi-articular muscles in complex movements. Journal of Anatomy 155: 1-5.

Winter, D.A., 1990. Biomechanics and Motor Control of Human Movement. Wiley-Interscience, New York, pp. 370.

Yang, J.F., Winter, D.A., 1984. Electromyographic amplitude normalization methods: improving their sensitivity as diagnostic tools in gait analysis. Archives of Physical Medicine and Rehabilitation 65, 517–521.

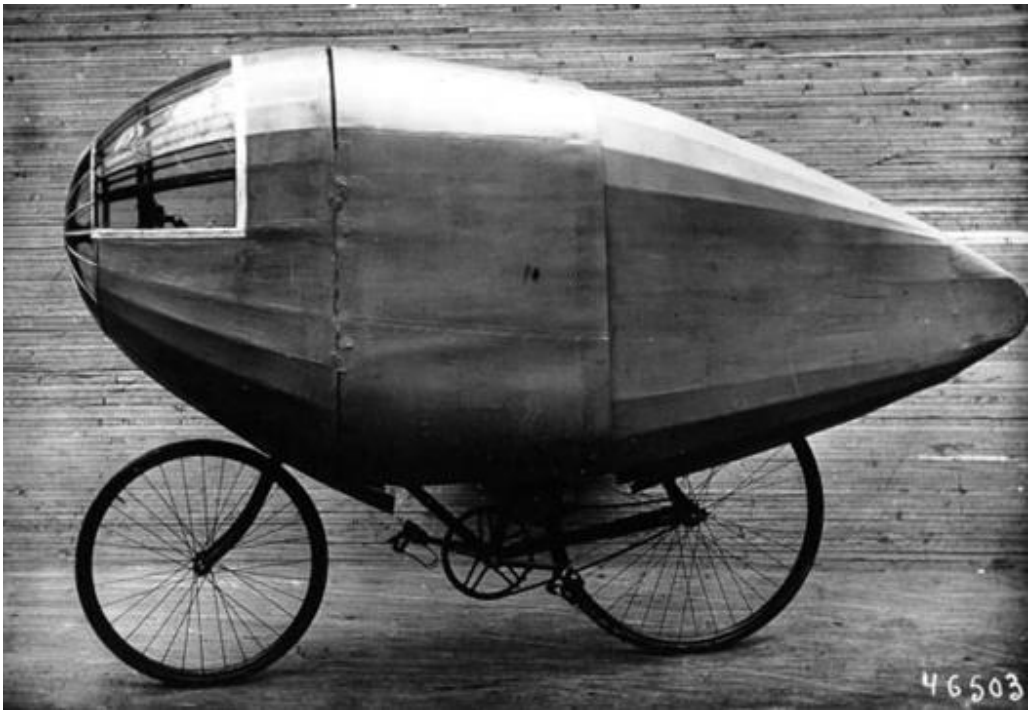

IV) Conclusion et Perspectives

Illustration : Le « Vélo-Torpille » inventé par Etienne Bunau-Varilla et Marcel Riffard (1913)

En résumé, les contributions personnelles apportées au cours de ces travaux de thèse s'articulent autour d'une nouvelle analyse de la transition assis-danseuse en cyclisme rendue possible grâce à l'utilisation d'un ergocycle entièrement instrumenté ayant permis l'étude de la dynamique des membres supérieurs et inférieurs.

Dans un premier temps, l'effet de la puissance de pédalage et de la position sur les contraintes mécaniques du membre supérieur ont été analysées. En révélant une augmentation des couples, puissances et travaux des articulations du membre supérieur lorsque la puissance au pédalier augmente et/ou lorsque la position en danseuse est choisie, cette étude indique la nécessité de prendre en compte les membres supérieurs lors de futures études biomécaniques du pédalage, en particulier lorsque le focus est sur des puissances élevées et/ou sur la position en danseuse, comme cela peut-être le cas par exemple lors d'une pratique cycliste de haut-niveau. D'autre part, en fournissant une première référence sur le niveau de sollicitation mécanique du membre supérieur, cet article ouvre la voie à de nouvelles investigations vers la recherche d'optimisation de la performance ou encore vers la prévention des blessures. Les perspectives directes en prolongement de ces travaux pourraient être l'analyse de nouvelles positions de pédalage, de nouvelles configurations de cintre, de populations différentes (enfants, seniors, haut-niveau...), et d'une application sur le terrain qui nécessiterait une instrumentation permettant une analyse cinématique et dynamique déplaçable à l'extérieur du laboratoire. La précision de l'analyse par procédé de dynamique inverse étant liée à celle de la détermination de ses trois types de données d'entrée que sont la cinématique, la mesure des efforts externes et l'anthropométrie, améliorer la finesse de ces mesures constituera un des enjeux de la future recherche en biomécanique.

Dans un second temps, notre objet d'étude a été la transition assis-danseuse en cyclisme. Lors de l'analyse des efforts mécaniques au niveau du membre supérieur, les premiers indices associés à la transition assis-danseuse ont été observés avec l'apparition de couples articulaires correspondant à une traction du membre supérieur sur le cintre assis et au niveau de puissance correspondant à la transition spontanée en danseuse. En plus de la traction sur le cintre, la poursuite de l'analyse a permis d'observer dans le même contexte des efforts de traction sur les pédales, ainsi qu'une diminution de la force verticale appliquée sur la selle. Conformément aux définitions des positions « assis » et « danseuse » proposées dans ces travaux, il semble que la diminution de la force verticale sur la selle observée simultanément à une augmentation des

forces appliquées sur les pédales constitue un déclencheur mécanique de la transition assis-danseuse en cyclisme. Les stratégies observées permettant de pédaler assis avec un niveau de force appliquée sur les pédales élevé autorisent le maintien de cette position, mais semblent coûteuses mécaniquement et pourraient faire l'objet de futures recherches ayant pour but l'optimisation de la performance. Afin de confirmer ces résultats, de nouvelles études sont nécessaires. En effet, d'après l'équation proposée dans l'article « A Reduction of the Saddle Vertical Force Triggers the Sit-Stand Transition in Cycling », des possibilités de manipulation de l'état d'équilibre des forces appliquées par et sur le cycliste peuvent être testées. Par exemple, une modification de la cadence de pédalage devrait en théorie modifier la puissance spontanée de transition, et il en est de même pour une modification du poids corporel. Une autre application de ces travaux est l'explication des mouvements effectués par le tronc, qui pourrait aboutir sur de nouvelles recommandations pratiques afin de maintenir une posture stable sur la bicyclette dans un contexte d'application de forces élevées sur les pédales. La corrélation et la minimisation des fonctions de coût mécaniques présentées dans la dernière partie de ces contributions personnelles dans la position spontanément choisie en cyclisme donne une nouvelle preuve des possibilités offertes par ce type de fonction représentative des efforts musculaires du membre inférieur. La suite logique serait de tester l'effet d'autres variables (réglages de la bicyclette, pente, fatigue, pratique de terrain...) sur ces fonctions de coût, qui pourraient s'avérer des outils puissants afin d'optimiser de façon individuelle l'intéraction homme-machine en cyclisme. L'utilisation de ces fonctions de coût hors du contexte du pédalage pourrait aussi offrir de nombreuses perspectives de recherche. Il est à noter que ces fonctions de coût pourraient être encore améliorées par une prise en compte du corps entier, ainsi que par leur visualisation en temps réel qui nécessiterait de nouvelles créations matérielles. L'approche pour la normalisation proposée sur les « Moment Cost Function » offre elle aussi de nouvelles perspectives. En effet, il n'est pas rare de voir les cyclistes mis en parallèle en fonction de « puissances-étalon », qui pourraient être rendues plus comparables en prenant en compte la masse (ce qui est parfois le cas), et la taille des cyclistes (ce qui est plus rare). Dans cette optique, les travaux récents effectués en collaboration avec David Villeger à propos de nouveaux nombres adimensionnels appliqués à la marche et à la course semblent transférables avec quelques modifications à l'analyse du cyclisme. Une ébauche d'approche adimensionnelle adaptée au cyclisme est présentée en annexe (section IV.5). Cette approche permettrait d'augmenter la puissance statistique de certaines études biomécaniques portant sur le cyclisme. Enfin, il est à noter que certaines problématiques à propos de la transition

assis-danseuse restent à approfondir. Les perspectives de ce travail, poursuivies en 2016 dans le cadre du Master II Recherche de Rémi Gouze seront d'étudier l'effet de la cadence de pédalage, et de la variation du poids corporel sur la transition assis-danseuse. D'autre part, la question de l'utilisation du poids du corps pour se propulser en danseuse est récurrente et mériterait une analyse approfondie. Enfin, et lorsque l'évolution technologique le permettra, les données recueillies lors de ces travaux seront à comparer avec celles obtenues dans un contexte écologique.

En catégorie « Annexe » sont présentées les études réalisées dans le cadre de mon année de Master II Recherche. Les enregistrements réalisés au cours de cette année d'étude ont été exploités en début de thèse et ont constitué une approche préliminaire à cette thèse, ayant fait l'objet de plusieurs articles portant sur la mécanique du pédalage et celle du mouvement humain.

V) Annexes

IV.1. INTRODUCTION

Dans cette partie « Annexes » sont présentés des travaux connexes au thème central de cette thèse et donc en lien avec l'optimisation spontanée du pédalage, et de façon plus générale avec l'optimisation spontanée du mouvement humain.

Ces derniers sont principalement associés aux travaux de mon année de Master II Recherche. C'est au cours de cette année que le laboratoire de biomécanique de l'Université de Toulouse a fait l'acquisition d'une paire de pédales instrumentées Sensix I-Crankset. Ces dernières, combinées au système de capture du mouvement Vicon, ont permis l'application d'un procédé de dynamique inverse sur des cyclistes réalisant une épreuve « force-vitesse » sur ergocycle. Un résultat surprenant observé au niveau du couple à la cheville a retenu notre attention. En effet, le moment d'extension de la cheville était supérieur lors du pédalage en comparaison sur ergomètre isocinétique. Ce résultat a été confirmé par électromyographie sur les muscles extenseurs de la cheville dans la littérature (Dorel et al. 2012). L'article associé à cette étude a été accepté pour publication par le « Journal of Human Kinetics ». Sa suite directe, s'interrogeant sur l'origine du résultat observé à la cheville a été publiée dans la revue « European Journal of Applied Physiology ».

Enfin, l'ébauche d'une approche adimensionnelle du cyclisme est proposée. Cette dernière a pour objectif de diminuer la part de variabilité des indices mécaniques mesurés chez le cycliste associée à leurs différences d'anthropométrie.

IV.2. ETUDE 7 : AN INVERSE DYNAMIC STUDY SUGGESTS THAT CYCLISTS MARGINALLY USE HIP JOINT TORQUE AT MAXIMAL POWER

Article associé à mes travaux de Master II Recherche, accepté et présenté par Bruno Watier au 24ème Congrès de la Société Internationale de Biomécanique (Natal, Brésil).

ISB 2013
BRAZIL
XXIV CONGRESS OF THE INTERNATIONAL SOCIETY OF BIOMECHANICS
XV BRAZILIAN CONGRESS OF BIOMECHANICS

AN INVERSE DYNAMIC STUDY SUGGESTS THAT CYCLISTS MARGINALLY USE HIP JOINT TORQUE AT MAXIMAL POWER

[1]Bruno Watier, [1]Antony Costes and [1]Pierre Moretto

[1]: Université de Toulouse; UPS; PRISMH-LAPMA ; 118, rte de Narbonne – 31062 Toulouse Cedex 09 – France
Bruno Watier (corresponding author): bruno.watier@univ-tlse3.fr

SUMMARY

This study aims to calculate net joint torques at ankle, knee and hip, using inverse dynamic during a maximal power cycling task on a cycle ergometer. These torques were then compared to maximum joint torques developed by each isolated articulation on isokinetic ergometer. Results show that subjects develop a maximal power (594±100W) during cycling at a pedaling frequency of 108±9RPM and an average torque at crank axis of 53.1±10Nm. Analyzing each joint torque reveals the leading part of the knee during the cycling task. Moreover, matching data from the isokinetic ergometer and from the cycling task, muscle force of hip extensors appears underused because only 33% of its maximal isometric torque is developed on the cycle ergometer.

INTRODUCTION

The inverse dynamic methods have been used in cycling tasks for a better understanding of geometric settings influence on the muscular torque developed at each joint of the lower limb. For some authors [1, 2], minimization of muscular torques is an important criterion of performance. Modifications of joint torques with standing mode, saddle height and power output level have already been analyzed [3, 4, 5, 6]. However, no comparison exists between torques developed by each joints during cycling and maximum capacity at these joints measured on isokinetic ergometer.

METHODS

Nine triathletes participated in this study. They were 32±10 years old, the mean height and body mass were 1.74±0.06m, and 64.6±6.8kg, respectively. They practice yearly 3100±1700km cycling since 11.7±10.9 years. The study consisted in two sessions spaced out of seven days.

The first test aimed to determine maximal power during cycling and associated nets joints torques at ankle, knee and hip. Usual settings of subjects were reproduced on the cycle ergometer in this sequence. A cycle ergometer Lode Excalibur with a crank length of 0,17m has been used. Subjects had to perform a protocol adapted from Vandewalle et al [7] consisting in six maximum pedaling phases of seven seconds against loads applied in random order with five minutes of passive rest between each. For each trial at maximal power, kinematics of lower limbs were analyzed using an optoelectronic Vicon system including ten cameras. Following ISB recommendations [8], three spherical markers were placed on anatomical landmarks corresponding to the hip, knee and ankle. Two additional markers were set up to identify cycle ergometer position. The cycle ergometer was instrumented with two pedals I-Crankset from Sensix to determine forces and torques applied by the foot on the crank. The acquisition frequency was set to 200Hz and the complete rotation of the cranks corresponding to the maximum power output was analyzed. Whole data have been filtered using a 4th order butterworth low pass filter with a cut off frequency of 6Hz for kinematic and 10Hz for forces and torques. Mixing anthropometric data from de Leva et al. [9], kinematic from Vicon, forces and torques data from instrumented pedals, inverse dynamic was used to calculate net joint torques at ankle, knee and hip using Newton-Euler formalism applied at the feet, the leg and the thigh. This study has been realized in the sagittal plane and torques were determined around transverse axis.

The second test consisted in a measure of maximum torque performed on isokinetic ergometer Biodex. Maximum joint torques were determined at ankle, knee and hip in flexion and extension with concentric contractions. Maximum torques were measured for the whole range of motion of each joint at a rotation speed of 20°/sec. This slow speed was chosen to approach isometric conditions. For each subject, joints have been tested in a random order. A four minutes rest period was allowed between each joint test.

Each result is presented as mean ± standard deviation. A two ways analysis of variance ($P<0.05$) has been conducted to discern the difference at measured joints during the cycling and ergometer tests.

RESULTS AND DISCUSSION

For the cycling test, results give torque evolution along a rotation at the crank axis (figure 1), the hip (figure 2), the knee (figure 3) and the ankle (figure 4). The calculated torque at the crank axis is the result of the contribution of the two lower limbs while torque at each joint is the torque for one leg.

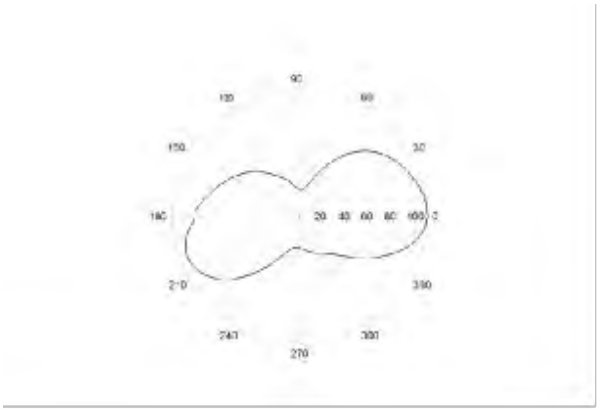

Figure 1 : Polar representation of the torque at crank axis

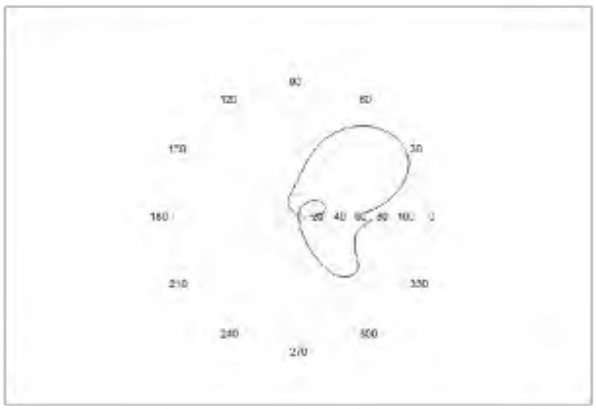

Figure 2: Polar representation of the torque at the hip

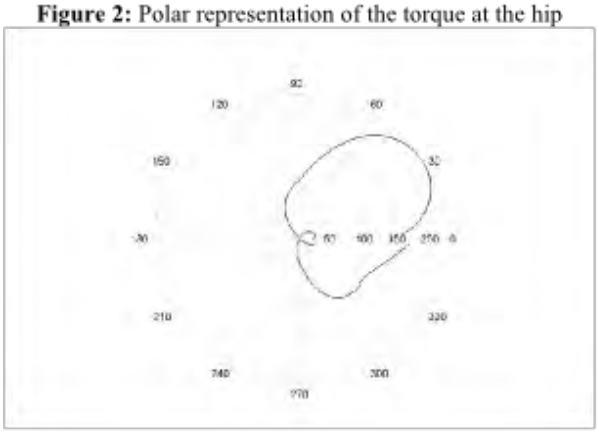

Figure 3: Polar representation of the torque at the knee

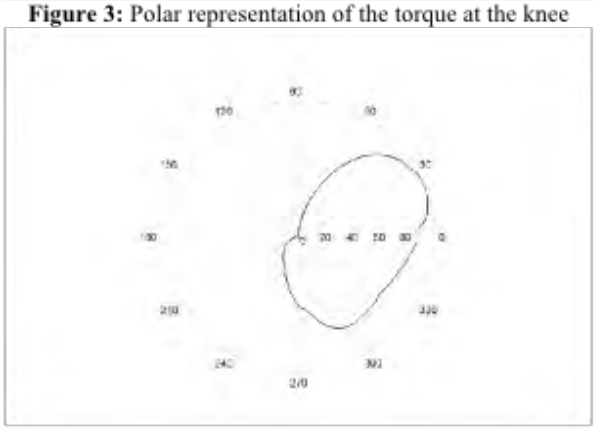

Figure 4 : Polar representation of the torque at the ankle

For this experience, subjects developed a maximal power of 594±100W at a 108±9RPM cadence and a mean torque of 53.1±10Nm at crank axis. For each joint, maximum torque is developed during the descent of the crank while joints are in concentric extension phase. During the rise of the crank, joints show a concentric flexion phase, meaning that subjects pull the clipless pedals during upstroke. When normalized to body mass, the maximum extension torque at the ankle is 1.14±0.27Nm/kg in extension and 0.18±0.09Nm/kg in flexion. At the knee, the maximum torque is 2.89±0.70Nm/kg in extension and 0.67±0.28N/kg in flexion. At the hip, it reaches 1.48±0.45Nm/kg in extension and 0.50±0.14Nm/kg in flexion. So, the knee develops torque value twice as large as those measured at the hip and at the ankle in extension. In flexion, peak torque at the knee and the hip is equivalent whereas it's rather low at the ankle.

Moreover, the comparison between maximum torques measured at each joint during cycling exercise and maximum torques measured on the ergometer reveals that hip is underused during maximum power cycling exercise. Indeed the ratio is by 33% of the isometric maximum torque reaches in extension during cycling, while ankle and knee are forced with respective ratios of 128% and 102%. In contrast, flexion capacity of each joint is rarely used with a mean ratio of 40%.

This shows that the cycling performance may be improved by better use of human capabilities especially at the hip and during flexion. However, this study is limited by speed movement which is approximately 500°/sec during cycling and only 20°/sec on ergometer, and according to Taylor et al. [10], higher speed results in a lower muscular torque. This outcome is not observed here particularly for ankle and knee extension. Moreover, bi-articular muscles can be extensor at one joint and flexor at another one. It can restrict maximum joint torques developed at the different level during overall movement like push-pull during cycling.

CONCLUSIONS

Finally, this study enables us to estimate net torque at each joint during maximal power exercise on cycling ergometer. Results show that triathletes well use ankle and knee during extension, while hip extension and flexion may be increased regarding the low solicitation level observed. A new way of pedaling thus remains to invent for a better utilization of each joint. New chainring and crankset types are perhaps future solutions to enhance the performance.

ACKNOWLEDGEMENTS

The authors wish to thank Sensix Company, Poitiers, France for its material assistance in this study.

REFERENCES

1. Neptune, et al J. Biomech **32**, 409-15, 1999
2. Hull, et al. *J. Biomech* **21,** 839-49, 1988.
3. Poirier, et al. *Science & Sport* **22**, 190-195, 2007.
4. Mornieux, et al. *European Journal of Applied Physiology* **102**, 11-18, 2007.
5. Horscroft, et al. *Med Sci Sport Exerc* **35**, S16, 2003.
6. Caldwell, et al. *Journal of applied biomechanics* **15**, 166-181, 1999.
7. Vandewalle, et al. *European Journal of Applied Physiology* **102**, 650-656, 1987.
8. Wu, G., et al. J Biomech **35**, 543-548, 2002.
9. de Leva, P. *J Biomech* **29**, 1223-1230, 1996
10. Taylor, N., et al. European Journal of Applied Physiology **62**, 116-121, 1991

IV.3. Etude 8 : Transferability Between Isolated Joint Torques and A Maximum Polyarticular Task : A Preliminary Study

Cet article accepté dans la revue « Journal of Human Kinetics » (sous presse) est associé aux travaux réalisés lors de mon Master II Recherche. L'objectif de cet article a été de mesurer les couples articulaires développés lors du pédalage à puissance maximale, puis de les comparer à ceux obtenus lors de mesures isolées sur ergomètre isocinétique afin d'étudier la corrélation entre ces mesures. Un objectif secondaire de cette étude a été de tester la corrélation entre les capacités de production de couple articulaire isolé à basse vitesse angulaire et la puissance maximale en cyclisme. Neuf cyclistes ont réalisé deux évaluations différentes de leurs couples articulaires maximaux au membre inférieur. Les couples articulaires isolés ont été évalués sur ergomètre isocinétique, alors que les mesures de couple articulaire lors du pédalage ont été effectuées par dynamique inverse à la cheville, au genou et à la hanche pour la flexion et l'extension pendant une épreuve de pédalage de type « force-vitesse ». Une analyse des corrélations entre les mesures isolées et celle calculées lors du pédalage a été effectuée pour chacun des mouvements articulaires [3 articulations x (flexion + extension)], ne montrant pas de corrélation significative. Une seule corrélation significative a été trouvée entre la puissance maximale de pédalage et le couple isolé d'extension du genou ($r=0.68$, $P<0.05$). L'absence de corrélation entre les mesures de couple isolées mesurées à faible vitesse angulaire et celles à la même articulation impliquée dans une tâche polyarticulaire montre que le transfert entre les deux n'est pas direct. Ces résultats pourraient être dûs aux différences de vitesse angulaire et à des capacités différentes de production de couple entre mouvements mono- et polyarticulaires. Cependant, cette étude confirme des résultats précédents indiquant que la puissance maximale en cyclisme est corrélée avec le couple articulaire isolé d'extension du genou obtenu à basse vitesse angulaire.

Journal of Human Kinetics volume 49/2015, 7-20
Section I – Kinesiology

DE GRUYTER OPEN

Transferability between Isolated Joint Torques and a Maximum Polyarticular Task: A Preliminary Study

by

Antony Costes[1], David Villeger[1], Pierre Moretto[1,2,3], Bruno Watier[1,4]

The aims of this study were to determine if isolated maximum joint torques and joint torques during a maximum polyarticular task (i.e. cycling at maximum power) are correlated despite joint angle and velocity discrepancies, and to assess if an isolated joint-specific torque production capability at slow angular velocity is related to cycling power. Nine cyclists completed two different evaluations of their lower limb maximum joint torques. Maximum Isolated Torques were assessed on isolated joint movements using an isokinetic ergometer and Maximum Pedalling Torques were calculated at the ankle, knee and hip for flexion and extension by inverse dynamics during cycling at maximum power. A correlation analysis was made between Maximum Isolated Torques and respective Maximum Pedalling Torques [3 joints x (flexion + extension)], showing no significant relationship. Only one significant relationship was found between cycling maximum power and knee extension Maximum Isolated Torque ($r=0.68$, $p<0.05$). Lack of correlations between isolated joint torques measured at slow angular velocity and the same joint torques involved in a polyarticular task shows that transfers between both are not direct due to differences in joint angular velocities and in mono-articular versus poly articular joint torque production capabilities. However, this study confirms that maximum power in cycling is correlated with slow angular velocity mono-articular maximum knee extension torque.

Key words: *cycling, isokinetic ergometer, inverse dynamics, force-velocity test.*

Introduction

Joint torque is a common measure for researchers and practitioners in strength and conditioning biomechanics to evaluate performance. Joint torques can be evaluated by two methods, which include direct and isolated evaluations using isokinetic ergometers, classical conditioning devices (Baroni et al., 2013; González-Ravé et al., 2014), or by indirect and polyarticular methods combining kinetic and kinematic measurements, namely inverse dynamics (Hull and Jorge, 1985).

Given the widespread use of strength and conditioning in sports training and rehabilitation, isolated joint torques assessments are often used to monitor the athlete's performance. This use has been questioned by Baker et al. (1994) who found no relationship between maximum isometric and dynamic force enhancements, and thus criticizing the use of isometric tests to monitor the athlete's performance. In cycling, winning a race is often determined by the ability to produce high power output in order to create high velocities; a high crank power output is crucial to scale the athlete's performance. To our knowledge, only one study in cycling examined the relationship between isolated joint torques and performance,

[1] - *PRISSMH, University of Toulouse, UPS, Toulouse, France.*
[2] - *University of Toulouse; UPS; Centre de Recherches sur la Cognition Animale; Toulouse Cedex 9, France.*
[3] - *CNRS; Centre de Recherches sur la Cognition Animale; Toulouse Cedex 9, France.*
[4] - *CNRS, LAAS, Toulouse, France.*

Authors submitted their contribution to the article to the editorial board.
Accepted for printing in the Journal of Human Kinetics vol. 49/2015 in December 2015.

represented by the maximum crank power output (Driss et al., 2002). In this study, the authors assessed correlations between maximum cycling power and knee extension joint torque at different velocities ranging from 0°·s-1 (isometric mode for a single knee angle of 120°) to 240°·s-1. They found significant correlations between maximum cycling power and knee extension joint torque. However, isolated joint measurements performed in non ecological conditions may not represent the performance in polyarticular dynamic tasks like running, cycling or rowing because of factors like energy storage/releasing, difference in joint angular velocity, inter-segmental coordination, or differences in torque production capabilities between mono-articular and polyarticular testing (Hahn et al., 2011). Indeed, it is not known if these limits are strong enough to preclude correlations between isolated joint torques and the same joint's torques in a polyarticular task given the possible correlations between low and high angular velocity joint torque capabilities (Anderson et al., 2007). For practitioners, the main outcome of this comparison is to establish if a strength/weakness of an isolated joint is found in the same joint involved in a multi-joint task despite muscular and articular redundancy. If both are correlated, it would remain an ideal diagnostic tool to direct training, and if they are not, it would restrict the interest of isolated joint testing when the goal is to develop capabilities on a polyarticular task.

While a series of studies are required to compare isolated joint torques with joint torques in all maximum polyarticular tasks, this one aimed to be the first to make this comparison, and was designed to examine cycling due to the prevalent use of inverse dynamics in this activity (for review, see Bini and Diefenthaeler, 2009). Two objectives were set: (a) to determine if isolated maximum joint torques are correlated with the same joint's torque during cycling at maximum power despite joint angular velocity differences, and (b) to evaluate if an isolated maximum joint torque is correlated with cycling performance, and so add the five other joint movements (i.e. ankle, knee, and hip flexion and extension) to the knee extension torque tested by Driss et al. (2002).

Material and Methods

Participants

Nine cyclists (32 ± 10 years old, body height 1.74 ± 0.06 m, body mass 64.6 ± 6.8 kg, annual cycling practice 3100 ± 1700 km) volunteered for the study. The subjects can be considered as recreational cyclists (Category 4 in Ansley and Cangley (2009) classification). This population was chosen in order to get a broad range of maximum crank power production capabilities given the goal of assessing correlations using this variable.

Measures

Two experimental sessions were realized, one to evaluate Maximum Isolated Torques (MITs) and one to evaluate Maximum Pedaling Torques (MPTs). MITs and MPTs were assessed for ankle, knee, and hip flexions and extensions.

MITs of each joint were assessed at low velocity in random order on an isokinetic ergometer (BIODEX, Shirley NY, United States of America). Then, to assess MPTs, the subjects first conducted a cycling torque-velocity test on an instrumented Excalibur cycle ergometer (LODE, Groningen, Nederland) that consisted of six maximum velocity pedalling sequences against various loads proposed in random order (Vandewalle et al., 1987). The MPT represented their instantaneous maximum joint torques during the most powerful crank cycle of the test. A time delay of 7 ±2 days was adopted between MIT and MPT assessments.

Maximum Isolated Torque (MIT) measurement

MIT determination was preceded by a 10 min warm-up on a cycling ergometer at a freely chosen cadence (Power = 100 W). Measures of maximum flexion and extension torques were realized separately at the ankle (from 10° of dorsiflexion to 50° of plantarflexion), the knee (from 50° of flexion to 60° of extension) and the hip (from 40° flexion to 50° in extension) on an isokinetic ergometer (BIODEX, Shirley NY, United States of America). The measurements were randomized across joint movements to avoid learning or sequence effect. Each torque was assessed using an isokinetic angular velocity of 20°/s with a maximum range-of-motion allowing to overlap the one used by the joint when pedalling. Differences of maximum joint torque between the isometric condition and such a low velocity can be considered as not significant on six movements assessed (Anderson et al., 2007). but with the advantage to allow assessing a complete range-of-motion and minimizing fatigue in

comparison to repeated isometric tests at different joint angles. Before each test, the rotation axis of the dynamometer was carefully aligned with the joint axis, using BIODEX recommendations of positioning for each joint. Two passive returns of the arm fixing the segment were done prior to each sequence in order to measure the torque due to the limb and the measurement tool weights. One sub-maximal trial of familiarization was first performed, and then the following one was selected for MIT evaluation. MIT for a given joint movement was the maximum torque value obtained during a full extension or flexion (i.e. one value for the optimal angle of the joint's range-of-motion). A rest period of 4 min was allowed between each unilateral joint movement test.

Determination of maximum cycling power

This session was separated by 7 ±2 days with regard to the MIT assessment. Subjects were placed on the ergometer according to their usual settings. The crank length was set at 0.17 m and the saddle height was adjusted if necessary to keep usual leg extension. The test began with an identical warm-up (10 min at 100 W, freely chosen cadence). Standardized instructions were given after the warming-up phase and no encouragement or feedback was provided. According to the classic recommendations for a torque-velocity test (Vandewalle et al., 1987), it consisted of six pedalling phases of 7 s at maximum velocity against loads presented in random order to avoid learning or sequence effect. Participants started each sprint with the load already applied and a horizontal and static crank position. Five minutes of passive rest were given between each sprint. The subjects were asked to pedal seated during the whole evaluation.

Maximum Pedalling Torques (MPT) evaluation

Kinematic data of the lower limbs were recorded in three dimensions at 200 Hz using an optoelectronic system composed of ten cameras (VICON, Oxford, United-Kingdom) located around the cyclist. Then, positions of the markers were projected in the sagittal plane of the cyclists. Three spherical reflective markers were placed on anatomical landmarks corresponding to the hip, knee and ankle joints, the great trochanter, the lateral femoral condyle and the lateral malleolus according to the International Society of Biomechanics (ISB) recommendations (Wu et al., 2002) adapted for a one-plane analysis. Two additional markers were placed on the heel and the toe for the foot to match the anthropometric model proposed by de Leva (1996). Two others markers were positioned on each side of the pedals to identify the position of the pedal spindle. Segments were considered rigid, with fixed centers of mass, fixed inertial parameters, and connected by frictionless joints. Figure 1 illustrates the theoretical model used to represent the cyclist.

Markers positions were filtered using a 4th order Butterworth low-pass filter with zero phase lag and a cutoff frequency of 6 Hz. The pedals were equipped with 3-dimensions force/torque sensors (I-Crankset-1, SENSIX, Poitiers, France), which recorded the applied reaction forces and moments at 1 kHz. Kinetics data were treated with a cutoff frequency of 10 Hz. Kinetics and kinematics were synchronized using the Nexus 1.7.1 system (VICON, Oxford, United-Kingdom).

A classic bottom-up inverse dynamics method (Hull and Jorge, 1985) written with Scilab 5.4.0 (SCILAB, Scilab Enterprises) was programmed to compute the MPTs in two dimensions during the crank cycle corresponding to the maximum power of the torque-velocity test. MPTs were selected as the maximum joint torques during the cycle corresponding to the maximum crank power.

Procedures

For the MIT, the data analyzed were the instantaneous maximum joints torques. MPT represented the instantaneous maximum torques for each of the six joints conditions [3 joints x (flexion + extension)] for each subject during the crank cycle corresponding to the maximum power output. A typical example of MPT and MIT processing according to crank power-velocity and crank torque-velocity relationships is presented in Figure 2. For both MPT and MIT, instantaneous values of torque were conserved. On the other hand, mean values of maximum cycling power during one cycle were retained given the involvement of each joint movement in this variable. Each participant was informed of the experimental procedure and signed an informed consent form before study initiation. The experimental design of the study was conducted in accordance with the declaration

of Helsinki and approved by the ethical committee of the University of Toulouse.

Statistical Analysis

All statistical analyses were performed using STATISTICA (StatSoft, Maisons-Alfort, France). Data normality was assessed using the Shapiro-Wilk's test, and homogeneity of variance was verified using the Levene's test. Correlations between MIT and MPT and between MIT and maximum cycling power were performed using the Pearson R test with the level of significance set at $p < 0.05$. For descriptive purposes, MPT/MIT ratios were compared using a repeated measure ANOVA. Data are presented as mean ± standard deviation and the p value below 0.05 was considered significant.

Results

Maximum cycling power was of 594 ± 110 W which represents 9.2 ± 1.7 W/kg of body mass. The mean cadence for this cycle was 108 ± 9 RPM, and the mean crank torque was 53.1 ± 10 Nm (0.82 ± 0.15 Nm/kg of body mass). Values of MPT and MIT at the ankle, knee and hip joints are presented in Table 1.

No significant correlations were found between MPT and MIT. Pearson's r-values ranged from 0.06 to 0.59 ($p > 0.05$) (Table 2).

Maximum crank power was correlated with knee extension MIT ($r = 0.68$, $p < 0.05$). Maximum crank power was not correlated with any other MIT (r ranging from 0.09 to 0.45).

This analysis showed that the ratios between MPT and MIT were highest for the ankle and knee extension when compared to other movements ($p < 0.05$), with no difference between the two mentioned. There was also a significant difference between knee flexion and hip flexion ($p < 0.05$). No other significant differences were detected (Figure 3).

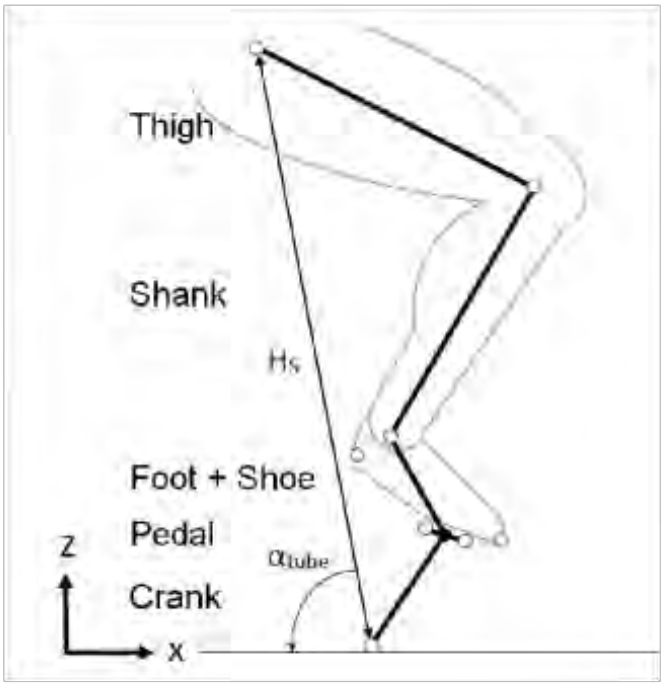

Figure 1

Theoretical model of the cyclist

α_{tube}: saddle tube angle. H_s: hip to crank axis length.
Each dot represents a reflective marker used for the kinematics analysis.

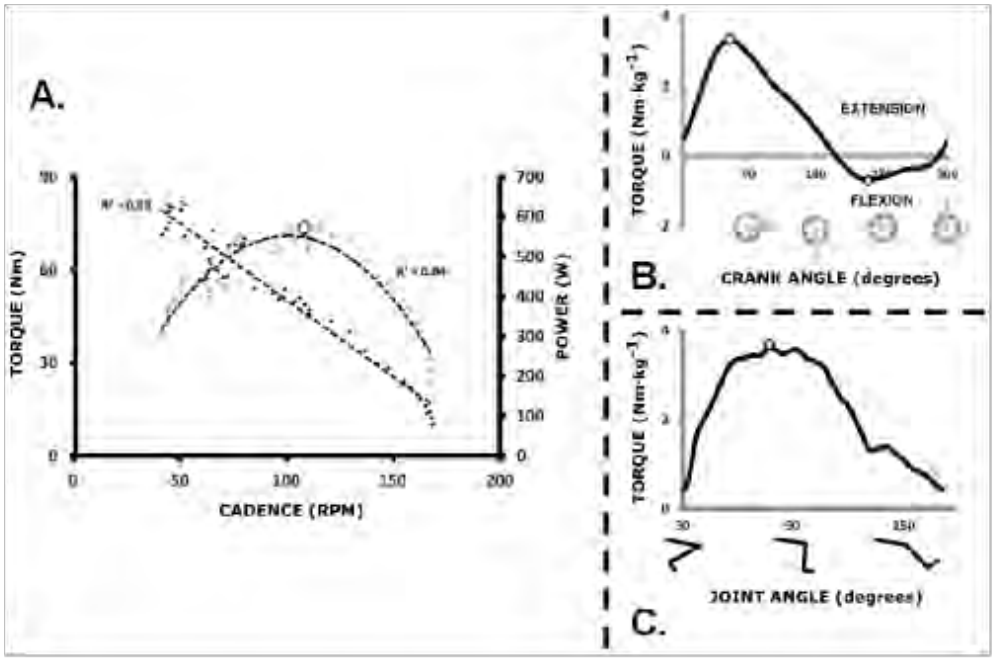

Figure 2

Power-Cadence, Torque-Cadence and Torque-Angles relationships.
A. Power as a function of the cadence (2nd order polynomial curve) and crank torque as a function of the cadence (linear relationship) for one participant during the maximum power determination test. One dot represents the average torque (black squares) or average power (white circles) for a whole crank revolution of the torque-velocity test. Data represent the six sprints. The diamond at maximum power indicates the studied cycle to compute MPT of each joint movement. B. MPT assessment for the same subject detailing knee joint torque as a function of the crank angle. The two diamonds indicate instantaneous maximum knee extension and flexion torques (MPT for these two joint movements). This process was repeated for the ankle and hip joints. C. MIT assessment of knee extension for the same subject as a function of the knee angle. The diamond represents the instantaneous maximum knee extension torque (MIT for this movement). This assessment was repeated for knee flexion, as well as ankle and hip flexion and extension.

Table 1

Mean values and standard deviations of the mechanical parameters assessed during the experimental protocol

Joint	Ankle		Knee		Hip	
Movement	Flexion	Extension	Flexion	Extension	Flexion	Extension
MPT ($Nm \cdot kg^{-1}$)	0.18±0.09	1.14±0.27	0.67±0.28	2.89±0.70	0.50±0.14	1.48±0.45
Joint Angular Velocity at MPT ($degrees \cdot s^{-1}$)	170±78	148±99	317±97	324±69	106±119	167±42
MIT ($Nm \cdot kg^{-1}$)	0.44±0.07	0.89±0.33	1.41±0.53	2.84±0.72	1.68±0.48	4.52±1.07

MPT: Maximum Pedaling Torque (maximum torque during the maximum power output pedaling cycle), MIT: Maximum Isolated Torque (maximum torque over the joint range of motion at 20°/s).

TABLE 2

Correlations (r) between MPT and MIT and between maximum cycling power and MIT (= significant p < 0 .05).*

	Ankle		Knee		Hip	
	Flexion	Extension	Flexion	Extension	Flexion	Extension
MPT *vs* MIT	0.34	0.45	0.49	0.59	0.06	0.50
Maximum Cycling Power *vs* MIT	-0.09	0.45	0.41	**0.68***	0.42	0.43

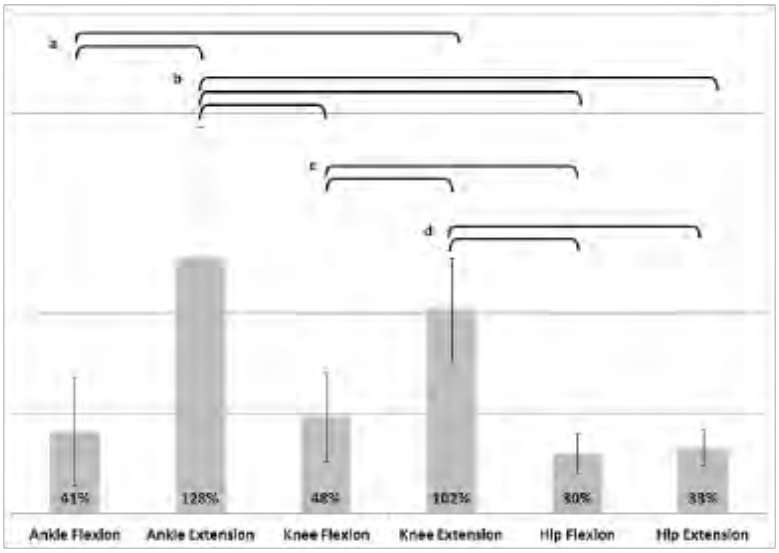

Figure 3

Ratios between Maximum Pedaling Torque (MPT) and Maximum Isolated Torque (MIT)

[a] Significant difference with Ankle Flexion, [b] Significant difference with Ankle Extension, [c] Significant difference with Knee Flexion, [d] Significant difference with Knee Extension.

Discussion

The first objective of this study was to verify if isolated measures of maximum joint torques using low velocity isokinetic testing similar to isometric conditions are correlated with torques on the same joints in a polyarticular task. Our data indicated that these correlations did not exist. This shows that the transfer between capabilities on isolated joints and the joint torques developed during a polyarticular task is not direct. A probable explanation for this result is the difference in joint angular velocity between MIT (20°·s-1) and MPT (see values for each joint in Table 1). This assumption was tested by Driss et al. (2002) who demonstrated that the correlation between maximum cycling power and isolated knee extension torque was better when using high joint velocities (i.e. 240°·s-1) during an isolated joint torque assessment (r=0.83 in their study) than when using isometric testing (r=0.54). Furthermore, another explanation for this lack of correlation may be the difference in joint torque development between isolated joints and a polyarticular joint action. In this sense, it has been shown that ankle torque production capability is higher when the ankle is involved in a polyarticular extension than in mono-articular testing (Hahn et al., 2011). Altogether, these results suggest that precautions are necessary in joint torque testing and conditioning in order to take into account the specificity of the task to develop in terms of joints involved and their angular velocities.

The second objective of our work was to determine if for the specific activity assessed, some isolated joint torque capabilities would be a better predictor of the athlete performance. This was the case for only one movement in the study with the knee extension maximum torque associated with better cycling power output. This finding is in line with the results of Driss et al. (2002) who demonstrated this correlation between maximum knee extension torque and maximum cycling power. However, lack of correlation for the other joint movements shown in this study gives more importance to the force development of muscles crossing the knee to improve cycling performance. The results regarding knee extension are in line with the findings of Elmer et al. (2011) and McDaniel et al. (2014) who described this joint movement as a large power generator during maximum cycling. The McDaniel et al.'s study also demonstrated the sensibility of joint power with regard to the crank angular velocity, showing that ankle plantar flexion power part in the total power production decreased with an increasing pedaling rate, whereas knee flexion and hip extension parts increased. In their study, hip joint power was presented as the main power generator whereas a relative low involvement of hip extension was found in our study (Figure 3). Nevertheless, this result is consistent with a recent study using electromyography of eleven muscles that compared ratios of peak activation between sprint pedalling and isolated isometric contractions (Dorel et al., 2012). Note that because of differences in the studied populations, non-linearity between EMG signals and joint torques (Caldwell and Li, 2000), and methodological aspects of the EMG normalization (Burden, 2010), precautions must be taken when comparing these results. Remarkably in their study, the soleus (ankle extensor) had a ratio of activation between sprint cycling and isometric contraction of 127%, the gastrocnemii medialis and lateralis (ankle extensors and knee flexors) of 101% and 99%, respectively, the tibialis anterior (ankle flexor) of 76%, the vastus lateralis and vastus medialis (knee extensors) of 104% and 92%, respectively, the rectus femoris (knee extensor and hip flexor) of 99%, the tensor fasciae latae (hip flexor) of 81%, the semitendinosus and semimembranosus (hip extensors and knee flexors) 71% and 60%, respectively, and the gluteus maximus (hip extensor) of 77%. Both results confirm the fact that flexion capabilities are sparsely used during maximum power cycling, and this is also the case for the hip extension whereas this joint exhibits the greatest possibilities of torque production. In contrast, polyarticular ankle and knee extension seem to be the most used joints during cycling at maximum power in regard to their isolated capabilities in pseudo-isometric conditions.

For descriptive purposes, ratios of joint torques used during cycling with isolated maximum (MIT) as reference were established (Figure 3). The observed MPT/MIT ratio of 128% for ankle extension was an unexpected result, meaning that the torque at this joint during a dynamic task at fast angular velocity exceeded the one during a pseudo-isometric condition. This result could be explained by the length variation of the biarticular muscle gastrocnemii between MIT and MPT, which may have lead to a difference in muscle/tendon force, and so in ankle extension torque (Hahn et al., 2011). During fast running at 6.5 m/s which probably involves a larger portion of "elastic" energy (Raasch and Zajac, 1999), even higher ankle extension torques were reported: 3.43 ± 0.49 Nm/kg of body mass (in our study 1.14 ± 0.27 Nm/kg MPT and 0.89 ± 0.33 Nm/kg MIT), which could have lead to an hypothetical ratio Maximum Running Torques on MIT around 385%. The interest to develop ankle extension torque capabilities has already been shown in cycling: a greater decrease in joint power production than in other joints (50% less power generated after 15 s of a 30 s maximum pedalling test, versus about 30% for other joint movements) was previously observed (Martin and Brown, 2009), and a lower contribution of the ankle extension torque at the end of a cycling test to exhaustion at constant power output was described (Bini et al., 2010).

To enhance the sensibility of our method and determine the task-specific muscular needs, an assessment of individual muscle forces is necessary. The method is still to be developed, but coupling inverse dynamics with electromyography (Raasch et al., 1997) or using supersonic shear imaging (Bouillard et al., 2013) could be applied to set references of in vivo muscle force and compare them during a polyarticular task.

To conclude, in order to improve the transferability of strength and conditioning to performance in polyarticular activities, practitioners and trainers should test force characteristics at appropriate angular velocity, and train the athletes in natural setting situations rather than choosing isolated and angular velocity different joint conditioning. However, if the relation between one isolated joint capability and performance in a specific activity is shown, then isolated conditioning of this joint may be justified. The results of this study confirm that this is the case for knee extension and cycling maximum power. As discussed with MPT/MIT ratios, improvement in cycling could also be achieved by strengthening the muscles involved in ankle extension (keeping in mind the need of a polyarticular extension to take into account the gastrocnemii characteristics) given their important involvement in maximum cycling in regard to their capabilities. The findings of this study indicate that transfers between isolated joint torques and the same joint torques involved in a polyarticular task are not direct.

Acknowledgements

The authors would like to thank the participants for their enthusiastic participation, together with Pr Pier-Giorgio Zanone for reviewing the manuscript.

References

Anderson DE, Madigan ML, Nussbaum MA. Maximum voluntary joint torque as a function of joint angle and angular velocity: Model development and application to the lower limb. *J. Biomech,* 2007; 40: 3105–3113

Ansley L, Cangley P. Determinants of "optimal" cadence during cycling. *Eur. J. Sport Sci,* 2009; 9: 61–85

Baker D, Wilson G, Carlyon B. Generality Versus Specificity - a Comparison of Dynamic and Isometric Measures of Strength and Speed-Strength. *Eur. J. Appl. Physiol,* 1994; 68: 350–355

Baroni BM, Rodrigues R, Franke RA., Geremia JM, Rassier DE, Vaz MA. Time Course of Neuromuscular Adaptations to Knee Extensor Eccentric Training. *Int. J. Sports Med,* 2013; 34: 904-911

Bini RR, Diefenthaeler F. Mechanical Work and Coordinative Pattern of Cycling: A Literature Review. *Kinesiology,* 2009; 41: 25–39

Bini RR, Diefenthaeler F, Mota CB. Fatigue effects on the coordinative pattern during cycling: Kinetics and kinematics evaluation. *J. Electromyogr. Kinesiol,* 2010; 20: 102–107

Bouillard K, Jubeau M, Nordez A, Hug F. Effect of vastus lateralis fatigue on load sharing between quadriceps femoris muscles during isometric knee extensions. *J. Neurophysiol,* 2013; 111: 768-776

Burden A. How should we normalize electromyograms obtained from healthy participants? What we have learned from over 25 years of research. *J. Electromyogr. Kinesiol,* 2010; 20: 1023–1035

Caldwell GE, Li L. How strongly is muscle activity associated with joint moments? *Motor Control,* 2000; 4: 53–59

Dorel S, Guilhem G, Couturier A, Hug F. Adjustment of Muscle Coordination during an All-Out Sprint Cycling Task. *Med. Sci. Sports Exerc,* 2012; 44: 2154–2164

Driss T, Vandewalle H, Le Chevalier JM, Monod H. Force-velocity relationship on a cycle ergometer and knee-extensor strength indices. *Can. J. Appl. Physiol,* 2002; 27: 250–262

Elmer SJ, Barratt PR, Korff T, Martin JC. Joint-Specific Power Production during Submaximal and Maximal Cycling. *Med. Sci. Sports Exerc,* 2011; 43: 1940–1947

González-Ravé JM, Juárez D, Rubio-Arias JA, Clemente-Suarez VJ, Martinez-Valencia MA, Abian-Vicen J. Isokinetic leg strength and power in elite handball players. *J. Hum. Kinet,* 2014; 41: 227–233

Hahn D, Olvermann M, Richtberg J, Seiberl W, Schwirtz A. Knee and ankle joint torque-angle relationships of multi-joint leg extension. *J. Biomech,* 2011; 44: 2059–2065

Hull ML, Jorge M. A method for biomechanical analysis of bicycle pedalling. *J. Biomech,* 1985; 18: 631–644

De Leva P. Adjustments to Zatsiorsky-Seluyanov's segment inertia parameters. *J. Biomech*, 1996; 29: 1223–1230

Martin JC, Brown NAT. Joint-specific power production and fatigue during maximal cycling. *J. Biomech*, 2009; 42: 474–479

McDaniel J, Behjani NS, Elmer SJ, Brown NA, Martin JC. Joint-specific power-pedaling rate relationships during maximal cycling. *J. Appl. Biomech*, 2014; 30: 423–430

Raasch CC, Zajac FE. Locomotor Strategy for Pedaling: Muscle Groups and Biomechanical Functions. *J. Neurophysiol*, 1999; 82: 515–525

Raasch CC, Zajac FE, Ma B, Levine WS. Muscle coordination of maximum-speed pedaling. *J. Biomech*, 1997; 30: 595–602

Vandewalle H, Peres G, Heller J, Panel J, Monod H. Force-velocity relationship and maximal power on a cycle ergometer. *Eur. J. Appl. Physiol*, 1987; 56: 650–656

Wu G, Siegler S, Allard P, Kirtley C, Leardini A, Rosenbaum D, Whittle M, D'Lima DD, Cristofolini L, Witte H, Schmid O, Stokes I. ISB recommendation on definitions of joint coordinate system of various joints for the reporting of human joint motion—part I: ankle, hip, and spine. *J. Biomech*, 2002; 35: 543–548

Corresponding author:

Antony Costes
PRISSMH, University of Toulouse, UPS, 118 route de Narbonne, 31062 Toulouse, France
Adress: Bureau 211, Pôle Sport, 118 route de Narbonne, 31062 Toulouse, France
Phone: +33 (0) 5 61 55 64 40;
Fax: +33 (0) 5 61 55 82 80
E-mail: address: antony.costes@univ-tlse3.fr

IV.4. ETUDE 9 : SELECTIVE MUSCLE CONTRACTION IS INCOMPATIBLE WITH MAXIMAL VOLUNTARY TORQUE ASSESSMENT

Cet article accepté dans la revue « European Journal of Physiology » est la suite directe de mes travaux de Master II Recherche. Une analyse de la littérature montrant une grande variabilité dans les mesures de couple articulaire à la cheville observées lors de la flexion plantaire, notre hypothèse a été que ces différences (pouvant atteindre 40% entre les différentes études), pourraient être attribuées à des consignes favorisant ou non une extension polyarticulaire.

Seize participants ont été testés sur un ergomètre isocinétique dans trois positions (en pronation, supination, et assis), avec la cheville en position neutre, et des consignes favorisant une mobilisation isolée des extenseurs (ISOL) de la cheville ou une extension polyarticulaire (ALL), dans les deux cas en isométrie. Le couple à la cheville, la cinématique du pied, et l'activité EMG de 7 muscles du membre inférieur ont été enregistrés.

Les résultats montrent que les couples articulaires étaient supérieurs en condition ALL en comparaison à ISOL ($p < 0,05$), avec des gains de 43,5%, 42,5% et 15,3% dans les positions supination, pronation et assis, respectivement. Les résultats de cette étude suggèrent que les forces musculaires créées par les muscles non liés directement à l'extension de cheville influencent les couples articulaires mesurés à la cheville. Cependant, les gains observés étaient associées à une plus grande activation des muscles extenseurs de la cheville, indiquant que la condition ISOL pourrait avoir conduit à une relative inhibition de l'activation de ces muscles.

En conclusion, les résultats de cette étude suggèrent que l'utilisation de contraction « isolées » semble ne pas être optimale pour la mesure de contractions maximales volontaires, en particulier pour les muscles extenseurs de la cheville, observés comme étant sensibles à ce type de conditions expérimentales.

Eur J Appl Physiol
DOI 10.1007/s00421-014-2900-3

ORIGINAL ARTICLE

Selective muscle contraction during plantarflexion is incompatible with maximal voluntary torque assessment

Nicolas A. Turpin · Antony Costes · David Villeger · Bruno Watier

Received: 23 October 2013 / Accepted: 22 April 2014

Abstract
Objective Large variations in maximal voluntary torque are reported in the literature during isometric plantarflexion contractions. We propose that these differences, which could reach 40 % across similar studies, could be explained by differences in the instructions provided, and notably by instructions as to favoring or not multi-joint contractions.
Method Sixteen participants were placed on an isokinetic ergometer in 3 different positions, supine, prone and seated, with the ankle in the neutral position, and instructed to create maximal force on the footplate by conforming to instructions that favored either isolated (ISOL) or multi-joint (ALL) isometric contractions. Torque, foot kinematics and the electromyographic activity of seven muscles of the lower limb have been recorded.
Results Joint torques were greater in ALL compared to ISOL ($p < 0.05$) with gains of 43.5 (25.4–170.6) %, 42.5 (1.4–194.6) % and 15.3 (9.3–71.9) % in the supine, prone and seated position, respectively [values are given as median (range)]. The results of this study suggested that forces created by muscles that do not span over the ankle joint significantly influenced the measured joint torque. Nevertheless, the observed gains in torque were associated with greater plantarflexor muscles activation, showing that the ISOL condition may have induced a form of inhibition of these muscles.
Conclusions The results of this study suggest that using isolated contractions, hence constrained testing protocols, cannot provide optimal conditions for MVC testing, notably for plantarflexor muscles, which seem to be extremely sensitive to such constrained conditions.

Keywords EMG, maximal voluntary contraction · Plantarflexion · Multi-joint contraction · Concurrent activation

Abbreviations

ALL	Multi-joint contractions condition
ANOVA	Analysis of variance
CR	Center of rotation
EMG	Electromyographic signal
EMG_{max}	Maximal electromyographic (EMG) value obtained over all conditions
GM	Gastrocnemius medialis
G_{max}	Gluteus maximus
ISOL	Isolated contractions condition
MVC	Maximal voluntary contraction
RF	Rectus femoris
SCoRE	Symmetrical centre of rotation estimation method
SCS	Segment coordinate system
SD	Standard deviation
Sol	Soleus
ST	Semi tendinosus
TA	Tibialis anterior
VL	Vastus lateralis

Communicated by Nicolas Place.

N. A. Turpin · A. Costes · D. Villeger · B. Watier
UPS, PRISSMH, University of Toulouse, 118 route de Narbonne, 31062 Toulouse Cedex 9, France

B. Watier
CNRS LAAS, 7 Avenue du colonel Roche, 31077 Toulouse, France

B. Watier (✉)
PRISSMH-EA 4561-F2SMH, Pôle Sport, 118 route de Narbonne, 31062 Toulouse Cedex 9, France
e-mail: bruno.watier@univ-tlse3.fr

Published online: 11 May 2014

Introduction

Maximal voluntary contraction (MVC) torque is an important measure to evaluate mechanical properties of the muscle and their progress with physical training (Klass et al. 2008; Van Cutsem et al. 1998) or in rehabilitation, to assess the evolution of musculoskeletal diseases and to quantify the beneficial effects of different therapeutic strategies (Moraux et al. 2013; McNeil et al. 2007). MVC at the ankle joint is especially critical to consider due to the important role of the plantarflexor and dorsiflexor muscles in maintaining balance and avoiding fall (Horak et al. 1989). Still, MVCs evaluation requires several precautions to be taken, because mechanical and neural factors could greatly influence torque output. Therefore, the present study will focus on isometric plantarflexion MVCs.

Regarding mechanical factors, even though ergometers have proven to be reliable instrument *per se* (Drouin et al. 2004), many biases are known to affect measurements, such as, (1) gravitational effects, (2) inertial effects, (3) compliance of the ergometer moment arm or deformation of the footplate and fasteners compliance, or (4) misalignments between the axis of rotation of the ergometer relative to that of the joint (Arampatzis et al. 2007; Herzog 1988; Deslandes et al. 2008), that, moreover, represents only an approximation of the actual functional axis of rotation of the joints (Ramos and Knapik 1978; Hicks 1953). In the isometric case, gravitational effects are easily eliminated and the inertial effects are supposed to be negligible (Deslandes et al. 2008). Compliance involves movement of the segment relative to the moment arm of the ergometer, and implies that muscles MVCs cannot be evaluated at the exact intended position. Adjustments can nevertheless be easily performed to correct positional changes observed when the muscles go from the passive to the active state (De Ruiter et al. 2008). Misalignment, on the other hand, is particularly critical for the evaluation of plantarflexion as compared to other group of muscles.

With some simplifications, torque at the ankle can be written (Arampatzis et al. 2007) as:

$$\tau_{\text{ankle}} = \frac{r_{\text{ankle}}}{r_{\text{dynamometer}}} \tau_{\text{dynamometer}} \quad (1)$$

with $\tau_{\bullet}$ the torque at either the ankle or the dynamometer axis, and $r_{\bullet}$ the moment arm of the reaction force to either the ankle or the dynamometer. This relation could be rewritten as:

$$\tau_{\text{ankle}} = \left(1 + \frac{\Delta r}{r_{\text{dynamometer}}}\right) \tau_{\text{dynamometer}}; \quad \Delta r = r_{\text{ankle}} - r_{\text{dynamometer}} \quad (2)$$

highlighting that, for a given misalignment Δr (order of magnitude = 1 cm), the bias is lower for knee extension testing (with large $r_{\text{dynamometer}}$ relative to Δr; $r_{\text{dynamometer}} \approx$ 30–40 cm, (Arampatzis et al. 2004; Deslandes et al. 2008) than for plantarflexion testing ($r_{\text{dynamometer}} \approx 17$ cm, assuming that the forces on the footplate act at the level of the metatarsophalangeal joint of the hallux, Van Cutsem et al. 1998). In addition, with misalignment, a moment arm is created between the ankle joint and the axis of rotation of the ergometer, and the reaction forces at the level of the ankle joint can thus create a torque on the footplate without any torque on the foot. Moreover, these forces can be easily manipulated by the participant using forces created by muscles not crossing the ankle joint (e.g., knee or hip extensors), and these accessory muscles can then have a mechanical influence on the measured joint torque.

At least two neural factors should be considered in this juncture: motivation and concurrent activation potentiation (Ebben et al. 2008a, 2010), also referred to as remote voluntary contraction (Cherry et al. 2010; Ebben et al. 2008b). Motivation is a well-known confound variable influencing performance which can be controlled following several recommendations (see Gandevia (2001) notably for a review). Concurrent activation potentiation is much less considered and captures the fact that contraction of accessory muscles (remote contraction) may increase the maximal activation level of primary movers (Ebben et al. 2008b). This phenomenon is commonly attributed to motor irradiation and/or to an increase in spinal excitability (Ebben 2006). Jaw clenching, Valsalva maneuver and hand gripping have been particularly investigated (see Ebben et al. 2008b for a review), but muscles from adjacent sites also prove to interact with the primary movers (Barry et al. 2008; Devanne et al. 2002; Kouchtir-Devanne et al. 2012). It is therefore likely that muscles that do not span over the ankle joint have also a neural influence on plantarflexor activity and hence on plantarflexion torque.

Since accessory muscles may come into play at both the neural and the mechanical level, the aim of this study was to test the maximal torque produced in plantarflexion using two modalities of instructions aimed at manipulating the degree of involvement of muscles not crossing the ankle joint. Furthermore, the various positioning used in the literature, notably the seated (Moraux et al. 2013; Simoneau et al. 2009), prone (Cresswell et al. 1995; Maganaris 2003) and supine positions (Danneskiold-Samsøe et al. 2009; Simoneau et al. 2007) are likely to favor specific patterns of muscle activity, and thus to influence the results in a different way. Therefore, in this study, these three positions have been tested. Offset of the rotation axes, ankle angle deviations and muscle activity have been recorded to set apart the neural and mechanical influences of the accessory muscles.

Materials and methods

Participants

16 healthy males participated to the study [mass = 76.8 ± 8.5 kg, range = (68–92); height = 1.77 ± 0.07 m, range = (1.62–1.87); age = 26.9 ± 6.4 years, range = (20–41)]. All of them were informed of the experimental procedures prior to giving their written consent to participate. The experimental design of the study was approved by the local ethical committee and the experiments were conducted in accordance with the Declaration of Helsinki (last modified in 2004).

General procedure

Ankle torque measurements were performed using an isokinetic dynamometer (Biodex III, Shirley Corporation, NY, USA). The right leg was evaluated in all participants. Participants were equipped of the reflective markers used for kinematic analysis and of the recording electromyographic (EMG) surface electrodes at their arrival at the laboratory (see details in sections Kinematics and Electromyographic acquisition). We first estimated the position of the real center of rotation of the ankle by moving passively the ankle on the dynamometer footplate in a procedure described in section Estimation of the ankle rotation axis and center of rotation. Afterward, participants performed a warm-up lasting 5 min which consisted of submaximal isometric plantarflexor contractions while seated on the ergometer. Participants were then successively placed in the PRONE, SUPINE or SEATED position in a random order to assess their isometric MVCs. For each of these positions, two modalities of instruction were randomly given to the participants. These constitute a total of 3 × 2 = 6 randomized conditions and for each of them 3 tries were given to the participant, resulting in a total of 18 MVCs.

Kinematics

A motion analysis system (Vicon Motion System, Lake Forest, CA, USA) equipped with 11 infrared cameras recorded the 3-dimensional position of 11 reflexives markers stuck on the participant and on the dynamometer. Markers were positioned on the right side of the body at the level of the external and internal maleolli, calcaneous (posterior point of the heel), 1st and 5th Metatarsal Head, fibula's head and tibiale's tuberosity. 4 reflexives markers were placed on the dynamometer such that the mid distance between two of the markers corresponds to the position of the dynamometer axis of rotation and that the two others, placed in a more backward position, allowed to recover the direction of this axis (Fig. 1). Kinematic data were recorded

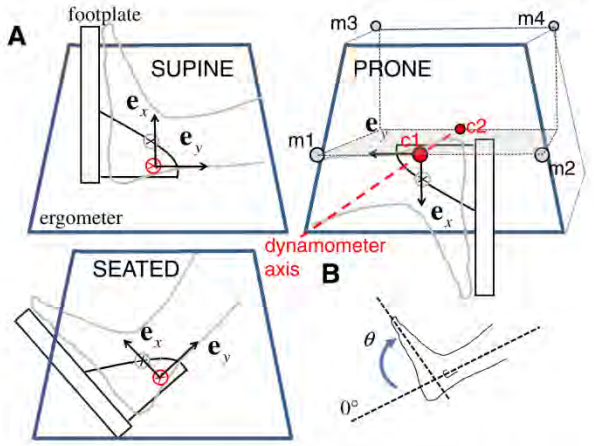

Fig. 1 Position of the foot relative to the ergometer. **a** The *circled red cross* designs the ergometer axis of rotation and the *circled black cross* the ankle axis of rotation (=CR). In all positions, the *X* axis associated with the vector $\mathbf{e}_x$ is the axis parallel to the footplate and pointing toward the participant toes and the *Y* axis associated with the vector $\mathbf{e}_y$ is the axis orthogonal to it and pointing toward the participant leg. The origin is centered at the level of the ergometer axis of rotation. The position of the reflexive markers (m1..0.4) and of the computed markers (c1 and c2) on the ergometer are illustrated. The midpoint between m1 and m2 (=the computed marker c1) gives the position of the axis of the ergometer. The position of c2 is computed as the midpoint between m3 and m4 projected on the horizontal plane containing m1 and m2. The dynamometer axis has been taken as the vector going from c2 to c1. **b** Definition of the ankle angle (θ)

at a sampling frequency of 200 Hz. Ankle angle represents the angle between the vector going from the calcaneous to the midpoint between 1st and 5th Metatarsal Head, and the vector going from the midpoint between fibula's head and tibiale's tuberosity to the midpoint between the two maleolli (see Fig. 1).

Electromyographic acquisition

Surface EMG was recorded from 7 muscles located on the right side of the body, namely, tibialis anterior (TA), soleus (Sol), gastrocnemius medialis (GM), vastus lateralis (VL), rectus femoris (RF), semi tendinosus (ST) and gluteus maximus (G_{max}). Prior to electrode application, the skin was shaved and cleaned with alcohol to minimize impedance. Pairs of Ag–AgCl disk electrodes of 8 mm diameter with inter electrode-distances of 2 cm were placed longitudinally with respect to the underlying muscle fibers arrangement according to the recommendations of Surface EMG for Non-Invasive Assessment of Muscles (SENIAM) (Hermens et al. 2000). The reference electrode was placed at the level of the great trochanter. EMG signals were amplified (×1,000), digitized (6–400 Hz bandwidth) at a sampling rate of 1 kHz (Biopac System Inc. Goleta, USA), recorded and synchronized using the motion analysis system.

Conditions of MVC testing and recording

The ankle joint torque was acquired with the isokinetic dynamometer and digitally synchronized at a sample rate of 1 kHz using the motion analysis system. During MVCs, participants were positioned on the ergometer and securely stabilized using two crossover shoulder harnesses and a belt across the abdomen. The right foot was strapped securely to the footplate with the ankle fixed at an angle of 90° i.e., at the neutral position with the sole of the foot perpendicular to the shank, and held in place by a heel block. The axis of the dynamometer was aligned with the anatomical ankle flexion–extension axis, estimated as the line passing through the tips of the maleolli (Wu et al. 2002; Lundberg et al. 1989). A clear start and stop signals were given. Each voluntary contraction lasted approximately 3–4 s and 1 min of rest was given between each contraction (Todd et al. 2004). Participants received no feedback of their performances during the tests.

Positions

Three positions were tested, PRONE, SUPINE and SEATED. For PRONE and SUPINE positions, the participants were lying on the dynamometer chair with the hip and the knee fixed at an angle of 0° (=full extension for both). In these positions, the thigh was stabilized using a belt. For the SEATED position, the chair was lifted up at an angle of 90° from the horizontal, and the knee and hip joints were both placed at an angle of 90°.

Instructions

For each position, MVCs were performed with two different modalities of instructions named ISOL and ALL. In the isolation condition (ISOL), participants were required to produce a force by rotating the footplate as hard as possible and to handle the shoulder harnesses. In this condition, they were invited to use only their calf muscles. In a second condition (ALL), the participants were invited to grip the ergometer handle and to use all the possible means to create forces against the footplate.

Estimation of the ankle joint rotation center

The ankle joint rotation center was estimated using the Symmetrical Centre of Rotation Estimation (SCoRE) method (Ehrig et al. 2006). In brief, the position of the center of rotation (CR) between two segments is determined by assuming a constant contact point between each and use the relation

$$\mathrm{CR} = \mathbf{o}_1 + \mathbf{R}_1\mathbf{u} = \mathbf{o}_2 + \mathbf{R}_2\mathbf{v} \quad (3)$$

where $\mathbf{o}_1$ and $\mathbf{o}_2$ are arbitrary points on segments #1 (the foot) and #2 (the leg), $\mathbf{R}_1$ and $\mathbf{R}_2$ are the rotation matrix transforming the segment coordinate system (SCS) to the global coordinate system and $\mathbf{u}$ and $\mathbf{v}$ are the vector linking, respectively, $\mathbf{o}_1$ and $\mathbf{o}_2$ to CR in the foot and leg coordinate system, respectively. The SCSs were defined according to Wu et al. (2002). For the estimation of the CR position, participants were seated on the ergometer chair with solely their right foot strapped on the footplate connected to the moment arm of the dynamometer and the ankle joint was moved passively at full but comfortable range of motion for about 10 flexion–extension cycles to localize an accurate joint center. The values of $\mathbf{u}$ and $\mathbf{v}$ were then used to estimate the position of the CR relative to the SCSs (foot and leg) in all experimental conditions.

Data analysis

EMG signals were filtered with a bandpass filter (4th order Butterworth) between 20 and 400 Hz. Linear envelopes for each muscle were obtained by low-pass filtering the fully rectified raw EMG signals with a 9-Hz low-pass filter (2nd order Butterworth, zero lag, (Shiavi et al. 1998). For each condition, the averaged value between −150 and 150 ms around the peak torque event was extracted (Fig. 2) and then normalized by the maximal value obtained over all conditions (=$\mathrm{EMG}_{\mathrm{max}}$). These calculations were performed for each muscle and each participant independently.

Joint torque and kinematic data were filtered by a 15-Hz low-pass filter [2nd order Butterworth filter (Winter 1990)]. Joint torque was corrected for gravity by subtracting the baseline, and for each condition the maximal value reached over the three tries given to the participant was extracted for analysis (Fig. 2).

Statistics

Normality of the data has been checked using Shapiro–Wilk tests. For normally distributed data, two-way repeated measure ANOVAs (instruction = ALL and ISOL × position = SUPINE, PRONE and SEATED) were performed after checking for violations of sphericity using Mauchly's test. Post hoc analyses were then performed using Bonferroni method (Maxwell 1980). For non-normal distribution, non-parametric Friedman ANOVAs (one-way repeated measures ANOVA on ranks) was chosen. Wilcoxon rank sum tests associated with Bonferroni–Dunn corrections were used when the null hypothesis was rejected.

The different biases mentioned in the introduction were rallied in kinematic deviations. They include (1) the ankle angle changes (in degrees) during the test due to the compliance of the ergometer moment arm, deformation of the footplate and fasteners compliance; (2) the alignment

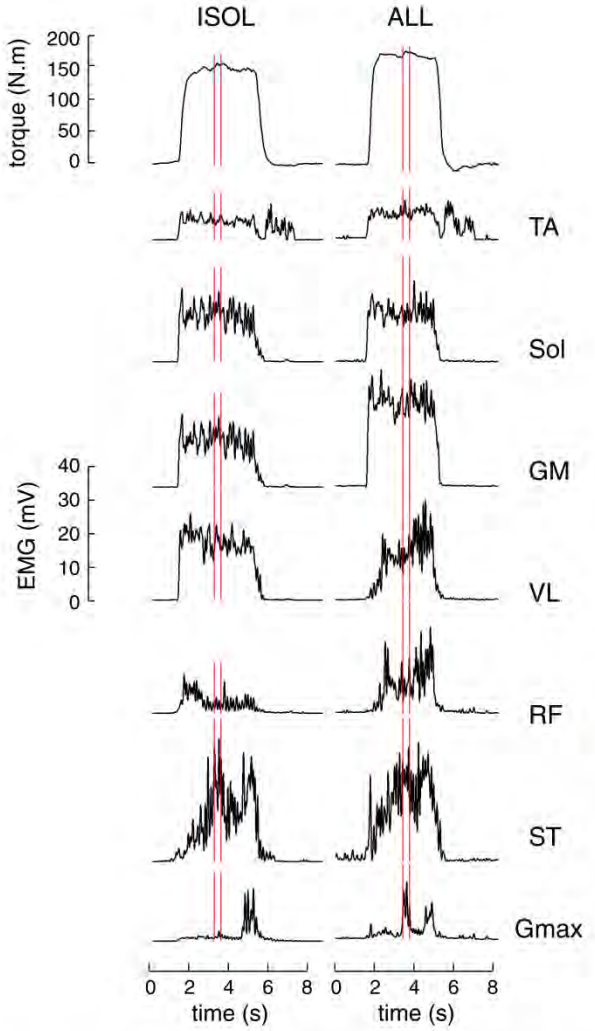

Fig. 2 Example of torque and EMG data for a typical participant. Condition = supine position. Smoothed torque and EMG envelope are processed as indicated in section "Data analysis". *Vertical lines* indicate the region around peak torque used for analysis.: tibialis anterior. SOL, soleus; GM, gastrocnemius medialis; VL, vastus lateralis; RF, rectus femoris; ST, semi tendinosus; G_{max}, gluteus maximus

errors (in mm) between the axis of the dynamometer and the functional ankle joint center of rotation in horizontal and vertical axis during the rest and the MVC. Kinematic deviations were compared to the reference using one-sample Student's *t* tests (reference value = 0). A description of the axes is given in Fig. 1.

We assessed the relationships between torque and other variables (i.e., kinematic deviations and EMG activity) using Pearson's correlation coefficient (*r*). For these analyses, values of each variable and for each participant were converted to *Z* scores, calculated by subtracting the

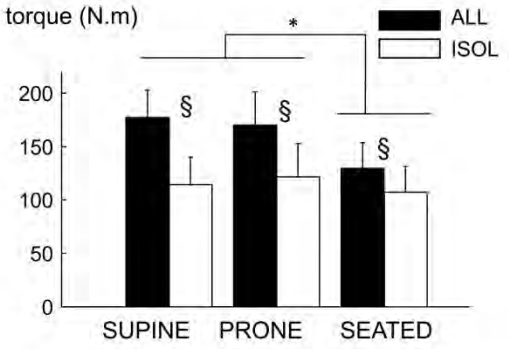

Fig. 3 Torque data. *Bars* represent the mean and error-bars one SD. § Indicates a significant difference ($p < 0.05$) between ALL and ISOL. *Indicates a significant difference between [SUPINE and PRONE] vs. SEATED ($p < 0.05$). See section "Results" for details

average (over all conditions) and dividing the result by the SD. Because correlation analysis is very sensitive to the presence of outliers in the data (Chatterjee and Hadi 1986), normality of each variable was checked and values of |Z-score| > 2.58 (corresponding to the 99th percentile of the distribution) were discarded from the analysis (Burke 2001). All available data were used (3 tries × 3 positions × 2 instructions × 16 subjects).

All statistical analyses were performed with the Statistica® software (Statistica®V6, Statsoft, Maison-Alfort, France). Values are reported as mean ± SD for normally distributed data and as median (range) instead. A *p* value below 0.05 was considered statistically significant.

Results

Torque

The results showed that MVCs were significantly affected by the positions [$F(2,30) = 13.2$, $p < 0.001$, $\eta_p^2 = 0.60$] and the instructions provided [$F(1,15) = 54.7$, $p < 0.001$, $\eta_p^2 = 0.80$; Fig. 3]. Post hoc analyses showed that MVCs were significantly greater in the SUPINE and PRONE positions compared to the SEATED position (pooled data SUPINE = 146.0 ± 40.5 Nm and PRONE = 145.7 ± 38.9 Nm vs. SEATED = 118.5 ± 31.2 Nm, $p < 0.001$). Torque was greater in the ALL condition compared to the ISOL condition for each position ($p < 0.001$), corresponding to gains of 43.5 (25.4–170.6) %, 42.5 (1.4–194.6) % and 15.3 (9.3–71.9) % for the SUPINE, PRONE and SEATED position, respectively. Gains were significantly lower in SEATED compared to SUPINE ($Z = 3.15$, $p < 0.001$) and PRONE ($Z = 2.43$, $p = 0.015$), but were similar between SUPINE and PRONE ($Z = 1.55$, $p = 0.121$).

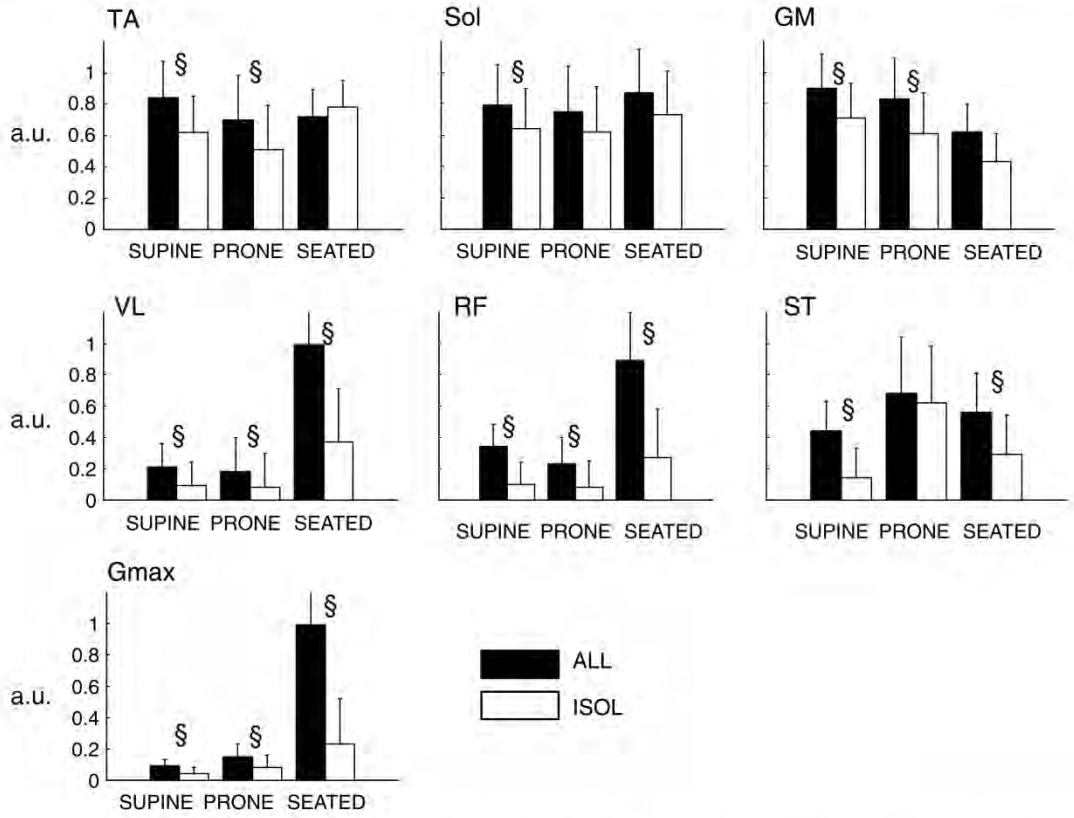

Fig. 4 Normalized EMG activities. *Bars* represent the mean and error-bars one SD. § Indicates a significant difference ($p < 0.05$) between ALL and ISOL

Muscle activation

EMG variables were not normally distributed. The activity level of TA was greater in ALL compared to ISOL [pooled data ALL = 89.6 (6.5–100) % vs. ISOL = 65.3 (2.7–100) %, $Z = 3.21$, $p = 0.001$], but this effect was present in the SUPINE and PRONE positions only ($Z = 3.31$, $p < 0.001$, and $Z = 2.53$, $p = 0.011$, respectively). Analysis revealed no main effect of the position on the activity of TA ($\chi^2 = 4.75$, $p = 0.093$; Fig. 4).

Overall positions, Sol activity was greater in ALL compared to ISOL [ALL = 85.7 (6.0–100) % vs. ISOL = 66.1 (0.7–100) %, Z = 2.84, $p = 0.004$], but post hoc analysis revealed significant differences in the SUPINE position only ($Z = 2.43$, $p = 0.015$). There was no main effect of the position on the activity of SOL ($\chi^2 = 2.25$, $p = 0.325$).

Activity of GM was greater in ALL compared to ISOL [i.e., pooled data ALL = 88.1 (15.8–100) % vs. ISOL = 61.5 (1.9–98.2) %; $Z = 4.24$, $p < 0.001$]. These differences held for the SUPINE and PRONE positions ($Z = 2.84$, $p = 0.004$ and $Z = 2.74$, $p = 0.006$, respectively), but no differences were found in the SEATED position ($Z = 1.76$, $p = 0.08$). Analysis revealed a main effect of the position ($\chi^2 = 17.69$, $p < 0.001$) i.e., GM was significantly less activated in the SEATED position [=49.9 (15.3–100) %,] compared to the PRONE [=79.4 (1.9–100) %., $Z = 3.78$, $p < 0.001$] and SUPINE [=0.83 (0.09–1) %, $Z = 3.72$, $p < 0.001$] positions.

ST was maximally activated in the PRONE position in 10 out of 16 participants. The activity of ST was significantly higher in ALL compared to ISOL in SUPINE ($Z = 3.46$, $p < 0.001$) and SEATED ($Z = 3.00$, $p = 0.003$), but no differences were found in the PRONE position ($Z = 0.67$, $p = 0.502$). A main effect of the position was found ($\chi^2 = 6.94$ $p = 0.03116$) i.e., there was higher ST activity in the PRONE position but differences were significant only when compared with the SUPINE's [i.e., pooled data = 74.6 (3.6–100) % vs. 8.0 (0.8–100) %, $Z = 3.22$, $p = 0.001$].

VL, RF and G_{max} activities possess the same patterns among the experimental conditions and were maximally activated in the SEATED position in most participants i.e., in 15, 13 and 15 out of 16 participants, respectively (Fig. 4). Friedman ANOVA confirmed the effect of position on VL,

Table 1 Kinematic variables

	SUPINE		PRONE		SEATED	
	ALL	ISOL	ALL	ISOL	ALL	ISOL
X_{rest}	**22.5 ± 13.5**	**20.9 ± 14.6**	**−14.8 ± 11.3**	**−14.7 ± 16.0**	**20.0 ± 15.3**	**22.1 ± 16.4**
Y_{rest}	3.9 ± 9.7	4.4 ± 10.8	−5.2 ± 12.8	−6.0 ± 11.3	**12.4 ± 10.4**	**15.4 ± 9.7**
X_{MVC}	**39.3 ± 14.1**	**36.1 ± 13.0**	−2.6 ± 13.6	−4.4 ± 17.0	**41.0 ± 18.0**	**36.2 ± 15.4**
Y_{MVC}	−0.7 ± 10.3	**11.6 ± 11.8**	**−12.5 ± 12.5**	1.5 ± 10.1	1.9 ± 14.1	**18.1 ± 12.1**
ΔX	**16.9 ± 5.8**	**15.2 ± 7.3**	**12.2 ± 12.7**	**9.8 ± 4.9**	**21.0 ± 5.3**	**14.1 ± 4.9**
ΔY	−4.6 ± 4.7	**7.3 ± 3.5**	**−7.1 ± 8.1**	**7.5 ± 7.5**	**−10.6 ± 9.3**	2.7 ± 5.4
$\Delta\theta$ ankle	**−6.71 ± 3.81**	**−7.70 ± 2.67**	**−9.51 ± 3.32**	**−9.63 ± 4.80**	**−14.29 ± 3.14**	**−10.70 ± 2.51**

X and Y are the position of the ankle joint (estimated by the SCoRe method) relative to the axis of rotation of the dynamometer in the x direction and y direction at rest (X_{rest} and Y_{rest}) and at the peak torque event (X_{MVC} and Y_{MVC}), given in mm. $\Delta X = X_{MVC} - X_{rest}$, and $\Delta Y = Y_{MVC} - Y_{rest}$. $\Delta\theta$ is the difference in joint angle in degree between MVC and rest. Bolded values indicate a significant difference from 0 (t test for single mean; $p < 0.05$).Values are given as mean ± SD

Table 2 Correlation coefficients

Torque vs.	SUPINE		PRONE		SEATED	
	ISOL	ALL	ISOL	ALL	ISOL	ALL
TA	0.10	**0.55****	0.29	**0.67****	0.29	0.10
Sol	−0.11	**0.42****	**0.41***	**0.64****	**0.59****	0.18
GM	**0.40***	0.16	0.30	**0.57****	**0.42***	**0.55****
VL	−0.28	−0.11	0.22	0.25	**0.38***	**0.35***
RF	−0.24	−0.10	0.19	**0.34***	0.24	0.16
ST	**0.31***	0.16	0.17	0.00	**0.54****	0.27
G_{max}	−0.29	−0.19	0.22	0.19	0.16	0.04
ΔX	0.17	0.01	0.23	0.03	0.27	0.24
ΔY	**0.30***	−0.17	−0.08	−0.24	−0.06	−0.29
$\Delta\theta$	−0.07	0.21	−0.28	−0.21	−0.26	**−0.37***
N	46	47	36	37	42	37

N refers to the number of values used to compute the Pearson's r. Bold values indicate significant correlations (* $p < 0.05$; ** $p < 0.001$)

RF and G_{max} (VL $\chi^2 = 31.75$, $p < 0.001$; RF $\chi^2 = 17.44$, $p < 0.001$; G_{max} $\chi^2 = 38.31$, $p < 0.001$). These muscles were significantly more activated in the SEATED compared to the SUPINE and PRONE positions [merged values in SEATED position VL = 97.1 (1.4–100) %, RF = 62.5 (0.6–100) % and G_{max} = 90.7 (1.3–100) % vs. SUPINE + PRONE VL = 6.2 (0.3–90.5) %, RF = 6.8 (0.3–100) % and G_{max} = 5.1 (0.4–54.9) %, Wilcoxon Z values ranged from 3.23 to 4.75, $p < 0.001$]. Analyses indicated that the activity of VL, RF and G_{max} was greater in the ALL compared to the ISOL condition in the 3 positions tested (Wilcoxon Z values and p values ranged from $Z = 2.84$, $p = 0.004$ to $Z = 3.51$, $p < 0.001$; Fig. 4).

Kinematic deviations

Kinematic results and statistics are summarized in Table 1. During MVCs, the ankle joint angle varied of −9.73° ± 4.15° in average i.e., from 91.0° ± 5.2° to 81.3° ± 4.9° overall conditions. From rest to MVC and overall conditions, the CR varied on $\mathbf{e}_x$ of ΔX =+14.8 ± 8.0 mm (i.e., from X_{rest} = 9.7 ± 22.1 mm to X_{MVC} = 24.7 ± 24.6 mm) and of ΔY = −0.71 ± 9.6 mm on $\mathbf{e}_y$ (i.e., from Y_{rest} = 3.9 ± 13.1 mm to Y_{MVC} = 3.0 ± 15.0 mm).

Correlations

All the results on correlation analyses are summarized in Table 2 and indicated that torque was significantly correlated with the activity of the plantar flexors in each position. VL, RF, ST and kinematic variables (ΔY and the variation in joint angle, $\Delta\theta$) were found to be significantly related to torque depending on the position and on the instruction (see Table 2).

Discussion

The aim of this study was to point out the differences in torque output during maximal voluntary contraction

(MVC) in isometric plantarflexion when activating either isolated or global muscle (conditions named ISOL and ALL, respectively). The ALL condition was associated with higher EMG activities in most of the recorded muscles, notably in plantarflexor muscles, and was associated with higher joint torque compared to ISOL.

Very large differences were observed between ALL and ISOL, with gains on joint torque of about 40 % in average (Fig. 3). Lower torque in seated position could be attributable to muscle mechanics, i.e., force–length relationships (Maganaris 2003), and to impairments in motor units recruitment, as already reported for this particular joint angle configuration (i.e., knee and ankle joint angles set at 90° of flexion) (Cresswell et al. 1995; Kennedy and Cresswell 2001). In line with our findings, a previous study showed that plantarflexion torque could be significantly enhanced (~+26 %) in multi-joint compared to isolated plantar flexion (Hahn et al. 2011). However, this study remained inconclusive regarding the differences in EMG activity resulting from these two conditions and used different methodologies to assess joint torque in the multi-joint and isolated contractions, i.e., they used inverse dynamic calculations and ergometer measurements, that proved to provide different results (Herzog 1988; Kaufman et al. 1995; Arampatzis et al. 2004). Sasaki et al. (1998) observed an increase in plantarflexion torque linked to jaw clenching, but the conclusions relied on integrated electromyographic activity per unit of time rather than EMG level, and did not check for the influence of mechanical factors, as they focused on jaw clenching only.

Interestingly, the value of 40 % found in the present study fits well to differences with that observed in similar studies examining ankle MVC, that is, values ranging from 134 up to 186 Nm, despite similar populations and protocols (Danneskiold-Samsøe et al. 2009; Cresswell et al. 1995; Maganaris 2003). More precisely, considering isometric plantarflexion MVCs in the supine and prone positions, and a population of young male adults, literature reports MVC values ranging from ~134 Nm [e.g., 142 ± 42, $N = 10$ (Danneskiold-Samsøe et al. 2009) or 134 ± 23 Nm, $N = 10$ (Cresswell et al. 1995)] up to ~186 Nm [e.g., 172 ± 15, $N = 8$ (Maganaris 2003) or 186 ± 28 Nm ($N = 9$) (Hahn et al. 2011)]. These differences may pertain to differences in the participants' fitness (i.e., more or less trained participants), but the results suggest that an explanation also bears on the nature of the instructions (ALL vs. ISOL).

Mechanical factors

Misalignment has been shown to induce bias of ~10 % in the estimation of joint torque (Arampatzis et al. 2007; Deslandes et al. 2008), but this factor is not expected to create large differences among studies, as the positioning of the foot is expected to be carefully executed Given the equation #1, positive deviations of CR in the x-direction, that decreases $\frac{r_{\text{ankle}}}{r_{\text{dynamometer}}}$, decrease the effectiveness of the ankle torque. The misalignments observed in this study on the X-axis are positive and then, they are not likely to explain the gains in torque. Nevertheless, misalignments may allow the auxiliary muscles, through joint reaction forces transmission, to influence the ankle torque.

One can first observe that positioning has an effect on the activity of knee extensors, knee flexors and hip extensors muscles (Fig. 4). For example, the seated position was associated with higher level of activity for VL, RF and G_{max} and the prone position was associated with higher ST activity (Fig. 4) but the correlation values between these muscles and the torque produced remained modest (Table 2), suggesting that the mechanical influence of these muscles is small. Furthermore, despite the fact that differences were observed in ST activity between PRONE and SUPINE, no differences were found in torque between these two positions. In addition, the large increase in G_{max}, VL and RF activity (Fig. 4) did not preclude to the force deficit associated with the seated position (Fig. 3). As a consequence, no major mechanical influence of these muscles is expected on the produced torque. Notwithstanding, at least two observations forbid ruling out the influence of such forces. Firstly, despite significant and positive correlations of the activity of Sol and GM with torque in the seated position (Table 2), the increase in torque was not associated with significant increases in the activity of these muscles i.e., SOL ($p = 0.255$) and GM ($p = 0.079$). And in this particular position, VL and ST were also correlated with torque (Table 2). These observations strongly suggest that the forces created by muscles that do not span over the ankle joint significantly influenced the measured joint torque, at least in the seated position. Secondly, provided that torque is mainly related to plantarflexor activity, as the relation between EMG and torque tends to be convex toward tension at high force levels (Perry and Bekey 1981; Lawrence and De Luca 1983), a given increase in torque in this portion of the curve should have been associated with a larger increase in EMG and not with a similar one (Figs. 3, 4). Suggesting that even in the supine and prone positions, plantarflexors are not the sole contributors of the increase in torque.

Neural factors

What can explain the higher muscle activity level in ALL compared to ISOL observed in this study? First, motivation is not likely to explain the differences observed between ALL and ISOL. Although motivation has not been explicitly assessed in this study, differences in motivation are not

expected, because the tests were randomized. In addition, we found high reliability between the 3 trials within all the conditions tested, with an average correlation coefficient of 0.95 [range = (0.90–0.98); model corresponding to case #1 in McGraw and Wong (1996)] and an average coefficient of variation of 5.8 % [range = (3.2–8.2)]. These reliability values are highly consistent with previous reports testing MVCs in plantarflexion (Webber and Porter 2010; Todd et al. 2004; Sleivert and Wenger 1994) and can be taken as evidences that MVC testing conditions carried out here can be truly compared to those imposed in previous studies. As a consequence, the lower values observed in ISOL are not likely to be due to a lack of motivation from the participants.

Nevertheless, in two subjects, the gains in torque from ISOL to ALL exceeded 150 % (in the prone and supine positions), values that were linked to very low values in the ISOL condition (i.e., 53 and 63 Nm). One explanation could be these participants, when attempting to isolate the calf muscles, tried to avoid a phenomenon named motor over flow or synkinesis (Todor and Lazarus 1986; Gandevia 2001). It appears in fact very difficult to isolate muscle contractions when effort increases and involuntary contractions of uninvolved muscles generally occur (Todor and Lazarus 1986; Dimitrijevic et al. 1992). It is therefore possible that these two participants, and maybe the others in a lesser extent, voluntarily reduced the neural drive to the muscles to avoid motor overflow and to conform with the instructions.

In ALL, participants were allowed to grasp the ergometer, which is not generally allowed in studies measuring ankle MVCs (cf. a representative setup in Figure #1 of Simoneau et al. (2009), so that concurrent activation potentiation could be induced (Ebben et al. 2008a, b, 2010; Cherry et al. 2010). Jaw clenching or Valsalva maneuver has been reported to improve the level of maximal activation of the contracting muscles (Ebben et al. 2008b; Sasaki et al. 1998). However, most of these studies focused on the knee extensors muscles (Ebben et al. 2008b, 2010), and not on plantarflexors. Furthermore, improvements in peak torque due to jaw clenching and Valsalva maneuver have been reported to be of ~15 % for the quadriceps muscles (Ebben et al. 2008b, 2010), that is, far less than the differences observed in the present study (i.e., ~40 %). This may suggest a particular sensitivity of the plantarflexors to the phenomenon. In fact, contrary to other muscles such as elbow flexors (Herbert et al. 1998) or ankle dorsiflexors (Kent-Braun et al. 2002), activation of plantarflexor muscles is rarely complete (Todd et al. 2004; Cresswell et al. 1995). Without training or adequate testing conditions, plantarflexor muscles are not maximally activated by volition, and only reach about 80–90 % of voluntary activation (Cresswell et al. 1995; Maffiuletti et al. 2002). This is in line with the finding that the neural drive to these muscles can be significantly improved by a strength training (Shield and Zhou 2004) or imagined strength training (Zijdewind et al. 2003; Sidaway and Trzaska 2005), whereas such is not the case for the elbow flexors, for example which possess a high initial level of voluntary activation (Herbert et al. 1998). The work of Devanne and collaborators (Devanne et al. 2002; Kouchtir-Devanne et al. 2012) is particularly interesting in this respect. They observed that the excitability of the cortical neurons associated with the first dorsal interosseus was lower during isolated (contraction of first dorsal interosseus only) vs. global muscle contractions (precision grip implying the thumb and the finger). This indicates that the cortical excitability of a given muscle depends on its functional interconnections at the cortical level.

Overall, these findings support the idea that isolated contractions, which explicitly or implicitly (through instructions) require a selection of the contracting muscles, may induce inhibition, incompatible with the objectives of MVC testing. Allowing global muscle activation or not is then a critical aspect of the instructions.

Conclusions

This study reports that activation of plantarflexor muscles is superior during global muscle activation compared to isolated joint contraction, entailing very large differences in motor-output. It emphasizes the pertinence of using isolated vs. unconstrained MVC testing protocols, notably for muscles that are not maximally activated by volition.

References

Arampatzis A, Karamanidis K, De Monte G, Stafilidis S, Morey-Klapsing G, Brüggemann G-P (2004) Differences between measured and resultant joint moments during voluntary and artificially elicited isometric knee extension contractions. Clin Biomech 19(3):277–283

Arampatzis A, De Monte G, Morey-Klapsing G (2007) Effect of contraction form and contraction velocity on the differences between resultant and measured ankle joint moments. J Biomech 40(7):1622–1628

Barry B, Riley Z, Pascoe M, Enoka R (2008) A spinal pathway between synergists can modulate activity in human elbow flexor muscles. Exp Brain Res 190(3):347–359

Burke S (2001) Missing values, outliers, robust statistics & non-parametric methods. LC-GC Europe Online Supplement, Statistics & Data Analysis 2:19–24

Chatterjee S, Hadi AS (1986) Influential observations, high leverage points, and outliers in linear regression. Stat Sci 1(3):379–393

Cherry EA, Brown LE, Coburn JW, Noffal GJ (2010) Effect of remote voluntary contractions on knee extensor torque and rate of velocity development. J Strength Cond Res 24(9):2564–2569

Cresswell AG, Löscher W, Thorstensson A (1995) Influence of gastrocnemius muscle length on triceps surae torque development and electromyographic activity in man. Exp Brain Res 105(2):283–290

Danneskiold-Samsøe B, Bartels E, Bülow P, Lund H, Stockmarr A, Holm C, Wätjen I, Appleyard M, Bliddal H (2009) Isokinetic and isometric muscle strength in a healthy population with special reference to age and gender. Acta Physiol 197(s673):1–68

De Ruiter CJ, Hoddenbach JG, Huurnink A, De Haan A (2008) Relative torque contribution of vastus medialis muscle at different knee angles. Acta Physiol 194(3):223–237

Deslandes S, Mariot J-P, Serveto S (2008) Offset of rotation centers creates a bias in isokinetics: a virtual model including stiffness or friction. J Biomech 41(10):2112–2120

Devanne H, Cohen LG, Kouchtir-Devanne N, Capaday C (2002) Integrated motor cortical control of task-related muscles during pointing in humans. J Neurophysiol 87(6):3006–3017

Dimitrijevic MR, McKay WB, Sarjanovic I, Sherwood AM, Svirtlit L, VrbovÃ G (1992) Co-activation of ipsi- and contralateral muscle groups during contraction of ankle dorsiflexors. J Neurol Sci 109(1):49–55

Drouin JM, Valovich-mcLeod TC, Shultz SJ, Gansneder BM, Perrin DH (2004) Reliability and validity of the Biodex system 3 pro isokinetic dynamometer velocity, torque and position measurements. Eur J Appl Physiol 91(1):22–29

Ebben WP (2006) A brief review of concurrent activation potentiation: theoretical and practical constructs. J Strength Cond Res 20(4):985–991

Ebben WP, Flanagan EP, Jensen RL (2008a) Jaw clenching results in concurrent activation potentiation during the countermovement jump. J Strength Cond Res 22(6):1850–1854

Ebben WP, Leigh DH, Geiser CF (2008b) The effect of remote voluntary contractions on knee extensor torque. Med Sci Sports Exerc 40(10):1805–1809

Ebben WP, Petushek EJ, Fauth ML, Garceau LR (2010) EMG analysis of concurrent activation potentiation. Med Sci Sports Exerc 42(3):556–562

Ehrig RM, Taylor WR, Duda GN, Heller MO (2006) A survey of formal methods for determining the centre of rotation of ball joints. J Biomech 39(15):2798–2809

Gandevia SC (2001) Spinal and supraspinal factors in human muscle fatigue. Physiol Rev 81(4):1725–1789

Hahn D, Olvermann M, Richtberg J, Seiberl W, Schwirtz A (2011) Knee and ankle joint torque–angle relationships of multi-joint leg extension. J Biomech 44(11):2059–2065

Herbert R, Dean C, Gandevia S (1998) Effects of real and imagined training on voluntary muscle activation during maximal isometric contractions. Acta Physiol Scand 163(4):361–368

Hermens HJ, Freriks B, Disselhorst-Klug C, Rau G (2000) Development of recommendations for SEMG sensors and sensor placement procedures. J Electromyogr Kinesiol 10(5):361–374

Herzog W (1988) The relation between the resultant moments at a joint and the moments measured by an isokinetic dynamometer. J Biomech 21(1):5–12

Hicks J (1953) The mechanics of the foot: I. The joints. J Anat 87(Pt 4):345

Horak FB, Shupert CL, Mirka A (1989) Components of postural dyscontrol in the elderly: a review. Neurobiol Aging 10(6):727–738

Kaufman KR, An K-N, Chao E (1995) A comparison of intersegmental joint dynamics to isokinetic dynamometer measurements. J Biomech 28(10):1243–1256

Kennedy P, Cresswell A (2001) The effect of muscle length on motor-unit recruitment during isometric plantar flexion in humans. Exp Brain Res 137(1):58–64

Kent-Braun JA, Ng AV, Doyle JW, Towse TF (2002) Human skeletal muscle responses vary with age and gender during fatigue due to incremental isometric exercise. J Appl Physiol 93(5):1813–1823

Klass M, Baudry S, Duchateau J (2008) Age-related decline in rate of torque development is accompanied by lower maximal motor unit discharge frequency during fast contractions. J Appl Physiol 104(3):739–746

Kouchtir-Devanne N, Capaday C, Cassim Fo, Derambure P, Devanne H (2012) Task-dependent changes of motor cortical network excitability during precision grip compared to isolated finger contraction. J Neurophysiol 107(5):1522–1529

Lawrence JH, De Luca C (1983) Myoelectric signal versus force relationship in different human muscles. J Appl Physiol 54(6):1653–1659

Lundberg A, Svensson O, Nemeth G, Selvik G (1989) The axis of rotation of the ankle joint. J Bone Joint Surg Br Vol 71(1): 94–99

Maffiuletti NA, Pensini M, Martin A (2002) Activation of human plantar flexor muscles increases after electromyostimulation training. J Appl Physiol 92(4):1383–1392

Maganaris CN (2003) Force-length characteristics of the in vivo human gastrocnemius muscle. Clin Anat 16(3):215–223

Maxwell SE (1980) Pairwise multiple comparisons in repeated measures designs. J Educ Behav Stat 5(3):269–287

McGraw KO, Wong S (1996) Forming inferences about some intraclass correlation coefficients. Psychol Methods 1(1):30

McNeil CJ, Vandervoort AA, Rice CL (2007) Peripheral impairments cause a progressive age-related loss of strength and velocity-dependent power in the dorsiflexors. J Appl Physiol 102(5):1962–1968

Moraux A, Canal A, Ollivier G, Ledoux I, Doppler V, Payan C, Hogrel J-Y (2013) Ankle dorsi-and plantar-flexion torques measured by dynamometry in healthy subjects from 5 to 80 years. BMC Musculoskelet Disord 14(1):104

Perry J, Bekey GA (1981) EMG-force relationships in skeletal muscle. Crit Rev Biomed Eng 7(1):1–22

Ramos MU, Knapik J (1978) Instrumentation and techniques for the measurement of muscular strength and endurance in the human body. DTIC Document

Sasaki Y, Ueno T, Taniguchi H, Ohyama T (1998) Effect of teeth clenching on isometric and isokinetic strength of ankle plantar flexion. J Med Dental Sci 45(1):29

Shiavi R, Frigo C, Pedotti A (1998) Electromyographic signals during gait: criteria for envelope filtering and number of strides. Med Biol Eng Comput 36(2):171–178

Shield A, Zhou S (2004) Assessing voluntary muscle activation with the twitch interpolation technique. Sports Med 34(4):253–267

Sidaway B, Trzaska A (2005) Can mental practice increase ankle dorsiflexor torque? Phys Ther 85(10):1053–1060

Simoneau E, Martin A, Van Hoecke J (2007) Effects of joint angle and age on ankle dorsi-and plantar-flexor strength. J Electromyogr Kinesiol 17(3):307–316

Simoneau EM, Billot M, Martin A, Van Hoecke J (2009) Antagonist mechanical contribution to resultant maximal torque at the ankle joint in young and older men. J Electromyogr Kinesiol 19(2):e123–e131

Sleivert GG, Wenger HA (1994) Reliability of measuring isometric and isokinetic peak torque, rate of torque development, integrated electromyography, and tibial nerve conduction velocity. Arch Phys Med Rehabil 75(12):1315–1321

Todd G, Gorman RB, Gandevia SC (2004) Measurement and reproducibility of strength and voluntary activation of lower limb muscles. Muscle Nerve 29(6):834–842

Todor JI, Lazarus J-AC (1986) Exertion level and the intensity of associated movements. Dev Med Child Neurol 28(2):205–212

Van Cutsem M, Duchateau J, Hainaut K (1998) Changes in single motor unit behaviour contribute to the increase in contraction speed after dynamic training in humans. J Physiol 513(1):295–305

Webber SC, Porter MM (2010) Reliability of ankle isometric, isotonic, and isokinetic strength and power testing in older women. Phys Ther 90(8):1165–1175

Winter DA (1990) Biomechanics and motor control of human movement. Wiley, New York

Wu G, Siegler S, Allard P, Kirtley C, Leardini A, Rosenbaum D, Whittle M, D'Lima DD, Cristofolini L, Witte H (2002) ISB recommendation on definitions of joint coordinate system of various joints for the reporting of human joint motion—part I: ankle, hip, and spine. J Biomech 35(4):543–548

Zijdewind I, Toering ST, Bessem B, van der Laan O, Diercks RL (2003) Effects of imagery motor training on torque production of ankle plantar flexor muscles. Muscle Nerve 28(2):168–173

IV.5. Proposition d'Approche Adimensionnelle du Cyclisme

Dans le cas de l'étude du mouvement humain, il est possible de diminuer la part de variabilité liée à l'anthropométrie en utilisant des conditions expérimentales adaptées, basées sur une combinaison de nombres adimensionnels adaptés pour l'analyse de la marche et de la course (Delattre, Lafortune, et Moretto 2009; Villeger et al. 2014; Villeger et al. 2015). Il s'agit de placer les participants dans des conditions expérimentales similaires, tenant compte de leurs différences d'anthropométrie. A ce jour, aucune approche de ce type n'a été proposée pour l'étude du cyclisme. Dans cette optique, l'ébauche d'une approche adimensionnelle du cyclisme sera presentée ci-après. Cette approche n'a pas encore été modélisée de façon complète, ni validée de façon expérimentale.

La première étape consisterait en un positionnement standardisé sur la bicyclette. En particulier, l'angle du tube de selle (variable adimensionnelle) devrait être constant, et la hauteur de selle, proportionnelle à la longueur de la jambe en extension complète du cycliste. La longueur séparant le centre articulaire de la hanche de l'axe de la pédale lorsque la jambe est en extension complète constitue une longueur caractéristique pour chaque sujet, qui sera utilisée par la suite. Il est à noter que dans le cadre de cette approche, la longueur des manivelles devrait aussi être proportionnelle à la longueur de jambe des sujets.

La seconde étape serait la définition d'une vitesse similaire entre les participants, quelle que soit leur anthropométrie. Le nombre de Froude permet d'étudier un mouvement périodique soumis à un champ gravitationnel. En utilisant ce nombre (N_{fr}), il est possible d'exprimer des vitesses similaires pour un champ gravitationnel donné en fonction d'une longueur caractéristique telles que :

$$v_{sim} = \sqrt{N_{fr} \times g \times l_j} \qquad \text{(Equation 8)}$$

Où g est l'accélération gravitationnelle, et l_j la longueur caractéristique de la jambe énoncée précédemment. Pour une population d'anthropométrie proportionnelle (*i.e.* de masse volumique identique), ces vitesses ont été modélisées (Figure 29).

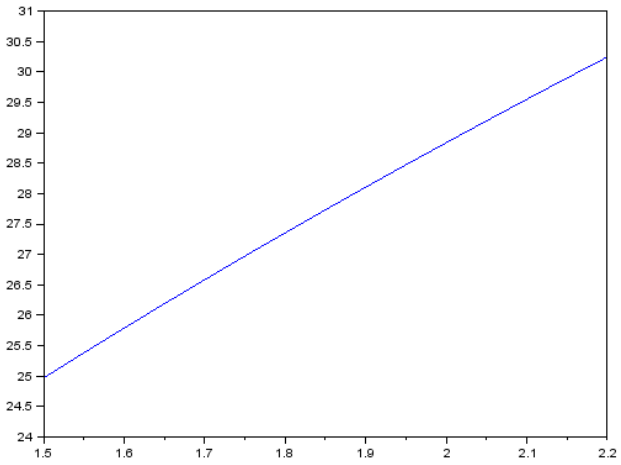

Figure 29 : vitesse de déplacement similaire exprimée en km.h^{-1} en fonction de la taille du cycliste, pour une population de masse volumique de 12,5 et un nombre de Froude de 6.

Etant donnée l'influence majeure des conditions environnementales en cyclisme (pente, coefficient de traînée aérodynamique, masse volumique de l'air...), notre proposition est de faire correspondre les vitesses similaires à des puissances mécaniques développées similaires. Considérant l'égalité :

$$V = \frac{P}{Rtot} \qquad \text{(Equation 9)}$$

Où V est la vitesse de déplacement, P la puissance mécanique développée (par la roue arrière sur le sol) et R_{tot} la somme des résistances extérieures appliquée au cycliste telles que (Martin et al. 2006) :

$$R_{tot} = 0{,}5\ \rho\ S\ C_x\ V^2 + C_r\ m\ g + \ m\ g\ sin\ \alpha \qquad \text{(Equation 10)}$$

Où ρ est la masse volumique de l'air, S le maître-couple du système cycliste+bicyclette, Cx le coefficient de traînée aérodynamique, V la vitesse de l'air (représentée dans le cas sans vent par la vitesse du cycliste), Cr le coefficient de friction global (en première approximation, celui des pneus sur le sol), m masse du cycliste, g l'accélération gravitationnelle et α la pente. En considérant les vitesses similaires proposées au-dessus, et les conditions environnementales suivantes : ρ = 1,2 (valeur pour 20°C à 0 m d'altitude) ; C_r = 0.007 (revêtement de qualité moyenne) ; α = 0 (terrain plat), et SC_x défini en fonction de la taille du sujet selon la régression taille = 0.7335 * SC_x – 1.0817 (Grappe 2009), nous obtenons les puissances similaires (P_{sim}) suivantes :

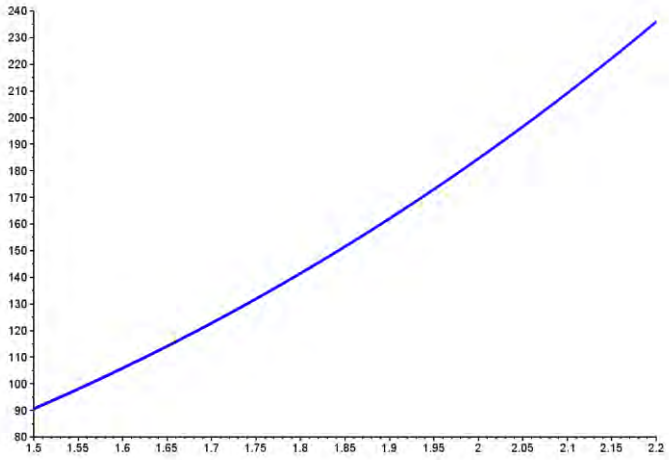

Figure 30 : puissances mécaniques similaires exprimées en km.h^{-1} en fonction de l'anthropométrie du cycliste pour des conditions plates et sans vent, et un nombre de Froude de 6.

Enfin, une dernière étape serait la définition d'une fréquence « similaire » (f_{sim}). A l'aide du nombre de Strouhal (N_{ST}), et sur la base des données précédentes de longueur caractéristique du système et de vitesse similaire, il est possible d'écrire la relation suivante :

$$f_{sim} = \frac{N_{st} \times V_{sim}}{l_j}$$ (Equation 11)

En considérant que la fréquence exprimée est une fréquence caractéristique du système, il paraît logique d'y associer la fréquence de pédalage. En considérant les mêmes données que précédemment, et pour un nombre de Strouhal de 0,2 nous obtenons la relation suivante :

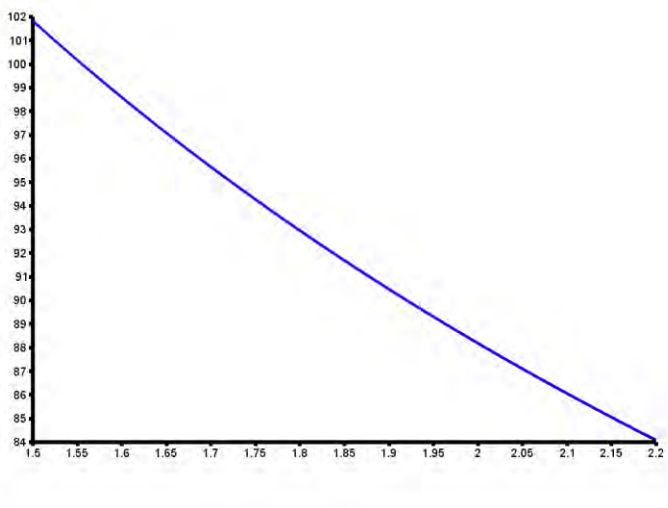

Figure 31 : fréquences de pédalage similaires exprimées en RPM (Rotations Par Minute) exprimées en fonction de l'anthropométrie des cyclistes.

Pour résumer, cette approche propose la détermination de conditions expérimentales similaires adaptées au cyclisme en utilisant une combinaison des nombres adimensionnels de Froude et de Strouhal. Son objectif est de diminuer la variabilité du comportement des individus liée à leurs différences d'anthropométrie. Dans l'exemple proposé précédemment, pour placer deux cyclistes de masse volumique proportionnelle et ayant pour taille 1,60m et 1,90m dans des conditions expérimentales similaires, le premier aurait à développer 105 W à 98,5 RPM tandis que le second devrait développer 158 W à 90,5 RPM (pour N_{fr} = 6 et N_{st} = 0,2). Toutefois, cette approche théorique reste à valider expérimentalement afin de démontrer son intérêt pour la diminution de la variabilité des données mécaniques liée aux différences anthropométriques entre les cyclistes.

IV.6. ETUDE 10 : VARIABILITY IN THE SPATIAL STRUCTURE OF MUSCLE COORDINATION ASSOCIATED WITH THE SIT-TO-STAND TRANSITION IN PEDALING

Article accepté pour présentation au congrès « Motor Control Summer School XI » (Bled, Slovénie).

MCSS XI, Slovenia

Variability in the Spatial Structure of Muscle Coordination associated with the Sit-To-Stand Transition in Pedaling

Nicolas A. Turpin[1], Antony Costes[1], Pierre Moretto[1], Bruno Watier[1,2]
[1]University of Toulouse, PRISSMH , France, [2]CNRS, LASS, Toulouse, France

SUMMARY
Hypothetical structures named muscle synergy vectors (MSV) or M-modes have been proven to organize the variations of multiple muscle activity in several tasks, including pedaling. Seventeen participants performed 12 randomized trials in either the standing or the seated position in pedaling, at intensities corresponding to 20%, 40%, 60% 80%, 100%, and 120% of the seat-to-stand transition power. For each trial, MSV were extracted from 15 pedaling cycles and used to fit subparts of the same dataset. The average and standard deviation of the R^2 of the reconstructed muscle patterns was used as a quantification of MSV variability inside a given condition. Non Negative Matrix Factorization was used to extract the MSV. Three MSV were extracted for all subjects. The analyses revealed large consistency of the MSV over cycles independent of the position used (mean R^2=0.94±0.02% range [0.88-0.98]). Power output affected both mean and SD of reconstruction R^2. The effect on SD, that decrease with increasing power output was likely to be attributable to changes in signal to noise ratio. The change in mean R^2, that increased in the standing position at low power output is linked to a trend for EMG variance to be well captured by only two MSV in these conditions. As a conclusion the change in position in cycling is not associated with changes in variability of the MSV.

INTRODUCTION
During movement, EMG patterns of multiple muscles could be decomposed into elemental unit bursts activating multiple muscles in synchrony. Muscle activation magnitudes during each burst are linearly related and the weightings of the muscles define vectors named muscle synergy vectors (MSV) or muscle modes. Several evidences suggested a certain degree of flexibility in the MSVs (Robert and Latash 2008; Gizzi et al. 2010; Berger et al. 2013; Muceli et al. 2014) and the goal of this study was to quantify MSVvariability associated with the spontaneous transition from the seated to the standing position in cycling.

METHODS
17 participants volunteers to the study (age, mass). Participants first performed a sit-to-stand transition test, lasting approximately 10 minutes, and consisting in an incremental pedaling exercise, performed in the seated position at the beginning, to determine the power at which subjects spontaneously raise to the standing position (named $P_{transition}$). In all tests, subjects were required to maintain a pedaling rate of 90 RPM. The second test consisted in 12 randomized trials lasting 10 seconds each, performed in either the standing or the seated position, and at intensities corresponding to 20%, 40%, 60% 80%, 100%, and 120% of $P_{transition}$. EMG signal from 7 muscles from the right side of the body was recorded i.e., *tibialis anterior*, *soleus*, *gastrocnemius lateralis*, *vastus medialis*, *rectus femoris*, *biceps femoris*, and *gluteus maximus*. EMG signals were amplified (× 1000), digitized (6-400 Hz bandwidth) at a sampling rate of 1 kHz (Bagnoli 16, Delsys, Inc. Boston, USA) and next, band-pass filtered (20-400 Hz, Butterworth filter), rectified and smoothed (9 Hz low pass filter) to obtain the EMG envelopes. For each muscle, EMG envelopes were normalized by the mean value obtained over all conditions. A first step has been to determine the number of MSV composing the dataset. Non-Negative-Matrix-Factorization (Lee and Seung 2001) have been used to extract the MSV. We iterated the analysis by varying the number of MSV extracted between 1 and 6 and computed the R^2 for each extraction(=1-SSE/SST, SSE:sum of squared residual and SST: sum of squared EMG data). The point when the averaged R^2 overreach 0.9 defined N, the number of MSV. Afterward, the global MSV corresponding to this particular number was extracted and used to fit each of the ~15 cycles of the same trial (=cross-validation procedure). The standard deviation and average R^2 of the reconstructed muscle patterns served as measures of consistency of the MSV within each trials and for each subject. A similar fitting procedure have been performed using random MSV to determine the reconstruction R^2 expected by chance. In this procedure, EMG data in each condition have been shuffled across time and muscles before extraction. R^2 values have been transformed into Fisher's Z before being subject to a three-way repeated measures ANOVA (position={seated *vs.* standing} and power-output={20%, 40%, 60% 80%, 100%, and 120%} as repeated measures factors and type={regular MSV *vs.* random MSV} as a categorical predictor) after checking for normality using Shapiro-Wilks tests. Post-hoc tests were performed using the Bonferroni's method.

RESULTS
Using the average R^2 over all conditions, three MSV have been extracted for all subjects (Fig.1.), a result that is consistent with a previous report (Hug et al. 2011). Mean reconstruction R^2 was high (overall conditions =0.94±0.02 range [0.88-0.98] at N=3) and always higher than chance level (Fig. 2A., p<.001) suggesting that MSV were robust across cycles. The analyses revealed no main effect of the position (p=.146) nor of the power-output (p=.232) on mean R^2. The significant interaction position×power-output×type (p<.001) leads to pursue inferences using post-hoc analysis. There was no change in the mean R^2 values in the seated position across power-output (Fig.2A.) but mean R^2 tended to increase with

decreasing power-output in the standing position, i.e., R^2 at 20% was greater than those observed at 60% up to 120% (Fig.2A.). Additionally, higher mean R^2 were observed in seated compared to standing at 20% and 40% ($p<.001$; Fig.2A.). This result represents the tendency for muscle coordination to be well captured by only 2 MSV in these conditions (i.e., R^2 close to 0.9 was found in the standing position at N=2-Fig.1).

The standard deviation of R^2 significantly decreases with increasing power output i.e., from 0.17±0.01 at 20% to 0.12±0.01 at 120% (values averaged over the two positions). No effect of the position was found (p=0.483; Fig.2B.). This decrease in the variability of the R^2 may be linked to an increase in signal-to-noise ratio with power output, an interpretation consistent with the increase in chance level R^2 observed with power-output (Fig.2A).

CONCLUSIONS

Variability in the structure of muscle coordination during pedaling do not depend on the position used (standing or seated).Power output is likely to affect this variability by mean of a change in signal to noise ratio.

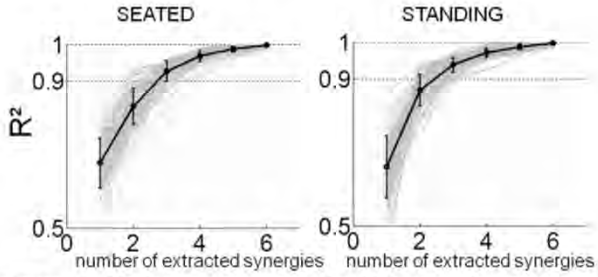

Figure 1. Variance accounted for (R^2) as a function of the number of extracted MSV. Each gray line is a plot for one subject and one condition of power-output (17 subjects × 6 power-outputs). Dark tick lines represent the mean±SD computed over all subjects and conditions of power-output.

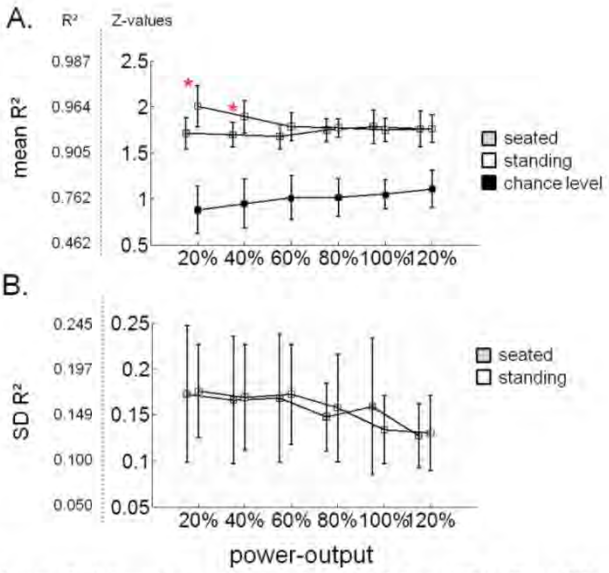

Figure 2. Mean (**A**.) and standard deviation (SD) (**B**.) of the reconstruction R^2. Values are given as mean ± SD. Statistical tests have been performed on Z-transformed values. Corresponding R^2 values are given on the left side of the figures. Red stars indicate significant differences between seated and standing at 20% and 40% ($p<.05$).

REFERENCES

Berger, D. J., R. Gentner, T. Edmunds, D. K. Pai and A. d'Avella (2013). "Differences in adaptation rates after virtual surgeries provide direct evidence for modularity." The Journal of Neuroscience **33**(30): 12384-12394.

Gizzi, L., J. r. F. k. Nielsen, F. Felici, Y. P. Ivanenko and D. Farina (2010). "Impulses of activation but not motor modules are preserved in the locomotion of subacute stroke patients." Journal of Neurophysiology **106**(1): 202-210.

Hug, F., N. A. Turpin, A. Couturier and S. Dorel (2011). "Consistency of muscle synergies during pedaling across different mechanical constraints." J Neurophysiol. ***106***(1): 91-103.

Lee, D. D. and H. S. Seung (2001). "Algorithms for Non-negative Matrix Factorization." Adv Neural Info Proc Syst **13**: 556-562.

Muceli, S., D. Falla and D. Farina (2014). "Reorganization of muscle synergies during multidirectional reaching in the horizontal plane with experimental muscle pain." J Neurophysiol. doi: 10.1152/jn.00147.2013.

Robert, T. and M. L. Latash (2008). "Time evolution of the organization of multi-muscle postural responses to sudden changes in the external force applied at the trunk level." Neuroscience Letters **438**(2): 238-241.

Bibliographie

Alexander, R.M. 1989. “Optimization and Gaits in the Locomotion of Vertebrates.” *Physiological Reviews* 69 (4): 1199–1227.

Amarantini, D. 2003. Thèse “Estimation Des Efforts Musculaires À Partir de Données Périphériques : Application À l’Analyse de La Coordination Pluri-Articulaire”. Grenoble: Université de Grenoble.

Amarantini, D., Martin, L., 2004. “A Method to Combine Numerical Optimization and EMG Data for the Estimation of Joint Moments under Dynamic Conditions.” *Journal of Biomechanics* 37 (9): 1393–1404. doi:10.1016/j.jbiomech.2003.12.020.

Begon, M., T. Monnet, and P. Lacouture. 2007. “Effects of Movement for Estimating the Hip Joint Centre.” *Gait & Posture* 25 (3): 353–59. doi:10.1016/j.gaitpost.2006.04.010.

Bertucci, W., Taiar, R., Grappe, F., 2005. “Differences between Sprint Tests under Laboratory and Actual Cycling Conditions.” *The Journal of Sports Medicine and Physical Fitness* 45 (3): 277–83.

Bini, R.R., Hume, P., Kilding, A.E., 2014. “Saddle Height Effects on Pedal Forces, Joint Mechanical Work and Kinematics of Cyclists and Triathletes.” *European Journal of Sport Science* 14 (1): 44–52. doi:10.1080/17461391.2012.725105.

Bizzi, E., Cheung, V.C.K., d’ Avella, A., Saltiel, P., Tresch, M., 2008. “Combining Modules for Movement.” *Brain Research Reviews* 57 (1): 125–33. doi:10.1016/j.brainresrev.2007.08.004.

Bolourchi, F., Hull, M.L., 1985. “Measurement of Rider Induced Loads During Simulated Bicycling.” *International Journal of Sport Biomechanics* 1 (4): 308–29.

Cahouët, V., Martin L., Amarantini D., 2002. “Static Optimal Estimation of Joint Accelerations for Inverse Dynamics Problem Solution.” *Journal of Biomechanics* 35 (11): 1507–13.

Caldwell, G., Hagberg, J.M., McCole, S.D., Li L., 1999. “Lower Extremity Joint Moments During Uphill Cycling.” *Journal of Applied Biomechanics* 15 (2): 166–81.

Caldwell, G., Li L, McCole, S.D., Hagberg, J.M., 1998. “Pedal and Crank Kinetics in Uphill Cycling.” *Journal of Applied Biomechanics* 14 (3): 245–59.

Caldwell, G., van Emmerik, C., Hamill, J., 2000. “Movement Proficiency: Incorporating Task Demands and Constrains in Assessing Human Movement.” In *Energetics of Human Activity*, 66–95. Human Kinetics. Champaign, Illinois: W. Sparrow.

Chapman, A.R., Vicenzino, B., Blanch, P., Knox, J.J., Hodges, P.W., 2010. “Intramuscular Fine-Wire Electromyography during Cycling: Repeatability, Normalisation and a Comparison to Surface Electromyography.” *Journal of Electromyography and Kinesiology* 20 (1): 108–17. doi:10.1016/j.jelekin.2008.11.013.

Coast, J. R., Welch, H.G., 1985. “Linear Increase in Optimal Pedal Rate with Increased Power Output in Cycle Ergometry.” *European Journal of Applied Physiology and Occupational Physiology* 53 (4): 339–42.

Dahmane, R., Djordjevic, S., Simunic, B., Valencic, V., 2005. “Spatial Fiber Type Distribution in Normal Human Muscle Histochemical and Tensiomyographical Evaluation.” *Journal of Biomechanics* 38 (12): 2451–59. doi:10.1016/j.jbiomech.2004.10.020.

Day, S.J., Hulliger, M., 2001. “Experimental Simulation of Cat Electromyogram: Evidence for Algebraic Summation of Motor-Unit Action-Potential Trains.” *Journal of Neurophysiology* 86 (5): 2144–58.

De Leva, P. 1996. “Adjustments to Zatsiorsky-Seluyanov’s Segment Inertia Parameters.” *Journal of Biomechanics* 29 (9): 1223–30.

De Luca, C.J., 1997. “The Use of Surface Electromyography in Biomechanics.” *Journal of Applied Biomechanics* 13 (2): 135–63.

Delattre, N., Lafortune, M.A., Moretto, P., 2009. “Dynamic Similarity during Human Running: About Froude and Strouhal Dimensionless Numbers.” *Journal of Biomechanics* 42 (3): 312–18. doi:10.1016/j.jbiomech.2008.11.010.

Demeny, G., 1904. *Mécanisme et Éducation Des Mouvements*. Vol. 99. F. Alcan.

Dorel, S., Guilhem, G., Couturier, A., Hug; F., 2012. “Adjustment of Muscle Coordination during an All-out Sprint Cycling Task.” *Medicine and Science in Sports and Exercise* 44 (11): 2154–64. doi:10.1249/MSS.0b013e3182625423.

Duc, S., Bertucci, W., Pernin, J.N., Grappe, F., 2008. “Muscular Activity during Uphill Cycling: Effect of Slope, Posture, Hand Grip Position and Constrained Bicycle Lateral Sways.” *Journal of Electromyography and Kinesiology* 18 (1): 116–27. doi:10.1016/j.jelekin.2006.09.007.

Dumas, R., Camomilla, V., Bonci, T., Cheze, L., Cappozzo, A., 2014. “Generalized Mathematical Representation of the Soft Tissue Artefact.” *Journal of Biomechanics* 47 (2): 476–81. doi:10.1016/j.jbiomech.2013.10.034.

Ebben, W.P., Leigh, D., Geiser, C.F., 2008. “The Effect of Remote Voluntary Contractions on Knee Extensor Torque.” *Medicine and Science in Sports and Exercise* 40 (10): 1805–9. doi:10.1249/MSS.0b013e31817dc4ad.

Ehrig, R.M., Taylor, W.R., Duda, G.N., Heller, M.O., 2006. “A Survey of Formal Methods for Determining the Centre of Rotation of Ball Joints.” *Journal of Biomechanics* 39 (15): 2798–2809. doi:10.1016/j.jbiomech.2005.10.002.

Elmer, S.J., Barratt, P.R., Korff, T., Martin, J.C., 2011. “Joint-Specific Power Production during Submaximal and Maximal Cycling.” *Medicine and Science in Sports and Exercise* 43 (10): 1940–47. doi:10.1249/MSS.0b013e31821b00c5.

Farina, D., Merletti, R., Enoka, R.M., 2004. “The Extraction of Neural Strategies from the Surface EMG.” *Journal of Applied Physiology* 96 (4): 1486–95. doi:10.1152/japplphysiol.01070.2003.

Gonzalez, H., Hull, M.L., 1989. “Multivariable Optimization of Cycling Biomechanics.” *Journal of Biomechanics* 22 (11-12): 1151–61.

Gregersen, C.S., Hull, M.L., 2003. “Non-Driving Intersegmental Knee Moments in Cycling Computed Using a Model That Includes Three-Dimensional Kinematics of the Shank/foot and the Effect of Simplifying Assumptions.” *Journal of Biomechanics* 36 (6): 803–13. doi:10.1016/S0021-9290(03)00014-9.

Hansen, E.A., Waldeland, H., 2008. “Seated versus Standing Position for Maximization of Performance during Intense Uphill Cycling.” *Journal of Sports Sciences* 26 (9): 977–84. doi:10.1080/02640410801910277.

Harnish, C., King, D., Swensen, T., 2007. “Effect of Cycling Position on Oxygen Uptake and Preferred Cadence in Trained Cyclists during Hill Climbing at Various Power Outputs.” *European Journal of Applied Physiology* 99 (4): 387–91. doi:10.1007/s00421-006-0358-7.

Hayot, C., 2010. Thèse “Analyse Biomécanique 3D de La Marche Humain : Comparaison Des Modèles Mécaniques”. Poitiers: Université de Poitiers.

Henneman, E., Somjen, G., Carpenter, D.O., 1965. “Functional Significance Of Cell Size In Spinal Motoneurons.” *Journal of Neurophysiology* 28 (May): 560–80.

Hermens, H.J., Freriks, B., Disselhorst-Klug, C., Rau, G., 2000. “Development of Recommendations for SEMG Sensors and Sensor Placement Procedures.” *Journal of Electromyography and Kinesiology* 10 (5): 361–74.

Hoes, M.J., Binkhorst, R.A., Smeekes-Kuyl, E., Vissers, A.C., 1968. “Measurement of Forces Exerted on Pedal and Crank during Work on a Bicycle Ergometer at Different Loads.” *Arbeitsphysiologie* 26 (1): 33–42. doi:10.1007/BF00696088.

Hof, A.L., 1996. “Scaling Gait Data to Body Size.” *Gait & Posture* 4 (3): 222–23. doi:10.1016/0966-6362(95)01057-2.

Hoyt, D.F., Taylor, C.R., 1981. “Gait and the Energetics of Locomotion in Horses.” *Nature* 292 (July): 239–40. doi:10.1038/292239a0.

Hug, F., Turpin, N.A., Couturier, A., Dorel, S., 2011. “Consistency of Muscle Synergies during Pedaling across Different Mechanical Constraints.” *Journal of Neurophysiology* 106 (1): 91–103. doi:10.1152/jn.01096.2010.

Hull, M.L., Gonzalez, H., 1988. “Bivariate Optimization of Pedalling Rate and Crank Arm Length in Cycling.” *Journal of Biomechanics* 21 (10): 839–49.

Hull, M.L., Jorge, M., 1985. “A Method for Biomechanical Analysis of Bicycle Pedalling.” *Journal of Biomechanics* 18 (9): 631–44.

Kamen, G., Gabriel, D., 2010. *Essentials of Electromyography*. Human Kinetics.

Kautz, S.A., Hull, M.L., Neptune, R.R., 1994. “A Comparison of Muscular Mechanical Energy Expenditure and Internal Work in Cycling.” *Journal of Biomechanics* 27 (12): 1459–67.

Keenan, K.G., Farina, D., Maluf, K.S, Merletti, K., Enoka, R.M., 2005. “Influence of Amplitude Cancellation on the Simulated Surface Electromyogram.” *Journal of Applied Physiology* 98 (1): 120–31. doi:10.1152/japplphysiol.00894.2004.

Knight, C.A., Kamen, G., 2005. “Superficial Motor Units Are Larger than Deeper Motor Units in Human Vastus Lateralis Muscle.” *Muscle & Nerve* 31 (4): 475–80. doi:10.1002/mus.20265.

Li, L., Caldwell, G., 1998. “Muscle Coordination in Cycling: Effect of Surface Incline and Posture.” *Journal of Applied Physiology* 85 (3): 927–34.

Lucía, A., Hoyos, J., Chicharro, J.L., 2001. "Preferred Pedalling Cadence in Professional Cycling." *Medicine and Science in Sports and Exercise* 33 (8): 1361–66.

MacIntosh, B.R., Neptune, R.R., Horton, J.F., 2000. "Cadence, Power, and Muscle Activation in Cycle Ergometry." *Medicine and Science in Sports and Exercise* 32 (7): 1281–87.

Marey, E.J. 1884. *Le Mouvement*. Masson.

Marsh, A.P., Martin, P.E., 1993. "The Association between Cycling Experience and Preferred and Most Economical Cadences." *Medicine and Science in Sports and Exercise* 25 (11): 1269–74.

Marsh, A. P., Martin, P.E., Sanderson, D.J., 2000. "Is a Joint Moment-Based Cost Function Associated with Preferred Cycling Cadence?" *Journal of Biomechanics* 33 (2): 173–80.

Martin, J.C., Brown, N.A., 2009. "Joint-Specific Power Production and Fatigue during Maximal Cycling." *Journal of Biomechanics* 42 (4): 474–79. doi:10.1016/j.jbiomech.2008.11.015.

Martin, J.C., Gardner, A.C., Barras, M., Martin, D.T., 2006. "Modeling Sprint Cycling Using Field-Derived Parameters and Forward Integration." *Medicine and Science in Sports and Exercise* 38 (3): 592–97. doi:10.1249/01.mss.0000193560.34022.04.

McDaniel, J., Behjani, N.S., Elmer, S.J., Brown, N.A., Martin, J.C., 2014. "Joint-Specific Power-Pedaling Rate Relationships during Maximal Cycling." *Journal of Applied Biomechanics* 30 (3): 423–30. doi:10.1123/jab.2013-0246.

McLester, J.R., Green, J.M., Chouinard, J.L., 2004. "Effects of Standing vs. Seated Posture on Repeated Wingate Performance." *Journal of Strength and Conditioning Research* 18 (4): 816–20. doi:10.1519/14073.1.

Mesin, L., Merletti, R., Rainoldi, A., 2009. "Surface EMG: The Issue of Electrode Location." *Journal of Electromyography and Kinesiology* 19 (5): 719–26. doi:10.1016/j.jelekin.2008.07.006.

Millet, G.P., Tronche, C., Fuster, N., Candau, R., 2002. "Level Ground and Uphill Cycling Efficiency in Seated and Standing Positions." *Medicine and Science in Sports and Exercise* 34 (10): 1645–52. doi:10.1249/01.MSS.0000031482.14781.D7.

Monnet, T, Desailly, E., Begon, M., Vallée, C., Lacouture, P., 2007. "Comparison of the SCoRE and HA Methods for Locating in Vivo the Glenohumeral Joint Centre." *Journal of Biomechanics* 40 (15): 3487–92. doi:10.1016/j.jbiomech.2007.05.030.

Muybridge, E. 1883. "The Attitudes of Animals in Motion." *Journal of The Franklin Institute* 115 (4): 260–74.

Neptune, R.R., Hull, M.L., 1995. "Accuracy Assessment of Methods for Determining Hip Movement in Seated Cycling." *Journal of Biomechanics* 28 (4): 423–37.

Neptune, R.R., Hull, M.L., 1996. "Methods for Determining Hip Movement in Seated Cycling and Their Effect on Kinematics and Kinetics." *Journal of Applied Biomechanics* 12 (4): 493–507.

Poirier. 2009. Thèse "Influence de paramètres biomécaniques et électrophysiologiques sur la technique de propulsion : transition de la posture classique vers la posture danseuse chez le cycliste." Toulouse: Université Toulouse III Paul Sabatier.

Poirier, E., Do, M., Watier, B., 2007. “Le Passage de La Posture Classique À La Posture En Danseuse Par Le Cycliste Répond-Il À Une Recherche de Minimisation de L’effort Musculaire ?” *Science & Sports* 22 (5): 190–95. doi:10.1016/j.scispo.2007.08.002.

Rao, G., Amarantini, D., Berton, E., Favier, D., 2006. “Influence of Body Segments’ Parameters Estimation Models on Inverse Dynamics Solutions during Gait.” *Journal of Biomechanics* 39 (8): 1531–36. doi:10.1016/j.jbiomech.2005.04.014.

Raynor, A.J., Yi, C.J., Abernethy, B., Jong, Q.J., 2002. “Are Transitions in Human Gait Determined by Mechanical, Kinetic or Energetic Factors?” *Human Movement Science* 21 (5–6): 785–805. doi:10.1016/S0167-9457(02)00180-X.

Redfield, R., Hull, M.L., 1986. “On the Relation between Joint Moments and Pedalling Rates at Constant Power in Bicycling.” *Journal of Biomechanics* 19 (4): 317–29.

Reiser, R.F., Maines, J.M., Eisenmann, J.C., Wilkinson, J.C., 2002. “Standing and Seated Wingate Protocols in Human Cycling. A Comparison of Standard Parameters.” *European Journal of Applied Physiology* 88 (1-2): 152–57. doi:10.1007/s00421-002-0694-1.

Ryschon, T.W., Stray-Gundersen, J., 1993. “The Effect of Tyre Pressure on the Economy of Cycling.” *Ergonomics* 36 (6): 661–66. doi:10.1080/00140139308967927.

Sargeant, A.J., Davies, C.T., 1977. “Forces Applied to Cranks of a Bicycle Ergometer during One- and Two-Leg Cycling.” *Journal of Applied Physiology: Respiratory, Environmental and Exercise Physiology* 42 (4): 514–18.

Stone, C., Hull, M.L., 1995. “Rider/Bicycle Interaction Loads During Standing Treadmill Cycling.” *Journal of Applied Biomechanics* 9 (3): 202–18.

Tanaka, H., Bassett, D.R.,Best, S.K., Baker, K.R., 1996. “Seated versus Standing Cycling in Competitive Road Cyclists: Uphill Climbing and Maximal Oxygen Uptake.” *Canadian Journal of Applied Physiology* 21 (2): 149–54.

Thouzé, A., Monnet, T., Lacouture, P., Begon, M. 2013. “A Numerical Approach to Assess the Soft Tissue Artefact during Human Movement Analysis.” *Computer Methods in Biomechanics and Biomedical Engineering* 16 Suppl 1: 59–60. doi:10.1080/10255842.2013.815894.

Turpin, N.A., Costes, A., Villeger, D., Watier, B., 2014. “Selective Muscle Contraction during Plantarflexion Is Incompatible with Maximal Voluntary Torque Assessment.” *European Journal of Applied Physiology* 114 (8): 1667–77. doi:10.1007/s00421-014-2900-3.

Villeger, D., 2014. Thèse “Restitution d’Energie Elastique et Locomotion (REEL) : Une Approche Adimensionnelle”. Toulouse: Université de Toulouse.

Villeger, D., Costes, A., Watier, B., Moretto, P., 2014. “Modela-R as a Froude and Strouhal Dimensionless Numbers Combination for Dynamic Similarity in Running.” *Journal of Biomechanics* 47 (16): 3862–67. doi:10.1016/j.jbiomech.2014.10.012.

Villeger, D., Costes, A., Watier, B., Moretto, P., 2015. “Walking Dynamic Similarity Induced by a Combination of Froude and Strouhal Dimensionless Numbers: Modela-W.” *Gait & Posture* 41 (1): 240–45. doi:10.1016/j.gaitpost.2014.10.016.

Winter, D.A. 1990. *Biomechanics and Motor Control of Human Movement*. New York: Wiley.